On the role of Spin, Pairing and Statistics for Composite Fermions in the Fractional Quantum Hall Effect

Dissertation
zur Erlangung des Doktorgrades
des Fachbereichs Physik
der Universität Hamburg

vorgelegt von

Eros Mariani

aus Genova (Italien)

Hamburg
2003

Gutachter der Dissertation: 1. Prof. Dr. Bernhard Kramer
2. Prof. Dr. Franco Napoli

Gutachter der Disputation: 1. Prof. Dr. Bernhard Kramer
2. Dr. Stefan Kettemann

Datum der Disputation: 08.07.2003

Vorsitzender des Prüfungsausschusses: Prof. Dr. D. Fay

Vorsitzender des Promotionsausschusses:
Prof. Dr. R. Wiesendanger

Dekan des Fachbereichs Physik: Prof. Dr. G. Huber

In this work we investigate the role of spin and of the pairing instabilities for Composite Fermions (CF). These quasiparticles are presently confirmed to describe many of the collective electronic properties of interacting two-dimensional Fermi systems under strong magnetic fields, in the Fractional Quantum Hall regime.

The first part of the work deals with almost free quasiparticles including their spin degree of freedom. The allowed spin-polarization eigenstates are derived and direct quantitative comparison with recent experiments is driven.
Several quantum phase transitions are expected already at this mean field level. We analyze the role of finite temperatures, spin-orbit coupling and disorder in affecting the phase transition regions and the low energy excitation sector.

In the second part of the work we concentrate on two different scenarios where CF pairing can take place.
An s-wave strong-pairing superconductive phase is considered close to the degeneracy of two Landau Levels with opposite spins. The consequent rigidity of the Ground State is argued to be responsible for the recently observed partly polarized states in the Fractional Quantum Hall regime at moderate magnetic fields.
A different p-wave CF-paired state (the "Pfaffian" state) is expected to describe the 5/2 Fractional effect. We consider the Pfaffian in the BCS-wavefunction picture, devoting particular attention to the nature of its vortex-like excitations. The zero-energy states in the core of the vortices are responsible for a macroscopic Ground State degeneracy in the many-vortices configuration. The consequent non-Abelian quantum statistics of vortex-like quasiparticles is studied by explicitly identifying the degenerate Ground State subspace.
In parallel we address the nature of the Cooper pairs wavefunctions in the inhomogeneous p-wave case.

In dieser Arbeit untersuchen wir die Rolle des Spins und der Paarbildungsinstabilitäten fr Composite Fermions (CF). Diese Quasiteilchen beschreiben viele der elektronischen Eigenschaften wechselwirkender zweidimensionaler Systeme von Fermionen in starken Magnetfeldern: dem Bereich des fraktionalen Quanten-Hall-Effektes.

Der erste Teil der Arbeit behandelt fast freie Quasiteilchen einschliesslich ihres Spinfreiheitsgrades. Die erlaubten Eigenwerte der Spinpolarisation werden hergeleitet und ein direkter quantitativer Vergleich mit neuen Experimente gezogen. Bereits auf diesem Mean-Field-Niveau werden einige Phasenübergänge erwartet. Wir analysieren den Enfluss endlicher Temperaturen, der Spin-Bahn-Wechselwirkung und von Unordnung auf den Bereich der Phasenübergänge sowie auf den Bereich niedriger Anregungsenergien.

Im zweiten Teil der Arbeit konzentrieren wir uns auf zwei unterschiedliche Szenarien, in denen CF-Paarildung stattfinden kann. Eine s-Wellen supraleitende Phase stark gekoppelter Cooper-Paare wird in der Nähe der Entartung zweier Landau-Niveaus mit entgegengesetztem Spin betrachtet. Die Stabilität des Grundzustandes wird verantwortlich gemacht für die kürzlich beobachtete teilweise Polarisierung der Zustände im Bereich des fraktionalen Quanten-Hall-Effektes bei mittleren Magnetfeldern.
Von einem anderen p-Wellen CF-Paarzustand (dem "Pfaffschen" Zustand) wird erwartet, dass er den fraktionalen Quanten-Hall-Effekt bei Füllfaktor $5/2$ beschreibt. Wir untersuchen den Pfaffschen Zustand im BCS-Bild, wobei wir besondere Aufmerksamkeit den vortexartigen Anregungen widmen. Die Zustände verschwindender Energie im Zentrum der Vortizes sind verantwortlich für eine makroskopische Entartung des Grundzustandes in Konfigurationen mit vielen Vortizes. Die folglich nicht-abelsche Quantenstatistik der vortexartigen Quasiteilchen wird untersucht, indem der entartete Unterraum des Grundzustandes explizit bestimmt wird.
Parallel dazu studieren wir die Natur der Cooper-Paar-Wellenfunktionen für den Fall inhomogener p-Wellen.

To my parents

CONTENTS

INTRODUCTION

In the last few decades there has been a ever-growing interest in the physics of electronic systems with reduced dimensionality.
The role of interactions, disorder, quantum fluctuations and their relative interplay in affecting the electronic and transport properties of realistic samples soon became, and still is, the crucial issue in condensed matter research.

Homogeneous interacting systems in more than one dimension are described within the theory of Fermi liquids (Landau 1956) in terms of Landau quasiparticles, sort of electrons with interaction-dependent effective mass and lifetime, their concept being best defined close to the Fermi level. In one dimension the quasiparticle picture breaks down and the only stable excitations are collective charge and spin-density fluctuations (Tomonaga-Luttinger 1950), in terms of which the exactly solvable Luttinger model is diagonalized.

On the other side, at first, theoretical investigations on *disordered* fermion liquids started addressing the localization properties of non-interacting systems in one, two and three dimensions (1D, 2D, 3D) (Abrahams, Anderson, Licciardello and Ramakrishnan 1979).
While 1D systems are expected to be robust insulators and 3D ones exhibit a clear density-dependent metal-insulator transition, the 2D electronic liquids lye at the edge between metallic and insulating.

Motivated by both theoretical issues and by the increased experimental skill in the production of confined systems, experimental and theoretical scientists started devoting significative effort in the analysis of 2D electronic systems, which soon played a major role in the field of condensed matter physics.
In this panorama the Quantum Hall Effect represented one of the crucial discoveries (von Klitzing 1980), showing the unique features coming out of the interplay between two-dimensionality and high magnetic fields in both the disorder and interaction-dominated regimes.
Indeed, the presence of magnetic fields induces a 2D localization-delocalization transition which can be directly analyzed in transport experiments.

In the Quantum Hall Regime macroscopic quantum phenomena show up, where both the electron kinetics in the inhomogeneous disorder potential as well as interactions can contribute on equal footing. In some sense the beauty of this phenomenon lies in its complexity.
The so-called *Integer Quantum Hall Effect* (IQHE) is ascribed to a single-particle disorder-dominated regime while electron-electron interactions play the leading role in producing the *Fractional Quantum Hall Effect* (FQHE).

The truly collective nature of the Fractional effect has been for long time ad-

dressed in terms of trial Ground State wavefunctions (Laughlin 1983) or with numerical simulations on small size systems.
Recently a different picture emerged, based on the introduction of a new quasiparticle, called *Composite Fermion*, made out of one electron and an even number of flux quanta attached to it (Jain 1989). The role of the flux quanta is to partly compensate for the external magnetic field so that many of the features observed in the FQHE can be addressed already at the non-interacting CF quasiparticle level.
As for all the other quasiparticles which have been introduced in the past to describe different collective phenomena, the improvement brought by the invention of CF has been huge. They allow a unified picture of both compressible and incompressible FQH states and a formal field theoretical treatment can be set up on their basis (Halperin, Lee and Read 1993).
Indeed the formal apparatus of Chern-Simons field theories can be applied to evaluate interaction-induced corrections to the non-interacting mean-field results, like the CF effective mass or their excitation spectrum (Stern and Halperin 1995).
The CF have been shown to be exceptionally effective in describing or even predicting experimental results. Their quasiparticle nature has been directly probed with focusing techniques as well as with geometric resonance experiments.

In recent years the increased sample quality (i.e. the ever-improving mobility) allowed the investigation of QH effects in the low magnetic field regime and the observation of previously unexpected features.
Spin effects come into play affecting both the Ground State structure as well as the excitation spectrum, in contrast to the standard picture of fully polarized electrons in the high field region.
Moreover, in both single 2D samples as well as in bilayer QH systems, for certain choices of parameters, low temperature phase transitions are observed, ascribed to quasiparticle pairing instabilities.

Therefore, in order to both describe the recent experimental issues and to dig deeper into the theoretical understanding of the CF it has become necessary to investigate the spin-related properties of these quasiparticles as well as the interaction-induced broken symmetries in the FQHE.
These will be the main topics addressed in this thesis.

After introducing the general theory of the IQHE and FQHE in the first chapter and the spinless CF picture in the second one, we will consider the spinful CF at the non-interacting level (chapter 3) to grasp the essential features observable in spin polarization measurements in the FQH regime.
The residual interactions between spinful CF will be shown to induce the tendency to quasiparticle pairing, somehow like the superconducting instability for Landau quasiparticles.
Therefore chapter 4 will be devoted to an introduction to the theory of superconductivity, both along the BCS wavefunction line and in the more formal field theoretical framework of many-body Green's functions with broken symmetries. These techniques will be combined, in chapter 5, with the Chern-Simons field theories with spin to address the CF pairing instabilities and its consequencies on experiments.
A particular FQHE, the so-called 5/2 state, will be investigated in chapter 6. It

can be interpreted as a p-wave superconductive condensate of spin-polarized CF whose vortex-like excitations fulfill a peculiar non-commutative quantum statistics. The nature of the Ground State producing such effects will be addressed in two different ways, highlighting its complex entangled structure and identifying the Cooper pairs in the inhomogeneous p-wave paired phase.

1. INTRODUCTION TO THE QUANTUM HALL EFFECT

In this first chapter we will give a brief introduction to the physics of the Quantum Hall Effects.
After a short overview of the Classical Hall Effect we will present the deviations occurring in the high magnetic field regime where quantum phenomena become prominent.
In order to describe the phenomenon we will first consider the behaviour of two-dimensional (2D) electronic systems in presence of strong magnetic fields. The resulting single particle spectrum shows energy quantization and a density dependent compressibility.
The introduction of inhomogeneities ("disorder" in general terms) affects the physical properties of the system inducing a 2D localization-delocalization transition responsible for the Integer Quantum Hall Effect (IQHE).
When electron-electron interaction is taken into account additional incompressibilities show up. In the regime of weak disorder they are the origin of the Fractional Quantum Hall Effect (FQHE).
As far as this chapter is concerned, the correlation effects in the FQH regime will be presented in the "standard" wavefunction picture. We will see later how new techniques emerged recently, leading to the introduction of quasiparticles able to catch the main physics related to correlations between the original electrons.

Before entering the fascinating topics related to the quantum phenomena of two-dimensional electronic systems in strong magnetic fields we will briefly describe the classical picture of the Hall effect within the framework of the Drude theory of metals [1].

1.1 The Classical Hall Effect

The Classical Hall Effect was discovered by E. H. Hall in 1879 [2] while studying the transport properties of metallic wires subject to an external magnetic field. We can describe the geometry of his experiment considering a three dimensional (3D) wire along the x direction, subject to a magnetic field $\mathbf{B} = B\hat{\mathbf{z}}$ along the z direction, as shown in Fig (1.1).

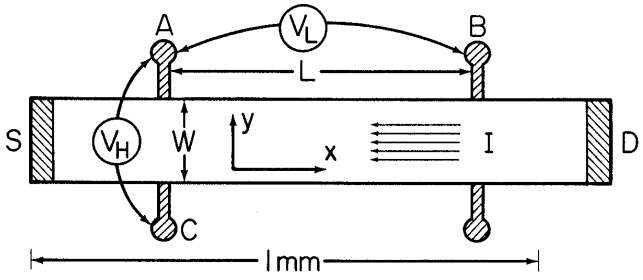

Fig. 1.1: The top view of a Hall bar in the (x, y) plane. The magnetic field is along the z direction. In the original experiment by Hall [2] the sample was 3-dimensional, having a finite thickness along z. For further interest in the Quantum Hall Effect we will have to deal with a pure 2D system as the one shown in the picture. Current is injected in the x direction and both the longitudinal and Hall voltage drops (V_{L} and V_{H}) are probed.

Hall imposed a current along the x direction and measured both the resistance along the same direction (longitudinal or *magnetoresistance*) and along the perpendicular (y) one (transverse or *Hall* resistance) as functions of the external magnetic field. He found out that the magnetoresistance was independent on B while the Hall resistance scaled linearly with the magnetic field.

We can interpret his results qualitatively by considering that the electrons in the sample feel an initial force along the x direction due to the external voltage; the Lorentz force bends their motion to the y direction where they tend to accumulate on the sample side. This accumulation builds in an additional electric field that, at regime, balances the Lorentz contribution, preventing further electronic accumulation. The additional electric field is responsible for the Hall voltage drop (and finally for the Hall resistance) along the y direction and has to be proportional to B in order to compensate for the Lorentz term. On the other side, *at regime* the motion of the electrons along the x direction is not affected by the formation of the Hall field and is essentially governed by scattering with impurities, which is B independent.

We can analyze the situation depicted above in more detail via a Drude-model calculation. The rate of momentum change for an electron of charge $-e$ and band

mass m is given by the Drude formula

$$\frac{\mathrm{d}\mathbf{p}}{\mathrm{d}t} = \mathbf{f} - \frac{\mathbf{p}}{\tau} \tag{1.1}$$

where $\mathbf{p}$ is the momentum, $\mathbf{f}$ is the force experienced by the electron and $\mathbf{p}/\tau$ is the frictional damping term introduced by the impurity scattering (τ the relaxation time). The electrons in the sample are subject to the force

$$\mathbf{f} = -e\left(\mathbf{E} + \frac{\mathbf{p}}{mc} \times \mathbf{B}\right) . \tag{1.2}$$

At regime, the average momentum per electron is independent on time ($\mathrm{d}\mathbf{p}/\mathrm{d}t = 0$) and, by writing the momentum in terms of the current density, $\mathbf{p} = -m\mathbf{j}/\rho e$ (ρ the average electron density) from (1.1) we get

$$\begin{aligned} E_x &= \frac{B}{\rho e c}\, j_y + \frac{m}{\rho e^2 \tau}\, j_x \\ E_y &= -\frac{B}{\rho e c}\, j_x + \frac{m}{\rho e^2 \tau}\, j_y \, . \end{aligned} \tag{1.3}$$

By imposing that the transverse current density j_y vanishes, and using the definition of the resistivity tensor

$$E_\alpha = \rho_{\alpha\beta} j_\beta \tag{1.4}$$

we obtain the longitudinal and transverse resistivities

$$\begin{aligned} \rho_{xx} &= \frac{m}{\rho e^2 \tau} \\ \rho_{yx} &= -\frac{B}{\rho e c} \, . \end{aligned} \tag{1.5}$$

The first coincides with the Drude resistivity, it is unaffected by the magnetic field and is essentially scattering-related while the second is proportional to B, as anticipated above qualitatively.
A useful quantity to define is the so-called Hall coefficient $R_{\mathrm{H}} = E_y/j_x B$. This comes out to be

$$R_{\mathrm{H}} = -\frac{1}{\rho e c} \tag{1.6}$$

and is therefore sensitive to the carrier concentration and to the sign of the carrier charge.
Indeed it came as a huge surprise that some metals, like Al, In, Mg and others, experimentally show a *positive* Hall coefficient, signature of positively charged carriers.
This apparent mystery had to wait for the quantum theory of solids to be explained, and lead to the introduction of the concept of *holes*.

From the previous discussion we saw that the z direction is completely decoupled from the interesting dynamics. In view of the later interest in the Quantum Hall Effect (QHE), we can from now on concentrate on a purely two-dimensional

electron system (2DES) in the (x, y) plane. In the next section we will discuss why 2D is an important issue in the QHE and how it is experimentally possible to produce 2DES with controllable physical properties.
Here we just notice that, similarly to the definition (1.4), the conductivity tensor σ can be introduced as

$$j_\alpha = \sigma_{\alpha\beta} E_\beta. \tag{1.7}$$

It is easy to verify that in the Hall regime the Onsager relations hold [3]: $\sigma_{yy} = \sigma_{xx}$ and $\sigma_{yx} = -\sigma_{xy}$. We can therefore obtain the relation between the tensors $\hat{\rho}$ and $\hat{\sigma}$

$$\hat{\rho} = \hat{\sigma}^{-1} = \frac{1}{\sigma_{xx}^2 + \sigma_{xy}^2} \begin{pmatrix} \sigma_{xx} & \sigma_{xy} \\ -\sigma_{xy} & \sigma_{xx} \end{pmatrix}. \tag{1.8}$$

From (1.8) we notice a curious property: if $\sigma_{xx} = 0$ *and* $\sigma_{xy} \neq 0$, as in the *disorder-free* ($\tau \to \infty$) Hall case with a *finite* magnetic field, also $\rho_{xx} = 0$. We will see that this relation holds in the plateau regions of the QHE as well.
In such conditions the sample on one side looks like a perfect insulator ($\sigma_{xx} = 0$) and on the other side like an ideal conductor with $\rho_{xx} = 0$. This apparently contradictory statement simply means that the current runs exactly perpendicular to the voltage.

Having discussed the general features of the Classical Hall regime we now start considering the experiment that lead to the discovery of the Quantum Hall Effect. The experimental outcomes of Hall measurements at high magnetic fields were dramatically different from the simple scalings observed originally by Hall and a full quantum treatment is finally needed in order to address the problem theoretically.

1.2 The Integer and Fractional Quantum Hall Effects: Experiments

The Quantum Hall Effect (QHE) was measured for the first time in 1980 by Klaus von Klitzing, roughly 100 years after the discovery of the Classical Hall Effect [4]. His experiment was performed at very low temperatures on a 2D Si-MOSFET inversion layer subject to a large perpendicular magnetic field.
Two essential deviations from the Classical behaviour were observed:

- Contrary to the classical linear scaling with the external field, the Hall resistance showed plateaux around some of the classically expected values. The resistance in the plateaux was found to be quantized as

$$\boxed{R_{\mathrm{H}} = \frac{h}{\nu e^2} \quad \nu = \text{integer}}. \tag{1.9}$$

- In the same region where the plateau forms, the magnetoresistance goes to *zero* within experimental uncertainties, contrary to the classically expected constant and *finite* value.

With improving sample quality the quantization is now observed up to a precision of 10^{-10} and the resistance has universal values, independent on all microscopical

details of the sample, its material, the amount of disorder (unless the sample mobility becomes too low), etc.
The quantization value $R_K = h/e^2 = 25812.81 \pm 0.05\,\Omega$ is presently used to maintain the standard metrological unit for resistances, and together with the speed of light c guarantees a very accurate determination of the fine structure constant $\alpha = e^2/\hbar c \approx 1/137$. It is impressive that such a precision is achieved in a *real* sample, with disorder, contacts, finite temperature...
For his discovery, Klaus von Klitzing was awarded the Nobel Prize for Physics in 1985.

Having a 2DEG is important for the universality of the results. In fact the resistance R and resistivity ρ of a d-dimensional hypercubic sample of size L scale as $R = \rho L^{2-d}$. Thus when $d = 2$ the resistance is scale-invariant and geometrical details of the sample do not matter, as well as their accurate measurement is not needed in order to improve the quantization accuracy.
Exactly two-dimensional electronic systems can be produced by imposing a strong potential confinement to the electrons in one of the three dimensions of a bulk sample (let's say the z direction) such that only the first level of the confining potential is occupied at the typical experimental densities. In the end electrons can move in an effectively 2D plane with a very small thickness due to the finite z-extension of the confinement potential wavefunctions (see Fig (1.2)).

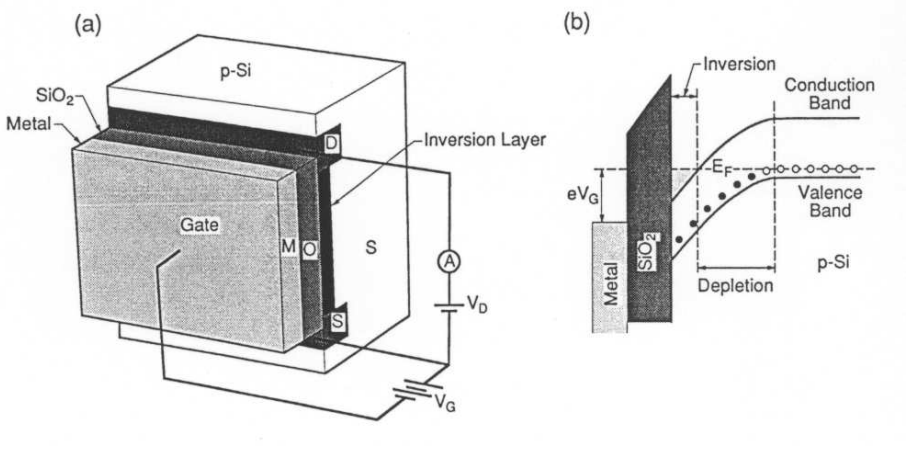

Fig. 1.2: The schematic view of a 2DEG formed in the inversion layer (b) produced in a MOSFET (a). The Source-Drain contacts are used to induce currents in the 2DES while the voltage modulation on the metallic Gate tunes the 2D electronic density.

Such a situation can be achieved in the Metal-Oxide-Semiconductor-Field-Effect-Transistors (MOSFETs) or in semiconductor heterojunctions. Via a modulation of the voltage on a metallic gate separate from the 2DEG the carrier concentration can

be changed in the sample.
The density modulation at a constant magnetic field of 19 T was originally considered in the experiment by von Klitzing depicted in Fig.(1.3). Clearly several plateaux in the Hall resistance were observed, together with a vanishing longitudinal resistance.

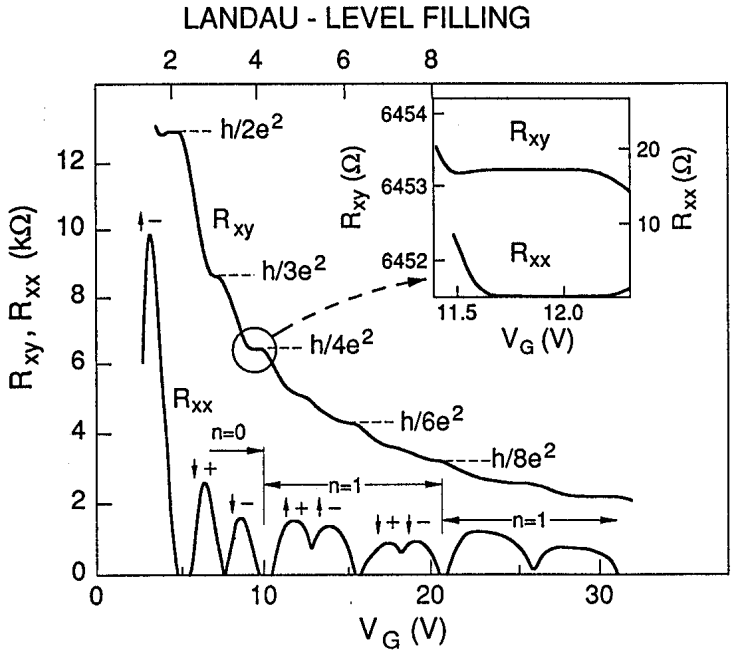

Fig. 1.3: The Quantum Hall effect observed in the longitudinal and Hall resistance as a function of the electronic density (tuned by the gate voltage V_G) for a fixed magnetic field of 19 T [5]. The temperature is kept constant at 1.5 K. The oscillations in R_{xx} are labelled by Landau Level index (see later), spin and valley degeneracy.

In analogy it is possible to perform QHE experiments at constant carrier density by sweeping the magnetic field. Due to the limited ability in changing the electron concentration via back-gate modulation, this last technique typically guarantees a wider range of observable plateaux.

In 1982 D. C. Tsui and H. L. Stormer, while performing high field Hall measurements on extremely clean GaAs 2DES, observed Hall resistance quantizations like (1.9) with ν being a fraction (the most pronounced was $\nu = 1/3$, see Fig (1.4)) [6]. With increasing efforts many more fractions were observed, with both ν larger and smaller than 1, belonging to precise rational series.

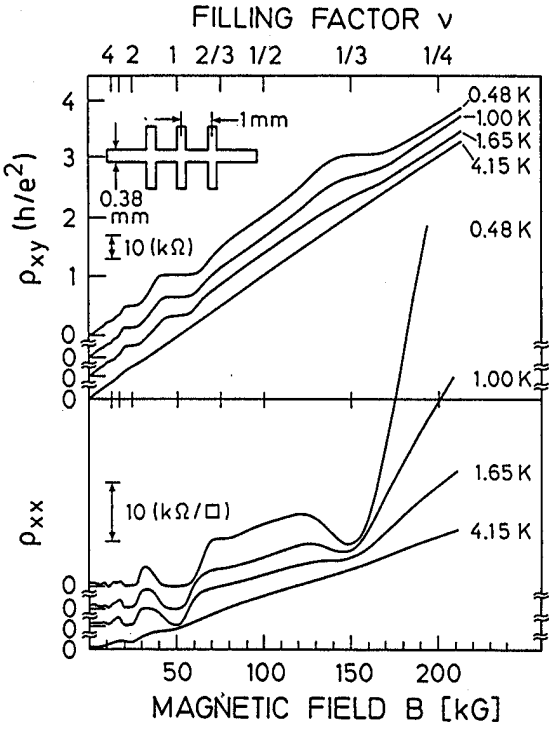

Fig. 1.4: The first observation of the Fractional Quantum Hall Effect [6]. A plateau at $\rho_{xy} = 3\,h/e^2$ shows up for low enough temperatures (upper panel). As it frequently happens at the early stage of observation of new plateaux, the longitudinal resistivity does not drop exactly to zero in the plateaux region but shows a minimum getting stronger for lower temperatures. In subsequent measures on cleaner samples the zero in ρ_{xx} was clearly observed (see, for example, Fig (1.5)).

The stable plateaux observed up to now for $\nu < 1$ fulfill the relation

$$\boxed{\nu = \frac{p}{2mp \pm 1} \qquad p, m \in \mathbb{N}}\,, \tag{1.10}$$

their stability decreasing with increasing p. Similar families of states are observed adding integers to the fractions described in (1.10).
As previously, in correspondence with the plateau in $R_{\rm H}$ a vanishing longitudinal resistance was measured. Figure (1.5) shows a QHE transport experiment in a wide range of magnetic fields. Many Integer as well as Fractional states are clearly evident.

For obvious reasons the effect discovered by von Klitzing was called "Integer Quan-

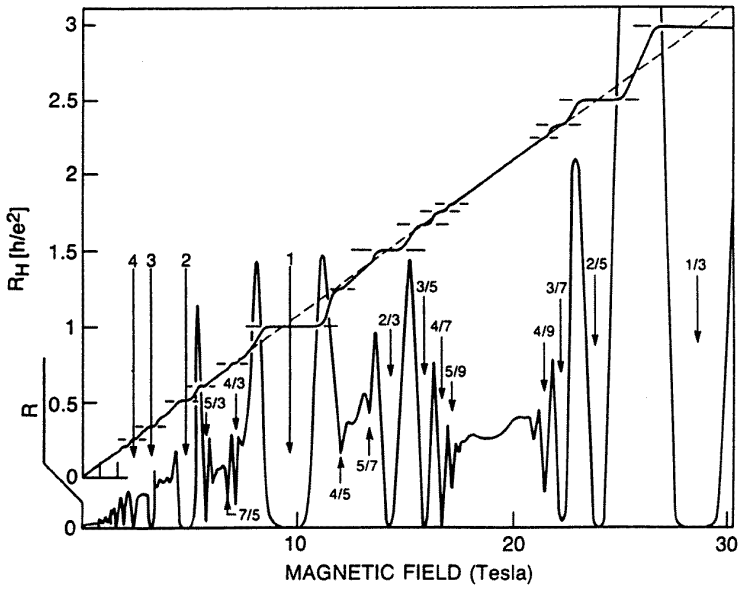

Fig. 1.5: The longitudinal and transverse resistances $R \equiv R_{xx}$ and $R_{\rm H} \equiv R_{xy}$ as functions of the magnetic field [7]. Many Quantum Hall plateaux show up in both the Integer and Fractional regimes. The values of ν in the plateaux are explicitly indicated. Notice that the regime of validity of the Classical Hall Effect ranges only up to less than 1 Tesla.

tum Hall Effect" (IQHE) while that measured by Tsui became the "Fractional Quantum Hall Effect" (FQHE).
Despite the similar experimental outcomes, the origin of these two effects is quite different, as we will see. The IQHE is mainly a disorder-related phenomenon while electron-electron interactions plays the major role in the explanation of the FQHE. Further experimental details will be presented in the section dedicated to spin polarization measurements in the Quantum Hall regime. Now we will introduce the theory of the Integer as well as of the Fractional Quantum Hall Effects.

1.3 The Integer Quantum Hall Effect: theoretical introduction

In this section we will present a theoretical introduction to the IQHE: the basic understanding of the phenomenon can be achieved by considering non-interacting fermions subject to a strong magnetic field in presence of a disorder potential. Our discussion of the Integer as well as of the Fractional QHE will be limited to zero temperature. Finite (but not too large) temperatures do not significantly alter the qualitative behaviour, as we will see.
The essence of the IQHE can be briefly described as follows

- The energy spectrum of the 2D electrons in presence of a strong perpendicular magnetic field is made of discrete levels corresponding to an harmonic oscillator with characteristic energy determined by the magnetic field itself. Each of these levels (Landau Levels) is hugely degenerate.
- The introduction of disorder removes the degeneracy producing a broadened density of states (DOS) for each Landau Level (LL) and induces a localization-delocalization transition. More precisely the states with energy close to the center of the LL are extended, meaning that their localization length diverges exactly at the LL center. All the states whose localization length is larger than the typical size of the sample contribute to the linear transport at $T = 0$ while all the localized states give a vanishing conductivity.
- By varying the electron density at a constant magnetic field (or viceversa) the chemical potential shifts and pins to either localized or extended states. In the former case we expect an insulating behaviour with $\sigma_{xx} = 0$ and the transport properties of the sample remain unchanged (plateaux) until the extended states start being occupied. At this point $\sigma_{xx} \neq 0$ and the transition region between different plateaux is reached.

A schematic view of the previous argument is given in Fig (1.6)

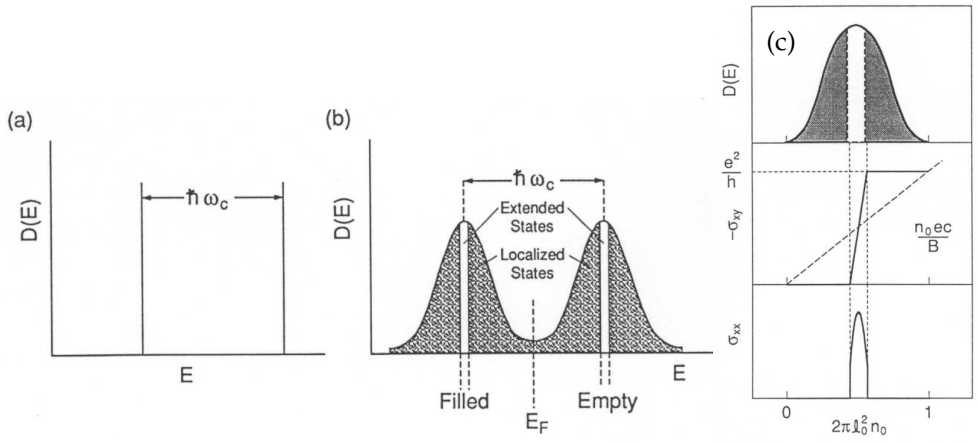

Fig. 1.6: Schematic view of the theory of the IQHE. In (a) the discrete energy levels (Landau Levels) are shown. Disorder broadens the Density of States (b), producing localized states in the tails of the Landau bands and extended states in their centers. In (b) the Fermi energy is pinned in the fully localized regime, implying the QHE plateau in the Hall resistance and the vanishing magnetoresistance, as shown in (c). The transition regions between different plateaux and the peaks in the longitudinal resistance are achieved by moving the Fermi energy in the band of extended states.

In the following sections we will first consider 2D electrons subject to a magnetic

field and obtain their spectrum. We will then show how the introduction of disorder affects the DOS of the system. Then we will present a couple of arguments about the existence of extended states in a Landau band, later supported by numerical investigations. Finally, it will be described how gauge invariance is responsible for the exactness of the plateau quantization.

1.3.1 2D electrons in a strong magnetic field: the Landau Levels

Let us start considering free spinless electrons in the 2D (x, y)-plane with a parabolic dispersion $\varepsilon_{\mathbf{k}} = \hbar^2 k^2/2m$, $\mathbf{k}$ their 2D wavenumber. Their Density of States is constant and equals $\mathrm{DOS}(\varepsilon) = m/2\pi\hbar^2$.
The introduction of the external uniform magnetic field $\mathbf{B} = B\hat{\mathbf{z}}$ induces a change in the Hamiltonian of the system which is now

$$H = \sum_i \frac{1}{2m}\left(\mathbf{p}_i + \frac{e}{c}\mathbf{A}(\mathbf{r}_i)\right)^2 \tag{1.11}$$

where the sum runs over the particles, $\mathbf{p}$ is the canonical momentum and $\mathbf{A}(\mathbf{r})$ is the vector potential generating $\mathbf{B} = \nabla \times \mathbf{A}(\mathbf{r})$.
Notice that, although the system is translationally invariant and all the physical properties are, the Hamiltonian is not!
Choosing the Landau gauge $\mathbf{A}(\mathbf{r}) = xB\hat{\mathbf{y}}$ the single particle Hamiltonian becomes

$$H = \frac{1}{2m}\left(p_x^2 + \left(p_y + \frac{eB}{c}\,x\right)^2\right) \tag{1.12}$$

and still preserves translation symmetry along the y direction. This implies that the eigenfunctions can be factorized as

$$\psi_k(x, y) = e^{iky} f_k(x) \tag{1.13}$$

with e^{iky} a planewave eigenstate with momentum eigenvalue $\hbar k$ along y and where $f_k(x)$ satisfies the Schrödinger equation

$$h_k f_k(x) = \varepsilon_k f_k(x) \tag{1.14}$$

with

$$h_k = \frac{1}{2m}\,p_x^2 + \frac{1}{2m}\left(\hbar k + \frac{eB}{c}\,x\right)^2 \equiv \frac{1}{2m}\,p_x^2 + \frac{1}{2}\,m\omega_{\mathrm{c}}^2\left(x + k\ell^2\right)^2. \tag{1.15}$$

Thus $f_k(x)$ satisfies the equation for a *one-dimensional* harmonic oscillator with the cyclotron frequency

$$\omega_{\mathrm{c}} = \frac{eB}{mc} \tag{1.16}$$

whose center is shifted by the amount $-k\ell^2$, with the magnetic length $\ell = \sqrt{\hbar c/eB}$.
The presence of the magnetic field thus introduces several characteristic scales: the

cyclotron frequency is the rotation frequency of a classical electron subject to B, while the magnetic length is defined as the radius of a circle enclosing half a magnetic flux quantum

$$2\pi\ell^2 B = \Phi_0 = \frac{hc}{e} \ . \tag{1.17}$$

The energy spectrum is then simply [8]

$$\boxed{E_{n,k} = \left(n + \frac{1}{2}\right)\hbar\omega_{\mathrm{c}}} \tag{1.18}$$

and gives rise to a DOS made out of delta's centered on the various $E_{n,k}$. Thus we have *discrete* energy levels, named Landau Levels (LL), degenerate with respect to the internal quantum number k.
In order to determine the degeneracy of the LL we directly look at the wavefunctions $f_k(x)$. Being solutions of a 1D harmonic oscillator, in the n-th LL they are

$$f_{nk}(x\,) = \mathcal{N} H_n(x + k\ell^2) e^{-\frac{1}{2\ell^2}(x+k\ell^2)^2} \ , \tag{1.19}$$

where H_n is the n-th Hermite polynomial. Due to the fast decay of the gaussian factor, they are strongly localized, in the x direction, around the center $-k\ell^2$ (determined by the wavevector k in the y direction) with a typical width ℓ.
Let us imagine to have a rectangular sample with side lengths (L_x, L_y), extending from $x = -L_x$ to $x = 0$, with periodic boundary conditions in the y direction. The center coordinate $-k\ell^2$ lies inside the sample if k ranges from 0 to L_x/ℓ^2, otherwise a different index n has to be chosen. We can then deduce that the total number of states in a given LL (the degeneracy) is

$$N_\Phi = \frac{L_x L_y}{2\pi\ell^2} \ . \tag{1.20}$$

By direct comparison with the definition of the magnetic length (1.17) we deduce that the degeneracy coincides with the total number of flux quanta penetrating the sample at a given magnetic field. When B is sufficiently large N_Φ becomes huge. A quantitative understanding of the degeneracy comes if we consider that

$$\ell(B) = \frac{25.7}{\sqrt{B[\mathrm{T}]}} \ \mathrm{nm}. \tag{1.21}$$

A typical sample with characteristic linear size of the order of 1mm at the (not so large) magnetic field of 1T already contains a macroscopic number of flux quanta.
The presence of the magnetic field therefore "breaks" the continuous parabolic energy spectrum into a sum of discrete degenerate levels where the kinetic energy is completely quenched. This aspect is crucial for many of the fascinating phenomena connected to the QHE.
The magnetic field introduces a new energy scale, the so-called "cyclotron energy" $\hbar\omega_{\mathrm{c}}$. When it becomes significatively larger than the level spacing, the Landau quantization becomes crucial.

If we calculate the number of states per unit area enclosed in an energy window $\hbar\omega_c$ of the parabolic dispersion (i.e. without magnetic field) we get $\hbar\omega_c m/2\pi\hbar^2 = N_\Phi/L_xL_y$, exactly as for the LL. Somehow it looks like if the magnetic field breaks the 2D DOS by shrinking all the states in the energy windows $\hbar\omega_c$ into one enormously degenerate LL.
We can now define the *filling factor* as the ratio between the total number N of electrons and the LL degeneracy

$$\nu = \frac{N}{N_\Phi} = \frac{\rho\Phi_0}{B} \ . \tag{1.22}$$

This quantity will come out to be one of the most important indicators of different Quantum Hall States. As mentioned in the introduction to the QHE experiments there are two ways of tuning the filling factor: either by changing the carrier density or by sweeping the magnetic field. We will see that interesting results come out by performing experiments at constant filling, by tuning density and B together.

Up to this point the system is still translationally invariant and no Quantum Hall Effect can arise in these conditions. We can rewrite the Hall conductivity in terms of the filling factor as

$$\sigma_{xy} = \frac{\rho ec}{B} = \frac{ec\nu}{\Phi_0} = \frac{\nu e^2}{h} \ . \tag{1.23}$$

But this relation has nothing to do with the QHE: it simply says that in a translationally invariant 2DES, by varying the filling continuously (e.g. via density modulation or magnetic field change), also σ_{xy} varies linearly with ν.
In particular, when ν is an integer, it assumes the correct value observed in the QHE plateaux: but the plateaux themselves are absent.

We need to break the translational invariance to explain the plateaux, as we will see. This invariance-breaking naturally appears in a *real* sample, since it always contains a certain amount of defects and inhomogeneities. In the next sections we investigate what is the role of disorder in affecting the electronic spectrum and the transport properties of Quantum Hall Systems.

1.3.2 The role of disorder in the DOS of Landau Levels

Electrons in real 2D samples move in an imperfect lattice of positive charges. The imperfections at very small temperatures consist essentially of lattice defects and ionized donors outside the 2D gas. Their presence affects both the conductivity at zero field by introducing a finite mean scattering time as well as the electronic density of states in presence of the Landau quantization.
In the absence of disorder we saw that the DOS of a Quantum Hall System is just a sum of delta functions at energies $(n+1/2)\hbar\omega_c$, each of them having a weight N_Φ. Disorder essentially removes the LL degeneracy and broadens the delta's into Landau bands with a finite width inversely proportional to the mean scattering time.
We can physically understand this effect already by considering classical electrons

performing circular orbits in presence of a uniform magnetic field. If the impurities are few and their average distance is much larger than the cyclotron radius, some electrons will keep performing their circular motion in regions not affected by the disorder potential, thus having their energy unaltered. Other electrons will move around the impurities thereby experiencing a shift in energy.
Quantum mechanically we can estimate the DOS of LLs by considering the impurity scattering as a perturbation to the free electron propagation [9].
We will consider the Hamiltonian

$$H = H_0 + H_{\text{Dis}} = \sum_i \left(\frac{1}{2m} \left(\mathbf{p}_i + \frac{e}{c} \mathbf{A}(\mathbf{r}_i) \right)^2 + V(\mathbf{r}_i) \right) . \tag{1.24}$$

The disorder potential can be described as

$$V(\mathbf{r}) = \sum_j v(\mathbf{r} - \mathbf{R}_j) \tag{1.25}$$

where $\mathbf{R}_j$ is the 3D position of the j-th impurity ion, generating the electrostatic potential $v(\mathbf{r} - \mathbf{R}_j)$.
In a real sample the relevant impurities are located outside the 2DEG and in principle they could generate different potentials v. For simplicity of treatment we can imagine to have *identical* impurities placed within the 2D layer. In the case of charged impurities, $v(\mathbf{r})$ is a screened Coulomb potential, obtained in principle by solving selfconsistently the dielectric function problem.
In many calculations, however, a Gaussian model potential

$$v(\mathbf{r}) = \frac{\lambda}{2\pi a^2} e^{-r^2/2a^2} \tag{1.26}$$

has been used to highlight the main physical influence of impurities. In Eq. (1.26) λ is the coupling constant and a the range of the potential. A final simplifying assumption can be performed, considering a zero range ($a \to 0$) random potential.
We will denote with a bar the averages over the impurity distributions for a generic function f,

$$\overline{f} = \int \prod_j \frac{\mathrm{d}\mathbf{R}_j}{A} f(\mathbf{R}_1, ..., \mathbf{R}_N) \tag{1.27}$$

with A the area of the sample.
The single particle DOS in presence of the disorder potential is obtained as [10]

$$\text{DOS}(E) = \frac{1}{A} Tr\{\overline{\delta(H - E)}\} = -\frac{1}{\pi A} Tr\{\text{Im}\, g^{\text{R}}(E)\} \tag{1.28}$$

with $g^{\text{R}}(E) = \overline{G^{\text{R}}(E)}$ the impurity averaged retarded single particle Green's function, where $G^{\text{R}}(z) = 1/(z - H)$, $z = E + i0^+$.
The Green's function $G(z)$ and averaged Green's function $g(z)$ obey the Dyson's equations

$$G = G_0 + G_0 V G \tag{1.29}$$
$$g = G_0 + G_0 \Sigma\, g \tag{1.30}$$

with $G_0(z) = 1/(z - H_0)$ the free electron Green's function and Σ the selfenergy. Owing to the rotational invariance of the disorder potential with respect to the z axis, $g(z)$ is diagonal in the LL basis and does not depend on the internal momentum k. For the n-th LL with energy E_n we can write

$$g_n^{\mathrm{R}}(z) = \frac{1}{z - E_n - \Sigma_n(z)} \tag{1.31}$$

where, in general, we can decompose Σ into its real and imaginary parts

$$\Sigma_n(z) = \Delta_n(E) - i\,\Gamma_n(E)\ . \tag{1.32}$$

Thus the DOS (1.28) becomes

$$\mathrm{DOS}(E) = \frac{1}{2\pi\ell^2} \sum_n \frac{1}{\pi} \frac{\Gamma_n(E)}{\left[E - E_n - \Delta_n(E)\right]^2 + \Gamma_n^2(E)}\ . \tag{1.33}$$

In order to evaluate (1.32) we rescale the disorder potential with respect to its average, such that $\overline{V} = 0$. Thus the first non-trivial contribution to the self-energy is, to lowest order in λ and in the LL basis

$$\Sigma_{n,k} = \sum_{n',k'} \overline{\left|V_{n,k;n',k'}\right|^2}\, g_{0n'} \tag{1.34}$$

where we use the standard notation for the set of LL quantum numbers (n, k) and where $V_{n,k;n',k'}$ is the projection of the disorder potential on the LL wavefunctions. The selfconsistent generalization of (1.34), the so-called Self-Consistent Born Approximation (SCBA), is obtained by replacing the free Green's function with the exact one, giving

$$\Sigma_{n,k} = \sum_{n',k'} \overline{\left|V_{n,k;n',k'}\right|^2}\, g_{n'} = \sum_{n',k'} \frac{\overline{\left|V_{n,k;n',k'}\right|^2}}{E - E_{n'} - \Sigma_{n',k'}} \tag{1.35}$$

depicted by the diagram of Fig (1.3.2). For strong magnetic fields, such that $\hbar\omega_{\mathrm{c}} \gg \Gamma_n$, we can neglect the admixtures of LL with $n \neq n'$ and (1.35) reduces to

$$\Sigma_n(E) = \frac{a_n}{E - E_n - \Sigma_n(E)} \tag{1.36}$$

with $a_n = \sum_{k'} \overline{\left|V_{n,k;n,k'}\right|^2}$.
From (1.36) we can extract

$$\Sigma_n(E) = \frac{1}{2}\left(E - E_n - \sqrt{(E - E_n)^2 - 4a_n}\right) \tag{1.37}$$

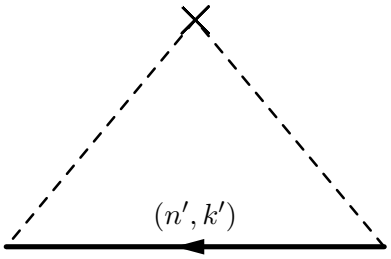

Fig. 1.7: The electronic selfenergy in the SCBA. The exact fermionic Green's function is used as internal line and the average of two disorder potentials is represented by joining the dashed lines into the scattering impurity.

whence

$$\Delta_n(E) = \frac{1}{2}\left(E - E_n\right) \tag{1.38}$$

and

$$\Gamma_n(E) = \frac{1}{2}\,\Theta\left(4a_n - \left(E - E_n\right)^2\right)\sqrt{4a_n - \left(E - E_n\right)^2} \tag{1.39}$$

with $\Theta(x)$ the step function equal to 1 for $x \geq 0$ and 0 elsewhere.
Inserting (1.38) and (1.39) in (1.33) we obtain a DOS made out of semi-ellipses centered around the LL energies, with a width $W_n = 2\sqrt{a_n}$. The coefficients a_n have been calculated [9] by projecting the disorder potential onto the LL functions (1.13,1.19) with the final result for the level width

$$W_n = \sqrt{\frac{2}{\pi}\hbar\omega_c\frac{\hbar}{\tau}} \tag{1.40}$$

with τ the relaxation time in the Born approximation. Thus the LL broadening is independent on the index n and scales as $\sqrt{B}$, justifying the high field approximation of neglecting LL mixing.

Already at the SCBA level we see that disorder breaks the huge LL degeneracy and produces a broad and smooth DOS. The approximation produces a semi-elliptic DOS with unphysical singularities at the band edges. For the case of δ-correlated impurity potentials the DOS for the lowest LL has been calculated *exactly* by Wegner with a resulting Gaussian shape [16], see Fig (1.8). The SCBA and exact DOS agree quite nicely near the LL center and the band-width scale in the same way. In both cases, however, the DOS does not show any sign of the mentioned localization-delocalization transition.

In the next section we will consider the issue of localization in the Quantum Hall Regime and the exactness of the plateau quantization. With these considerations we will then procede to analyze the Fractional Quantum Hall regime.

1.3.3 The percolation picture for the Localization-Delocalization transition

According to the scaling theory of localization for noninteracting electrons [17], in two dimensions all the states should be localized in the absence of a magnetic field

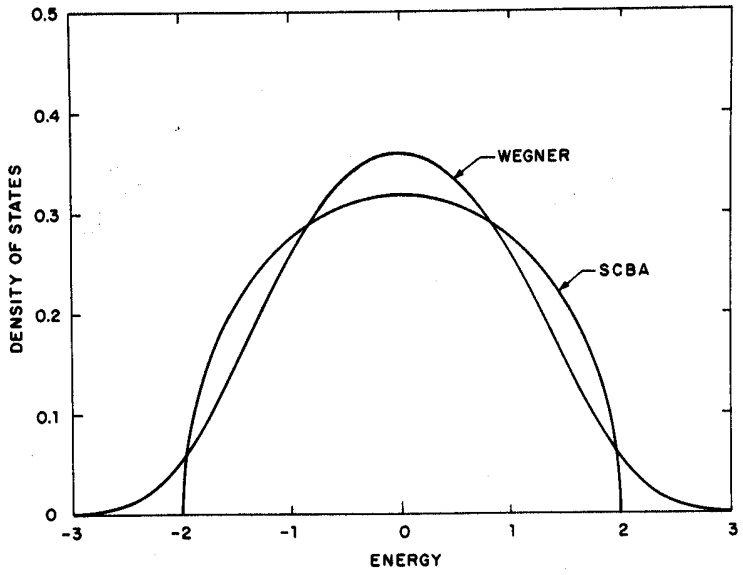

Fig. 1.8: The DOS of the first LL in presence of a delta-correlated random potential. The Self-Consistent Born Approximation [9] as well as the exact result by Wegner [16] are shown.

(if spin-orbit effects are neglected). One of the intriguing aspects of the QHE is the observation of localization-delocalization transitions in 2D.
In order to get a physical picture of this quantum phase transition we can start considering the high field limit for a 2D sample with a long-range correlated disorder potential. This is the dominant inhomogeneity induced, for example, by donors in a δ-doping layer or spread over the 3D wafer. They induce an electrostatic potential $V(\mathbf{r})$ which looks like a mountain landscape, with tops and valleys.
Let us consider the high magnetic field regime, where the magnetic length is much smaller than the correlation length of the potential landscape, and neglect the e-e interactions. We can restrict to the lowest LL physics if we consider the limit of having a cyclotron energy much larger that the variance of the disorder potential. Since the kinetic energy is quenched for all the electrons, the single particle eigenstates are given by equipotential lines of $V(\mathbf{r})$ (in the limit $B \to \infty$, where the magnetic length is zero). If the magnetic length is finite but small we can describe the electronic behaviour semiclassically as a cyclotron rotation (with characteristic size ℓ) accompanied by a drift along the equipotential lines of the disorder landscape due to the $\mathbf{E} \times \mathbf{B}$ force. In recent experiments with scanning tunneling spectroscopy techniques [18] these percolating electronic wavefunctions have been directly observed and their lateral size has been measured to be compatible with the magnetic length, see Fig (1.9).
Let us imagine we start with no electrons in this disordered LL. If we now increase

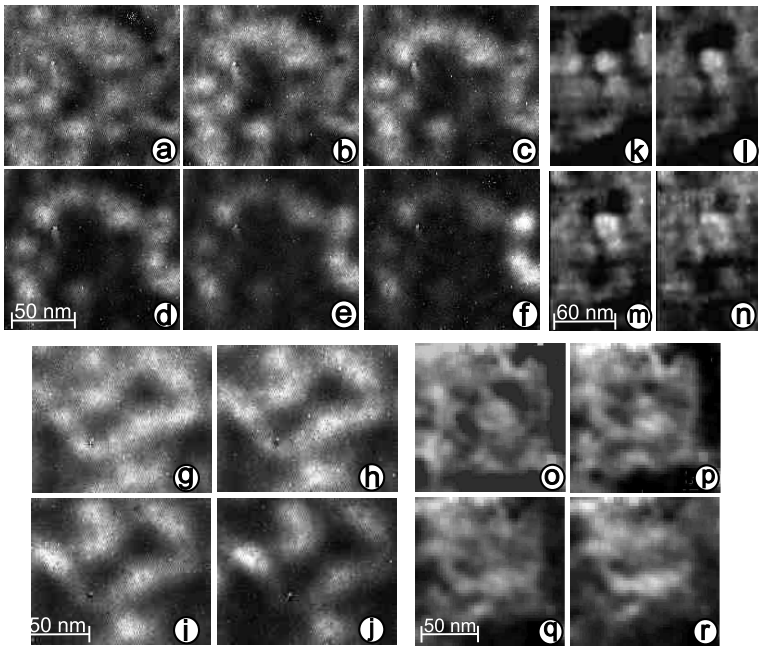

Fig. 1.9: Localized percolating states in the tails of a Landau Level [19], probed by scanning tunneling spectroscopy [18] (see the paper for quantitative details). The percolating states are indicated by bright drifting orbits whose lateral size has been measured to be compatible with the magnetic length. The different series of pictures (a-f), (g-j), (k-n) and (o-r) have been taken in four regions of the sample. Within each series the electron density was tuned via gate modulation, thereby shifting the chemical potential slightly. Clearly, it is possible to observe the effective size of the structures getting larger while moving closer in energy to the LL center (series a-j), or shrinking while moving away from it (k-r).

the number of particles we will first occupy percolating states along the dips of the potential V, effectively looking like the shores of lakes formed in the minima of the inhomogeneous landscape. These states will clearly be localized and will not contribute to the transport structures. Thus, if we vary the density and still occupy these states we will describe the plateaux of the QHE experiments.
By increasing the density further (thus rising the chemical potential) the percolating states will grow in effective size until they will meander around the whole sample. This will occur roughly around the energy corresponding to the middle between the maximum and minimum of V. These are the extended states within the percolation model and pinning the chemical potential to them would induce variations in the conductivity, thereby describing the transition region between different plateaux.
A further increase of the chemical potential will be associated to localized states

percolating along the top of the mountains (see Fig (1.10)), describing the next conductivity plateau.
This semiclassical model offers a clear pictorial description of the density induced

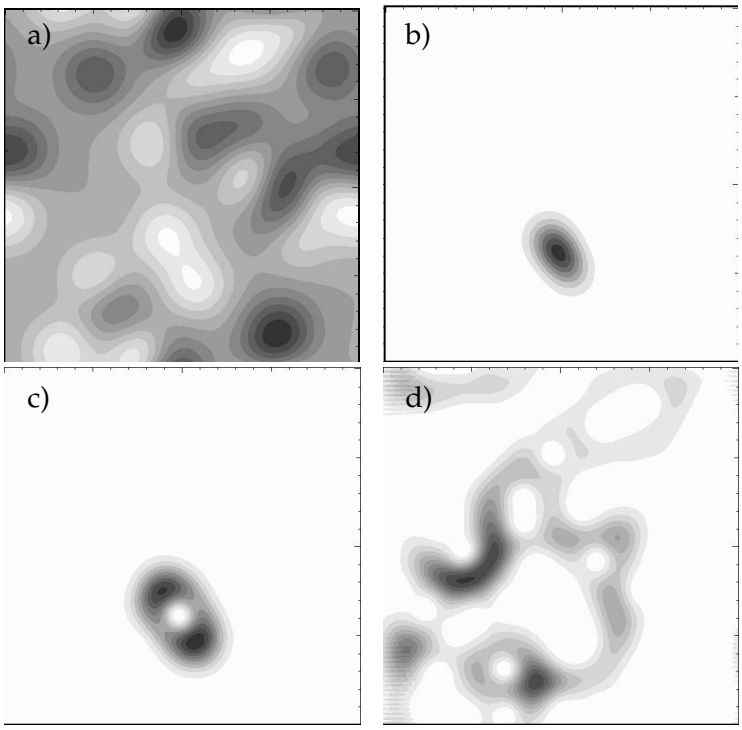

Fig. 1.10: Percolating states in the disordered first Landau Level [20]. In a) the landscape potential is depicted, the bright regions corresponding to minima and the dark regions to maxima of the disorder modulation. In b) a localized state in the tails of the LL is shown to live in the valley minimum (darker gray means larger wavefunction amplitude) while c) describes a state with a very small energy deviation from b). The overall support of the two states is similar but the state c) already feels the "double-well" shape of the local potential (see a)). Finally, d) describes an extended wavefunction close to the LL center.

localization-delocalization transition and its beauty relies on the high field quenching of the single particle kinetic hamiltonian.
Within the classical percolation theory the localization length of the equipotential lines (the effective diameter of the percolating path) for energies close to the center of the levels has been found to diverge as

$$\xi_{\rm cl}(E) \sim |E - E_n|^{-4/3} \tag{1.41}$$

where E_n is the energy of the n-th LL [21].
Quantum mechanically, whenever a classical percolating path of finite width ℓ is close to another, the inclusion of tunneling between the two states enhances the localization length. Indeed, the quantum mechanical localization length has been numerically shown [22] to diverge as

$$\xi_{\rm qm}(E) \sim |E - E_n|^{-\gamma} \tag{1.42}$$

with $\gamma \simeq 2.34$. It is currently believed that this exponent is universal and independent on the LL index n.

The percolation model offers a nice pictorial view of the QHE and of the existence of a 2D localization-delocalization transition. Whenever the localization length $\xi(E)$ exceeds the linear sample size L we expect a peak in σ_{xx} which vanishes as soon as the Fermi energy is pinned to states with $\xi(E) < L$. The energies at which the condition $\xi(E_{\rm M}) = L$ is fulfilled are called "mobility edges" and determine the width of the conductivity peaks.
With this picture we can address also the scaling of the σ_{xx} peak width with respect to a characteristic external energy source (like temperature, or frequency). Indeed, the new energy scale $E_{\rm ext}$ can excite localized states outside the mobility edge into the region of the extended states, if they fulfill $|E - E_{\rm M}| \leq E_{\rm ext}$. This means effectively shifting the mobility edge, with the result that the conductance peak broadens. A detailed analysis of the scaling of the QHE peaks with respect to external parameters can be found in [23].
The *qualitative* behaviour of the IQHE is not altered by a finite temperature T as long as $K_{\rm B}T$ is smaller than the smallest energy gap (in our case the cyclotron gap). Larger temperatures would shrink the plateaux and merge the different magnetoresistance peaks, thereby washing the effect away.

1.3.4 Gauge arguments: extended states and exactness of the quantization

One of the extraordinary features of the IQHE is the exactness of the quantization of σ_{xy} as an integer multiple of the conductance quantum e^2/h. Soon after the discovery of the effect, Laughlin realized that this feature had to do with something really deep and fundamental [24]. He proposed an argument to explain the quantization as a consequence of gauge invariance. One year later an extension of the gauge argument was proposed by Halperin [25] to include disorder effects: as a byproduct, this argument also showed the necessary existence of extended states within the LLs. In the remaining part of this section we will briefly present this last argument.

The QHE is essentially a bulk phenomenon, in the sense that it is not significantly influenced by the shape or size of the sample. Thus we can freely choose the geometry of our gedanken-experiment.
Let us consider a Corbino-disk 2D gas (the 2DEG is simply shaped as a disk with a hole in the center) placed in the $x - y$ plane, with the external uniform magnetic field B along the z direction. In addition let us imagine to have an infinitely thin solenoid inside the hole, through which we can adiabatically induce a variable magnetic flux (see Fig (1.11)). The 2DEG does not feel the corresponding additional

magnetic field but only the associated vector potential. In particular, only the states extending throughout the whole disk and encircling the hole (i.e. the extended states, if they exist) can be affected by the Aharonov-Bohm phase connected to the varying flux. The localized states not encircling the hole cannot be affected by the gauge flux variation and, in particular, their occupation cannot change during the adiabatic flux insertion. By "adiabatic" we mean slowly with respect to the inverse of the minimum bulk energy gap.

Let us imagine that the sample is made out of three concentric regions, bounded by radii $r_1 < r_1' < r_2' < r_2$ and that the disordered region is confined to the internal disk between r_1' and r_2' while the external "guard rings" are free from impurities. Let us also assume that the variance of the disorder potential is much smaller than the cyclotron energy.
We then have a DOS which is made of δ-like LL in the external rings and by broader Landau bands in the disordered central region, the broadening still being smaller than the LL spacing (see Fig (1.11)).

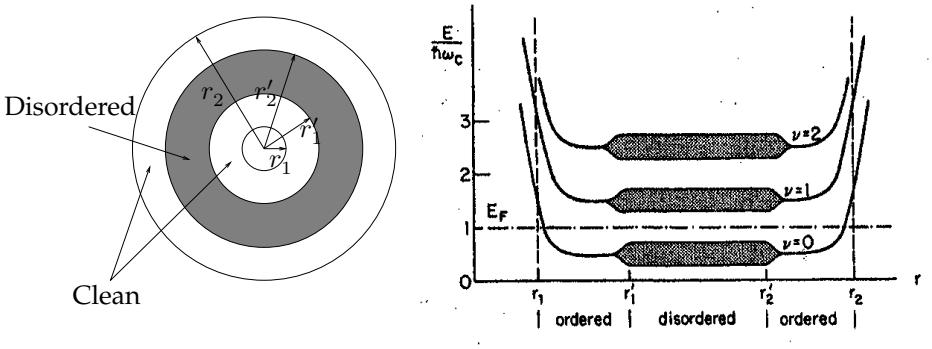

Fig. 1.11: The Corbino-like geometry for the gedanken-experiment of the gauge argument (left) and the corresponding schematic DOS (right) [25]. Disorder is active only between radii r_1' and r_2' inducing a broadening, still smaller than the LL separation. The delta-like LL in the clean areas are bent upwards close to r_1 and r_2 due to the confining potential. The Fermi energy lies in the gapped region, and an integer number of "clean" LL is occupied.

We can have two different possibilities:

- Either the states in the disordered region are localized at all energies with a maximum localization length much smaller that the sample size (supposed arbitrarily large)
- Or some extended states have to exist within the disordered region as well.

We will assume the first hypothesis and show that it leads to a contradiction.
Let us start fixing the Fermi energy in the gap between two LL of the perfect re-

gions, thus having a fixed number i of occupied LL. We know that, in the perfect regions, the conductance will be ie^2/h.
Let us now turn the adiabatic flux on. The flux variation will generate an azimuthal electric field satisfying

$$\oint_{\mathcal{C}} \mathrm{d}\mathbf{r} \cdot \mathbf{E} = -\frac{1}{c}\,\partial_t \Phi \tag{1.43}$$

where the close path $\mathcal{C}$ encircles the flux tube in one of the perfect regions. Since $\sigma_{xx} = \sigma_{yy} = \rho_{xx} = \rho_{yy} = 0$ the electric field produces a purely radial current density, pushing charge away from the solenoid

$$\mathbf{E} = \rho_{xy}\,\mathbf{j} \times \hat{\mathbf{z}} \tag{1.44}$$

so that

$$\rho_{xy} \oint_{\mathcal{C}} \mathbf{J} \cdot (\hat{\mathbf{z}} \times \mathrm{d}\mathbf{r}) = -\frac{1}{c}\,\partial_t \Phi. \tag{1.45}$$

The integral on the left hand side represents the total current flowing into the region enclosed by the contour. Thus the charge transferred through this region obeys

$$\rho_{xy}\,\frac{\mathrm{d}Q}{\mathrm{d}t} = -\frac{1}{c}\,\frac{\mathrm{d}\Phi}{\mathrm{d}t}. \tag{1.46}$$

After one quantum of flux has been added the final transferred charge is

$$Q = \frac{1}{c}\,\sigma_{xy}\Phi_0 = \frac{h}{e}\,\sigma_{xy} = ie. \tag{1.47}$$

Once the adiabatic insertion of one flux quantum has been completed, all the states have their original wavefunctions and energies since the Aharonov-Bohm phase due to such a process is an integer multiple of 2π, and the added flux can be removed away via a gauge transformation.
Now, let us say that the charge comes from the external guard ring pointing towards the internal one. If, according to our choice, in the disordered region all the states below the Fermi energy are localized, there is no way for them to transport charge, since they are not affected by the adiabatic flux insertion and their population cannot change. Therefore we deduce that there must be some delocalized states within the impurity region below the Fermi energy.
Having shown the existence of extended states within the disordered band, we understand that they are responsible for the adiabatic charge transfer. Thus, the gauge argument shows that the conductivity of the whole sample is the same as that of the perfect regions as long as the chemical potential lies in a gap between the LL in the guard rings. The disorder broadening helps us in producing bands of localized states where the Fermi energy can be pinned continuously as the density is varied, still preserving the conductance properties of the pure sample.

We have presented an introduction to the basic issues related to the IQHE. Essentially all the discussed properties can be understood within a model of non-interacting electrons in presence of a disorder potential. The role of the disorder is

to localize electronic wavefunctions in the tails of the Landau bands and to give a reservoir of states where the Fermi energy can be pinned without contribution to the transport dissipation.
Interactions between electrons have been entirely neglected. Recent investigations [26] of the role of interactions in affecting electronic and transport properties in the IQH regime surprisingly found no relevant changes with respect to the independent particle system.
Interactions play a major role in the FQH regime, inducing incompressibility out of a partially filled LL as we will see in the next section. Disorder, in this case, will induce localization of the quasiparticles describing the excitations with respect to the GS (not of electrons), producing the plateaux in analogy with the Integer case. The description of the FQHE GS and of the nature of its quasiparticle excitations will be the subject of the following section.

1.4 The Fractional Quantum Hall Effect: wavefunction picture

In the present section we introduce the wavefunction picture of the Fractional Quantum Hall Effect as formulated by Laughlin [27] soon after the experimental discovery by Tsui and Stormer [6]. The discovery and explanation of the FQHE was awarded the Nobel Prize for Physics in 1998 (given to Laughlin, Stormer and Tsui) as an outstanding manifestation of interaction-induced macroscopic quantum phenomenon.

The most prominent FQHE plateau was observed at $\nu = 1/3$ in high mobility GaAs heterostructures. As already discussed in the previous section it is crucial, for the QHE to be realized, to have incompressibility at certain values of magnetic field-dependent densities.
For the Integer case the incompressibility was present at the single particle level, and was induced by the LL quantization. If we stop at that level and consider $\nu = 1/3$, we do not find any reason for incompressibility to appear. The lowest LL is partly filled and there are plenty of states to be occupied before jumping to the next LL.
It was soon realized that incompressibility had to come out of interactions between electrons. When $1/3$ filling is reached interactions produce a Ground State (GS) which is separated from all the possible excitations by an energy gap.
A perturbation approach is out of question due to the enormous degeneracy of the problem. In fact the filling $1/3$ is obtained by having N particles and $N_\Phi = 3N$ states in the lowest LL. There are $(3N)!/(2N)!N!$ different ways of redistributing the particles in the degenerate states, all of them giving rise to degenerate many particle states before the introduction of the interactions. The $e-e$ repulsion has to be considered in this hugely degenerate subspace, and this is the reason why perturbation theory cannot be of help in tackling the problem, except for very small systems.
The breakthrough in understanding the incompressibility came with the proposal by Laughlin of a many body state candidate to represent the GS. This state was shown to have energy gaps for the introduction of quasiparticle and quasihole ex-

citations. The quasiparticles of the Laughlin state were shown to have exotic properties, like fractional charge and statistics. Few years ago the direct experimental observation of fractional charges in noise experiments in the FQHE finally confirmed the Laughlin picture [28, 29].

In the original experiments by Stormer the $\nu = 1/3$ FQHE was observed in the extreme high magnetic field regime ($\sim 15\,\mathrm{T}$). In this limit the cyclotron energy scale as well as the Zeeman splitting (both proportional to B) are much larger than the typical Coulomb repulsion $e^2/\epsilon\ell \propto \sqrt{B}$ and the disorder induced broadening of the levels Γ_{Dis}. Thus the theory by Laughlin was developed for *fully spin polarized* electrons neglecting the interaction-induced LL mixing, and disorder was considered as the smallest characteristic energy in the problem:

$$\hbar\omega_c, E_Z \gg E_{\mathrm{Coul}} \gg \Gamma_{\mathrm{Dis}}. \tag{1.48}$$

In recent years, due to the improved quality of the samples, it has become possible to observe FQH states at much lower magnetic fields. In these cases the Coulomb scale easily mixes different spin channels, producing interesting spin polarization transitions that will be the subject of the following chapters. For the time being let us describe the fully polarized Laughlin theory within the regime (1.48).

1.4.1 General considerations about many body states in the lowest LL

Let us start by considering the single particle problem in a different, so-called symmetric, gauge

$$\mathbf{A} = \frac{B}{2}(-y, x, 0)\ . \tag{1.49}$$

Contrary to the previously considered Landau gauge preserving translational invariance in one direction, this choice preserves rotational symmetry and the good quantum number is now the angular momentum.
If we concentrate on the lowest LL, where $\nu = 1/3$ shows up, the solutions to the free particle Schrödinger equations with the angular momentum $\hbar m$, m a non-negative integer, are

$$\varphi_m(z) = \frac{1}{\sqrt{2\pi\ell^2 2^m m!}}(\frac{z}{\ell})^m e^{-\frac{1}{4\ell^2}|z|^2} \tag{1.50}$$

where $z = (x + iy)$ is the complex coordinate of a particle in the 2DEG.
All these eigenstates are degenerate and any linear combination of them is also a solution to the Schrödinger equation. In particular, any many-body wavefunction formed completely out of electrons in the lowest LL must be a sum of products of the lowest LL one-body wavefunctions. Therefore any function of the form

$$\Psi(z) = f(z)e^{-\frac{1}{4\ell^2}|z|^2} \tag{1.51}$$

represents electrons restricted to the lowest LL if and only if f is *analytic* in its argument [30]. In particular, arbitrary polynomials of any degree N

$$f(z) = \prod_{j=1}^{N}(z - z_j) \tag{1.52}$$

are allowed, defined by the locations of their N zeros $\{z_j; j = 1, 2, \ldots, N\}$.
In this language we can write arbitrary many-electrons wavefunctions as

$$\Psi(z_1, ..., z_N) = f(z_1, ..., z_N) \prod_{j=1}^{N} e^{-\frac{1}{4\ell^2}|z_j|^2} . \tag{1.53}$$

In order to preserve the fermionic nature of electrons the function f has to be *anti-symmetric* with respect to the interchange of the coordinates of two particles. This condition implies that f has to vanish whenever two electrons approach each-other. If we imagine to fix the positions of all the particles except one, say z_N, which will be used as a test electron, the fermionic constraint implies that $f(z_1, ..., z_{N-1}, z_N)$, viewed as a function of z_N only, has at least one zero at the positions $z_1, ..., z_{N-1}$. If we move adiabatically z_N around a *single* zero, the global phase accumulated by Ψ is 2π, exactly as if we encircled a vortex. Hence the zero's in the many particle wavefunctions are usually called vortices.
Let us now move the test charge adiabatically around an area $\mathcal{A}$. The Aharonov-Bohm phase accumulated by the electron is

$$e^{i\frac{2\pi}{\Phi_0}\oint \mathbf{A}\cdot d\mathbf{l}} = e^{i2\pi\Phi/\Phi_0} \tag{1.54}$$

where $\Phi = \mathcal{A}B$ is the total flux enclosed. However, as mentioned above, the analyticity of the wavefunction also demands that the accumulated phase is given by $\exp(i2\pi N_z)$ where N_z is the number of zeros of the wavefunction enclosed in the loop. Comparing these two results, we find that any lowest Landau level wavefunction must have B/Φ_0 zeros per unit area, i.e. as many as the magnetic flux quanta crossing the unit area.
Recalling the definition of LL degeneracy we find out that there are as many states in a LL as magnetic flux quanta across the sample as zeros in the lowest LL many-particle wavefunction.

These considerations lead us to write down the form of the many-fermions wavefunction describing a completely filled LL, i.e. $\nu = 1$. The GS wavefunction, apart from the ubiquitous gaussian factors, is given by the Slater determinant (Vandermond polynomial)

$$\sum_p \text{sign}(p)\, z_{p(1)}^0 z_{p(2)}^1 ... z_{p(N)}^{N-1} \tag{1.55}$$

where p denotes a permutation of N objects with sign(p). It can be shown that the Vandermond polynomial can be rewritten as

$$\prod_{j<k} (z_j - z_k) \tag{1.56}$$

showing that we have N particles and N vortices, and the fermionic constraint forces us to place exactly one vortex per electron. As a result

$$\Psi_{\nu=1}(z_1, ..., z_N) = \prod_{i<j=1}^{N} \frac{z_i - z_j}{\ell} \prod_{j=1}^{N} e^{-\frac{1}{4\ell^2}|z_j|^2} . \tag{1.57}$$

Within the approximation of neglecting LL mixing (suitable for the large B, or small mass, regime) this is the *exact* GS independently on the $e-e$ interaction at filling $\nu = 1$.

1.4.2 The Laughlin state and its quasiparticle excitations

In his original paper, Laughlin proposed a many body wavefunction for filling factors $\nu = 1/(2m+1)$ (m integer, not to be confused with the angular momentum quantum number) as

$$\boxed{\Psi_{\nu=\frac{1}{2m+1}}(z_1,...,z_N) = \prod_{i<j=1}^{N}\left(\frac{z_i - z_j}{\ell}\right)^{2m+1}\prod_{j=1}^{N} e^{-\frac{1}{4\ell^2}|z_j|^2}} \,. \tag{1.58}$$

Its form is reminiscent of the Vandermond wavefunction (1.57) and reduces to that for $m = 0$. Let us consider the properties of the Laughlin state in more detail.
In analogy to what we did before, we can think to freeze the coordinates of all but one electron which is used as a test particle. Then this state has a $(2m+1)$-fold zero at the position of each particle. This automatically means that it describes a filling fraction $\nu = 1/(2m+1)$ in the lowest LL, and since $2m$ is even, the correct fermionic statistics is fulfilled.
The peculiarity of the Laughlin state is the positioning of the zeros. In fact we already knew that, at $1/(2m+1)$ filling, we had N particles and $(2m+1)N$ zeros, but their position (apart from the obligatory single zero per particle due to the statistics) was otherwise arbitrary. In this state a choice is made to put $2m+1$ zeros *exactly* on top of each electron. This implies that the probability of finding two particles very close to each other is very small, with the effect of lowering drastically the energy contribution due to $e-e$ interactions. All the zeros are used to this purpose, and no one is wasted in the space between the particles.
The Laughlin wavefunction has been shown to be the exact GS for hard core $e-e$ interactions and numerical calculations proved it to have an excellent (99.7 %) overlap with the exact GS even for the Coulomb repulsion [31].
Thermal activation experiments unambiguously showed the incompressibility of the FQHE GS [32] and the gap was observed to scale as the Coulomb interaction, especially in the large B regime, where the spin degree of freedom is frozen by the Zeeman energy and LL mixing can be neglected. This feature can be understood given the quenching of the kinetic energy into the degenerate cyclotron term, leaving us with the only energy scale determined by the interactions.
Incompressibility was theoretically proven by numerical calculations of the creation energy for the charged quasiparticle excitations of the GS. If we imagine to shift the filling factor slightly away from $1/(2m+1)$, e.g. by inserting one flux quantum, the final effect on the many body state is the insertion of an additional zero. This minimal damage will produce a quasi-hole at position Z, whose wavefunction in the Laughlin state is written as [27]

$$\Psi_Z^{(+)}(z_1,...,z_N) = \prod_{j=1}^{N}\left(\frac{z_j - Z}{\ell}\right)\Psi_{\nu=\frac{1}{2m+1}}(z_1,...,z_N) \,. \tag{1.59}$$

The wavefunction for a quasiparticle, appearing when a flux quantum is *removed* from the GS, was introduced by Laughlin as

$$\Psi_Z^{(-)}(z_1,...,z_N) = \prod_{j=1}^{N} \left(\frac{2\partial_{z_j} - Z^*}{\ell} \right) \Psi_{\nu=\frac{1}{2m+1}}(z_1,...,z_N) \ . \tag{1.60}$$

The creation energy of a quasiparticle and a quasihole were evaluated numerically by Chakraborty [33] and by Morf and Halperin [34] to be $\Delta_- = 0.025\ e^2/\epsilon\ell$ and $\Delta_+ = 0.026\ e^2/\epsilon\ell$ respectively, for $\nu = 1/3$, in the case of the Coulomb interaction. It comes out that these excitation energies depend quite significantly on the interaction parameters and range.
The quasiparticle excitations carry fractional charge and statistics, as we will see in the next section. This means that they can be thermally excited only in neutral pairs, resulting in a charge excitation gap $\Delta = \Delta_+ + \Delta_-$, in the limit of neglecting the interaction between the quasiparticles.
We would like to stress that in experiments the excitation gap can be proven in many different ways, e.g. by studying the activation of the transport plateaux with temperature, or by spectroscopic techniques. The outcoming gaps can be quite different with respect to each other and to the theoretical estimates of the intrinsic quasiparticle excitation energies. Activation measurements are typically quite sensitive to the disorder effects in the sample, while spectroscopic analysis seem to give cleaner informations.
From the theoretical point of view, the effects of disorder, LL mixing and finite thickness of the 2DEG affect the quantitative values obtained in the numerical evaluations (see Fig (1.12)). In the end it is crucial to ask what is really observed in experiments in order to attempt a direct comparison with theory.

In order to finally explain the plateaux in the Hall conductivity, in analogy to the integer case, disorder will play the role of localizing the excess charge carriers (in this case the quasiparticles and quasiholes) thus preventing the transport coefficients from changing with the filling. If the density is changed significantly from the value of $1/(2m+1)$ filling, the quasiparticles tend to delocalize and eventually condense again into an incompressible Laughlin-like state. This line of thinking was introduced to explain the additional FQH states observed around the principal one and leads to the hierarchical family of states with filling $p/(2mp \pm 1)$ (p integer). We will not dwell on the hierarchical picture of the FQHE but the principal sequence of observed states will be obtained in a different way in the following chapter.

We will now consider the issue of fractionalization of charges and statistics for the FQHE quasiparticles.

1.4.3 Fractional Charges and Fractional Statistics

In his original work, Laughlin analyzed the properties of his many-body GS using a mapping to a plasma system of fake charges interacting with a 2D Coulomb repul-

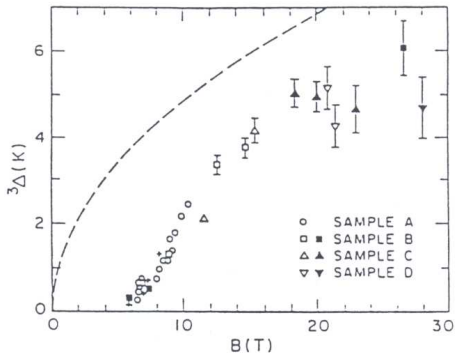

Fig. 1.12: The activation gap for two *constant* fillings of the principal FQH sequence (filled symbols indicate $\nu = 1/3$, open symbols $\nu = 2/3$) as a function of the perpendicular magnetic field [32]. Different samples with different base densities where used in order to span a larger range of magnetic fields, the filling being kept constant via back-gate density modulation. The dashed line represents the curve $C\, e^2/\epsilon\ell$ with $C = 0.03$. This is *half* the value of the lowest theoretical prediction obtained without finite thickness corrections, disorder effects and LL mixing. It is clear that a precise quantitative prediction of the gap can be extremely difficult and the result is often significantly sample-dependent.

sion. One of the outcomes of his analysis was the existence of fractionally charged quasiparticle excitations. We will not present here the plasma analogy and the interested reader can find an exhaustive treatment of this issue in references [31] and many others in literature.
On the contrary we will address the quasiparticle charge at first with an elegant argument (again by Laughlin) and subsequently we will review a unified treatment of both charge and statistics fractionalization considering the Berry phases accumulated by charged objects performing loops in the Laughlin GS. This issue will come useful again in the last chapter, in connection with the non-abelian statistics of vortices in p-wave superconductors.

In order to obtain the fractional charge of the Laughlin quasiparticles we will use three basic ingredients:

- the GS has a finite excitation gap Δ
- in the FQH plateau $\sigma_{xx} = 0$ and $\sigma_{xy} = \nu e^2/h$
- gauge invariance is preserved.

Let us think to pierce the 2D FQH system at filling ν with an infinitely thin solenoid through which a magnetic flux is adiabatically turned on. By adiabatically we mean that the turning on must be slow with respect to the time scale $\hbar/\Delta$. In this way we know via the adiabatic theorem that the GS evolves continuously as an eigenstate

of the changing Hamiltonian. Once a single flux quantum $\Phi_0 = hc/e$ has been inserted we stop.
At this point we notice that a single δ-like flux quantum is invisible to the particles since the Aharonov-Bohm phase factor accumulated by an electron while turning around the flux tube is

$$\exp\left(i\frac{e}{\hbar c}\oint \delta\mathbf{A}\cdot \mathrm{d}\mathbf{r}\right) = e^{\pm 2\pi i} = 1, \tag{1.61}$$

where $\delta\mathbf{A}$ is the additional vector potential due to the solenoid. As a matter of fact the quantized flux can be removed by a singular gauge transformation, the so-called Chern-Simons transformation. We will analyze this issue in detail in the chapter dedicated to the Chern-Simons gauge theory of the FQHE.
To conclude the gauge argument we analyze what has been the effect of the flux insertion. In analogy to what has been shown while discussing the gauge arguments for the exactness of the plateau quantization in section 1.3.4, during the variation of the magnetic flux through the solenoid a net charge is pushed away from the position of the attached flux.
On the quantized Hall plateau at filling factor ν, where $\sigma_{xy} = \nu\, e^2/h$ we have, in analogy with (1.47), the resulting quasihole charge

$$Q = \nu e. \tag{1.62}$$

Reversing the sign of the added flux would reverse the sign of the charge.
This argument highlights the deep connection between plateau quantization, incompressibility and the fractional charge of the excitations.
Once the fractional charge was proposed a lot of debate rose about what was the statistics of the Laughlin quasiparticles.

It is possible to analyze in a unified treatment the fractionalization of charge and statistics by considering the Berry phases accumulated by the quasiparticles performing closed loops [35]. A clean and short introduction to Berry phases is presented in [36] and in the beautiful original paper by Berry [37].
Let us consider a Hamiltonian H_Z dependent on a parameter Z (in the following it will be the position of the quasiparticle) and let $\psi(t)$ be an eigenstate of the time dependent Schrödinger equation separated by a finite gap from all the other states. Let us now move $Z = Z(t)$ in a closed loop in a time T so long that the corresponding characteristic energy $\hbar/T \ll \Delta_{\text{min}}$, where Δ_{min} is the minimum value of the gap encountered along the closed path. In this way the state will evolve adiabatically as an eigenstate of the instantaneous Hamiltonian $H_{Z(t)}$ with energy $E(t)$, and admixture with other levels can be neglected.
While $Z(t)$ slowly transverses a loop, in addition to the dynamical phase $\int^t E(t')dt'$, $\psi(t)$ will acquire an additional phase γ which is independent on the speed with which the loop was transversed and just depends on the geometry of the loop itself. This additional phase, the Berry phase, satisfies the equation

$$\frac{\mathrm{d}\gamma}{\mathrm{d}t} = i\langle\psi(t)|\frac{\mathrm{d}\psi(t)}{\mathrm{d}t}\rangle\ . \tag{1.63}$$

Let us apply the Berry phase calculation for the case in which $Z(t)$ is the position of a Laughlin quasi-hole being slowly transported along a closed loop. Let us say that we perform a circular loop of radius R much larger than the typical quasihole size, of the order ℓ.
Having the Laughlin quasihole wavefunction, given by (1.59), we deduce

$$\frac{\mathrm{d}\Psi^{(+)}_{Z(t)}}{\mathrm{d}t} = \sum_{j=1}^{N} \frac{\mathrm{d}}{\mathrm{d}t} \ln\left(\frac{z_j - Z(t)}{\ell}\right) \Psi^{(+)}_{Z(t)} \,. \tag{1.64}$$

We can then write the Berry phase equation as

$$\frac{\mathrm{d}\gamma}{\mathrm{d}t} = i\langle\Psi^{(+)}_{Z(t)}| \frac{\mathrm{d}}{\mathrm{d}t} \sum_{j=1}^{N} \ln\left(\frac{z_j - Z(t)}{\ell}\right) |\Psi^{(+)}_{Z(t)}\rangle \,. \tag{1.65}$$

Now, using the expression for the one-particle density of the quasihole

$$\rho^{(+)}_{Z(t)}(z) = \langle\Psi^{(+)}_{Z(t)}| \sum_{j=1}^{N} \delta\left(z_j - z\right) |\Psi^{(+)}_{Z(t)}\rangle \tag{1.66}$$

we can write (1.65) as

$$\frac{\mathrm{d}\gamma}{\mathrm{d}t} = i \int \mathrm{d}z\, \rho^{(+)}_{Z(t)}(z) \frac{\mathrm{d}}{\mathrm{d}t} \ln\left(\frac{z - Z(t)}{\ell}\right) \,. \tag{1.67}$$

We can expand the density $\rho^{(+)}_{Z(t)}(z)$ around its uniform value $\rho = \nu B/\Phi_0$ and neglect the small correction due to the vicinity of the quasihole position. The density correction due to the finite quasihole size scales as $(\ell/R)^2$ and can therefore be neglected if $R \gg \ell$.
After dragging the quasihole around the complete clockwise loop, all the vectors $z - Z(t)$ with z *inside* the circle underwent a phase change of 2π while all those with z *outside* the circle have their phases unchanged. Therefore only the points z inside the circle contribute to the integral in (1.67), bringing

$$\gamma = -i \int_{|z|<R} dz\; \rho\; 2\pi i = 2\pi N_R = 2\pi\nu \frac{\Phi}{\Phi_0} \tag{1.68}$$

where N_R is the mean number of electrons in the circle with radius R.
Finally we can compare the obtained result with the phase that a generic particle of charge Q picks up while performing a loop in presence of the external magnetic field. This is simply given by

$$\frac{Q}{\hbar c} \oint \mathrm{d}\mathbf{r} \cdot \mathbf{A} = 2\pi \frac{Q\Phi}{e\Phi_0}. \tag{1.69}$$

By comparison with (1.68) we deduce that the Laughlin quasihole charge is $Q = \nu e$, as stated previously. Analogous arguments lead to the Laughlin quasiparticle

charge of $-\nu e$.
The Berry phase calculation can also account for the quasiparticle statistics. Indeed let us compare the previous results with the phase we get by dragging the quasihole around the same loop but with another quasihole inside. This latter phase will be obtained from the former by replacing N_R with $N_R - \nu$. The difference between the two Berry phases is then

$$\Delta\gamma = 2\pi\nu. \tag{1.70}$$

Finally we notice that encircling a quasihole with another corresponds to interchanging them twice, up to a translation, so that their true statistics factor is $\Delta\gamma/2 = \pi\nu$.
In particular we can recover the correct fermionic statistics for electrons at $\nu = 1$, when the two-electron interchange gives the phase π, corresponding to the sign change in the many fermion wavefunction.
The Laughlin quasiparticles at $\nu = 1/3$ have a statistical factor $\pi/3$ for their interchange. Their statistics is therefore neither fermionic nor bosonic, but somewhat "in the middle": such objects have been called *anyons*. Still, by interchanging two anyons, we get a phase belonging to the $U(1)$ group. These sort of statistical factors are assigned to the so-called *abelian* (or commutative) statistics, since the product of many $U(1)$ phases is a commutative operation and it does not matter the order of the particle interchanges we perform.
In the last chapter we will face the exotic case of *non-abelian* statistics for the quasiparticle excitations of a particular many-body GS showing up at $\nu = 5/2$ filling, the so-called *Pfaffian* state.

Up to this point the presence of the electronic spin has never been considered in neither the many body GS nor in its excitations. This is due to the fact that, at the origin of the FQHE, the magnetic fields needed to observe fractional structures were so large that the Zeeman energy scale was frozen out of the observable range of parameters.
We will see in the next chapters that a lot of interesting effects related to the spin degree of freedom have been recently observed in experiments. They will be presented in the framework of the Chern-Simons field theoretical treatment of the FQHE. For the time being we will still confine to the wavefunction picture of the GS and briefly present a class of many-body states originally introduced by Halperin [38] to describe different spin populations within a Laughlin-like treatment.

1.4.4 GS with spin: the Halperin states

If we considered the LLs of 2D electrons in vacuum their cyclotron energy would be

$$\hbar\omega_{\mathrm{c}}^{\mathrm{vac}} = \frac{\hbar eB}{m_0 c} \tag{1.71}$$

with the free electron mass m_0. Analogously, the Zeeman energy would be

$$E_{\mathrm{Z}}^{\mathrm{vac}} = g\mu_{\mathrm{B}}B = g\frac{\hbar e}{2m_0 c}B \tag{1.72}$$

with μ_B the Bohr magneton. In vacuum, the electronic g-factor is 2 so that the cyclotron and Zeeman energy coincide. This would mean that, except from the lowest spin split LL, the other levels would be degenerate in couples, with opposite spin and LL index different by a factor 1.
Experiments however are made on doped semiconducting 2DES where electrons can be characterized by an effective band mass m determined by the complicated crystal structure. The g factor is not the bare one as well, due to the spin orbit scattering experienced by electrons. Both the m and g can finally depend on the electronic density via $e-e$ interactions.
Many of the present QHE experiments are performed in GaAs heterostructures: in these materials the electronic band mass is typically 14 times smaller than the free mass, while the g-factor ranges around -0.44. The result is that the typical ratio between cyclotron and Zeeman energies is as high as 70. By choosing the sample carefully it is indeed possible to tune this ratio to different values.
Due to these considerations, the spin splitting is typically much smaller than expected and LLs with opposite spin can be easily mixed via interaction effects if not by temperature, especially if the magnetic field is not too strong.
In a beautiful paper immediately after the original explanation of the FQHE by Laughlin, Halperin considered the possibility of having many-body GS with some reversed spin population [38]. In the case when half of the spins are parallel to the external field and half are antiparallel, he wrote a Laughlin-like GS of the form

$$\begin{aligned}\Psi &= \prod_{i<j=1}^{N_\uparrow}\left(\frac{z_i-z_j}{\ell}\right)^m \prod_{\alpha<\beta=1}^{N_\downarrow}\left(\frac{z_\alpha-z_\beta}{\ell}\right)^m \prod_{i,\alpha=1}^{N_\uparrow=N_\downarrow}\left(\frac{z_i-z_\alpha}{\ell}\right)^n \times \\ &\times \prod_{j=1}^{N_\uparrow} e^{-\frac{1}{4\ell^2}|z_j|^2} \prod_{\alpha=1}^{N_\downarrow} e^{-\frac{1}{4\ell^2}|z_\alpha|^2}. \qquad (1.73)\end{aligned}$$

Here roman indices are associated to spin up particles while greek indices relate to spin down electrons.
As in the Laughlin state the particles are kept apart by the relative zeros in the polynomial factors. Moreover the electrons are in the lowest LL, thus minimizing the kinetic energy, while the factor m has to be chosen as an odd integer to preserve the fermionic antisymmetry by interchanging two electrons with the same spin.
The Halperin state describes an unpolarized configuration, and it has been shown to be associated to the filling factor $\nu = 2/(m+n)$. In particular, with $m=3$ and $n=2$ we get $\nu = 2/5$. It is interesting to have a candidate unpolarized GS at $\nu = 2/5$ since experimental evidence of a spin polarization transition at this filling was observed. In later chapters we will dwell on systematic observations of the degree of spin polarization of the FQHE GS for several filling fractions.
After Halperin, a systematic study of many-body wavefunctions with spin reversed populations have been attempted, especially within finite size numerical calculations. The interested reader is referred to the review books [31, 39, 40] and references therein.

After giving this brief introduction to the standard interpretation of the QHE,

we will now concentrate on the Fractional case, by looking the problem from a quite different perspective. The next aim will be to describe a field theoretical picture of the effect.
It will be shown how new quasiparticles, called *Composite Fermions* (CF), can be introduced and a systematic perturbative treatment of the collective phenomenon will be presented. However, as we will see, the starting point for the introduction of the CF is still the many-body Laughlin wavefunction.

While concluding this introduction we would like to mention that many other issues connected with both the Integer and the Fractional regimes have been omitted. Among them we mention the presence of the edge states due to the finite size of the sample, the collective excitations out of the FQH GS, the Temperature and Frequency scaling of the conductivity, the mechanisms for the breakdown of the QHE and many others. After more than 20 years of investigations of the QHE the amount of studied features is quite impressive and an attempt to present them would be out of the purpose of the present work: but still there is a vast amount of unanswered questions awaiting further investigations, on technical as well as on fundamental levels.
Nonetheless we believe that the main ingredients for the understanding of the effect have been presented, especially in view of the topics still to be covered in the next chapters.

2. COMPOSITE FERMIONS AND THE CHERN-SIMONS THEORY OF THE FQHE

In this chapter we will present a different picture of the FQHE based on the introduction of a new quasiparticle called "Composite Fermion" (CF).
The CF is an electron with an even number of flux quanta bound to it. As we saw in the Laughlin picture of the FQHE it is energetically very convenient to bind vortices (or "zeros of the wavefunction", or "flux quanta", for the equivalence we proved) to the electrons. The correlation holes implied by the flux attachment is the mechanism that prevents electrons to come close to each other and keeps the GS energy low.
Composite Fermions were first introduced starting from the wavefunction picture of the FQHE but later a field theoretical treatment was set down to describe the new quasiparticles, based on previously developed Chern-Simons theories.
We will then start from the Laughlin state and observe the first direct consequencies of the flux attachment at the mean field level. To develop further levels of approximation we will then resort to the Chern-Simons field theories and deduce the CF propagators, effective interactions and so on. The final part of the chapter will be focused on some of the physical properties of the new quasiparticle as deduced from a Fermi-Liquid like picture of the CF system.

Clearly, having identified a quasiparticle that grasps the essential physics of the collective FQHE is a significant improvement. Many experimental features will be then addressed in a straightforward way in terms of quasi-free CFs.
As far as this chapter is concerned we will consider spinless CFs. From the next chapter on we will investigate further properties of the quasiparticles, introducing their spin and addressing the role of their residual interactions in modifying their single particle properties as well as inducing instabilities that will produce a restructuration of the GS.

2.1 The wavefunction picture of Composite Fermions

The most important feature of the Laughlin wavefunction we described in the last chapter was the binding of zeros to the position of the electrons. This prevented particles from coming close thereby paying a large Coulomb energy contribution. We also noticed the equivalence between zeros, or vortices, and flux quanta, highlighted also by the gauge argument about the Laughlin quasiholes. Finally, the Vandermonde polynomial entering the Laughlin state,

$$\prod_{i<j} (z_i - z_j)^{2m+1} \qquad (m \in \mathbb{N}) \,, \tag{2.1}$$

described fermionic statistical phases while two of the electrons are interchanged, due to the odd exponent. In particular, $m = 0$ describes the GS at filling factor $\nu = 1$ and $m = 1$ the FQH state at $\nu = 1/3$.
The Laughlin states describe GS at fillings $\nu = 1/(2m + 1)$. Indeed, for $m = 1, 2, 3$ the related FQHE has been observed, while the higher values of m correspond to very low electron densities. In these cases a Wigner crystal is more favourable to form compared to the liquid nature of the FQHE GS.
One aspect which is not directly grasped by the Laughlin picture is the full sequence of observed FQH states. As already mentioned, incompressible fractions have been observed for $\nu = p/(2mp \pm 1)$, $(p, m \in \mathbb{N})$ in the lowest LL. The Laughlin states describe the case $p = 1$.
In order to get the other fractions a hierarchical picture had been proposed [41]. According to it, the quasiparticle and quasihole excitations, induced by varying the magnetic field with respect to where the Laughlin state forms, condense on their turn in further Laughlin states giving rise to incompressibility. The outcoming FQH states have been shown to be centered around the correct sequence for $p > 1$.

Let us perform the apparently trivial step to write the Vandermonde polynomial as

$$\prod_{i<j} (z_i - z_j)^{2m} \prod_{i<j} (z_i - z_j) \qquad (m \in \mathbb{N}) \,. \tag{2.2}$$

The first polynomial has an *even* exponent and the corresponding statistical factor for electron interchange is always 1. Thus, the statistical properties of fermions are not altered by this first term and just lie in the second polynomial factor. By inspection we directly see that this second term is the Vandermonde polynomial for the IQHE at filling factor 1 (i.e. it is associated to the Laughlin state for $m = 0$), see (1.57).
The global polynomial (2.1) is then factorized in a first term which preserves the statistics and a second one describing an IQHE GS. The first statistical factor has the further crucial function of binding an even number of zeros to the electrons, implementing part of the correlation hole attachment.
It thus looks like the FQH state described by the Laughlin wavefunction can be interpreted as IQH (at filling 1) of *fermions* made up from electrons bound to an even number ($2m$) of flux quanta. These objects will be called "Composite Fermions" (CF) and were introduced for the first time by Jainendra Jain in 1989 [42].

At this level we then identify the FQHE for electrons at $\nu = 1/(2m+1)$ as the IQHE for CF at filling $\nu_{\rm CF} \equiv p = 1$.
Composite Fermions clearly feel a reduced number of flux quanta. Indeed, let us say we have N electrons in the system and N_Φ flux quanta, leading to a filling factor $\nu = N/N_\Phi$. After the flux attachment $2mN$ flux quanta have been used to produce CFs and $N_\Phi - 2mN$ are still remaining. Thus the CF filling factor is

$$\nu_{\rm CF} \equiv p = \frac{N}{N_\Phi - 2mN} = \frac{1}{\frac{1}{\nu} - 2m} \ , \tag{2.3}$$

with the inverse relation

$$\nu = \frac{p}{2mp+1} \ . \tag{2.4}$$

A negative CF filling factor could be conceived in the case when the residual number of flux quanta is negative (for $N_\Phi < 2mN$). If we replace $p \to -p$ in (2.4) we get also

$$\nu = \frac{p}{2mp-1} \ . \tag{2.5}$$

Formulas (2.4,2.5) describe exactly the principal sequence of observed FQH states for electrons *if* the CF filling factor p is an integer.
This is quite a remarkable result. By defining a new quasiparticle out of the physical intuition borrowed from the Laughlin state we obtain *the whole* principal sequence of FQH fractions as IQH states of CF. Therefore we can use the knowledge of the integer effect (essentially a single particle phenomenon) to describe properties of the collective FQHE.
One problematic aspect already at this level is that, by writing the fermionic wavefunction at integer CF filling p (for $p \geq 2$) together with the flux-attachment polynomial, the outcoming electronic wavefunction is no longer confined to the lowest LL. This is obviously due to the fact that the CFs fill more that one CFLL. In a wavefunction theory it will then be necessary to project the total electronic state in the lowest LL at the end of the calculations. This issue is crucial for many numerical evaluations on small size systems, although it frequently happens that already the unprojected wavefunction has a good overlap with the exact solution.

Up to now we obtained the correct mapping of the fractional to integer states but know little about the properties of the new quasiparticles. In order to procede in this direction we will consider a more formal approach to the problem which will lead, finally, to the field theoretical Chern-Simons picture of the FQHE.

2.2 The Chern-Simons transformation

In the previous section we considered the introduction of CF from the knowledge of the physical properties of the Laughlin states. Now we know that building up CFs out of electrons can lead to the interesting mapping of fractional and integer effects.
Indeed, one of the features that were soon observed in the early transport experiments in the FQH regime was the striking similarity with the integer effect (see

Fig 1.5). Apart from the fractional values of the plateaux in the Hall resistance the two effects looked essentially identical. It was surprising that the theoretical understandings of them were so different. The introduction of CF allows to understand the two phenomena in an essentially unified way as well as to directly investigate many more states than the ones described by the Laughlin sequence.

In what said up to now the zeros that we bind to the electrons to produce CFs are already present in the GS wavefunction. However flux attachment can also be performed acting on the many-body state using the so-called Chern-Simons transformation. A nice discussion about the difference in the two approaches can be found in [43] and in the review books [39, 44].

Let us consider a many-body wavefunction for N spinless (or fully spin polarized) electrons, $\Psi_e(\mathbf{r}_1, ..., \mathbf{r}_N)$, solution of the Schrödinger's equation

$$H_e \Psi_e = E \Psi_e \ . \tag{2.6}$$

Here the electronic Hamiltonian is

$$H_e = \sum_j \frac{1}{2m} \left(\mathbf{p}_j + \frac{e}{c} \mathbf{A}(\mathbf{r}_j) \right)^2 + \sum_{i<j} V(\mathbf{r}_i - \mathbf{r}_j) \tag{2.7}$$

where m is the electronic band mass, e is the modulus of the electronic charge, $\mathbf{A}$ is the vector potential producing the homogeneous external magnetic field $\mathbf{B} = B\,\hat{\mathbf{z}}$ and $V(\mathbf{r}_i - \mathbf{r}_j)$ is the Coulomb interaction.
Let us now act on the function Ψ_e with a *unitary* operation, the Chern-Simons transformation, to produce the new many-body state

$$\boxed{\Phi(\mathbf{r}_1, ..., \mathbf{r}_N) = \left[\prod_{i<j} e^{-i\tilde{\varphi}\theta(\mathbf{r}_i - \mathbf{r}_j)} \right] \Psi_e(\mathbf{r}_1, ..., \mathbf{r}_N)} \tag{2.8}$$

where $\theta(\mathbf{r}_i - \mathbf{r}_j)$ is the angle between the vector $\mathbf{r}_i - \mathbf{r}_j$ and the x axis (arbitrarily chosen), while $\tilde{\varphi}$ is a free parameter, for the time being.
Under permutation of two particles, say $i \leftrightarrow j$, $(i \neq j)$, we have $\theta(\mathbf{r}_j - \mathbf{r}_i) = \theta(\mathbf{r}_i - \mathbf{r}_j) + \pi$, while Ψ_e picks up a minus sign due to the fermionic statistics of electrons. Thus we have

$$\Phi(..., \mathbf{r}_j, ..., \mathbf{r}_i, ...) = -\, e^{-i\tilde{\varphi}\pi}\, \Phi(..., \mathbf{r}_i, ..., \mathbf{r}_j, ...) \ . \tag{2.9}$$

According to the choice of $\tilde{\varphi}$ several possibilities are open. If $\tilde{\varphi}$ is an even integer the new function Φ has a fermionic nature like Ψ_e, if it is an odd integer Φ describes an ensemble of bosons. Finally, if $\tilde{\varphi}$ is chosen to be a non-integer number, Φ describes a many-body state of anyons, particles with fractional abelian statistics (as the Laughlin quasiparticles we saw in the previous chapter).
Therefore we see directly that the Chern-Simons transformation is a statistical transmutation operation on the many electron system. In the following we will concentrate on a transmutation that preserves the particle statistics and choose

$$\tilde{\varphi} = 2m \qquad (m \in \mathbb{N}) \ . \tag{2.10}$$

Apart from the properties connected with the statistics, the Chern-Simons (CS) transformation produces other interesting effects.
Indeed, let us define explicitly the CS transformation as

$$U_{\mathrm{CS}} = \prod_{i<j} e^{-i\tilde{\varphi}\theta(\mathbf{r}_i - \mathbf{r}_j)} \tag{2.11}$$

and consider the following operation

$$U_{\mathrm{CS}}^{-1} \left(\mathbf{p}_i + \frac{e}{c}\mathbf{A}(\mathbf{r}_i) \right) U_{\mathrm{CS}} \ . \tag{2.12}$$

Acting with $\mathbf{p}_i = -i\hbar\nabla_i$ on U_{CS} we obtain the derivatives of the statistical angles and finally we get

$$U_{\mathrm{CS}}^{-1} \left(\mathbf{p}_i + \frac{e}{c}\mathbf{A}(\mathbf{r}_i) \right) U_{\mathrm{CS}} = \mathbf{p}_i + \frac{e}{c}\mathbf{A}(\mathbf{r}_i) - \frac{e}{c}\boldsymbol{\mathcal{A}}(\mathbf{r}_i) \tag{2.13}$$

with the Chern-Simons vector potential

$$\boldsymbol{\mathcal{A}}(\mathbf{r}_i) = \frac{\tilde{\varphi}\Phi_0}{2\pi} \sum_{j\neq i} \nabla_i \theta(\mathbf{r}_i - \mathbf{r}_j) \tag{2.14}$$

where we used the flux quantum definition $\Phi_0 = hc/e$. Thus if we define the modified Hamiltonian

$$H = \sum_j \frac{1}{2m} \left(\mathbf{p}_j + \frac{e}{c}\mathbf{A}(\mathbf{r}_j) - \frac{e}{c}\boldsymbol{\mathcal{A}}(\mathbf{r}_j) \right)^2 + \sum_{i<j} V(\mathbf{r}_i - \mathbf{r}_j) \tag{2.15}$$

we just showed, through (2.13), the equivalence

$$H = U_{\mathrm{CS}}^{-1} \, H_e \, U_{\mathrm{CS}} \ . \tag{2.16}$$

This finally means that, if (2.6) holds, we also have

$$H\Phi = E\Phi \ . \tag{2.17}$$

Thus we formally know the full mapping between the original fermionic problem and the Chern-Simons transformed one.
In order to understand physically the implications of the Chern-Simons vector potential we can evaluate the fictitious "magnetic field" generated by it. Using the density $\rho(\mathbf{y}) = \sum_j \delta(\mathbf{y} - \mathbf{r}_j)$ and the relation $\theta(\mathbf{v}) = \arctan(v_y/v_x)$ (for a generic 2D vector $\mathbf{v}$) we can rewrite (2.14) as

$$\boldsymbol{\mathcal{A}}(\mathbf{x}) = \frac{\tilde{\varphi}\Phi_0}{2\pi} \int d\mathbf{y}\, \rho(\mathbf{y})\, \nabla_{\mathbf{x}} \theta(\mathbf{x} - \mathbf{y}) = \frac{\tilde{\varphi}\Phi_0}{2\pi} \int d\mathbf{y}\, \rho(\mathbf{y})\, \hat{\mathbf{z}} \times \frac{\mathbf{x} - \mathbf{y}}{|\mathbf{x} - \mathbf{y}|^2} \ . \tag{2.18}$$

But this is just the solution to the differential equation

$$\boxed{\nabla \times \boldsymbol{\mathcal{A}}(\mathbf{x}) = \hat{\mathbf{z}}\, \tilde{\varphi}\Phi_0\, \rho(\mathbf{x})} \tag{2.19}$$

in the Coulomb gauge $\nabla \cdot \boldsymbol{\mathcal{A}} = 0$, leading to the Chern-Simons magnetic field

$$\boldsymbol{\mathcal{B}}(\mathbf{x}) = \hat{\mathbf{z}}\, \tilde{\varphi} \Phi_0\, \rho(\mathbf{x}) = \hat{\mathbf{z}}\, \tilde{\varphi} \Phi_0 \sum_j \delta(\mathbf{x} - \mathbf{r}_j)\ . \tag{2.20}$$

Being $\boldsymbol{\mathcal{A}}(\mathbf{x})$ a gradient we could already anticipate its curl to vanish for every $\mathbf{x} \neq \mathbf{r}_i$ but it is the singular nature of the CS vector potential to lead to the interesting consequences.
From (2.20) we see that the physical effect of the CS transformation is to attach an even number of flux quanta to the position of each electron. Thus the transformation (2.8) maps a many-electron state into a many-CF wavefunction.
The Chern-Simons approach therefore implements directly the flux attachment in the electronic wavefunction, independently from the original many-body state Ψ_e. In this picture additional fictitious (since they come out of a gauge transformation (2.8)) flux quanta are added to the ones due to the real external magnetic field. Of course, the CF satisfy the equation (2.17) and feel both real and gauge flux quanta.

In the previous section we considered the vortex binding from the wavefunction of the system and the CF was formed by "capturing" some of the already present flux quanta. Notwithstanding the difference in approach, the new quasiparticles are subject to reduced effective magnetic fields that coincide.
To see this, we consider a mean field approximation, replacing the density operator $\rho(\mathbf{x})$ with its average value $\langle \rho \rangle$, constant in space. This corresponds to imagine the flux attachment to be uniformly spread over the entire system. Replacing the density fluctuations with their constant average implies that the Coulomb part of the Hamiltonian just contributes as an uninteresting constant energy shift and the fermions can be treated as free. The resulting CS magnetic field (2.20) is also constant and opposite to the homogeneous external one (see the relative sign between $\mathbf{A}$ and $\boldsymbol{\mathcal{A}}$ in (2.15)).
The effective magnetic field for CFs at mean field level is

$$\boxed{\mathbf{B}^* = \mathbf{B} - \langle \boldsymbol{\mathcal{B}} \rangle = \hat{\mathbf{z}}\, (B - \tilde{\varphi} \Phi_0 \langle \rho \rangle) = \hat{\mathbf{z}}\, B\, (1 - \tilde{\varphi} \nu)} \tag{2.21}$$

where we used the definition of the electronic filling factor. Since the densities of electrons and of CF are equal, we can define the CF filling factor

$$p = \frac{\langle \rho \rangle \Phi_0}{B^*} = \frac{\nu}{1 - \tilde{\varphi} \nu}\ . \tag{2.22}$$

The inverse relation yields

$$\nu = \frac{p}{\tilde{\varphi} p + 1} \tag{2.23}$$

as we found previously in (2.4). Again, if $\nu > 1/\tilde{\varphi}$ the effective field B^* becomes negative and leads us to the "negative p" sequence

$$\nu = \frac{p}{\tilde{\varphi} p - 1}\ . \tag{2.24}$$

At mean field level, the quasiparticles are then free fermions in a uniform effective magnetic field. They form LLs with an effective cyclotron gap $\hbar \omega_{\mathrm{CF}} = \hbar e B^* / mc$

and the corresponding incompressibility results in the IQHE at integer CF filling. As indicated by (2.23) this CF IQHE is the equivalent of the electronic FQHE.

The mean field approximation grasps the incompressibility but the predicted energy gaps are not correct. In fact, since we still speak about electronic states with fractional filling smaller than 1 (well inside the first LL) we know that the only relevant energy scale is the Coulomb repulsion. But the CF cyclotron gap is not affected (at mean field) by the interaction part, which has been completely neglected being just a constant.
In order to get the correct energy scaling, Halperin, Lee and Read (HLR) [45] proposed the introduction of an interaction dependent CF effective mass m^*. Up to now this is just a phenomenological argument. We will see later how to obtain the proper scaling by considering the CF interactions beyond mean-field. For a fixed filling factor in the principal FQH sequence we write

$$\hbar\omega_{\mathrm{CF}} = \frac{\hbar eB(1-\nu\tilde{\varphi})}{m^*c} = \frac{\hbar eB}{(\tilde{\varphi}p \pm 1)m^*c} \propto \frac{e^2}{\epsilon\ell} \,. \tag{2.25}$$

Considering the magnetic field scaling $e^2/\epsilon\ell \propto \sqrt{B}$ we can formally write the effective CF mass *at fixed filling*

$$m^*(B) = m_0\alpha\sqrt{B\,[\mathrm{T}]} \,. \tag{2.26}$$

Here α is a fit parameter, whose value and meaning will be discussed in detail in the next chapter.

One could ask what would happen considering fractional fillings of CF. That is, if a FQHE for CFs took place due to their residual interactions neglected so far, what should we expect for the electronic fractions?
Curiously enough, in the first CFLL, the answer is "nothing new".
Indeed, let us imagine to consider a CF filling factor of the principal sequence form $p = p'/(2m'p'+\sigma')$, with $p', m' \in \mathbb{N}$ and $\sigma' = \pm 1$ and let us insert it into the principal electronic sequence $\nu = p/(2mp+\sigma)$. The filling factors we would get are

$$\nu = \frac{p'}{2(m+\sigma m')p' + \sigma\sigma'} \tag{2.27}$$

which clearly belong to the principal sequence again.
Something new happens if we considered a CF FQH state in the second LL, e.g. $p = 4/3 = 1 + 1/3$. This state would generate an electronic filling $\nu = 4/11$ which cannot be obtained from the principal sequence.
All of this would be just a speculation if we did not have any evidence for the formation of similar states. Very recently, however, the FQHE at $\nu = 4/11$ has been clearly observed by Pan et al. [46], see Fig (2.1). In tilted field configurations the state has been shown to be essentially unaffected, suggesting its full spin polarization. This measurement is the first direct evidence of the possible formation of FQH states for CFs and indicates the importance of the residual quasiparticle interactions.

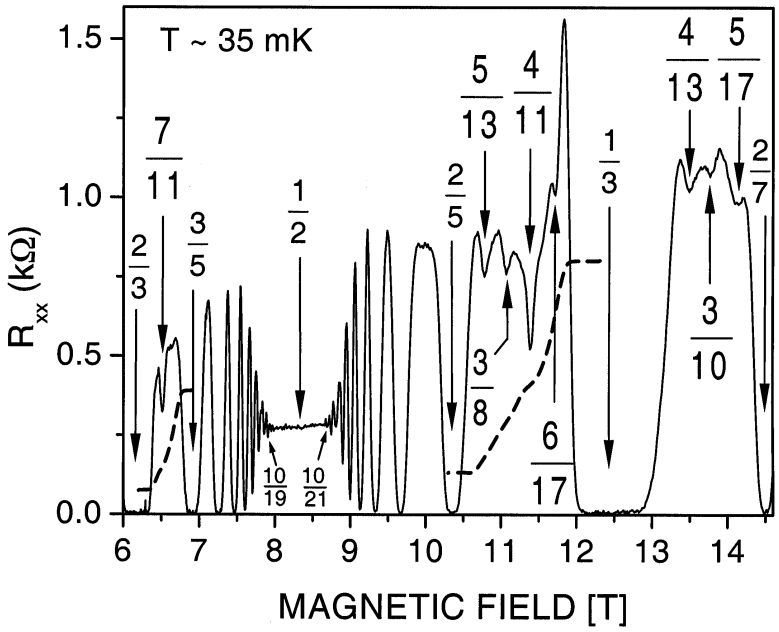

Fig. 2.1: The magnetoresistance in the interval $\nu = 2/3 - 2/7$ at T=35 mK [46]. The arrows indicate the main observed FQH states. Notice the formation of minima at $\nu = 4/11$ and $\nu = 7/11$, not belonging to the principal sequence. The dashed lines sketch the simultaneous behaviour of the Hall resistance, showing the initial formation of a plateau at $4/11$.

Having determined the mean field B^* (2.21), if we imagine to sweep the electronic filling factor ν (for instance by varying the external B *at constant density*) we see that, at $\nu = 1/\tilde{\varphi}$, B^* vanishes. Since the fermionic statistics forces to have $\tilde{\varphi} = 2m$, an even number, we see that the even denominator states $\nu = 1/2m$ are expected, at mean field, to be described as many-body CF systems in a vanishing effective field. In such a case the expected behaviour would be to have a Fermi Gas with a well developed Fermi surface and a parabolic quasiparticle dispersion. This state should be compressible and should not show any sign of FQHE. Indeed, up to now, experimentally, the even denominator states do not show FQHE, except for the two isolated cases of $\nu = 5/2$ and $\nu = 7/2$ (see Fig (2.2)). We will return on them later in Chapter 6.

The residual CF interactions neglected at mean field should modify the single-particle fermionic properties leading to Fermi Liquid like corrections, as we will investigate in more detail later.

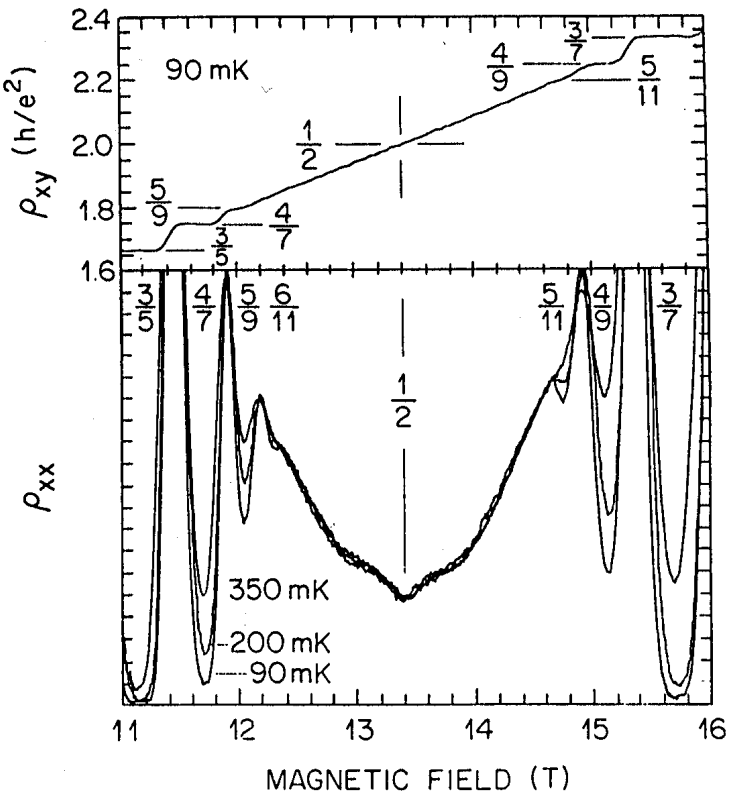

Fig. 2.2: Magnetotransport measurement close to $\nu = 1/2$ [47]. No sign of FQHE shows up, even in the extremely small temperature regime. The $1/2$ state is quite insensitive to temperature variations, while the incompressible states shown in the graph are destroyed by a very small temperature increase.

Having an average CF density ρ, we can extract their Fermi wavenumber

$$k_{\rm F} = \sqrt{4\pi\rho} = \frac{1}{\sqrt{m}\,\ell}\,. \tag{2.28}$$

If we are close to, but not at, the magnetic field where the $\nu = 1/2m$ forms, the cancellation is not exact and a small effective field B^* is still present. The CF are then expected to move in long cyclotron orbits with radius

$$R_{\rm C} = \frac{\Phi_0 k_{\rm F}}{2\pi\, B^*}\,, \tag{2.29}$$

independent on their mass. These orbits have been observed in experiments close to $\nu = 1/2$, with periodic density modulation on the 2D systems [48]. Whenever the cyclotron radius is commensurate with the period of the modulation, peaks in the

longitudinal conductivity are observed that vanish until the next commensurability is matched. Thus R_{xx} shows oscillations (named Weiss oscillations) as a function of B close to the even denominator states, see Fig (2.3). The direct observation of Weiss oscillations gave strong support to the picture of the CF Fermi liquid forming at half LL filling.

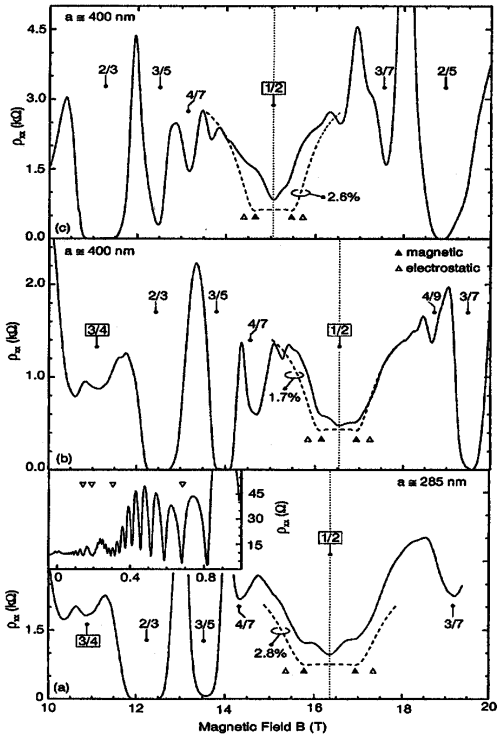

Fig. 2.3: The commensurability oscillations close to $\nu = 1/2$ [48]. The density modulation imposed on the 2DEG has a period of 285 nm in (a) and 400 nm in (b,c). In (b) and (c) the periodic potential has different intensity, the percentage indicating the density modulation with respect to its average.

Moreover the FQHE gap has been observed to vanish linearly close to the even denominators as a function of B^* for fixed density [49], as expected according to (2.21,2.25), see Fig (2.4).

Here we want to stress the extreme versatility of the CF theory. Already at mean field level we obtain the correct sequence of FQH states and interpret their incompressibility in terms of a single particle IQHE. Moreover we grasp the structure of the compressible even denominator states.

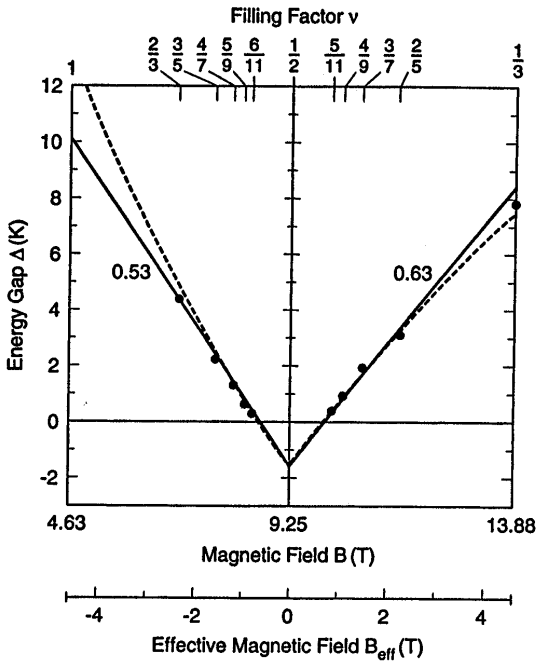

Fig. 2.4: The activation gap as a function of the magnetic field close to $\nu = 1/2$, [49]. The gap vanishes roughly linearly with B_{eff}. The finite negative intercept for $B_{\text{eff}} = 0$ is due to the disorder "closing" the gap before the Fermi liquid is reached. The dashed lines describe the theoretical expectation of the gap, taking into account the magnetic field dependence of m^* close to $B_{1/2} = 2\rho\Phi_0$, see (2.26).

We note in passing that, if we considered the even powers in the Laughlin wavefunction we would not get the proper fermionic statistics of electrons. Indeed, these states were for long time quite mysterious and the introduction of CFs was the crucial step towards their understanding.

We showed that the two problems (2.6) and (2.17) are *completely equivalent*. However the CF Hamiltonian looks even more complicated than the original electronic one, which we were not able to treat because of the huge degeneracy of many-body permutations in the fractional fillings.
The improvement induced by the CS transformation is to produce quasiparticles that feel a reduced magnetic field. We can therefore find situations where there is no further many-body state degeneracy for the non-interacting CF problem. Thus we can in principle start to treat the residual interactions in a perturbative way. In particular we saw that the original fractional effect for electrons is mapped onto CFs at integer filling (which is a non-degenerate configuration). Analogously, the even

denominator electronic states are mapped into Fermi Gases of CF (again with a non degenerate free many-body GS). The price we pay for that improvement is the fact that CF interact not only with each other via the Coulomb term but also with the gauge fields. We will show later how to deal with the effective interactions between CF keeping trace of both the contributions.

The mean field (MF) approximation we presented gets many correct results in a very simple way. It is natural then to use it and its GS as a starting point for further improvement. The need to go beyond mean-field is motivated by some incorrect expectations coming out of the approximation. The incorrect scaling of the MF CF cyclotron gap is one example.
Another issue we can address is the transverse resistance. For the principal incompressible fractions at electronic filling ν we know that $R_{xx} = 0$ and $R_{xy} = h/\nu e^2$. If we use the MF CF approach to describe them we have free CFs at integer filling p. We would then expect $R_{xx}^{\mathrm{CFMF}} = 0$ and $R_{xy}^{\mathrm{CFMF}} = h/pe^2$, an incorrect result. Thus, although incompressibility is obtained, the value of the resistance in the FQH plateaux is not correct.

In order to improve the MF we have to understand how CFs interact. Apart from the Coulomb repulsion due to their charge, CF also feel an additional coupling due to the flux attachment, the so-called Chern-Simons interaction. Physically it can be understood as follows. If a CF moves, it carries its flux quanta. Other CFs then feel a CS magnetic field that varies in time, leading to an electric field through the Faraday's law. This electric field is the additional interaction contribution between the quasiparticles.
To evaluate it explicitly, let us say we have a CF current I along the x direction entering an imaginary closed path $\mathcal{C}$. The current density $\mathbf{j}$ is associated to a variation in CS magnetic field through (2.20). In fact, taking the time derivative of (2.20) and using the continuity equation $\partial_t \rho = -\nabla \cdot \mathbf{j}$ we deduce

$$\hat{\mathbf{z}} \cdot \partial_t \boldsymbol{\mathcal{B}} = -\tilde{\varphi} \Phi_0 \nabla \cdot \mathbf{j} \, . \tag{2.30}$$

Thus the variation of magnetic flux through $\mathcal{C}$ induces an electric field along the path equal to

$$\mathbf{e}^{\mathrm{CS}} = \frac{1}{ec} \, \tilde{\varphi} \Phi_0 \, \hat{\mathbf{z}} \times \mathbf{j} \, . \tag{2.31}$$

Writing (2.31) in the form

$$\mathbf{e}^{\mathrm{CS}} = \hat{\rho}^{\mathrm{CS}} \mathbf{j} \tag{2.32}$$

we get the CS resistivity tensor $\hat{\rho}^{\mathrm{CS}}$, a 2×2 matrix with indices (x, y),

$$\hat{\rho}^{\mathrm{CS}} = \frac{h\tilde{\varphi}}{e^2} \begin{pmatrix} 0 & 1 \\ -1 & 0 \end{pmatrix} \, . \tag{2.33}$$

Within the linear response theory the electronic conductivity tensor can be expressed as a current-current correlation function. Having identified the contribution of the CS term we can treat it in Random Phase Approximation (RPA). We will consider this issue on a formal level in the next sections. For the time being we

mention that the RPA resistivity is obtained by isolating the CS term contribution and treating the remaining system at mean field. Since we know the mean field result $\rho_{xy}^{\mathrm{CFMF}} = h/pe^2$ we can deduce the RPA Hall resistivity

$$\rho_{xy} = \rho_{xy}^{\mathrm{CS}} + \rho_{xy}^{\mathrm{CFMF}} = \frac{h}{e^2}\left(\tilde{\varphi} + \frac{1}{p}\right) = \frac{h}{\nu e^2}\ , \tag{2.34}$$

which is the correct value observed in the FQH plateaux.

Thus we saw that CF allow direct investigation of many issues in the FQH regime already at MF level. The incorrect results coming out of the MF approximation are due to the residual interactions being too crudely neglected. The systematic formal treatment of the residual interactions is the topic to be still addressed. In this direction we are helped by having removed the free many-body GS degeneracy through the flux attachment. A perturbative treatment can then be set down in terms of the standard many-body techniques.
In the following we will concentrate on the Chern-Simons field theoretical treatment of the FQH problem, deriving the free CF Green's function and considering the corrections due to the residual interactions.
We will mainly focus on the case of the even denominator states, where the effective average magnetic field vanishes. In the following chapters, in fact, the MF knowledge of the incompressible fractions will be enough for our purposes, while we will need a more sophisticated treatment of the CF Fermi Liquid forming at half LL filling. The residual interactions in the even denominator configurations modify the single particle properties of the unperturbed Fermi Gas producing a CF Fermi Liquid with peculiar characteristics, as we will see.
For the interested reader, however, we mention that the field theoretical treatment of the incompressible fractions has been investigated in detail in ref.[50].

Finally, we would like to mention that a lot of work has been done to address the Laughlin FQH states from the bosonic Chern-Simons point of view. At fillings $\nu = 1/(2m+1)$ the parameter $\tilde{\varphi}$ can be chosen to be odd, $\tilde{\varphi} = 2m+1$, thereby producing Composite Bosons in a vanishing average field. The incompressibility is then interpreted in terms of a gapped bosonic mode induced by the long range forces between the quasiparticles. A nice presentation of these results can be found in [51].
Essentially one is free to choose the parameter $\tilde{\varphi}$ to cancel the external magnetic field, on the average, at the filling factor of interest. The resulting theory is based on composite particles with, in general, fractional statistics. This approach has been followed by some authors [52].

In the following we will only treat fermionic quasiparticles and the fractions with generic odd denominators will be obtained with a finite effective magnetic field.

2.3 The Chern-Simons field theory of the FQHE

We already observed how the Chern-Simons transformation produces a new fermionic Hamiltonian (2.15) where the CF interact via the direct Coulomb interaction besides being also coupled to the fictitious gauge field $\boldsymbol{\mathcal{A}}$. The link between the two fields is implemented by the flux attachment condition (2.20).
It is possible to formulate the *same* problem in the Lagrangian formalism where the free fermions, free gauge fields and their coupling are directly evident. The flux attachment is fixed by introducing a Lagrangian multiplier and the propagators are directly obtained as kernels of the free field actions.

The total real-time Lagrangian density of the system with Hamiltonian (2.15) is (from now on we consider $\hbar = c = 1$, $e > 0$),

$$\mathcal{L}(\mathbf{r},t) = \mathcal{L}_0(\mathbf{r},t) + \mathcal{L}_{\rm CS}(\mathbf{r},t) + \mathcal{L}_{\rm Coul}(\mathbf{r},t)\ . \tag{2.35}$$

We will now specify the various terms in (2.35) and then show the equivalence with the original hamiltonian problem (2.15).
The first term

$$\begin{aligned}\mathcal{L}_0(\mathbf{r},t) \quad = \quad & \psi^\dagger(\mathbf{r},t)\Big\{ i\partial_t + \mu + e\left(A_0 - \mathcal{A}_0(\mathbf{r},t)\right) + \\ & -\frac{1}{2m}\Big[i\nabla - e\Big(\mathbf{A}(\mathbf{r}) - \boldsymbol{\mathcal{A}}(\mathbf{r},t)\Big)\Big]^2\Big\}\psi(\mathbf{r},t)\,,\end{aligned} \tag{2.36}$$

describes Fermions with chemical potential μ. The vector potential of the homogeneous external magnetic field, $\mathbf{B} = \nabla \times \mathbf{A}$, is included as well as a scalar component A_0 which would be present in the case of an external electric field (in the following we will not consider this case and set $A_0 = 0$). Finally we introduced the gauge fields $(\mathcal{A}_0, \boldsymbol{\mathcal{A}})$ with $\boldsymbol{\mathcal{A}} = (\mathcal{A}_x, \mathcal{A}_y)$.
The action corresponding to (2.36) clearly contains the free CF propagator as kernel of the pure fermionic part, as well as the vertices connecting fermions with gauge fields.
The gauge field component $\mathcal{A}_0(\mathbf{r},t)$ acts as a Lagrange multiplier to impose the boundary condition associated to the correct flux attachment. To implement it completely in fact we introduced the pure gauge field term (the Chern-Simons Lagrangian density)

$$\mathcal{L}_{\rm CS}(\mathbf{r},t) = \frac{e}{\tilde{\varphi}\,\Phi_0}\,\mathcal{A}_0(\mathbf{r},t)\,\hat{\mathbf{z}}\cdot\nabla\times\boldsymbol{\mathcal{A}}(\mathbf{r},t)\ . \tag{2.37}$$

The flux attachment is evident by minimizing the action of the first two Lagrangian densities with respect to $\mathcal{A}_0(\mathbf{r},t)$. In fact, by imposing

$$0 = \frac{\delta\left(\mathcal{S}_0 + \mathcal{S}_{\rm CS}\right)}{\delta\mathcal{A}_0(\mathbf{r},t)} \equiv \frac{\delta}{\delta\mathcal{A}_0(\mathbf{r},t)}\left[\int \mathrm{d}t \int \mathrm{d}\mathbf{r}\ \left(\mathcal{L}_0(\mathbf{r},t) + \mathcal{L}_{\rm CS}(\mathbf{r},t)\right)\right] \tag{2.38}$$

we obtain

$$\hat{\mathbf{z}}\cdot\nabla\times\boldsymbol{\mathcal{A}}(\mathbf{r},t) = \tilde{\varphi}\Phi_0\,\psi^\dagger(\mathbf{r},t)\psi(\mathbf{r},t) \equiv \tilde{\varphi}\Phi_0\,\rho(\mathbf{r},t)\ , \tag{2.39}$$

exactly as in (2.19).
Finally, the Lagrangian density of the Coulomb interaction between the fermions is

$$\mathcal{L}_{\rm Coul}(\mathbf{r},t) = -\frac{1}{2}\int \mathrm{d}\mathbf{r}'\, \rho(\mathbf{r},t)\, V(\mathbf{r}-\mathbf{r}')\, \rho(\mathbf{r}',t) \tag{2.40}$$

with $V(\mathbf{r}) = e^2/\epsilon r$. Using the constraint (2.39) we can cast $\mathcal{L}_{\rm Coul}$ into a pure gauge field Lagrangian density term

$$\mathcal{L}_{\rm Coul}(\mathbf{r},t) = -\frac{1}{2(\tilde{\varphi}\Phi_0)^2}\int \mathrm{d}\mathbf{r}'\, \hat{\mathbf{z}}\cdot\nabla\times\boldsymbol{\mathcal{A}}(\mathbf{r},t)\, V(\mathbf{r}-\mathbf{r}')\, \hat{\mathbf{z}}\cdot\nabla\times\boldsymbol{\mathcal{A}}(\mathbf{r}',t)\,. \tag{2.41}$$

Thus the action associated to $\mathcal{L}_{\rm CS}+\mathcal{L}_{\rm Coul}$ will contain the free gauge field propagator as kernel.

In order to show the equivalence between the Lagrangian and the Hamiltonian problems we remind the relation

$$\mathcal{H}\,[q,p] = p\,\dot{q} - \mathcal{L}\,[q,\dot{q}] \tag{2.42}$$

between a Lagrangian density in the configuration space and the corresponding Hamiltonian density in the phase space. In our case we will have $q=\psi(\mathbf{r},t)$, $\dot{q}=\partial_t\psi(\mathbf{r},t)$ and

$$p = \frac{\partial\mathcal{L}\,[q,\dot{q}]}{\partial\dot{q}} = \frac{\delta\mathcal{L}\,[\psi,\partial_t\psi]}{\delta(\partial_t\psi)} = i\,\psi^\dagger(\mathbf{r},t)\;. \tag{2.43}$$

If we use the constraint (2.39) to specify the form of the gauge field $\boldsymbol{\mathcal{A}}$ we keep trace of the CS lagrangian density as well as of the fictitious field $\mathcal{A}_0$. Then we can obtain the Hamiltonian density from (2.42) as

$$\begin{aligned}
&\mathcal{H}\left[\psi,\psi^\dagger\right] = i\psi^\dagger\partial_t\psi - \mathcal{L}_0\left[\psi,\partial_t\psi\right] - \mathcal{L}_{\rm Coul}\left[\psi,\partial_t\psi\right] = \\
&= -\frac{1}{2m}\left|\left(-i\nabla + \frac{e}{c}\left(\mathbf{A}(\mathbf{r},t) - \boldsymbol{\mathcal{A}}(\mathbf{r},t)\right)\right)\psi(\mathbf{r},t)\right|^2 + \\
&+\frac{1}{2}\int \mathrm{d}\mathbf{r}'\, \rho(\mathbf{r},t)\, V(\mathbf{r}-\mathbf{r}')\, \rho(\mathbf{r}',t)
\end{aligned} \tag{2.44}$$

which is exactly the second quantized version of the original Hamiltonian (2.15).

In the following we will concentrate on even denominator fractions of the form $\nu = 1/\tilde{\varphi}$. The Fermi Liquid theory of the even denominator states has been essentially carried out in a seminal paper by Halperin, Lee and Read (HLR) [45] and in a series of subsequent connected works.
As already shown in the previous sections, with the choice $\nu = 1/\tilde{\varphi}$ the effective magnetic field acting on the fermions

$$B^*(\mathbf{r},t) = B - \tilde{\varphi}\Phi_0\rho(\mathbf{r},t)\;, \tag{2.45}$$

vanishes, on the average. Therefore we will consider the fluctuations of the gauge field with respect to its average introducing

$$a_\mu = \mathcal{A}_\mu - \langle\mathcal{A}_\mu\rangle \tag{2.46}$$

and clearly $\langle a_\mu \rangle = 0$.
The flux attachment constraint reads now

$$\rho(\mathbf{r},t) - \langle \rho \rangle = \frac{1}{\tilde{\varphi}\Phi_0}\, \hat{\mathbf{z}} \cdot \nabla \times \mathbf{a}(\mathbf{r},t)\,. \tag{2.47}$$

In this way the effect of the external vector potential $\mathbf{A}$ in $\mathcal{L}_0$ is compensated by $\langle \boldsymbol{\mathcal{A}} \rangle$. Moreover, since the average density contributes to the interaction Lagrangian just as an uninteresting constant, we can rewrite $\mathcal{L}_{\text{Coul}}$ in terms of fermionic density fluctuations, and then use the constraint (2.47) to cast it into a pure gauge fluctuation term.
The total Lagrangian density (2.35) is then rewritten as

$$\begin{aligned}
&\mathcal{L}(\mathbf{r},t) = \mathcal{L}_0(\mathbf{r},t) + \mathcal{L}_{\text{CS}}(\mathbf{r},t) + \mathcal{L}_{\text{Coul}}(\mathbf{r},t) \qquad (2.48)\\
&\mathcal{L}_0(\mathbf{r},t) = \psi^\dagger(\mathbf{r},t)\Big\{ i\partial_t + \mu - e a_0(\mathbf{r},t) \\
&\qquad\qquad -\frac{1}{2m}\Big[i\nabla + e\mathbf{a}(\mathbf{r},t)\Big]^2 \Big\}\psi(\mathbf{r},t)\,, \\
&\mathcal{L}_{\text{CS}}(\mathbf{r},t) = \frac{e}{\tilde{\varphi}\,\Phi_0}\, a_0(\mathbf{r},t)\, \hat{\mathbf{z}} \cdot \nabla \times \mathbf{a}(\mathbf{r},t)\,, \\
&\mathcal{L}_{\text{Coul}}(\mathbf{r},t) = -\frac{1}{2(\tilde{\varphi}\,\Phi_0)^2} \int \mathrm{d}\mathbf{r}'\, \hat{\mathbf{z}} \cdot \nabla \times \mathbf{a}(\mathbf{r},t)\, V(\mathbf{r}-\mathbf{r}')\, \hat{\mathbf{z}} \cdot \nabla \times \mathbf{a}(\mathbf{r}',t)\,.
\end{aligned}$$

In (2.48) we can identify three parts, describing free fermions, free gauge fields and the vertices between them. The resulting three terms are

$$\begin{aligned}
\mathcal{L}(\mathbf{r},t) &= \mathcal{L}_{\text{F}}(\mathbf{r},t) + \mathcal{L}_{\text{G}}(\mathbf{r},t) + \mathcal{L}_{\text{Int}}(\mathbf{r},t) && (2.49)\\
\mathcal{L}_{\text{F}}(\mathbf{r},t) &= \psi^\dagger(\mathbf{r},t)\Big\{ i\partial_t + \mu + \frac{\nabla^2}{2m} \Big\}\psi(\mathbf{r},t) && (2.50)\\
\mathcal{L}_{\text{G}}(\mathbf{r},t) &= \frac{e}{\tilde{\varphi}\,\Phi_0}\, a_0(\mathbf{r},t)\, \hat{\mathbf{z}} \cdot \nabla \times \mathbf{a}(\mathbf{r},t) + && (2.51)\\
&\quad -\frac{1}{2(\tilde{\varphi}\,\Phi_0)^2} \int \mathrm{d}^2 r'\, \hat{\mathbf{z}} \cdot \nabla \times \mathbf{a}(\mathbf{r},t)\, V(\mathbf{r}-\mathbf{r}')\, \hat{\mathbf{z}} \cdot \nabla \times \mathbf{a}(\mathbf{r}',t) \\
\mathcal{L}_{\text{Int}}(\mathbf{r},t) &= -\psi^\dagger(\mathbf{r},t)\Big\{ e a_0(\mathbf{r},t) + \frac{ie}{2m}\Big[\nabla \cdot \mathbf{a}(\mathbf{r},t) + \mathbf{a}(\mathbf{r},t) \cdot \nabla \Big] + \\
&\quad + \frac{e^2}{2m}\, \mathbf{a}(\mathbf{r},t) \cdot \mathbf{a}(\mathbf{r},t) \Big\}\psi(\mathbf{r},t)\,. && (2.52)
\end{aligned}$$

The total action of our system is then

$$\mathcal{S} = \int \mathrm{d}t \int \mathrm{d}\mathbf{r}\; \mathcal{L}(\mathbf{r},t)\,. \tag{2.53}$$

The free propagators and the vertices of interaction between fermions and gauge fields can be obtained as kernels of the action (2.53), as we will see.
In the following it will be more convenient to work in the energy-momentum space

with the definitions (for a generic field ϕ_μ)

$$\phi_\mu(\mathbf{r},t) = \int \frac{\mathrm{d}\mathbf{k}}{(2\pi)^2}\,\frac{\mathrm{d}\omega}{2\pi}\,e^{i(\mathbf{k}\cdot\mathbf{r}-\omega t)}\phi_\mu(\mathbf{k},\omega) \tag{2.54}$$

$$\phi_\mu(\mathbf{k},\omega) = \int \mathrm{d}\mathbf{r}\,\mathrm{d}t\,e^{-i(\mathbf{k}\cdot\mathbf{r}-\omega t)}\phi_\mu(\mathbf{r},t)\ . \tag{2.55}$$

2.3.1 The free fermion propagator

Let us first consider the free fermionic action

$$\mathcal{S}_\mathrm{F} = \int \mathrm{d}t \int \mathrm{d}\mathbf{r}\,\mathcal{L}_\mathrm{F}(\mathbf{r},t). \tag{2.56}$$

In the Fourier space it reads

$$\mathcal{S}_\mathrm{F} = \int \frac{\mathrm{d}\mathbf{k}}{(2\pi)^2}\,\frac{\mathrm{d}\omega}{2\pi}\,\psi^\dagger(\mathbf{k},\omega)\,[\omega-\varepsilon_\mathbf{k}]\,\psi(\mathbf{k},\omega) \tag{2.57}$$

with the definition $\varepsilon_\mathbf{k} = k^2/2m - \mu$. On the other side we know that this action is linked to the fermionic Green's function via the relation [53]

$$\mathcal{S}_\mathrm{F} = \int \frac{\mathrm{d}\mathbf{k}}{(2\pi)^2}\,\frac{\mathrm{d}\omega}{2\pi}\,\psi^\dagger(\mathbf{k},\omega)\,\left[G^0(\mathbf{k},\omega)\right]^{-1}\psi(\mathbf{k},\omega) \tag{2.58}$$

whence we deduce the time-ordered free propagator

$$\boxed{G^0(\mathbf{k},\omega) = \frac{1}{\omega-\varepsilon_\mathbf{k}+i\,0^+\,\mathrm{sign}(\omega)}}\ . \tag{2.59}$$

The sign of the small imaginary part has been chosen in agreement with the analytical properties of the time-ordered Green's functions [10, 11, 12, 13, 14].

2.3.2 The free gauge field propagator

In analogy to what done before, we now derive the propagator of the gauge fields out of the free action

$$\mathcal{S}_\mathrm{G} = \int \mathrm{d}t \int \mathrm{d}\mathbf{r}\,\mathcal{L}_\mathrm{G}(\mathbf{r},t)\ . \tag{2.60}$$

We choose the transverse gauge, $\nabla\cdot\mathbf{a} = 0$ which, in the Fourier space, becomes $\mathbf{q}\cdot\mathbf{a}(\mathbf{q}) = 0$. If we then project the vector $\mathbf{a}(\mathbf{q})$ on the 2D versors orthogonal ($\hat{e}_\mathrm{T}(\mathbf{q}) = \hat{\mathbf{z}}\times\mathbf{q}/q$) and parallel ($\hat{e}_\mathrm{L}(\mathbf{q}) = \mathbf{q}/q$) to $\mathbf{q}$,

$$\mathbf{a}(\mathbf{q}) = a_1(\mathbf{q})\,\hat{e}_\mathrm{T}(\mathbf{q}) + a_2(\mathbf{q})\,\hat{e}_\mathrm{L}(\mathbf{q})\ , \tag{2.61}$$

the gauge choice implies $a_2(\mathbf{q}) = 0$.
From now on we will use the notation a_μ, ($\mu = 0, 1$), and we have

$$a_0^\dagger(\mathbf{q}) = a_0(-\mathbf{q})\ , \qquad a_1^\dagger(\mathbf{q}) = -a_1(-\mathbf{q})\ . \tag{2.62}$$

The relations (2.62) have been obtained imposing the reality of $a_\mu(\mathbf{r},t)$, considering that $\hat{e}_{\rm T}(-\mathbf{q}) = -\hat{e}_{\rm T}(\mathbf{q})$.
Using the identity $\hat{\mathbf{z}}\cdot\mathbf{q}\times(\hat{\mathbf{z}}\times\mathbf{q}) = q^2$, we get

$$\begin{aligned}\int \mathrm{d}\mathbf{r}\, a_0(\mathbf{r})\,\hat{\mathbf{z}}\cdot\nabla\times\mathbf{a}(\mathbf{r}) &= i\int\frac{\mathrm{d}\mathbf{q}}{(2\pi)^2}\,q\,a_0(\mathbf{q})\,a_1(-\mathbf{q})\\ \int \mathrm{d}\mathbf{r}\,\mathrm{d}\mathbf{r}'\ (\hat{\mathbf{z}}\cdot\nabla\times\mathbf{a}(\mathbf{r}))\ V(\mathbf{r}-\mathbf{r}')\ (\hat{\mathbf{z}}\cdot\nabla\times\mathbf{a}(\mathbf{r}')) &= \\ = -\int\frac{\mathrm{d}\mathbf{q}}{(2\pi)^2}\,q^2\,V(q)\,a_1(\mathbf{q})\,a_1(-\mathbf{q}) \quad .\end{aligned} \tag{2.63}$$

Thus, the gauge fields action $\mathcal{S}_{\rm G}$ becomes

$$\begin{aligned}\mathcal{S}_{\rm G} = \int\frac{\mathrm{d}\mathbf{q}}{(2\pi)^2}\,\frac{\mathrm{d}\Omega}{2\pi}\Big\{a_0(\mathbf{q},\Omega)\,\frac{ieq}{\tilde{\varphi}\,\Phi_0}\,a_1(-\mathbf{q},\Omega) + \\ + a_1(\mathbf{q},\Omega)\,\frac{q^2V(q)}{2(\tilde{\varphi}\,\Phi_0)^2}\,a_1(-\mathbf{q},\Omega)\Big\}\end{aligned} \tag{2.64}$$

and can be written as

$$\mathcal{S}_{\rm G} = \frac{1}{2}\sum_{\mu\nu}\int\frac{\mathrm{d}\mathbf{q}}{(2\pi)^2}\,\frac{\mathrm{d}\Omega}{2\pi}\,a^\dagger_\mu(\mathbf{q},\Omega)\left[D^0_{\mu\nu}(\mathbf{q},\Omega)\right]^{-1}a_\nu(\mathbf{q},\Omega) \tag{2.65}$$

with the free inverse gauge field propagator

$$\left[D^0_{\mu\nu}(\mathbf{q},\Omega)\right]^{-1} = \begin{pmatrix} 0 & \frac{ieq}{\tilde{\varphi}\Phi_0} \\ -\frac{ieq}{\tilde{\varphi}\Phi_0} & -\frac{q^2V(q)}{\tilde{\varphi}^2\Phi_0^2}\end{pmatrix}. \tag{2.66}$$

The diagonal free gauge field Green's functions, obtained inverting the matrix (2.66), are

$$\boxed{D^0_{\mu\nu}(\mathbf{q},\Omega) = \begin{pmatrix} \frac{V(q)}{e^2} & \frac{i\tilde{\varphi}\Phi_0}{eq} \\ -\frac{i\tilde{\varphi}\Phi_0}{eq} & 0\end{pmatrix}}. \tag{2.67}$$

We can notice that the propagators (2.67) do not have any dynamics. In the next section we will concentrate on the RPA approximation and we will see how the dynamics comes in through the coupling with the fermions.
For a pure Coulomb interaction we see that each element of $D^0_{\mu\nu}(\mathbf{q},\Omega)$ scales as q^{-1} and is therefore dominant at small momenta. This is exactly the regime where RPA is more effective in summing up the leading diverging series. It is thus expected to be an excellent approximation for the treatment of the dynamical screening of the gauge field fluctuations by the fermions.

2.3.3 Interactions and vertices between fermions and gauge fields

The last part of the Lagrangian density (2.49) to be considered is $\mathcal{L}_{\text{Int}}$ describing the vertices between the fermions and the gauge field fluctuations. In the Fourier space it has the form

$$\mathcal{L}_{\text{Int}}(t) = -\int \frac{\mathrm{d}\mathbf{k}}{(2\pi)^2}\frac{\mathrm{d}\mathbf{q}}{(2\pi)^2}\Big[\psi^\dagger(\mathbf{k}+\mathbf{q},t)\Big(ea_0(\mathbf{q},t) - \frac{e}{2m}(2\mathbf{k}+\mathbf{q})\cdot\mathbf{a}(\mathbf{q},t)\Big)\psi(\mathbf{k},t) + \\ -\int \frac{\mathrm{d}\mathbf{k}'}{(2\pi)^2}\psi^\dagger(\mathbf{k}+\mathbf{q},t)\Big(\frac{e^2}{2m}\mathbf{a}(\mathbf{q},t)\cdot\mathbf{a}(\mathbf{q}',t)\Big)\psi(\mathbf{k}+\mathbf{q}',t)\Big] \ . \tag{2.68}$$

It can be rewritten as

$$\mathcal{L}_{\text{Int}}(t) = \int \frac{\mathrm{d}\mathbf{k}}{(2\pi)^2}\frac{\mathrm{d}\mathbf{q}}{(2\pi)^2}\Big[\sum_\mu v_\mu(\mathbf{k},\mathbf{q})\psi^\dagger(\mathbf{k}+\mathbf{q},t)a_\mu(\mathbf{q},t)\psi(\mathbf{k},t) + \\ +\frac{1}{2}\sum_{\mu,\nu}\int\frac{\mathrm{d}\mathbf{k}'}{(2\pi)^2}\,w_{\mu\nu}(\mathbf{q},\mathbf{q}')\,\psi^\dagger(\mathbf{k}+\mathbf{q},t)a_\mu(\mathbf{q},t)a_\nu(\mathbf{q}',t)\psi(\mathbf{k}-\mathbf{q}',t)\Big] \tag{2.69}$$

with the vertices

$$v_\mu(\mathbf{k},\mathbf{q}) = \begin{cases} -e, & \text{for } \mu = 0 \\ -\frac{e}{m}\,\hat{\mathbf{z}}\cdot\frac{\mathbf{k}\times\mathbf{q}}{q}, & \text{for } \mu = 1 \end{cases} \\ w_{\mu\nu}(\mathbf{q},\mathbf{q}') = -\frac{e^2}{m}\,\frac{\mathbf{q}\cdot\mathbf{q}'}{qq'}\,\delta_{\mu 1}\delta_{\nu 1}\ . \tag{2.70}$$

In diagrammatic terms they are represented in Fig (2.3.3).

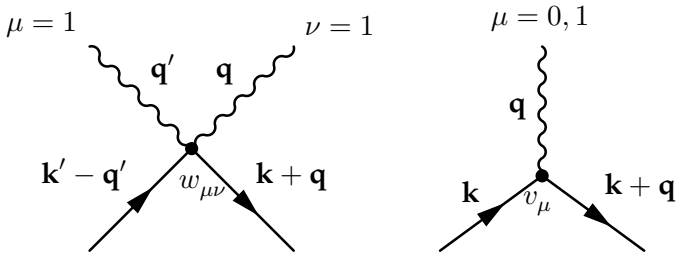

Fig. 2.5: The interaction vertices between fermions and gauge fields. Momentum conservation has already been implemented.

Having introduced the free Green's functions for fermions and gauge fields and their actions we can start considering the perturbation expansion of the propagators in terms of the vertices described by the Lagrangian (2.69).
The exact gauge field propagator is defined as

$$D_{\mu\nu}(\mathbf{q},t) = -i\,\langle\mathcal{T}\left[a_\mu(\mathbf{q},t)a_\nu^\dagger(\mathbf{q},0)\right]\rangle \tag{2.71}$$

analogously to the fermionic Green's function

$$G(\mathbf{k},t) = -i\,\langle\mathcal{T}\left[\psi(\mathbf{k},t)\psi^\dagger(\mathbf{k},0)\right]\rangle\ , \tag{2.72}$$

where $\mathcal{T}$ is the time ordering operator. They can also be obtained as

$$D_{\mu\nu}(\mathbf{q},t) = -\frac{i}{\mathcal{Z}} \int \mathcal{D}\psi^\dagger_{\mathbf{k}}\, \mathcal{D}\psi_{\mathbf{k}}\, \mathcal{D}a_\mu(\mathbf{q})\, e^{i\mathcal{S}} a_\mu(\mathbf{q},t) a^\dagger_\nu(\mathbf{q},0) \tag{2.73}$$

and the analogous for G, with $\mathcal{S} = \int \mathrm{d}t\, \mathrm{d}\mathbf{r}\, \mathcal{L}(\mathbf{r},t)$ and the partition function

$$\mathcal{Z} = \int \mathcal{D}\psi^\dagger_{\mathbf{k}}\, \mathcal{D}\psi_{\mathbf{k}}\, \mathcal{D}a_\mu(\mathbf{q})\, e^{i\mathcal{S}} \ . \tag{2.74}$$

The expression (2.73) is particularly suitable for the perturbation treatment. We will in fact expand the exponential of the interaction action contained in $\mathcal{S}$ as

$$e^{i\mathcal{S}_{\mathrm{int}}} = \sum_{n=0}^{\infty} \frac{i^n}{n!} (\mathcal{S}_{\mathrm{int}})^n \tag{2.75}$$

and then make all the possible contractions of couple of fermions and gauge field operators to produce the corresponding Green's functions according to (2.71) and (2.72). That is, using Wick's theorem we will break the average of the product of many operators into contractions of couples of them, with the relations

$$\langle a_\mu(\mathbf{q},t) a_\nu(\mathbf{q}',t')\rangle = i\,(-1)^\nu\, D^{(0)}_{\mu\nu}(\mathbf{q}, t-t')\, \delta(\mathbf{q}+\mathbf{q}') \tag{2.76}$$

$$\langle \psi(\mathbf{k},t) \psi^\dagger(\mathbf{k}',t')\rangle = i\, G^{(0)}(\mathbf{k}, t-t')\, \delta(\mathbf{k}-\mathbf{k}') \ . \tag{2.77}$$

As usual, the total effect of the contractions giving rise to non-connected diagrams will compensate for the partition function in the denominator due to the interaction action [10, 11, 12, 13, 14]. In the end we will just have to consider connected diagrams with free internal Green's functions.

With the formal apparatus of perturbation theory we can now address the Random Phase Approximation for the gauge field propagators.

2.4 The RPA for the Gauge field propagator

In order to obtain the dynamics of the gauge field propagators we consider the Dyson equation for $D_{\mu\nu}(\mathbf{q},\Omega)$

$$D_{\mu\nu} = D^0_{\mu\nu} + \sum_{\gamma\delta} D^0_{\mu\gamma}\, \Pi_{\gamma\delta}\, D_{\delta\nu} \tag{2.78}$$

where momenta and frequency dependencies have been omitted. Here D is the *exact* gauge field propagator and Π is the *exact irreducible* polarization function acting as a selfenergy for the Green's function D (see Fig (2.4)).

The Random Phase Approximation (RPA) corresponds to taking the polarization function to lowest order in the vertices and with *free* fermionic Green's functions, the so-called Π^0. In our case it will correspond to have the vertex w at first order and v at the second order, since the average of a single bosonic field vanishes.

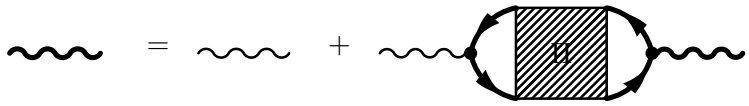

Fig. 2.6: The Dyson equation for the gauge field propagator. The thick wiggly line is the exact function D while the thin wiggly line is the free Green's function D^0. The exact irreducible polarization Π has been included.

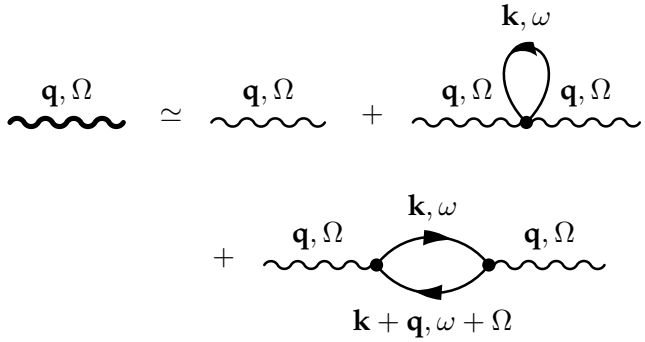

Fig. 2.7: The gauge field propagator at lowest orders in the vertices. Integration over internal momenta and frequencies is implied.

In order to identify Π^0 we consider the two lowest order corrections to the free gauge field propagators iD^0, represented in Fig (2.4).

These two corrections amount to

$$
\begin{aligned}
&-\sum_{\gamma\delta} D^0_{\mu\gamma}(\mathbf{q},\Omega) w_{\gamma\delta}(\mathbf{q},\mathbf{q}) \int \frac{\mathrm{d}\mathbf{k}}{(2\pi)^2}\,\frac{\mathrm{d}\omega}{2\pi}\, G^0(\mathbf{k},\omega)\, e^{i\omega 0^+} D^{(0)}_{\delta\nu}(\mathbf{q},\Omega) + \\
&+\sum_{\gamma\delta} D^0_{\mu\gamma}(\mathbf{q},\Omega) \int \frac{\mathrm{d}\mathbf{k}}{(2\pi)^2}\,\frac{\mathrm{d}\omega}{2\pi}\, v_\gamma(\mathbf{k},\mathbf{q})\, G^0(\mathbf{k}+\mathbf{q},\omega+\Omega) \times \\
&\times G^0(\mathbf{k},\omega)\, v_\delta(\mathbf{k},\mathbf{q})\, D^{(0)}_{\delta\nu}(\mathbf{q},\Omega). \qquad (2.79)
\end{aligned}
$$

By direct comparison with the Dyson equation (2.78) we deduce the free polarization

$$
\begin{aligned}
&\Pi^0_{\mu\nu}(\mathbf{q},\Omega) = i\, w_{\mu\nu}(\mathbf{q},\mathbf{q}) \int \frac{\mathrm{d}\mathbf{k}}{(2\pi)^2}\,\frac{\mathrm{d}\omega}{2\pi}\, G^0(\mathbf{k},\omega)\, e^{i\omega 0^+} + \qquad (2.80)\\
&-i \int \frac{\mathrm{d}\mathbf{k}}{(2\pi)^2}\,\frac{\mathrm{d}\omega}{2\pi}\, v_\mu(\mathbf{k},\mathbf{q})\, G^0(\mathbf{k}+\mathbf{q},\omega+\Omega) G^0(\mathbf{k},\omega)\, v_\nu(\mathbf{k},\mathbf{q})\ .
\end{aligned}
$$

These polarization terms correspond to the diagrams of Fig (2.4).

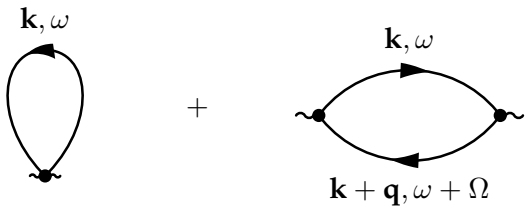

Fig. 2.8: The free polarization $\Pi^0(\mathbf{q}, \Omega)$.

The first term, stemming from the vertex $w_{\mu\nu}(\mathbf{q}, \mathbf{q})$, is constant while the second is dynamically more interesting. It depends on the momentum of the incoming gauge field and on its frequency.
We can directly see why the RPA is particularly effective for small momenta and energy: in fact, whenever Ω and $\mathbf{q}$ tend to zero, the poles of the two fermionic Green's functions get closer and closer, thereby giving a large contribution to the final integral.

Our purpose in the following is to describe the quasiparticle properties for the CF Fermi Liquid forming at half LL filling [45]. The gauge field propagator will act as the mediator of the effective quasiparticle interaction, keeping trace of both the original Coulomb and CS coupling terms. As in the usual Fermi Liquids we will concentrate on the small energy sector, where the Landau quasiparticles are well defined, their lifetime diverging at the Fermi level. The small energy excitations, moreover, are the relevant ones for the linear transport properties of the system.
Among the interesting quantities to be considered, we will mainly concentrate on the single particle fermionic Green's function, focusing on the properties of its pole close to the Fermi energy. The issue of the renormalized quasiparticle effective mass will be addressed directly, and we will see how the gauge field fluctuations drastically affect the small energy sector of the spectrum [54].
Being interested in the dominant scattering for fermions close to the Fermi level, we will need the small energy behaviour of the gauge field propagator mediating the coupling. To get this limiting scaling we then consider the polarization Π^0 in the regime $|\Omega| \ll v_{\mathrm{F}} q \ll v_{\mathrm{F}} k_{\mathrm{F}}$. The result (see Appendix A) is

$$\Pi^0(\mathbf{q}, \Omega) \simeq \begin{pmatrix} -\frac{m\, e^2}{2\pi}\left(1 + i\frac{|\Omega|}{v_{\mathrm{F}} q}\right) & 0 \\ 0 & \frac{q^2 e^2}{24\pi m} - i\frac{2\rho e^2 |\Omega|}{m v_{\mathrm{F}} q} \end{pmatrix} . \tag{2.81}$$

Replacing this result in the exact polarization present in the Dyson equation (2.78) we get the propagator in Random Phase Approximation

$$D(\mathbf{q}, \Omega) \simeq \frac{1}{\chi_q + i\gamma\frac{|\Omega|}{v_{\mathrm{F}} q}} \begin{pmatrix} \tilde{\chi}_q + i\tilde{\gamma}_q |\Omega| & -i\beta q \\ i\beta q & \frac{m}{2\pi} \end{pmatrix} \tag{2.82}$$

where $\beta = e/\tilde{\varphi}\Phi_0$, $\tilde{\chi}_q = -q^2V(q)/\tilde{\varphi}^2\Phi_0^2 = -q\,e^2/\epsilon\tilde{\varphi}^2\Phi_0^2$, $\chi_q = \tilde{\chi}_q\, m/2\pi$, $\tilde{\gamma}_q = 2\rho/k_{\rm F}q$ and $\gamma = \rho/\pi$.
Clearly the D_{11} component is the dominant one, being the only non-vanishing small energy-small momentum matrix element. It comes out to be

$$\boxed{D_{11}(\mathbf{q},\Omega) \approx \left[-\frac{q\,e^2}{\epsilon\tilde{\varphi}^2\Phi_0^2} + i\,\frac{2\rho\,|\Omega|}{k_{\rm F}q}\right]^{-1}}\,. \tag{2.83}$$

This is the leading gauge field channel mediating effective interactions between the fermions. By inspection we see that $D(\mathbf{q},\Omega)$ has a pole (for the retarded propagator) at

$$\Omega = -i\,\frac{2\pi e^2}{k_{\rm F}\epsilon\tilde{\varphi}^2\Phi_0^2}\,q^2\ . \tag{2.84}$$

Such an imaginary pole means that the dominant coupling is mediated by a slowly decaying channel rather than a conventional stable mode. However the decay time diverges for very small momenta as q^{-2}.

Having obtained the RPA gauge field propagator we will now concentrate on the Fermi Liquid corrections to the single quasiparticle Green's function. Among the physical properties to be extracted from it we will observe a peculiar diverging CF effective mass close to the Fermi level [54].

2.5 Selfenergy correction to the fermionic Green's function: CF effective mass

Let us consider the selfenergy correction to $iG(\mathbf{k},\omega)$ at first order in the leading gauge field propagator D_{11}. We will be interested in the fermionic properties close to the Fermi level, where the concept of quasiparticle in the Fermi Liquid is well defined. Thus, we will mainly look at $k \simeq k_{\rm F}$ and $\omega/E_{\rm F} \to 0$.

The fermionic Dyson equation for the exact Green's function is

$$G(\mathbf{k},\omega) = G^0(\mathbf{k},\omega) + G^0(\mathbf{k},\omega)\Sigma(\mathbf{k},\omega)G(\mathbf{k},\omega) \tag{2.85}$$

with $\Sigma(\mathbf{k},\omega)$ the *exact irreducible* selfenergy (see Fig(2.5)).

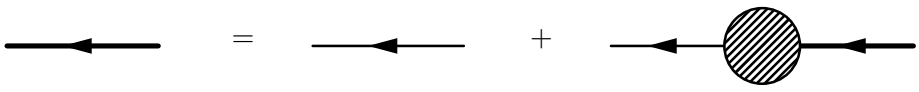

Fig. 2.9: The Dyson equation for the fermionic propagator. The thick line is the exact function G while the thin line is the free Green's function G^0. Arrows come out of the creation operators and indicate the momentum transfer. The exact irreducible selfenergy Σ has been included as a dashed circle.

In terms of $\Sigma(\mathbf{k},\omega)$, we can deduce the renormalized spectrum of the single particle excitations out of the pole of $G(\mathbf{k},\omega)$ by solving the selfconsistent equation

$$\varepsilon^*(\mathbf{k}) = \varepsilon(\mathbf{k}) + \mathrm{Re}\left[\Sigma\left(\mathbf{k},\varepsilon^*(\mathbf{k})\right)\right] \tag{2.86}$$

where $\varepsilon(\mathbf{k})$ and $\varepsilon^*(\mathbf{k})$ are the free and renormalized fermionic dispersions, respectively. On the same footing the quasiparticle lifetime is

$$\tau = \frac{1}{\mathrm{Im}\left[\Sigma\left(\mathbf{k},\varepsilon^*(\mathbf{k})\right)\right]} \ . \tag{2.87}$$

It is possible to define an effective quasiparticle mass m^* from (2.86) by insisting that the renormalized dispersion has the form

$$\varepsilon^*(\mathbf{k}) \equiv \frac{k^2}{2m^*} - \mu \ . \tag{2.88}$$

Thus, taking the derivative of (2.86) with respect to k at the Fermi level we get

$$\frac{k_\mathrm{F}}{m^*} = \frac{k_\mathrm{F}}{m} + \frac{\partial\Sigma}{\partial\varepsilon(\mathbf{k})}\Big|_{k=k_\mathrm{F}} \cdot \frac{k_\mathrm{F}}{m} + \frac{\partial\Sigma}{\partial\omega}\Big|_{\omega=\varepsilon^*(\mathbf{k})} \cdot \frac{k_\mathrm{F}}{m^*} \tag{2.89}$$

whence the equation for the renormalized effective mass

$$\boxed{\frac{m^*}{m} = \frac{1 - \frac{\partial\Sigma}{\partial\omega}\Big|_{\omega=\varepsilon^*(\mathbf{k})}}{1 + \frac{\partial\Sigma}{\partial\varepsilon(\mathbf{k})}\Big|_{k=k_\mathrm{F}}}} \ . \tag{2.90}$$

In order to analyze the fermionic selfenergy and deduce the outcoming quasiparticle effective mass we start considering the Green's function up to first order in the gauge field propagator (see Fig. (2.5))

$$\begin{aligned} iG(\mathbf{k},\omega) &\simeq iG^0(\mathbf{k},\omega) - G^0(\mathbf{k},\omega) \times \\ &\times \left(\int \frac{\mathrm{d}\mathbf{k}'}{(2\pi)^2} \frac{\mathrm{d}\Omega}{2\pi} \, v_1(\mathbf{k},\mathbf{k}')^2 G^0(\mathbf{k}',\omega-\Omega) D_{11}(\mathbf{k}-\mathbf{k}',\Omega) \right) G^0(\mathbf{k},\omega) \ . \end{aligned} \tag{2.91}$$

Here we neglected the first order contribution coming from the vertex w and from the Hartree correction since they are just constants, at most renormalizing the chemical potential.
By direct comparison with the Dyson equation (2.85) we extract the first order selfenergy correction

$$\Sigma(\mathbf{k},\omega) \simeq i \int \frac{\mathrm{d}\mathbf{k}'}{(2\pi)^2} \frac{\mathrm{d}\Omega}{2\pi} \, v_1(\mathbf{k},\mathbf{k}')^2 G^0(\mathbf{k}',\omega-\Omega) D_{11}(\mathbf{k}-\mathbf{k}',\Omega) \ , \tag{2.92}$$

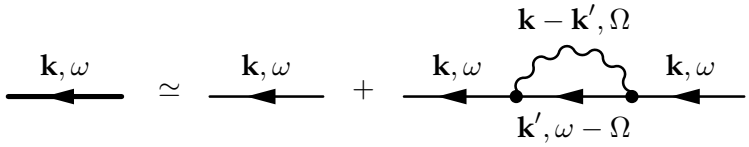

Fig. 2.10: The fermionic Green's function up to first order in the gauge field propagator. The first order contributions coming from the vertex $w_{\mu\nu}$ and the Hartree correction have been neglected since they are just constants renormalizing the chemical potential. The Fock-type selfenergy insertion is clearly visible.

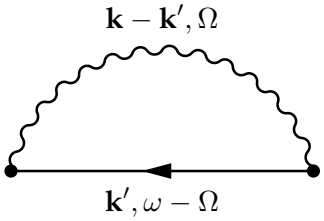

Fig. 2.11: The Fock type selfenergy correction to the single particle fermionic Green's function $G^0(\mathbf{k},\omega)$. Integration over internal momenta and frequency is implied.

represented by the Fock-type diagram of Fig (2.5).

Having a dynamical bosonic mode as mediator of the interaction, as in the theory of superconductivity for example, it is often more convenient to evaluate $\delta\Sigma(\mathbf{k},\omega) = \Sigma(\mathbf{k},\omega) - \Sigma(\mathbf{k},0)$ [55]. Thus our task is to calculate

$$\delta\Sigma(\mathbf{k},\omega) \simeq i \int \frac{\mathrm{d}\mathbf{k}'}{(2\pi)^2} \frac{\mathrm{d}\Omega}{2\pi} v_1(\mathbf{k},\mathbf{k}')^2 D_{11}(\mathbf{k}-\mathbf{k}',\Omega) \left[G^0(\mathbf{k}',\omega-\Omega) - G^0(\mathbf{k}',-\Omega)\right] . \tag{2.93}$$

It is convenient to introduce $q \equiv |\mathbf{k}-\mathbf{k}'|$ and replace

$$v_1(\mathbf{k},\mathbf{k}')^2 = \frac{e^2}{m^2} \frac{k^2 k'^2}{q^2} \sin^2\theta \tag{2.94}$$

where θ is the angle between $\mathbf{k}$ and $\mathbf{k}'$. The measure is then changed into

$$\int \mathrm{d}\mathbf{k}' = \int_0^\infty k' \mathrm{d}k' \int_0^{2\pi} \mathrm{d}\theta = 2 \int_0^\infty \mathrm{d}k' \int_{|k-k'|}^{k+k'} \mathrm{d}q \, \frac{q}{k \sin\theta} \tag{2.95}$$

with

$$\sin\theta = \sqrt{1 - \left[\frac{k^2 + k'^2 - q^2}{2kk'}\right]^2} . \tag{2.96}$$

For quasiparticle scattering at the Fermi level and $q \ll k_{\rm F}$ we have $\sin\theta \simeq q/k$ such that the measure can be approximated to be 1, with $q \in [0, 2k_{\rm F}]$ and $v_1(\mathbf{k},\mathbf{k}')^2 \simeq k_{\rm F}^2 e^2/m^2$. The selfenergy (2.93) becomes

$$\delta\Sigma(\mathbf{k},\omega) \simeq i\frac{2e^2k_{\rm F}^2}{(2\pi)^3m^2}\int_{-\infty}^{\infty}{\rm d}\Omega\int_0^{2k_{\rm F}}{\rm d}q\,D_{11}(q,\Omega)\int_0^{\infty}{\rm d}k'\left[G^0(k',\omega-\Omega)-G^0(k',-\Omega)\right] \tag{2.97}$$

where we used the fact that the propagators depend only on the modulus of their momentum.
Let us consider first the integral over k'. For small ω we can approximate

$$\begin{aligned}&\int_0^{\infty}{\rm d}k'\left[G^0(k',\omega-\Omega)-G^0(k',-\Omega)\right]\simeq \qquad (2.98)\\ &\simeq\frac{1}{2}\int_{-\infty}^{\infty}{\rm d}k'\frac{\omega}{\left[\omega-\Omega-\varepsilon_{k'}+i0^+{\rm sign}(\omega-\Omega)\right]\left[\Omega+\varepsilon_{k'}+i0^+{\rm sign}(\Omega)\right]}\,.\end{aligned}$$

Linearizing the dispersion close to $E_{\rm F}$, $\varepsilon_{k'} \simeq v_{\rm F}(k'-k_{\rm F}) \equiv \eta$, we get

$$\frac{\omega}{2v_{\rm F}}\int_{-\infty}^{\infty}{\rm d}\eta\frac{1}{\left[\omega-\Omega-\eta+i0^+{\rm sign}(\omega-\Omega)\right]\left[\Omega+\eta+i0^+{\rm sign}(\Omega)\right]}\,. \tag{2.99}$$

If we concentrate on positive ω (meaning to investigate quasi-*particle* properties) we can perform the integration on η by closing the contour in the positive imaginary complex plane with the result that (2.99) becomes

$$-\frac{i\pi}{v_{\rm F}}\,\Theta(\Omega)\,\Theta(\omega-\Omega)\,, \tag{2.100}$$

with $\Theta(x)$ the step function equal to 1 for $x>0$ and 0 elsewhere.
The integration over q,

$$\int_0^{2k_{\rm F}}{\rm d}q\,D_{11}(q,\Omega)=\int_0^{2k_{\rm F}}{\rm d}q\,\frac{1}{-\frac{q\,e^2}{\epsilon\tilde{\varphi}^2\Phi_0^2}+i\frac{2\rho|\Omega|}{k_{\rm F}q}}\,, \tag{2.101}$$

can be easily carried out to give

$$\frac{\epsilon\tilde{\varphi}^2\Phi_0^2}{2e^2}\,\log\left[\frac{i\frac{2\rho|\Omega|}{k_{\rm F}}}{i\frac{2\rho|\Omega|}{k_{\rm F}}-4k_{\rm F}^2\frac{e^2}{\epsilon\tilde{\varphi}^2\Phi_0^2}}\right]\,. \tag{2.102}$$

Having shown that $\Omega \in [0,\omega]$ (see (2.100)) and being $\omega \ll v_{\rm F}q$, we can expand the result in $\Omega/v_{\rm F}q$ to be

$$\frac{\epsilon\tilde{\varphi}^2\Phi_0^2}{2e^2}\,\log\left[-\frac{i\frac{2\rho|\Omega|}{k_{\rm F}}}{4k_{\rm F}^2\frac{e^2}{\epsilon\tilde{\varphi}^2\Phi_0^2}}\right]\,. \tag{2.103}$$

Finally the integration over Ω brings

$$\begin{aligned}\delta\Sigma(\mathbf{k},\omega)&\simeq\frac{2e^2k_{\rm F}^2}{(2\pi)^3m^2}\,\frac{\pi}{v_{\rm F}}\,\frac{\epsilon\tilde{\varphi}^2\Phi_0^2}{2e^2}\int_0^{\omega}{\rm d}\Omega\,\log\left[-\frac{i\frac{2\rho|\Omega|}{k_{\rm F}}}{4k_{\rm F}^2\frac{e^2}{\epsilon\tilde{\varphi}^2\Phi_0^2}}\right]=\\ &\simeq\frac{k_{\rm F}\epsilon\tilde{\varphi}^2\Phi_0^2}{8\pi^2m}\,\omega\,\log\left[\frac{\epsilon\tilde{\varphi}^2\Phi_0^2}{8\pi k_{\rm F}e^2}\,\omega\right]-i\frac{k_{\rm F}\epsilon\tilde{\varphi}^2\Phi_0^2}{16\pi m}\,\omega\,.\end{aligned} \tag{2.104}$$

We can see directly that the imaginary part of the selfenergy is correctly producing a pole for the single particle Green's function in the negative imaginary plane for positive frequencies, as requested from its analytical properties. Moreover, the ratio between imaginary and real part of the selfenergy vanishes for small frequencies, indicating that the concept of quasiparticle is well defined close to the Fermi level.

Now let us discuss the physical consequencies of (2.104) for the CF effective mass. First of all the selfenergy is essentially frequency dependent and it is dominated by its real part for small frequencies. Inserting (2.104) into (2.90) we get the dominant scaling

$$m^* \sim -m \frac{k_{\rm F} \epsilon \tilde{\varphi}^2 \Phi_0^2}{8\pi^2 m} \log \omega \,, \tag{2.105}$$

that is, a logarithmic divergence at small energy.
Thus CF are well defined quasiparticles in the Landau Fermi-liquid sense but their renormalized parameters can show "anomalies". The origin of the diverging effective mass is the $1/q$ singularity of the gauge field propagator in the static limit. This gives rise to many infrared divergencies found while calculating response functions out of the original Lagrangian (2.48).
It is natural to ask whether the singular behaviour is just an artifact of the lowest order approximation we kept, and is removed by higher order corrections. This issue has been investigated in detail by Stern and Halperin [54] who showed the remarkable fact that the result (2.104) is *exact* at low energies. More specifically they show that, due to Ward identities valid in the limit $\omega \ll v_{\rm F} q$, the corrections to the internal fermionic Green's function leading to the exact G in the selfenergy (2.92) are cancelled by the vertex corrections. Thus, surprisingly, the first order calculation we performed gives the *exact* result, in the low energy sector.

Stern and Halperin considered also the case when a *small* residual effective magnetic field B^* exists, i.e. the limit of very large CF filling factor, $p \gg 1$. In particular the states at fillings $\nu = 1/\tilde{\varphi}$ can be looked at as $\lim_{p\to\infty} p/(\tilde{\varphi} p \pm 1)$. By studying the pole of the single particle Green's function in the CFLL basis they were able to extract the FQH energy gap $\Delta(p)$, and they found

$$\Delta(p) \simeq \frac{e^2 k_{\rm F} \pi}{\epsilon \tilde{\varphi}(\tilde{\varphi} p + 1)} \frac{1}{\ln(2p+1)} \,. \tag{2.106}$$

The origin of the logarithmic correction is the same as the one for vanishing residual field. In the limit $p \gg 1$ we can estimate $k_{\rm F} = \ell^{-1}\sqrt{2/\tilde{\varphi}}$ and $\ln(2p+1) \simeq \ln p$, so that

$$\Delta(p) \simeq \frac{e^2}{\epsilon \ell} \frac{\pi}{\tilde{\varphi}^2 p \ln p} \sqrt{\frac{2}{\tilde{\varphi}}} \,. \tag{2.107}$$

This is a very important result, since it shows how the gauge field mediated interaction induces incompressibility with the correct scaling determined by the Coulomb coupling. At least in the large p limit it is then possible to obtain the scaling predicted by HLR via dimensional analysis arguments (see (2.25)). Moreover the gaps are predicted to show a logarithmic dependence on the filling factor, which is linked to the diverging CF effective mass at the Fermi level for $\nu = 1/\tilde{\varphi}$.
Thus, an accurate measurement of the energy gaps close to even denominator states

would allow a direct test of the theoretically expected logarithmic divergence. Of course, since the gaps become smaller and smaller for increasing p, it is experimentally very difficult to obtain precise measurements, since the disorder tends to "close the gap" before the logarithmic corrections show up (see Fig (2.4)). There are claims [56] of the observation of a very large effective mass close to $\nu = 1/2$, but the issue is still experimentally not fixed.

2.6 Summary

To sum up the main results of this chapter we stress that Composite Fermions seem to work extremely well as quasiparticles for the FQHE.
The basic physical advantage of CF is that they naturally carry the correlation hole attachment that keeps the GS energy low and is the key issue in Laughlin's original explanation of the FQHE.
The new quasiparticles feel an effective magnetic field which is reduced with respect to the external one. The main interesting fractions, like the principal FQH sequence and the even denominator states, can be addressed already at mean field as manifestations of independent CF behaviour. In these states, in particular, the mean field CF starting point has a non-degenerate GS subspace, allowing for the treatment of the residual interactions in the perturbative framework.
Due to the composite nature of the quasiparticles, the effective interaction between them is affected by both the Coulomb repulsion and by the Chern-Simons coupling, and is mediated by dynamical gauge field fluctuations. The nature of the gauge field propagator is peculiar, having a decaying lifetime which diverges only in the very small energy-momentum regime. The $1/q$ divergence of the static gauge field Green's function is responsible for the anomalies observed in the perturbative corrections to the mean field GS. In particular, the CF effective mass at the Fermi level diverges logarithmically.

In the following we will elaborate on the CF model by introducing its spin-related properties. At first we will address the GS spin polarization for incompressible fractions and then we will consider the role of the gauge field fluctuations in the spinful CF Fermi Liquid. We will observe that they can induce a GS restructuration as well as enhance the singularity of the CF effective mass at the Fermi level.

3. COMPOSITE FERMIONS WITH SPIN

In the last chapter we gave an introduction to the field theoretical treatment of the FQHE in terms of Composite Fermions. All the features analyzed up to now have been presented in the fully spin polarized (or spinless) case. This is a good approximation for the large magnetic field regime, where the Coulomb repulsion between particles with the same spin orientation is the smallest energy scale into play.
However, as mentioned at the end of the first chapter, due to the characteristic parameters of the samples it is frequently possible that non fully spin polarized configurations rise naturally, especially in the small magnetic field regime.
In this chapter we will present a first introduction to the spin related properties in the FQHE. Along the line of thinking introduced by the CF picture, we will include the spin degree of freedom in the Chern-Simons treatment and see the main outcomes of a single particle analysis for CF with spin.
All the chapter will have close relations with recent experiments where the degree of electronic spin-polarization of the GS is directly probed. Our task is to analyze the various structures observable in the experiment in terms of the simplest possible CF model. We will see that the dominant structures are easily described by an independent CF picture, and corrections to it will be presented in order to account for smaller observed features.
A first part of the chapter will be devoted to a description of the experimental technique adopted in measuring the spin polarization and to the main results of that analysis. Then the independent picture for CF with spin will be introduced and the role of finite temperature, disorder and spin-orbit scattering will be considered. The direct comparison with the experimental results will allow us to associate to the CF an effective mass and a g-factor, altogether consistent with the small and large temperatures regimes of the measurements.

3.1 The GS spin polarization in the FQHE: experimental analysis

Originally, in the theory of the Fractional Quantum Hall Effect (FQHE) at large magnetic fields, it has been assumed that the Zeeman splitting is sufficiently large such that the spins of all electrons in a Landau band are completely polarized [27]. However, due to the small electronic effective mass $m_{\rm b}$ ($m_{\rm b} = 0.067\, m_0$, m_0 the electron mass) and the small g-factor ($g = -0.44$), in GaAs the Zeeman term is about 70 times smaller than the cyclotron energy

$$\begin{aligned} \hbar\omega_{\rm c}^{\rm GaAs} &\simeq 20\, B\,[{\rm T}]\,{\rm K} \\ E_{\rm Z}^{\rm GaAs} &\simeq 0.29\, B\,[{\rm T}]\,{\rm K} \end{aligned} \tag{3.1}$$

where magnetic fields are expressed in Tesla and energies in Kelvin [38].
In recent years, the improved quality of samples and their excellent mobility allowed to observe FQH structures down to few Tesla, where the Coulomb energy scale can easily mix the different spin channels. Spin effects have therefore to be taken into account in order to describe many recent interesting features.
As we saw at the end of Chapter 1, partly spin-polarized ground states (GS) have been proposed at various filling factors ν by Halperin [38]. An example is the state at $\nu = 2/5$ that has also been studied numerically. For this, the GS has been shown to be non-polarized [57] without Zeeman splitting. Exact diagonalization confirmed the Halperin wave function to be an excellent approximation of the true GS [58].

In order to observe spin related features in the Quantum Hall regime different techniques can be applied.
Let us start with the Integer case, where interaction effects seem non to play a crucial role. Apart from the disorder broadening that always has to be smaller than the other dynamical scales in order to observe Quantum Hall structures at all, the two energy scales we have to consider are the cyclotron and Zeeman energies. Both of them scale linearly with a purely perpendicular magnetic field. In such a configuration we do not expect any interesting spin-related feature. If the density is fixed and we sweep **B** (or viceversa) the different spin split LL come across the Fermi energy, giving rise to peaks in σ_{xx}. Thus the only effect would be the doubling of the peak structures with respect to the spinless case analyzed earlier.
It is however possible to tune the cyclotron and Zeeman energies *independently* by tilting the external magnetic field with respect to the direction orthogonal to the 2DES. In fact the cyclotron gap is related to the electronic motion *in the plane*, and is only sensitive to the component of **B** orthogonal to it, denoted as $B_\perp$. On the other side the Zeeman energy is sensitive to the *total* external **B**, which fixes the spin quantization axis. The only effect of the in-plane component of the magnetic field $B_\parallel$ would be to couple to the finite z-extent of the electronic wavefunctions (due to the finite thickness of the 2DES) thereby shrinking them. But the outcome of this correction will be observable in the effective e-e interaction. Indeed this comes out to be a crucial issue for a precise quantitative determination of the energy gap in the FQHE, but we won't dwell on that here.
It is then possible, in principle, to induce crossings between LL with different spin

by tilting the field. If we indicate with θ the angle of the total **B** with respect to the direction orthogonal to the 2DES we have $B_\perp = B\cos\theta$. By keeping B constant, the Zeeman and cyclotron energy can be made equal at a critical tilt angle $\theta_{\rm cr}$ solution of the equation

$$\hbar\,\frac{eB\cos\theta_{\rm cr}}{m_{\rm b}c} = g\mu_{\rm B}B = g\,\frac{\hbar eB}{2m_0c}. \tag{3.2}$$

With the typical parameters of GaAs the resulting $\theta_{\rm cr}$ is very large ($\theta_{\rm cr}\approx 89^\circ$). This makes the experimental realization difficult since we still need $B_\perp$ of the order of 1 T in order to observe reasonably stable QH states. The resulting total B would be unachievable at such large angles. Moreover, a large in plane component $B_\parallel$ induces a preferential direction in the sample, which tends to favour the formation of anisotropic structures in the GS.
In order to perform coincidence experiments in the Integer regime with a finite tilt it is then necessary to choose other materials with larger g-factor and bulk mass. Unfortunately their mobilities are typically much worse than the one observed in the best GaAs samples.
In recent experiment in the IQH regime on SiGe the LL crossing has been induced and the interesting outcome is the formation of anisotropic structures (stripes-like) orthogonal to the in plane field component. The main resulting effect is a strongly anisotropic transport in the directions parallel and perpendicular to $B_\parallel$ [59]. The theory for such a state has been worked out recently, with the curious discovery that an in plane field on an *isotropically* disordered sample induces *anisotropic* dominant small angle scattering [60].

In the following we will mainly concentrate on the FQH regime for states with filling factor smaller than 1. A very clean analysis of the possible spin-related phase transitions is possible if we consider experiments at *fixed filling factors* and this will be the focus in the next sections.
Since we deal with FQH states well inside the first LL we already know that the only dynamically interesting energy scale is the Coulomb coupling, scaling as $\sqrt{B}$. Since the Zeeman energy is still linear in the total magnetic field, we see that in the Fractional regime the crossover between the two relevant scales can be induced even *without tilt*. By tuning the *purely perpendicular* B together with the electronic density (in order to keep ν fixed) we can sweep from the spin polarized regime where $E_{\rm Z}$ dominates (large B) to an interesting regime where the Coulomb scale mixes the spin channels. Indeed this was the purpose of the experiment we will now briefly describe.

3.1.1 Experimental analysis of the spin polarization in the FQH regime

The experimental question was to directly observe the degree of electronic spin polarization of the FQH GS for different fillings as a function of the external magnetic field. Among the possible experimental techniques to measure the spin polarization of the 2DES we will focus on the magnetoluminescence. It was recently used in a series of investigations by Kukushkin et al. which constitute the main source of experimental input for our following analysis [61, 62, 63].
The essence of the magnetoluminescence experiments is to induce holes away from

the 2DES with a laser pulse and then observe the circular polarization of the light emitted by the process of recombination of the 2D electrons with the holes. This technique, contrary to the magnetotransport measurements exploring the electronic properties close to the Fermi energy, is able to give informations about the whole spectrum of the system.
At the beginning, the laser pulse was used to produce holes spread into the 3D sample. Later it was shown that a much better resolution of the peaks in the recombination spectrum is obtained if the holes are produced in a 2D layer with a finite separation from the 2DES. For this purpose, a δ-doping of acceptors (Be) is induced in the sample, at an optimized distance of 20-30 nm from the 2DES. The recombination spectrum is usually measured after the holes have thermalized, thus not immediately after the laser pulse.
By measuring the circular polarization of the outcoming photons in configurations where the electronic spin polarization is known (e.g. $\nu = 1$ fully polarized and $\nu = 2$ fully unpolarized) it is possible to calibrate the experiment and associate *univocally* a 2D spin polarization to the photonic circular polarization. More details on this technique will be found in [61] and references therein.
In the following we will directly speak about the *electronic spin polarization of the GS*.

Starting in 1999, Kukushkin et al. lead a systematic investigation of the spin properties of the FQHE GS via the radiative recombination technique described above.
At first they tried the spin-polarization measurements at constant 2D electron density, depicted in Fig (3.1).

It is possible to see that the value of the polarization observed at a certain filling depended strongly on the underlying density. Only few states, like $\nu = 1$ and $\nu = 1/3$ preserve full polarization while varying B. It is therefore difficult to get informations about the allowed GS spin configurations at a given filling with this technique.
Much cleaner results were obtained imposing a constant filling (via back-gate density modulation).
The first important data presented in Kukushkin's analysis concerned the very small temperature behaviour of the system. The experiments were performed at a starting temperature T_{in} where the first values of polarization were recorded. Then, while keeping the density and magnetic field fixed, the temperature was decreased to reach the minimum allowed by their refrigerator (of the order of 30 mK). Kukushkin realized that the value of the polarization tends to saturate at small temperatures. By plotting the $T \to 0$ saturation value as a function of B he produced the "zero temperature" polarization plot depicted in Fig (3.2).

A first important point to be noticed is the quality of the sample, allowing the observation of FQH structures down to magnetic fields as low as 1 T.
Here we would like to stress that these data should be looked at as the "zero temperature" behaviour of the system.
Several interesting features come out of this experiment:

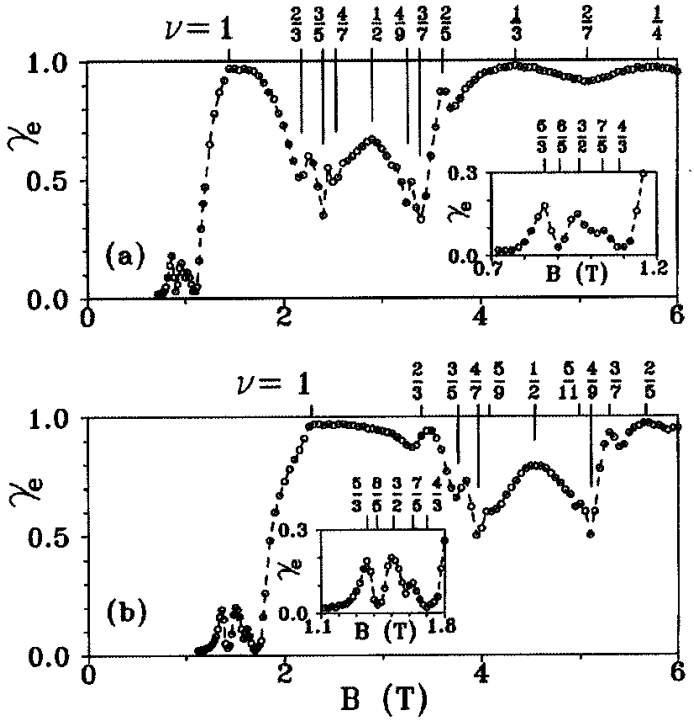

Fig. 3.1: The degree of spin polarization of a 2D GaAs-AlGaAs sample as a function of the purely perpendicular magnetic field for two different but fixed densities [61]: (a) $\rho = 3.5 \cdot 10^{10}\,\mathrm{cm}^{-2}$, (b) $\rho = 5.5 \cdot 10^{10}\,\mathrm{cm}^{-2}$. The magnetoluminescence signals are reported for the smallest temperatures achievable in the experiment. Many FQH states are probed: the spin polarization of the same filling factors varies in the two cases, except for $\nu = 1$ which is always fully polarized.

1. First of all, for all the measured *incompressible* fractions large plateaux were observed, where the spin polarization is constant although the magnetic field is changing
2. At certain critical values of magnetic field a crossover between one plateau and the following is observed, and the transition, although virtually at $T = 0$, is smooth, a feature which we will denote as "Zero Temperature Smoothening" (ZTS)
3. In *every* crossover region an additional structure, like a shoulder, shows up indicating a further stabilization of the polarization, at a value *exactly* half the way between the neighboring plateaux. We want to stress that this feature is *reproducible and generic*, indicating something happening whenever a po-

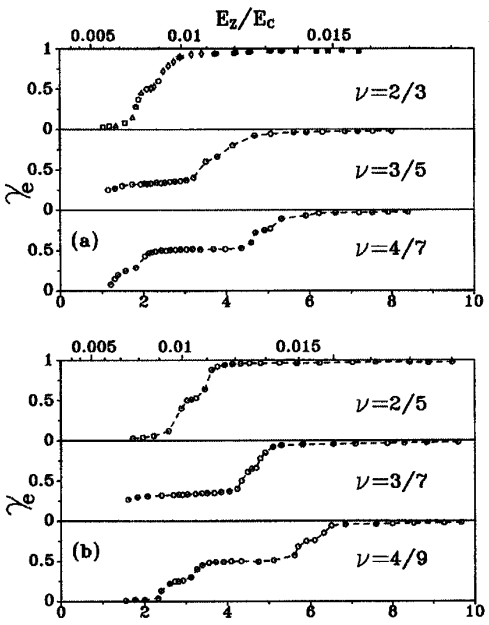

Fig. 3.2: The zero temperature expectation value of the degree of spin polarization of a 2D GaAs-AlGaAs sample as a function of the purely perpendicular magnetic field for some different but fixed filling factors corresponding to incompressible states of the principal sequence [61]. The fillings (indicated in the picture) are kept constant by a simultaneous back-gate density modulation. Notice the presence of wide plateaux where the polarization is constant as well as smooth crossover regions between different plateaux. Moreover, we can observe the reproducible formation of shoulders in every crossover region, with a value of polarization mid way between the neighbour large plateaux.

larization crossover takes place, independently on the magnetic field or the filling factor where the transition occurs

Later on the analysis of the spin polarization as a function of temperature was carried out. The temperature scaling for $\nu = 1/3, 2/3$ is presented in Fig (3.3) and a further analysis will be presented in Fig (3.9). By fitting the small temperature regime with an activated exponential scaling $\sim \exp[-\Delta/2\mathrm{K_B}T]$, it was experimentally possible to determine the energy gap involved in spin flip processes.

We notice that the state at $\nu = 2/5$ indeed shows a transition from unpolarized to fully polarized while increasing B, a feature previously discussed in connection with the partially polarized Halperin states.
It will be the purpose of the rest of the chapter to address the features presented in

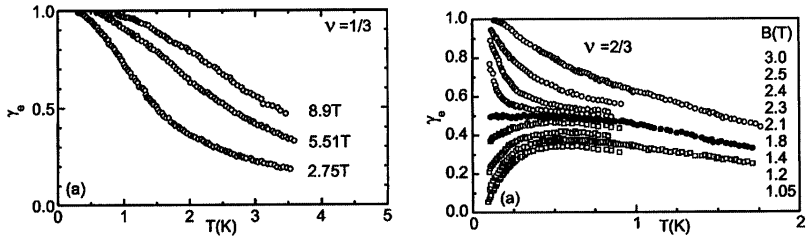

Fig. 3.3: The temperature dependence of the degree of spin polarization at constant $\nu = 1/3$ and $\nu = 2/3$ for different fixed magnetic fields (indicated in the picture) [63]. Notice the full polarization of $\nu = 1/3$ for $T \to 0$ independently on B.

1) and 2) above within the picture of CF with spin [64]. The shoulder mentioned in 3) will be addressed at the end of chapter 5.

We consider the most simple but non-trivial model with only one adjustable parameter, namely the prefactor α in the CF effective mass $m^*(B) = m_0\alpha\sqrt{B}$. We find that the model fits a surprisingly large number of experimental data quantitatively. This strongly indicates that quasi-free CF with spin are a perfect starting point for the theory of the FQHE, though a complete microscopic justification of the model is still lacking.

3.2 Composite Fermions with spin

The singular gauge transformation used up to now to introduce CFs was written for fully spin polarized (or spinless) systems. If we wanted to include the spin in this treatment we could in principle perform the flux attachment in many ways.
For the non-fully spin-polarized states it has been noted that interacting spin-1/2 electrons in two dimensions (2D) in a perpendicular magnetic field can be described as a $U1 \otimes U1$ gauge invariant liquid of spin-up and down electrons that interact with a doublet of Chern-Simons gauge fields [65, 66]. Then, the number of flux quanta associated with spin-up or down fermions can be different. However, one can show that for the principal FQH sequence the effective magnetic field is the same for both species. This generates the states at $\nu = (p_\uparrow + p_\downarrow)/2[(p_\uparrow + p_\downarrow) \pm 1]$ ($p_{\uparrow/\downarrow}$ numbers of filled spin-up/down CFLL).
At mean field we have equal cyclotron gaps $\hbar\omega^*_{c\uparrow} = \hbar\omega^*_{c\downarrow} \equiv \hbar\omega^*_c$. In the following, we focus on the principal sequence with $p = p_\uparrow + p_\downarrow$ (p integer).

As seen in the previous chapter, the mean field assumption has the problem of generating the energy gaps scaling incorrectly. The dimensional analysis of the spinless case by Halperin, Lee and Read [45] yields an activation cyclotron gap at fixed p,

$$\hbar\omega^*_c \propto \frac{1}{2p \pm 1}\frac{e^2}{\varepsilon\ell}\,, \tag{3.3}$$

since the Coulomb coupling $e^2/\varepsilon\ell$ (≈ 51 K$\sqrt{B[\mathrm{T}]}$) is the only energy scale for electrons in the first LL, with the dielectric constant ε ($\approx$ 12.8 for GaAs) and $\ell = (\Phi_0/2\pi B)^{1/2}$ the magnetic length.
Equation (3.3) can be obtained by assuming an effective CF mass $m^* \propto \sqrt{B}$. The activation gap is interpreted as the smallest energy needed to excite a CF from the GS into the first unoccupied CFLL without flips. The scaling law (3.3) has been confirmed by numerical diagonalization of small 2D systems on a sphere [67].

When spin is taken into account, a different energy gap can be introduced, associated with the reversal of the spin of a CF in the uppermost CFLL. In connection to this process, a new effective mass — the "polarization mass" — can be introduced [68, 69].
Both, the activation and the polarization masses scale as $\sqrt{B}$ but with different prefactors, due to their different physical origin.
Estimates for the magnitudes of these gaps have been obtained without taking into account disorder, finite thickness of the sample and LL-mixing. Thus, in experiments typically smaller energy gaps than the theoretically predicted ones are observed [32].
In order to discuss the results of the recent experiments, we consider in the following $m^*/m_0 = \alpha\sqrt{B}$. Such a dependence of m^* on B has been recently observed in experiments [70]. We use α as a fitting parameter that incorporates the mentioned corrections. We will show that the experimental results for *all of the different filling factors* can be described with an accuracy of about 10% by a *unique* choice of α.

The considerations above suggest the following form of the CF cyclotron gap

$$\hbar\omega_{\mathrm{c}}^*(p,B) = \frac{\hbar e}{m_0 c}\,\frac{\sqrt{B}}{\alpha(2p\pm 1)}\ . \tag{3.4}$$

These gaps are consistent with recent numerical investigations [71], especially for $p > 2$.
The Zeeman term can be easily included since it is not affected by the Chern-Simons transformation. It depends only on B. Thus,

$$E_{n_s ps}(B) = \left(n_s + \frac{1}{2}\right)\hbar\omega_{\mathrm{c}}^*(p,B) + \frac{s}{2}\,g\mu_{\mathrm{B}}B \tag{3.5}$$

are the energies of spin-up/down ($s = \pm 1$) CFLLs. The spectrum (3.5) is shown in Fig (3.2) as a function of the magnetic field.

The relevant feature to be stressed is the presence of crossings between LL with opposite spins and different LL index n. In contrast with the IQHE, we see that in the Fractional case crossings of quasiparticle LLs with opposite spin at a given filling can occur *without any in-plane field*, thus in a naturally *isotropic* phase.
With this spectrum in mind we can start analyzing the GS properties for fixed filling factors. We notice, in passing, that a fixed electronic filling implies a fixed CF filling.

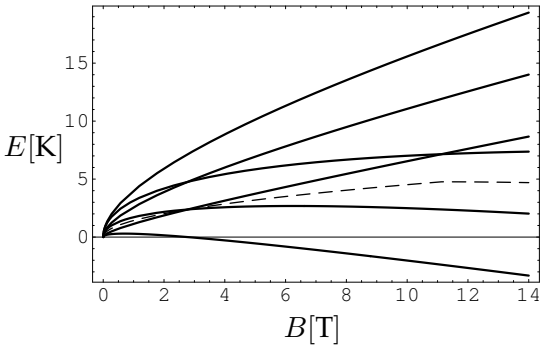

Fig. 3.4: The spectrum of spinful Composite Fermions Landau Levels as a function of the perpendicular magnetic field. Here the mass parameter $\alpha = 0.2$ was chosen, with $p = 2$, suitable for the filling factor $\nu = 2/5$. The Fermi energy is explicitly plot as a dashed line mid way between the second and third CFLL. Notice the occurrence of a CFLL crossing *at the Fermi energy* close to 3 T.

In order to find the ground state at $T = 0$ at a certain B we have to occupy the lowest p CFLLs, if we are interested in the principal sequence $\nu = p/(2mp \pm 1)$. At $T = 0$ the chemical potential lies *exactly in the middle between two CFLL*, as indicated in Fig (3.2). Since the LL degeneracy is the same for all of them, the corresponding zero temperature spin polarization is simply $\gamma_e(B) = [p_\uparrow(B) - p_\downarrow(B)]/p$.
The transitions between differently polarized GS are then given by the crossings between CFLL with different spins *at the Fermi energy*.
For example, the critical magnetic field B_{crit} at which the transition to the *completely* spin polarized GS takes place is obtained as the crossing point between the $n_- = 0$ and the $n_+ = p - 1$ CFLL,

$$B_{\text{crit}}(p) = \left[\frac{2(p-1)}{|g|\,\alpha(2p \pm 1)}\right]^2 . \tag{3.6}$$

We recover the $\nu = 1/2$-limit for $p \to \infty$.
The allowed values of polarization for the incompressible fractions with CFLL filling p are indicated in the table of Fig (3.2), and they agree with the experimentally observed ones in the large plateaux.

Thus, point 1) of the experimental outcomes is addressed at the mean field level with spin.
The comparison of (3.6) with experimentally measured $B_{\text{crit}}(p)$ [61] leads to a first striking result, namely a linear relation between $|g|\alpha$ and ν which is consistent with all the experimentally investigated filling factors, with best fit: $|g|\alpha = -0.075 + 0.787\,\nu$ (see Fig (3.6)).

p	γ_e
1	1
2	0 , 1
3	1/3 , 1
4	0 , 1/2 ,1

Fig. 3.5: The allowed values of the electronic spin polarization γ_e for the fixed filling factors of the principal sequence $\nu = p/(2p \pm 1)$.

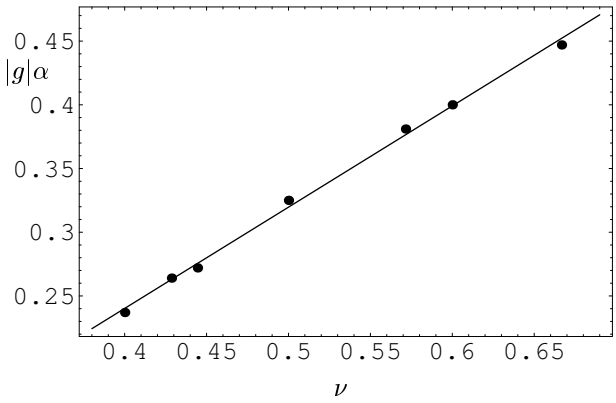

Fig. 3.6: Experimental values [61] for $|g|\alpha$ extracted from (3.6). Best fit $|g|\alpha = -0.075 + 0.787\,\nu$.

From this we can determine the g-factor for a given effective mass (tuned by α). A similar relation has been observed [72] for fractions belonging to the principal sequence of FQH states around $\nu = 3/2$, but in these experiments the crossings were produced by tilting the magnetic field at a constant electron density.
As a byproduct of our analysis we observe that, for $p = 1$, i.e. $\nu = 1/3$, there are no crossings whatsoever and the GS is therefore *always* fully polarized, a result known for a long time in the framework of the wavefunction theory of the FQHE.

Another interesting feature is related to the B dependence of $E_{n_s ps}(B)$ near the crossings. If we define the "slope" $S_{n_s ps}(B) = \partial_B E_{n_s ps}(B)$ it is easy to check that

$$\left| S_{n_\uparrow p\uparrow}(B_{n_\uparrow, n'_\downarrow}) - S_{n'_\downarrow p\downarrow}(B_{n_\uparrow, n'_\downarrow}) \right| = \frac{1}{2}\,|g|\,\mu_{\rm B}, \tag{3.7}$$

where $B_{n_\uparrow, n'_\downarrow}$ is the magnetic field where the two levels $E_{n_\uparrow p\uparrow}$ and $E_{n'_\downarrow p\downarrow}$ cross. Therefore the relative slopes of the two CFLL at the crossing is the same for all the possible crossings at a given filling factor. This is an interesting issue since it means that any fixed characteristic energy scale involved in processes close the

LL crossings will produce quantitatively similar effects *independently* on the chosen crossing point.

3.3 Temperature scaling of the polarization and the spin-flip gap

Having determined the energy spectrum of the CFLL with spin and considering the filling factor fixed, we know the position of the Fermi energy as well as the smallest excitation gap at any given value of B.
In particular we know that the energy gap vanishes at the spin polarization transitions, occurring when two CFLL of opposite spin cross at the Fermi level.
Let us call B_c the magnetic field where the transition takes place. Close to this point, the minimal excitation gap involves a spin-flip process to be overcome and is therefore called "spin-flip gap" (Δ_{sf}). Clearly, at this level, Δ_{sf} vanishes linearly with $B - B_c$. Finally, in the high magnetic field regime, the lowest CFLL have the same spin polarization and the smallest direct excitation gap does not imply spin-flips any longer. We will then recover the fully spin-polarized situation described in the last chapter, with a single particle CF gap given by (3.3).
In Fig (3.3) we show the CF energy gap for $\nu = 1/3, 2/3, 4/7$ ($p = 1, 2, 4$).

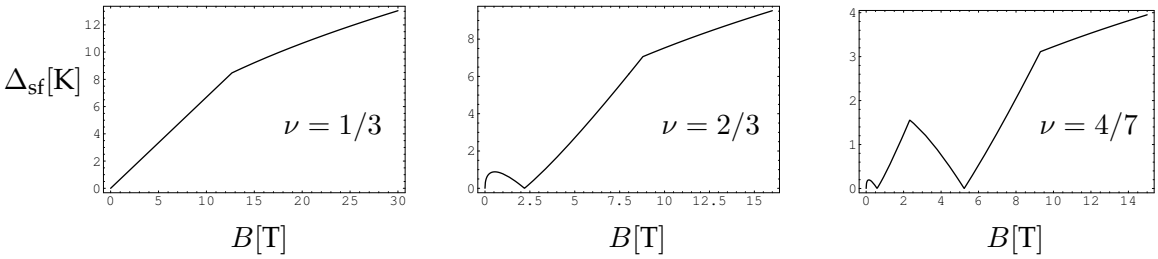

Fig. 3.7: The magnetic field dependence of the spin-flip gap Δ_{sf} for $\nu = 1/3, 2/3, 4/7$. Notice the kink for $\nu = 1/3$, separating the linear spin-related scaling from the Coulomb high-field regime, as well as the reentrant behaviours for $\nu = 2/3$ and $4/7$ associated to the spin polarization transitions.

The fully polarized (at $T = 0$) Laughlin state $\nu = 1/3$ has a gap showing a high field Coulomb scaling as well as a roughly linear small B behaviour, together with a kink separating the two regimes. This feature had been previously shown with numerical techniques [73] and is in agreement with what seen experimentally [32]. For the states with $p \geq 2$, notice the formation of multiple minima connected with the spin polarization transitions.

The spin-flip gap Δ_{sf} is experimentally determined by fitting $\gamma_e(T)$ for small temperatures as $\exp[-\Delta_{sf}/2K_B T]$, for the states whose polarization vanishes at $T = 0$, or as $1 - \exp[-\Delta_{sf}/2K_B T]$, for states with $\gamma_e(T) \to 1$ for $T \to 0$ [63].

With our model we can determine $\gamma_e(T)$ and the comparison with experiments fixes the free parameter α.
Indeed, to get $\gamma_e(T)$ for a certain CF filling and magnetic field, we have to consider the thermal occupation of the SCFLL and evaluate

$$\gamma_e(p,B,T) = \frac{1}{p}\sum_{n_s,s} s\cdot\mathcal{F}(n_s,p,s,B,T) \tag{3.8}$$

with $\mathcal{F}(n_s,p,s,B,T)$ the Fermi occupation of the energy level E_{n_sps} at magnetic field B and temperature T. Notice that the Fermi distribution depends on the chemical potential $\mu_p(B,T)$, which must be determined selfconsistently as a function of temperature by imposing that the sum of the spin up and spin down CF is equal to their total number. Dividing both the terms by the CFLL degeneracy we obtain the equation for $\mu_p(B,T)$

$$p = \sum_{n_s,s}\frac{1}{\exp\left[\left(E_{n_sps}(B)-\mu_p(B,T)\right)/\mathrm{K_B}T\right]+1}\ . \tag{3.9}$$

This equation can be solved numerically for a given p and B and the resulting scaling of μ with T is very weak at the typically interesting temperatures investigated in the experiments, see Fig (3.3).

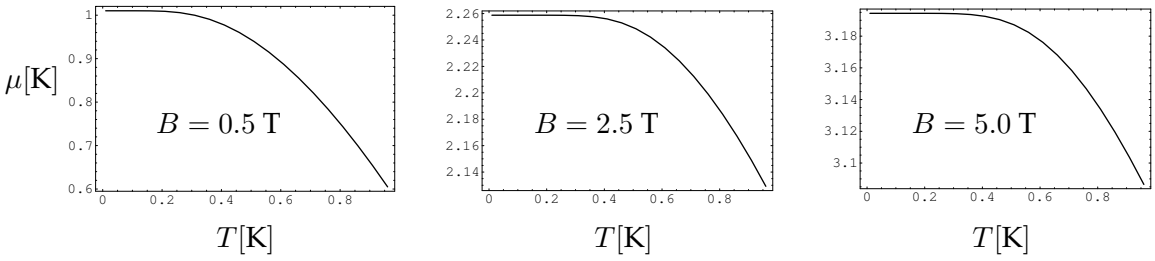

Fig. 3.8: The temperature dependence of the chemical potential at $\nu = 2/5$ for three different magnetic fields (indicated in the pictures). It is possible to see that, at small temperatures, $\mu(T)$ is essentially constant.

Some results for $\gamma_e(p,B,T)$ for various p's and B's are shown in Fig (3.9). The polarization for $\nu = 1/2$ has been obtained in the limit $p\to\infty$.
Comparing with experiments, one observes that the data in [61, 62, 63, 74] can be described within 10% by choosing α independently on the filling factor, i.e. once and for all for a given sample. The data obtained from the sample of Ref. [61, 62, 63] are well described by choosing $\alpha = 0.2$ (see Fig (3.9) a, b) while the measurements in [74] are better fitted by $\alpha = 0.6$ (an analysis of the data of Ref. [74] is presented also in [69]).
In order to improve the fit, in Fig (3.9)c we have plotted the lowest five modes with $\alpha = 0.24$ and the remaining four with $\alpha = 0.16$. The slightly better agreement obtained in this way could reveal a slight dependence of α on B.

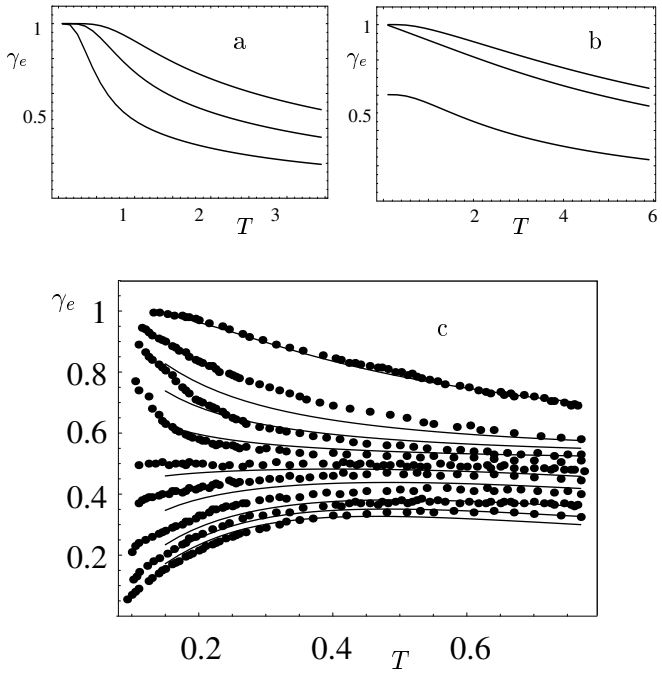

Fig. 3.9: Temperature dependence (T in Kelvin) of γ_e for fixed filling factors and magnetic fields. (a) $\nu = 1/3$ $B = 2.75, 5.51, 8.9$ T (bottom to top), to be confronted with Fig (3.3); (b) $\nu = 1/2$ $B = 3.3, 9.3, 12$ T (bottom to top); (c) $\nu = 2/3$ $B = 1.05, 1.2, 1.4, 1.8, 2.1, 2.3, 2.4, 2.5, 3.0$ T (bottom to top). Results (a) and (b) are obtained with $\alpha = 0.2$, while in (c) $\alpha = 0.24$ for $B \leq 2.1$ T and $\alpha = 0.16$ for $B > 2.1$ T. Experimental data (bullets, data from [63]) are obtained at the same B as the theoretical curves.

Having fixed the mass parameter α we obtain the excitation gaps depicted in Fig (3.3), to be compared with the experimentally extracted ones. The spin flip gap at $\nu = 2/3$ has been measured in [63] and shows a pronounced reentrant behaviour, close to the transition, consistent with our theoretical prediction (see Fig (3.10)).

The experimental determination of the gap is difficult close to B_c since Δ_{sf} becomes critically small. However it seems that a *small but finite* excitation energy survives near the criticality, with a typical scale of $0.2 - 0.3$ K. This is the energy scale involved in the additional structures present close to the spin polarization transition, i.e. the Zero Temperature Smoothening (ZTS) and the additional shoulder described at points 2 and 3 of our initial analysis. Having determined the spectrum, it can be directly checked that, indeed, this minigap is associated with a typical magnetic field deviation from B_c of the right order of magnitude for the comparison with experiments (see Fig (3.11)).

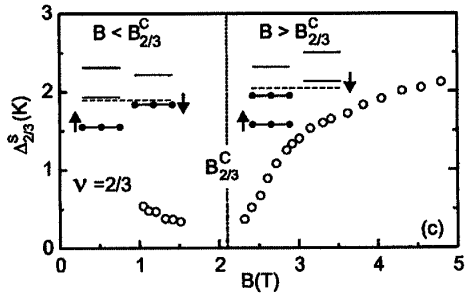

Fig. 3.10: The experimental spin-flip gap for fixed $\nu = 2/3$ as a function of B [63]. A reentrant behaviour is clearly visible. The typical energy scale involved in the smooth transition region is of the order of 0.3 K.

we will now concentrate on the mechanisms producing the ZTS, while the additional polarization shoulders will be addressed in Chapter 5.

3.4 Zero Temperature Smoothening (ZTS)

So far, at $T = 0$, the model predicts step-like transitions of $\gamma_e(B)$ at the magnetic fields for which the Fermi energy is at a crossing point between two spin-up/down CFLL. On the other hand, the experimental data, extrapolated to $T = 0$, show smooth cross-overs. In the following, we suggest different origins for such a behaviour.

3.4.1 The role of Disorder

A first contribution to the smoothening at $T = 0$ is the disorder-induced broadening of the CFLL. If the DOS of the crossing CFLL are broad, within a single particle picture it is easy to see that the Fermi energy lies in their overlap for the magnetic fields around the transition. The relative population of the two spin modes is then a continuous function of B even at $T = 0$, producing the observed smooth zero temperature spin polarization transition. It is therefore crucial to investigate the DOS of the CFLL in presence of a disorder potential.
At the filling factors considered, the random electrostatic potential is strongly screened and the residual disorder is dominated by a long-range randomly fluctuating magnetic field associated with the distribution of the fluxes connected to the screening charge density.
The problem of a charged quantum particle (electron or CF) constrained to move in two dimensions in a random magnetic field (RMF) has recently attracted a lot of theoretical and experimental interest [75, 76, 77, 78, 79]. So far, most of the work was concerned with RMFs with zero or small mean value, which are believed to effectively describe a 2DEG near filling factor $\nu = 1/2$.
The standard way to calculate the single-particle relaxation time of electrons in a

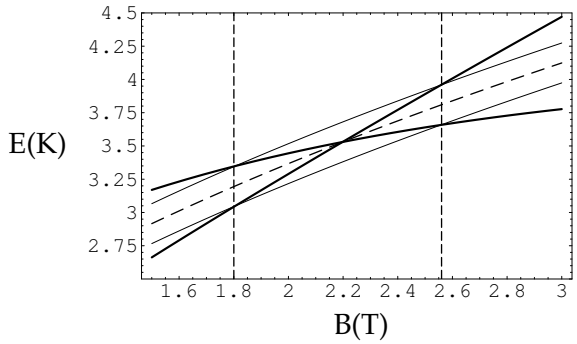

Fig. 3.11: The SCFLL crossing of interest for the spin polarization transition at $\nu = 2/3$ as functions of the magnetic field. Here the two crossing levels $|0,\downarrow\rangle$ and $|1,\uparrow\rangle$ are depicted as thick lines, together with the Fermi energy (dashed line) passing through the crossing point. The two thin lines represent the Fermi energy shifted upwards and downwards by 0.15 K, so to mimic a characteristic energy window of 0.3 K (in agreement with the experimental indications) close to the transition. This window is associated to a magnetic field region, "guarding" the critical field B_c, delimited by the two vertical lines. The magnetic field size of this region is in agreement with the transition region observed in the zero temperature measurements (see Fig (3.2)).

random scalar potential is via the momentum integral of the imaginary part of the self-energy Σ for the single-particle Green's function, as we saw in section 1.3.2.
In the RMF case, this approach is questionable because the single-particle Green's function is not a gauge invariant quantity. Moreover, for vanishing average field, within the self-consistent Born approximation (SCBA), the calculation of the self-energy is plagued by infrared divergencies [75] which are due to the long range nature of the correlator of the vector potentials.
To circumvent these difficulties, E. Altshuler et al. [77] calculated the DOS of electrons in a RMF in the semiclassical approximation, assuming that the energy E of the particle is much larger than both the cyclotron energy and $1/\tau$, where $1/2\tau$ is the width of LLs due to the RMF ($\hbar = 1$). This would correspond to consider large LL number ($p \gg 1$ for CF).
In the analogous semiclassical calculation for spinless CF, we would start with the Hamiltonian

$$H_{\text{Dis}} = \sum_i \frac{1}{2m^*} \left[\mathbf{p}_i + \frac{e}{c}\left(\mathbf{A}(\mathbf{r}_i) + \delta\mathbf{A}(\mathbf{r}_i)\right)\right]^2 \tag{3.10}$$

where $\mathbf{A}(\mathbf{r})$ is the vector potential generating the average mean magnetic field B^* and $\delta\mathbf{A}(\mathbf{r})$ generates the RMF. We also assume a Gaussian, δ-correlated RMF

$$\langle \delta B(\mathbf{r}) \delta B(\mathbf{r}') \rangle = B_0^2 \, \delta(\mathbf{r} - \mathbf{r}') \tag{3.11}$$

where $\langle ... \rangle$ indicates the average over the disorder. The corresponding vector potential correlator (in the momentum space) is

$$\langle \delta A_\alpha(\mathbf{q}) \delta A_\beta(\mathbf{q}') \rangle = \frac{B_0^2}{q^2}\, \delta_{\alpha\beta}\, \delta(\mathbf{q}+\mathbf{q}') \,. \tag{3.12}$$

In the semiclassical approximation, the Density of States DOS(E) (proportional to the imaginary part of the one point Green's function G(E)) can be shown to be given by the disorder averaged path integral over the closed classical trajectories, x_E

$$\mathrm{DOS}(E) = \frac{m^*}{2\pi}\left[1 + \mathrm{Re}\left\langle \oint \mathcal{D}x_E \;\exp\left(i\mathcal{S}[x_E]\right)\right\rangle\right] \,. \tag{3.13}$$

In the same spirit of the theory of the weak localization, the approximation is made to take the orbits as the free ones (i.e. closed cyclotronic circles in the effective field B^*) but with a phase influenced by the vector potential. In particular, using Stoke's theorem we can transform the phase contribution $\oint \mathrm{d}\mathbf{l}\cdot(\mathbf{A}+\delta\mathbf{A})$ into a surface integral and write the action on a generic path as

$$\mathcal{S} = \frac{e}{c}\int_{\mathrm{S}} \mathrm{d}\mathbf{r}\,(B^* + \delta B(\mathbf{r})) \tag{3.14}$$

where S is the area enclosed by the trajectory.
Assuming that the RMF is a small perturbation to the mean field B^* ($\hbar\omega_{\mathrm{c}}^* \gg m^* v_0^2$, where $v_0^2 = e^2 B_0^2/4m^{*2}c^2$), the classical trajectories are not affected by the RMF and are circles with radius $R_c = v/\omega_{\mathrm{c}}^*$ (v is the velocity of the particle); more precisely, every circle gives rise to infinitely many trajectories labelled by their winding number.
For the disorder average over a Gaussian RMF we have

$$\left\langle \exp\left(i\frac{e}{c}\int_S \mathrm{d}\mathbf{r}\;\delta B(\mathbf{r})\right)\right\rangle = \exp\Big(-\frac{e^2}{2c^2}\int_S \mathrm{d}\mathbf{r}\int_S \mathrm{d}\mathbf{r'}\,\left\langle \delta B(\mathbf{r})\,\delta B(\mathbf{r'})\right\rangle\Big) \,. \tag{3.15}$$

Hence, the DOS (3.13) can be calculated, with the averaged action on the trajectories

$$\mathcal{S}_{\mathrm{av}} = \frac{e}{c}\, S_{\mathrm{or}}\, B^* + \frac{e^2}{2c^2}\, B_0^2\, S_{\mathrm{nor}} \tag{3.16}$$

where S_{or} and S_{nor} are the oriented and non-oriented areas enclosed by the trajectory, respectively.
Carrying out the sum over the circles with different winding number, a Gaussian DOS is obtained (ℓ^* the magnetic length associated to B^*)

$$\mathrm{DOS}(E) = \frac{1}{2\pi\ell^{*2}}\sum_{n=0}^{\infty}\frac{\tau(E)}{\sqrt{\pi}}\;\exp\left(-\tau^2(E)\left[E-\left(n+\frac{1}{2}\right)\hbar\omega_{\mathrm{c}}^*\right]^2\right) \tag{3.17}$$

and the width of the levels is

$$W(E) \equiv \frac{1}{2\tau(E)} = \sqrt{\frac{Em^*v_0^2}{\pi}} \,. \tag{3.18}$$

In our system the mean magnetic field can be relatively strong (only few Landau levels are filled) and the semiclassical approximation is not fully justified but we believe that the expression (3.18) yields a reasonable semiquantitative estimate of the broadening in this regime as well.
In the case of CFLLs, m^* is the effective mass of the CF around the magnetic fields of interest for the spin polarization transition and $B_0^2 \approx \nu(\Phi_0/2\pi l)^2$ [80, 45]. The width of the n-th LL, W_n is then

$$W_n \equiv W\left((n+1/2)\hbar\omega_c^*\right) = \sqrt{\frac{(n+1/2)\hbar\omega_c^* m^* v_0^2}{\pi}} \tag{3.19}$$

showing weak LL number and magnetic field dependences.
Let us focus on the $\nu = 2/3$ state: assuming that $B \approx 2$ T (around which the polarization transition occurs) with the parameters of the GaAs-AlGaAs heterostructures we get, for the 0-th LL, $W_0 \approx 0.34$ K. As mentioned in the last section this is the typical energy scale involved in the experimental ZTS. Moreover the ZTS regions seem not to dependent significantly on the different spin polarization transitions, suggesting a weak energy scaling of the disorder induced CFLL broadening.
Of course, we have made some simplifying assumptions to get formula (3.19): in the experiments of Kukushkin et al., the δ-doped monolayer is separated from the 2DEG by an undoped spacer of width $d \approx 30$nm. Therefore, the range of the RMF generated by the density fluctuations (of the order of d) is longer than the magnetic length for $B^* > 1$ T. In order to describe more closely the experiments, a deeper analysis of the strong residual field and of the longer RMF correlations is needed.
In this direction, we performed preliminary calculations of the CF Green's function in the SCBA for the strong residual magnetic field case. If Landau level mixing is neglected, in analogy with the approximate treatment of random scalar potentials [81, 82], the fermionic self-energy is finite. Surprisingly enough, the LL widths obtained in this approximation have the same dependence on B^*, B_0^2 and n as formula (3.19). However singular terms appearing due to Landau level mixing lead to divergencies as in the zero mean field case. The treatment of these divergencies is presently a highly debated problem and further investigations of this delicate issue are under study.

3.4.2 Spin-orbit effects

The disorder-induced broadening of the CFLLs is not the only origin of the ZTS. One can also obtain it by anticrossing of the CFLL near the critical fields. In analogy with the IQHE [83], anticrossing could be driven by spin-orbit coupling.
In order to obtain the effective spin-orbit Hamiltonian for the CFLL involved in the transition, let us start with the single particle 2D Bychkov-Rashba term

$$V_{\text{Rashba}}^{\text{2D}} = \frac{\hbar e\langle E_z\rangle}{4m_0^2c^2}\,\hat{\mathbf{z}}\cdot\mathbf{s}\times\mathbf{\Pi}\,. \tag{3.20}$$

where $\langle E_z\rangle$ is the average electric field built into the heterojunction along the growth direction z.

We can write the kinetic momentum $\mathbf{\Pi}$ in terms of the interLL operators a, $a^\dagger$ (with $a^\dagger|n,k\rangle = \sqrt{n+1}\,|n+1,k\rangle$, where $|n,k\rangle$ describes the state of the n-th LL with internal momentum k): $\Pi_x = i\ell^*/\sqrt{2}\hbar(a^\dagger - a)$ and $\Pi_y = \ell^*/\sqrt{2}\hbar(a^\dagger + a)$ and the Pauli matrices s_x, s_y in terms of the rising and lowering spin operators $s_\pm = s_x \pm i s_y$. Then we obtain the effective Hamiltonian for two close CFLL with opposite spins

$$H_{\rm SO} = E_{n_\uparrow+1,p,\uparrow}(B)\; c^\dagger_{n_\uparrow+1,\uparrow} c_{n_\uparrow+1,\uparrow} + E_{n_\downarrow,p,\downarrow}(B)\; c^\dagger_{n_\downarrow,\downarrow} c_{n_\downarrow,\downarrow} + \\ + \left(V_{\rm SO}\; c^\dagger_{n_\uparrow+1,\uparrow} c_{n_\downarrow,\downarrow} + \text{h.c.}\right) \quad (3.21)$$

with $V_{\rm SO} = \sqrt{2}\hbar^2 e\langle E_z\rangle/4m_0^2c^2\ell^*$ and $c_{n_s,s}$ the annihilation operator for a particle in the state $|n_s,k\rangle$ and spin s. Notice that the spin-orbit coupling is diagonal in the internal momentum and the corresponding index has been omitted for simplicity. By diagonalizing (3.21) we get the resulting single particle split eigenmodes $\Psi_\pm$ as linear combinations of the CFLL eigenfunctions ψ_{n_s},

$$\Psi_\pm = \mathcal{N}\left[\psi_{n_\downarrow} + \left(\frac{\Delta(B)}{2V_{\rm SO}} \pm \sqrt{\left(\frac{\Delta(B)}{2V_{\rm SO}}\right)^2 + 1}\right)\psi_{n_\uparrow+1}\right] \quad (3.22)$$

where $\Delta(B) = E_{n_\uparrow+1,p,\uparrow}(B) - E_{n_\downarrow,p,\downarrow}(B)$ and $\mathcal{N}$ is a normalization factor. The new eigenenergies are

$$\epsilon_\pm(B) = \frac{E_{n_\uparrow+1,p,\uparrow}(B) + E_{n_\downarrow,p,\downarrow}(B)}{2} \pm \sqrt{\left(\frac{\Delta(B)}{2}\right)^2 + V_{\rm SO}^2}\,. \quad (3.23)$$

It can be seen how the eigenmodes (3.22) have expectation values of the spin that change smoothly from, say, $\downarrow$ to $\uparrow$ when B moves from the left to the right of $B_{n_\uparrow+1,n_\downarrow}$. By evaluating with these states $\gamma_e(B)$ at $T=0$ we obtain the cross-over behaviour shown in Fig (3.12) for $\nu = 2/5$ (dashed line).

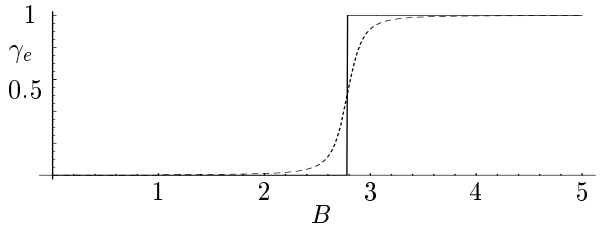

Fig. 3.12: Spin polarization of the GS at $T=0$ for $\nu = 2/5$ as a function of B (in Tesla), for $\alpha = 0.2$. Full line: with level crossing. Dashed line: with anticrossing ($V_{\rm SO} = 0.1$ K, see text).

The width of the crossover region in B is a function of $V_{\rm SO}$, which also represents half of the smallest energy separation (the gap) between the eigenmodes. The typical spin-orbit-induced splitting in GaAs heterostructures is of the order of 0.2-0.3

K. Again, we obtain the right energy scale needed to produce the observed ZTS. Similar results can be obtained for the other ν's considered in [61].
In a real experiment both the disorder induced broadening of the CFLL and the spin-orbit anticrossing contribute to the ZTS.

Up to now we never considered the role of the residual fermionic interaction close to the degeneracy point. This seems to be a crucial issue for the explanation of the observed shoulder in the polarization experiments.
The first attempt we could try in this direction is to treat the CF Coulomb interaction at Hartree-Fock level. This would keep memory of the CF charge neglecting the role played by the attached fluxes, and by the consequent Chern-Simons interaction. Of course, these are drastic approximations and we will see that, indeed, we will have to go beyond this level to grasp the nature of the partly polarized state.
In 1985 Giuliani and Quinn considered the problem of two LL of electrons brought to coincidence (via a tilted magnetic field configuration) and coupled by the Coulomb interaction [84]. The purpose of their investigation was to determine whether a spin-density wave GS close to the crossing is possible, or if otherwise the only stable configurations are obtain by pure occupations of one mode only.
By performing a direct (non self-consistent) Hartree-Fock calculation they deduced that a *first-order* phase transition should be expected in the polarization, and that no spin-density wave GS should form. In the following years a similar calculation has been performed in presence of inhomogeneities with the result that the first-order phase transition should still be the expected behaviour [85].
The existence of the shoulder in the polarization experiments shows that more complex structures come up near the degeneracy of two CFLLs, and that the Hartree-Fock analysis is not enough to describe them. The nature of these partly polarized states will be addressed in Chapter 5.

3.5 Summary

To summarize this chapter, we have considered the spin polarization of the ground state for the FQHE at fixed filling factors in terms of CFs with spin.
We have found that a large number of experimentally detected features, such as the temperature scaling of the polarization, as well as the B -dependence of the spin-flip gap, can be described quantitatively by fitting only one parameter for a given sample, namely α.
The analysis of the Random Magnetic Field-influence on the DOS of CFLL with large residual fields has been presented, as well as a study of the spin-orbit effects near the degeneracy of two CFLLs of opposite spins. The two effects act simultaneously to induce the Zero Temperature Smoothening of the spin polarization transitions.
Altogether, the results show the remarkable versatility of the single particle CF picture for the FQHE. The role of the residual interactions between CF close to the LL coincidence will be considered in detail in Chapter 5. The outcomes of that investigation could lead to the explanation of the shoulder mentioned in point 3) of

Kukushkin's experimental analysis as a condensation instability of the GS.

In order to address this issue and to set the basis for the topic to be presented in Chapter 6, we will need the physical and formal apparatus of the theory of superconductivity. The next Chapter is devoted to this purpose.

4. INTRODUCTION TO THE THEORY OF SUPERCONDUCTIVITY

In this chapter we will present a brief introduction to the theory of superconductivity. Together with the QHE, superconductivity is a remarkable example of quantum effects on a macroscopic scale.
This phenomenon was first observed in 1911 by H. Kamerlingh-Onnes [86] while studying the transport properties of Hg at very small temperatures. Onnes realized that by cooling down Hg under a critical temperature T_c (typically of the order of 2 K, via liquid He, a discovery he had made in 1910!) its properties changed dramatically.
The first surprising effect was the resistance dropping abruptly to zero below T_c. In the following years it was discovered that superconductors are perfect diamagnets (the magnetic field inside a bulk superconductor is zero) for not too high external magnetic fields, the so-called "Meissner-Ochsenfeld Effect" [87]. Moreover there exists a critical temperature-dependent magnetic field beyond which superconductivity is destroyed.
It is not the purpose of the present chapter to present a complete analysis of the experimental findings in the broad field of superconductivity. We will rather concentrate on the theoretical considerations that lead to the microscopical theory and dwell on the properties of the outcoming GS.
There is now a vast literature concerning the topic of superconductivity. Among the books I consulted, the ones by Schrieffer and de Gennes deserve a particular mention [55, 88]. Many issues not discussed here will be found in great detail there and in many introductory and specialistic reviews.

At the time of the discovery of superconductivity, no previously developed theory of metals including the Sommerfeld and Bloch pictures, not to mention the Drude model, was able to grasp the essential physics behind this phenomenon. Indeed, it took 46 years after Onnes' experiment before the microscopic theory of superconductivity by Bardeen, Cooper and Schrieffer (BCS) came out [89]. In the same years an independent treatment was presented by Bogoliubov and Valatin [90, 91], accounting for the existence of bizarre gapped quasiparticle excitations out of the GS condensate.
The BCS theory made the conceptual step of introducing what is now called the "spontaneous symmetry breaking", and the possibility of having anomalous operator averages on the condensed GS, as we will see.

In this chapter we will first present an introduction to the BCS theory within the many-body wavefunction picture, as originally formulated by the authors in 1957. We will consider the standard "s-wave pairing picture" and its modification

into "p-wave case", as this issue will come up again in our last chapter on the non-abelian quantum statistics.
In the second part of the chapter we will consider the field theoretical treatment of superconductivity within the framework of the many-body Green's functions technique, as originally introduced by Nambu and Gor'kov.

4.1 The BCS wavefunction theory

One of the first elements that was soon realized to lie at the basis of the superconductive behaviour was the existence of a finite excitation gap. By lowering the temperature below T_c the Fermi Liquid becomes unstable and the system gains a finite energy by rearranging the structure of the GS, a process called "condensation". In contrast with the behaviour of a Normal Fermi liquid, in the superconductive condensate, the GS is separated from its single-particle excitations by a finite energy, set by the effective interactions between electrons. External perturbations applied to the system with typical energy smaller than the gap cannot produce excitations: the system remains in its GS and the macroscopic properties are unaltered. In this way, by pushing a not too large electron current through the system, no dissipation can occur and the vanishing resistance is acquainted for. Analogously, the introduction of an external magnetic field with characteristic associated energy smaller than the gap will not move the system away from the GS, thereby not destroying its superconductive correlations.
By "condensation" it is meant that the occupation of the single particle states by electrons is different between the Normal (N) and the Superconducting (SC) state. Within the Landau theory of Fermi Liquids we know that, at $T = 0$, all the *quasiparticle* states below the Fermi energy are independently occupied according to the Pauli principle and all the states above it are empty. The role of interactions is incorporated in modifying the quasiparticle properties, like the effective mass we saw in Chapter 2. Finally we point out that the Landau theory is particularly suitable for describing the properties of the quasiparticles with energy close to the Fermi level, which are the crucial ones in all the low energy phenomena, like linear transport, specific heat, and so on. Since the energy gap in the SC phase opens up around the Fermi energy it is natural to assume the Fermi liquid states as the standard quasiparticle basis on which to write the effective low energy theory. We will see that, in the SC state at $T = 0$, the quasiparticle distribution differs from the Fermi-Dirac one around E_F and their occupation is no longer independent.

4.1.1 The Cooper instability for the one-pair problem

A major step towards the comprehension of the fundamental mechanism for the condensation was made by Leon Cooper by studying a model of two interacting fermions over a filled Fermi sea of non-interacting particles [92]. Although oversimplified, this study set the basis for the successive BCS form of the many-electrons GS.
Let us imagine to have two fermions interacting via a non-retarded two-body potential V, over a filled 3D Fermi sea at $T = 0$. The electrons in the sea are neither interacting with each other, nor with the two additional particles. Via the exclusion principle they simply forbid the additional particles from occupying states below the Fermi energy.
We assume the system to be translationally invariant. The center of mass momentum $\hbar\mathbf{q}$ and spin of the pair are therefore conserved quantities. If we introduce out of the two particle positions $\mathbf{r}_1$ and $\mathbf{r}_2$ the center of mass and relative coordinates

$\mathbf{R} = (\mathbf{r}_1 + \mathbf{r}_2)/2$ and $\mathbf{r} = \mathbf{r}_1 - \mathbf{r}_2$, the orbital wavefunction of the pair is written as

$$\psi(\mathbf{r}_1, \mathbf{r}_2) = \varphi_{\mathbf{q}}(\mathbf{r})\ e^{i\mathbf{q}\cdot\mathbf{R}}\ . \tag{4.1}$$

If we limit ourselves to the $\mathbf{q} = 0$ case, where the net current vanishes, the pair wavefunction is rotationally invariant and is therefore an eigenstate of the angular momentum. For the spin singlet case the orbital wavefunction has to be symmetric while the triplet is associated to an antisymmetric orbital state.
Let us consider for simplicity the spin singlet state with lowest ($l = 0$ or s-wave) angular momentum. The resulting pair state can be expanded in terms of plane waves as

$$\psi(\mathbf{r}_1, \mathbf{r}_2) = \varphi_{\mathbf{q}=0}(\mathbf{r}) = \sum_{\mathbf{k}} a_{\mathbf{k}}\ e^{i\mathbf{k}\cdot\mathbf{r}} = \sum_{\mathbf{k}} a_{\mathbf{k}}\ e^{i\mathbf{k}\cdot\mathbf{r}_1}\ e^{-i\mathbf{k}\cdot\mathbf{r}_2} \tag{4.2}$$

where the summation is extended to states with positive energy with respect to E_{F}. Thus the pair wavefunction is a *superposition* of configurations where the *pairs* of plane wave states $(\mathbf{k}, -\mathbf{k})$ are occupied.
The eigenstates of the pair are determined by solving the Schrödinger equation

$$E\ \psi = (H_0 + V)\psi \tag{4.3}$$

where H_0 is the free quasiparticle Hamiltonian

$$H_0 = \sum_{\mathbf{k},s} \varepsilon_{\mathbf{k}}\, c^{\dagger}_{\mathbf{k},s} c_{\mathbf{k},s} \tag{4.4}$$

and $\varepsilon_{\mathbf{k}}$ is the kinetic energy of a fermion with momentum $\hbar\mathbf{k}$ measured from E_{F}. From (4.2) we can rewrite (4.3) as

$$(E - 2\varepsilon_{\mathbf{k}})a_{\mathbf{k}} = \sum_{\mathbf{k}'} V_{\mathbf{k}\mathbf{k}'} a_{\mathbf{k}'} \tag{4.5}$$

where $V_{\mathbf{k}\mathbf{k}'}$ is the interaction matrix element describing the process where a pair $(\mathbf{k}, -\mathbf{k})$ is scattered into $(\mathbf{k}', -\mathbf{k}')$.
To simplify the treatment and solve (4.5) let us assume that the model interaction has the constant value λ and acts only between particles lying within an energy window ω_{D} around E_{F}. This means that $V_{\mathbf{k}\mathbf{k}'}$ is factorizable as

$$V_{\mathbf{k}\mathbf{k}'} = \lambda w_{\mathbf{k}} w^{*}_{\mathbf{k}'} \tag{4.6}$$

where $w_{\mathbf{k}} = 1$ if $0 \leq \varepsilon_{\mathbf{k}} \leq \omega_{\mathrm{D}}$ and 0 elsewhere. Up to now we let λ and the cutoff energy ω_{D} free. In the following we will comment about the effective interactions occurring in a metal and the cutoff will be given a physical meaning and range.
Equation (4.5) becomes

$$(E - 2\varepsilon_{\mathbf{k}})\, a_{\mathbf{k}} = \lambda\, w_{\mathbf{k}}\, C \tag{4.7}$$

with $C = \sum_{\mathbf{k}'} w^{*}_{\mathbf{k}'} a_{\mathbf{k}'}$. It follows that

$$a_{\mathbf{k}} = \frac{\lambda w_{\mathbf{k}} C}{E - 2\varepsilon_{\mathbf{k}}} \tag{4.8}$$

which, inserted into the definition of C leads to the consistency equation

$$\frac{1}{\lambda} = \sum_{\mathbf{k}} \frac{|w_{\mathbf{k}}|^2}{E - 2\varepsilon_{\mathbf{k}}} \equiv \Phi(E) \; . \tag{4.9}$$

The eigenenergies of our problem are thus determined by the crossing points between the function $\Phi(E)$ and the constant $1/\lambda$.
To get a feeling of the solutions let us consider the function $\Phi(E)$ in more detail. It clearly has poles at the *positive* energies $2\varepsilon_{\mathbf{k}}$ for all the allowed states $\mathbf{k}$ above the Fermi sea. For a finite system these energies are discrete but tend to become a continuous band in the thermodynamic limit. Finally, for negative E, $\Phi(E)$ is regular and goes as $1/E$ for large $|E|$. A plot of the shape of $\Phi(E)$ is shown in Fig (4.1).

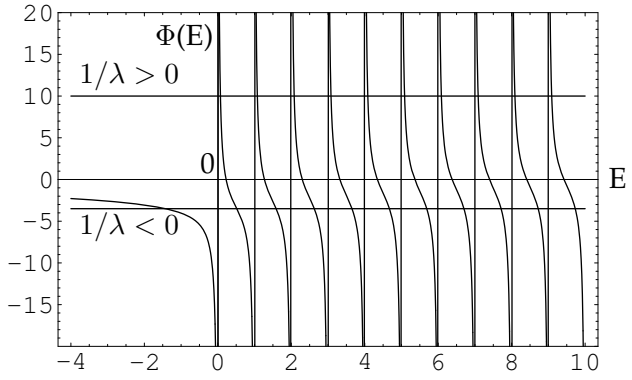

Fig. 4.1: The Cooper function $\Phi(E)$. In the comb region for positive energy, Φ has singularities at the discrete unperturbed energies (the level spacing has been chosen to be 1). Two constant values of $1/\lambda$ are shown, for both repulsive ($\lambda > 0$) as well as attractive ($\lambda < 0$) interaction. The pair energy is given by the intersections between $\Phi(E)$ and $1/\lambda$. Notice the negative energy solution for attractive interactions, associated to the Cooper pair bound state.

Two quite different results come out of the possible choices for λ. Indeed, for positive λ (repulsive interactions) the allowed eigenenergies solutions of (4.9) lie in the comb region $E > 0$ and in the thermodynamic limit they tend to the unperturbed values $2\varepsilon_{\mathbf{k}}$.
If, on the contrary, λ is negative (corresponding to an attractive interaction between electrons close to the Fermi energy) there always exists a solution with *negative* E, due to the intersection in the region where $\Phi(E)$ has the hyperbolic behaviour (see Fig (4.1)). This solution describes a *bound* state for the pair.
With our choice of $w_{\mathbf{k}}$ it is easy to evaluate the binding energy. We can in fact transform the sum over the $\mathbf{k}$'s into an energy integration up to ω_{D} by passing through the density of states. If the integration cutoff is much smaller than the Fermi energy

we can approximate the regular 3D DOS with its value at E_{F}, N_0, to get

$$\frac{1}{|\lambda|} = \frac{N_0}{2} \ln\left(\frac{|E| + 2\omega_{\mathrm{D}}}{|E|}\right) . \tag{4.10}$$

The binding energy therefore is

$$|E| = \frac{2\omega_{\mathrm{D}}}{\exp\left(\frac{2}{N_0|\lambda|}\right) - 1} . \tag{4.11}$$

It grows linearly with the cutoff energy but the more interesting scaling is with respect to the interaction strength λ. For a strong attractive interaction ($N_0|\lambda| \gg 1$) we can expand the exponential to get

$$|E| \simeq N_0|\lambda|\omega_{\mathrm{D}} \tag{4.12}$$

while the weak coupling regime $N_0|\lambda| \ll 1$ yields

$$|E| \simeq 2\omega_{\mathrm{D}} \exp\left(-\frac{2}{N_0|\lambda|}\right) . \tag{4.13}$$

The crucial point shown by this argument is the existence of a bound state for *arbitrarily weak attractive* interactions, whose binding energy is extremely sensitive to the interaction strength itself.
Cooper suggested that the condensation instability of the metallic GS at small temperatures had to do with an occupation rearrangement in which pair of electrons enter the bound states described in the previous analysis. If it is energetically advantageous to take two particles and let them form the mentioned bound state, it will be even more to let many particles enter the bound states. However we have to keep trace of the fermionic nature of electrons, forbidding an independent Bose-like condensation.
Along this line of thinking the BCS picture of the superconducting GS was conceived.

While discussing the Cooper problem we considered the wavefunction for two particles over an inert Fermi sea. The successive BCS treatment included *all* the particles in a properly antisymmetrized way, thanks to the automatic statistical treatment offered by the second quantization operators, as we will see.
Suppose we were to tackle the same N-particle problem in terms of the electron-pairs, i.e. we want to produce a trial wavefunction for the system at $T = 0$. Then we first have to produce an *antisymmetric* two body wavefunction $\varphi(\mathbf{r} - \mathbf{r}'; s, s')$. Then we associate to every possible pair of electrons *this* function and finally antisymmetrize with respect to the permutations leading to different pairing choices and normalize with a prefactor $\mathcal{N}$. The resulting many-electron state is

$$\begin{aligned} \Psi &= \mathcal{N}\{\varphi(\mathbf{r}_1 - \mathbf{r}_2; s_1, s_2)\varphi(\mathbf{r}_3 - \mathbf{r}_4; s_3, s_4)... + \\ &- \varphi(\mathbf{r}_1 - \mathbf{r}_3; s_1, s_3)\varphi(\mathbf{r}_2 - \mathbf{r}_4; s_2, s_4)...\}. \end{aligned} \tag{4.14}$$

This state has the correct symmetry properties and it is clear that, if we choose the function φ properly, so that the two particles in the pair get the maximum possible binding energy, this will automatically happen for all the particles in the condensate. This was the original line of thinking of Cooper, before the BCS condensation in the space of the states was introduced.
It will be the purpose of the next section to describe the BCS GS and its zero temperature properties.

4.1.2 The BCS Ground State

The Cooper argument presented above can be generalized to the case where the pair has a nonvanishing net momentum, describing a configuration with a finite current. However, Cooper showed that the pair state with $\mathbf{q} = 0$ is the most unstable, having the largest condensation energy.
The next logical step to formulate a picture of the SC GS is to start occupying pairs with opposite momenta, starting from the bottom of the free electron band. As in the previous section a spin singlet, $l = 0$ (s-wave) pair structure is considered and the GS parameters will be chosen to minimize the expectation value of the effective Hamiltonian of the system.
The essential physical point of the Cooper analysis was to isolate, among the interactions between electrons, the relevant contributions coming from correlations between particles with opposite momenta. The remaining electronic effects are merely treated by the Pauli exclusion principle.
The idea leading to the BCS GS was to write the many-body wavefunction *not as an antisymmetrized product of wavefunctions referring to different pairs of electrons*, but as a product of wavefunctions referring to the occupation of different *pairs of single-particle states* ($\mathbf{k}\uparrow, -\mathbf{k}\downarrow$).
Let us consider a single *pair of states* and associate *to it* an amplitude $u_{\mathbf{k}}$ for being empty and an amplitude $v_{\mathbf{k}}$ for being occupied. Then repeat the procedure for all $\mathbf{k}$'s.
The BCS state is therefore written as

$$\boxed{|\Psi_{\text{BCS}}\rangle = \prod_{\mathbf{k}} \left(u_{\mathbf{k}} + v_{\mathbf{k}} c^{\dagger}_{\mathbf{k},\uparrow} c^{\dagger}_{-\mathbf{k},\downarrow} \right) |\text{vac}\rangle} \quad . \tag{4.15}$$

In order to properly normalize the single pairs we have to impose that the complex numbers $u_{\mathbf{k}}$ and $v_{\mathbf{k}}$ fulfill the condition

$$|u_{\mathbf{k}}|^2 + |v_{\mathbf{k}}|^2 = 1 \tag{4.16}$$

and the s-wave requirement leads to

$$u_{-\mathbf{k}} = u_{\mathbf{k}} \quad , \quad v_{-\mathbf{k}} = v_{\mathbf{k}} \, . \tag{4.17}$$

It is possible to recover the Fermi Sea state from (4.15) with the choices

$$\text{Fermi Sea} \begin{cases} u_{\mathbf{k}} = e^{i\phi} \, \Theta(|\mathbf{k}| - k_{\text{F}}) \\ v_{\mathbf{k}} = e^{i\phi} \, \Theta(k_{\text{F}} - |\mathbf{k}|) \end{cases} \tag{4.18}$$

where $\Theta(x) = 1$ for $x > 0$ and 0 elsewhere, and ϕ is a generic phase.
Except from the special case (4.18), one peculiar aspect of the BCS state (4.15) is to be a *superposition of many-body states* with *different* (but even) number of particles. Therefore the total number of electrons in a state described by (4.15) is *not* fixed. Rather, its mean value N can be centered around a preferred number by tuning the parameters $u_{\mathbf{k}}$ and $v_{\mathbf{k}}$. It can be shown that the width of the distributions of the particle numbers scales as $\sqrt{N}$, implying that the deviations get smaller and smaller in the thermodynamic limit of large N. At the end of the section we will comment on what is the meaning of not having a fixed number of particles in a closed physical system (the 3D superconducting sample).
The normalization constraint on $u_{\mathbf{k}}$ and $v_{\mathbf{k}}$ and their symmetry relations allow us to define a *single* complex parameter, called "the gap" (we will see why) $\Delta_{\mathbf{k}}$ determining the GS, via the relations

$$\begin{aligned} u_{\mathbf{k}} &= \frac{E_{\mathbf{k}} + \varepsilon_{\mathbf{k}}}{\sqrt{|\Delta_{\mathbf{k}}|^2 + (E_{\mathbf{k}} + \varepsilon_{\mathbf{k}})^2}} \\ v_{\mathbf{k}} &= \frac{\Delta_{\mathbf{k}}}{\sqrt{|\Delta_{\mathbf{k}}|^2 + (E_{\mathbf{k}} + \varepsilon_{\mathbf{k}})^2}} \end{aligned} \tag{4.19}$$

having defined $E_{\mathbf{k}} = \sqrt{\varepsilon_{\mathbf{k}}^2 + |\Delta_{\mathbf{k}}|^2}$ (also this notation will acquire a physical meaning in the next section), with $\Delta_{\mathbf{k}} = \Delta_{-\mathbf{k}}$.
The previous relations imply

$$\begin{aligned} |u_{\mathbf{k}}|^2 &= \frac{1}{2}\left(1 + \frac{\varepsilon_{\mathbf{k}}}{E_{\mathbf{k}}}\right) \\ |v_{\mathbf{k}}|^2 &= \frac{1}{2}\left(1 - \frac{\varepsilon_{\mathbf{k}}}{E_{\mathbf{k}}}\right) . \end{aligned} \tag{4.20}$$

Unless macroscopic phase coherence is considered, as in the Josephson's effect, the functions $u_{\mathbf{k}}$ and $v_{\mathbf{k}}$ can be chosen to be real. We will however keep trace of their complex nature, although no physical effect presented here will depend on it.
The final step in the BCS analysis is to determine the function $\Delta_{\mathbf{k}}$ as to minimize the expectation value of the Hamiltonian on the proposed GS $|\Psi_{\text{BCS}}\rangle$.
Before doing that we briefly comment about the nature of the creation and annihilation operators of the pairs.
Indeed we can introduce the second quantization operators creating and destroying a pair of fermions with opposite momenta and spin as

$$\begin{aligned} b_{\mathbf{k}}^\dagger &= c_{\mathbf{k},\uparrow}^\dagger c_{-\mathbf{k},\downarrow}^\dagger \\ b_{\mathbf{k}} &= c_{-\mathbf{k},\downarrow} c_{\mathbf{k},\uparrow} . \end{aligned} \tag{4.21}$$

In the BCS state these operators repeatedly act on the vacuum generating states with even number of particles. If we study their commutation relations directly we realize that

$$\begin{cases} \left[b_{\mathbf{k}}, b_{\mathbf{k}'}^\dagger\right] = \delta_{\mathbf{k}\mathbf{k}'}\left(1 - n_{\mathbf{k},\uparrow} - n_{-\mathbf{k},\downarrow}\right) \\ \left[b_{\mathbf{k}}, b_{\mathbf{k}'}\right] = \left[b_{\mathbf{k}}^\dagger, b_{\mathbf{k}'}^\dagger\right] = 0 \end{cases} \tag{4.22}$$

where $n_{\mathbf{k},s} \equiv c^\dagger_{\mathbf{k},s} c_{\mathbf{k},s}$ is the particle number operator in the single particle electron state with momentum $\mathbf{k}$ and spin s.
We can therefore see that the pair operators fulfill usual bosonic commutation relations when acting on states with different momenta but not when their momentum coincide. It can be directly verified that $b^{\dagger 2}_{\mathbf{k}} = b^2_{\mathbf{k}} = 0$, so that the pair operators have a bosonic behaviour for different momenta and fulfill the Pauli principle when applied on the same state twice.
If a full Bose-Einstein statistics were satisfied by the $b_{\mathbf{k}}$'s the GS would be a bosonic condensate of pairs in the state with vanishing momentum. This is *not* the case for the superconductor, and this is the reason why the Fermi surface due to the exclusion principle still plays a crucial role in the properties of the SC GS.
Among the many curious properties of the BCS state, one which has deep consequences is the fact that the operator $b_{\mathbf{k}}$ (destroying two electrons in the GS) has a non vanishing expectation value on $|\Psi_{\text{BCS}}\rangle$.
This clearly has to do with the fact that the SC GS does not have a fixed number of particles and it represents a dramatic difference with respect to the usual "normal" Fermi liquid-like states. The existence of such "anomalous" averages will force us to consider an extension to the usual Green's functions techniques to account for the superconducting condensation effects, as we will see in the second part of this chapter. The anomalous average effect leads to the introduction and development of the concept of the spontaneous symmetry breaking mechanism which has now a broad range of applications in the theory of the phase transitions.
A simple example can directly show the existence of anomalous averages in the BCS state. Let us imagine to consider just a single momentum state $\mathbf{k}_0$, in the BCS GS. Thus

$$|\Psi^{(1)}_{\text{BCS}}\rangle = \left(u_{\mathbf{k}_0} + v_{\mathbf{k}_0} b^\dagger_{\mathbf{k}_0}\right)|\text{vac}\rangle = u_{\mathbf{k}_0}|0\rangle + v_{\mathbf{k}_0}|1\rangle \tag{4.23}$$

where $|0\rangle$ and $|1\rangle$ indicate the states where the *pair* $(\mathbf{k}_0\uparrow, -\mathbf{k}_0\downarrow)$ is empty or occupied, respectively. It is then easy to evaluate

$$\langle\Psi^{(1)}_{\text{BCS}}|b_{\mathbf{k}_0}|\Psi^{(1)}_{\text{BCS}}\rangle = \langle\Psi^{(1)}_{\text{BCS}}|c_{-\mathbf{k}_0,\downarrow}c_{\mathbf{k}_0,\uparrow}|\Psi^{(1)}_{\text{BCS}}\rangle = u^*_{\mathbf{k}_0} v_{\mathbf{k}_0}\ . \tag{4.24}$$

If the product $u^*_{\mathbf{k}_0} v_{\mathbf{k}_0}$ does not vanish the anomalous average survives: in a normal Fermi liquid state the same expectation value would be trivially zero.
Normal averages on the same $|\Psi^{(1)}_{\text{BCS}}\rangle$ state give

$$\langle\Psi^{(1)}_{\text{BCS}}|c^\dagger_{\mathbf{k}_0,s}c_{\mathbf{k}_0,s}|\Psi^{(1)}_{\text{BCS}}\rangle = \langle\Psi^{(1)}_{\text{BCS}}|c^\dagger_{-\mathbf{k}_0,s}c_{-\mathbf{k}_0,s}|\Psi^{(1)}_{\text{BCS}}\rangle = |v_{\mathbf{k}_0}|^2\ . \tag{4.25}$$

Let us now turn to the direct determination of the GS parameters $u_{\mathbf{k}}$ and $v_{\mathbf{k}}$ (or alternatively to the single order parameter $\Delta_{\mathbf{k}}$) by minimizing the energy of the system on the BCS state.

To be more precise, working in the grandcanonical ensemble, we plan to minimize the expectation value of $H - \mu N$ on the BCS state, where H is the Hamiltonian of our system, μ the chemical potential and N the operator of the total number of particles.
Since we work at $T = 0$ and the single particle energy $\varepsilon_{\mathbf{k}}$ is measured with respect

to the Fermi level, we can write

$$H-\mu N=\sum_{\mathbf{p},s}\varepsilon_{\mathbf{p}}\,c^{\dagger}_{\mathbf{p},s}c_{\mathbf{p},s}+\frac{1}{2}\sum_{\mathbf{p},\mathbf{p}',\mathbf{q},s,s'}V(\mathbf{p},\mathbf{p}',\mathbf{q})\,c^{\dagger}_{\mathbf{p}+\mathbf{q},s}c^{\dagger}_{\mathbf{p}'-\mathbf{q},s'}c_{\mathbf{p}',s'}c_{\mathbf{p},s}\ . \tag{4.26}$$

We will take expectation values on $|\Psi_{\rm BCS}\rangle$ considering the "normal" scattering terms (corresponding to Hartree and Fock energy corrections) as already incorporated in the single particle energy $\varepsilon_{\mathbf{p}}$. In the interaction part of the Hamiltonian we will then isolate only scattering processes where the pairing structure of both incoming and outgoing pairs of particles is preserved. This leads us to the relations $s'=-s$, $\mathbf{p}=-\mathbf{p}'$. Renaming $\mathbf{p}\equiv\mathbf{k}$ and $\mathbf{p}+\mathbf{q}\equiv\mathbf{k}'$ and defining $V(\mathbf{k},-\mathbf{k},\mathbf{k}'-\mathbf{k})=V_{\mathbf{k}'\mathbf{k}}$ we get the so-called *reduced* Hamiltonian

$$H_{\rm red}-\mu N=\sum_{\mathbf{k},s}\varepsilon_{\mathbf{k}}\,c^{\dagger}_{\mathbf{k},s}c_{\mathbf{k},s}+\frac{1}{2}\sum_{\mathbf{k},\mathbf{k}',s}V_{\mathbf{k}'\mathbf{k}}\,c^{\dagger}_{\mathbf{k}',s}c^{\dagger}_{-\mathbf{k}',-s}c_{-\mathbf{k},-s}c_{\mathbf{k},s}\ . \tag{4.27}$$

The scattering processes in the interaction parts of (4.26) and (4.27) are diagrammatically depicted in Fig (4.1.2).

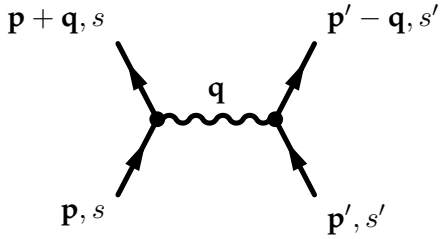

Fig. 4.2: The four fermion interaction diagram. Momentum conservation has been implemented. Notice the absence of spin-flip processes in the vertices. The interaction term in the reduced Hamiltonian (4.27) is obtained with $\mathbf{p}=\mathbf{k}$, $\mathbf{p}'=-\mathbf{k}$ and $\mathbf{q}=\mathbf{k}'-\mathbf{k}$.

The expectation value of (4.27) on (4.15) is then easily evaluated using what we learned in the simple examples (4.24,4.25). Indeed, since the occupations of different pairs are uncorrelated, the expectation value of the operator
$c^{\dagger}_{\mathbf{k}',s}c^{\dagger}_{-\mathbf{k}',-s}c_{-\mathbf{k},-s}c_{\mathbf{k},s}$ is factorized into

$$\langle c^{\dagger}_{\mathbf{k}',s}c^{\dagger}_{-\mathbf{k}',-s}c_{-\mathbf{k},-s}c_{\mathbf{k},s}\rangle=\langle c^{\dagger}_{\mathbf{k}',s}c^{\dagger}_{-\mathbf{k}',-s}\rangle\langle c_{-\mathbf{k},-s}c_{\mathbf{k},s}\rangle=(u_{\mathbf{k}'}v^{*}_{\mathbf{k}'})(u^{*}_{\mathbf{k}}v_{\mathbf{k}})\equiv F^{*}_{\mathbf{k}'}F_{\mathbf{k}}\ . \tag{4.28}$$

with $F_{-\mathbf{k}}=F_{\mathbf{k}}\equiv u^{*}_{\mathbf{k}}v_{\mathbf{k}}$. Thus we deduce

$$\langle H_{\rm red}-\mu N\rangle=\sum_{\mathbf{k}}2\varepsilon_{\mathbf{k}}|v_{\mathbf{k}}|^2+\sum_{\mathbf{k},\mathbf{k}'}V_{\mathbf{k}\mathbf{k}'}F^{*}_{\mathbf{k}}F_{\mathbf{k}'}\ . \tag{4.29}$$

We then have to minimize (4.29) with respect to the function $\Delta_{\mathbf{k}}$ entering $F_{\mathbf{k}}$.
In order to do that it is convenient to notice that $|\Delta_{\mathbf{k}}|^2/E_{\mathbf{k}}=2\Delta_{\mathbf{k}}F^{*}_{\mathbf{k}}$ and $\mathrm{d}E_{\mathbf{k}}/\mathrm{d}\Delta_{\mathbf{k}}=$

$2F^*_{\mathbf{k}}$ (the derivative being done so that $\Delta_{\mathbf{k}}$ and $\Delta^*_{\mathbf{k}}$ remain complex conjugates, and *not* at constant $\Delta^*_{\mathbf{k}}$), whence $E_{\mathbf{k}} = 2\int \mathrm{d}\Delta_{\mathbf{k}} F^*_{\mathbf{k}}$. Using (4.20) we get

$$\begin{aligned}\langle H_{\mathrm{red}} - \mu N\rangle &= \sum_{\mathbf{k}} \left(\varepsilon_{\mathbf{k}} - \frac{\varepsilon^2_{\mathbf{k}}}{E_{\mathbf{k}}}\right) + \sum_{\mathbf{k},\mathbf{k}'} V_{\mathbf{k}\mathbf{k}'} F^*_{\mathbf{k}} F_{\mathbf{k}'} \\ &= \sum_{\mathbf{k}} \varepsilon_{\mathbf{k}} + \sum_{\mathbf{k}} (-E_{\mathbf{k}} + 2\Delta_{\mathbf{k}} F^*_{\mathbf{k}}) + \sum_{\mathbf{k},\mathbf{k}'} V_{\mathbf{k}\mathbf{k}'} F^*_{\mathbf{k}} F_{\mathbf{k}'} \ , \end{aligned} \tag{4.30}$$

so that, integrating $E_{\mathbf{k}}$ by parts,

$$\langle H_{\mathrm{red}} - \mu N\rangle = \sum_{\mathbf{k}} \varepsilon_{\mathbf{k}} + 2\sum_{\mathbf{k}} \int \mathrm{d}F^*_{\mathbf{k}}\ \Delta_{\mathbf{k}} + \sum_{\mathbf{k},\mathbf{k}'} V_{\mathbf{k}\mathbf{k}'} F^*_{\mathbf{k}} F_{\mathbf{k}'} \ . \tag{4.31}$$

Differentiating with respect to $F^*_{\mathbf{k}}$ and imposing the vanishing of the derivative, we finally get the BCS equation at $T = 0$

$$\Delta_{\mathbf{k}} = -\sum_{\mathbf{k}'} V_{\mathbf{k}\mathbf{k}'} F_{\mathbf{k}'} = -\sum_{\mathbf{k}'} V_{\mathbf{k}\mathbf{k}'} \frac{\Delta_{\mathbf{k}'}}{2E_{\mathbf{k}'}} \ . \tag{4.32}$$

The solution of this equation can be difficult, depending on the form of the matrix element $V_{\mathbf{k}\mathbf{k}'}$. However, following the single-pair Cooper problem, we can use the factorized interaction (4.6), i.e.

$$V_{\mathbf{k}\mathbf{k}'} = \begin{cases} \lambda < 0, & \text{for } |\varepsilon_{\mathbf{k}}| \text{ and } |\varepsilon_{\mathbf{k}'}| < \omega_{\mathrm{D}} \\ 0, & \text{elsewhere} \end{cases} \ . \tag{4.33}$$

With this choice we get

$$\Delta_{\mathbf{k}} \begin{cases} \Delta_0, & |\varepsilon_{\mathbf{k}}| < \omega_{\mathrm{D}} \\ 0, & \text{elsewhere} \end{cases} \tag{4.34}$$

where

$$\Delta_0 = \frac{\omega_{\mathrm{D}}}{\sinh\left(\frac{1}{N_0|\lambda|}\right)} \ . \tag{4.35}$$

We can then substitute the obtained expression for $\Delta_{\mathbf{k}}$ into (4.19) and finally into (4.29) to get the condensation energy. In fact, by taking the difference between the GS energy $\mathcal{E}$ for the normal phase (4.18) and the resulting (4.29) in the SC state, we obtain

$$\mathcal{E}_{\mathrm{N}} - \mathcal{E}_{\mathrm{SC}} = \frac{1}{2} N_0 \Delta_0^2 \ . \tag{4.36}$$

We therefore see that the total energy of the system has been decreased by the phenomenon of condensation. The reorganization of the normal GS into the BCS state leads to a net gain in energy at $T = 0$.
We can understand how the BCS state differs from a normal phase by directly looking at the occupation distribution of the $\mathbf{k}$ eigenstates. The probability amplitude for the pair $(\mathbf{k}\uparrow, -\mathbf{k}\downarrow)$ to be occupied is given by $v_{\mathbf{k}}$. In Fig (4.3) we plot the typical form of $|v_{\mathbf{k}}|$ as a function of $|\mathbf{k}|$.

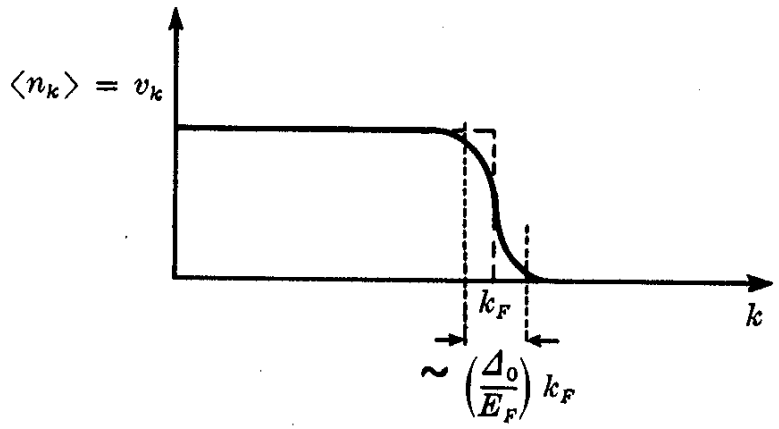

Fig. 4.3: The typical occupation distribution of the momentum eigenstates in the BCS Ground State.

We see that the condensation implies a smoothening of the occupation distribution around the Fermi energy, in comparison with the sharp Fermi-liquid like drop.

In the following section we will investigate the spectrum of the excitations out of the BCS GS and see that it is indeed gapped. This accounts for the rigidity of the superconducting phase to the external perturbations of low enough energy, and finally to the vanishing resistance. Moreover we will present the temperature dependence of the gap and show that there is a critical temperature above which the SC state becomes unstable and a normal Fermi-liquid like phase is preferred.

4.1.3 Quasiparticle excitations of the BCS theory

Let us consider the addition of a single electron to the BCS GS in the single particle state $|\mathbf{p}\uparrow\rangle$ and calculate the energy required for such a process.
Since the paired state $|-\mathbf{p}\downarrow\rangle$ is empty the interaction terms included in the reduced Hamiltonian (4.27) are unable to scatter the electron out of its state. Thus the pair state $(\mathbf{p}\uparrow, -\mathbf{p}\downarrow)$ gives no contribution to the pairing interaction. The total energy involved in this single particle excitation process is obtained by adding the kinetic term $\varepsilon_{\mathbf{p}}$ of the electron and subtracting the energy of the pair, i.e.

$$\varepsilon_{\mathbf{p}}\left(1-2|v_{\mathbf{p}}|^2\right) - 2\sum_{\mathbf{k}'} V_{\mathbf{p}\mathbf{k}'} F^*_{\mathbf{p}} F_{\mathbf{k}'} = \varepsilon_{\mathbf{p}}\left(1-2|v_{\mathbf{p}}|^2\right) + 2\Delta_{\mathbf{p}} F^*_{\mathbf{p}} \,. \tag{4.37}$$

Using the definitions of $F_{\mathbf{p}}$, $E_{\mathbf{p}}$ and together with the (4.19), we obtain the excitation energy

$$\frac{\varepsilon^2_{\mathbf{p}} + |\Delta^2_{\mathbf{p}}|}{E_{\mathbf{p}}} = E_{\mathbf{p}} \,. \tag{4.38}$$

Thus the function $E_{\mathbf{p}}$ is just the energy required to create a single-particle excitation with momentum $\mathbf{p}$. In Fig (4.4) we plot $E_{\mathbf{p}}$ as a function of $|\mathbf{p}|$ for the case (4.34).

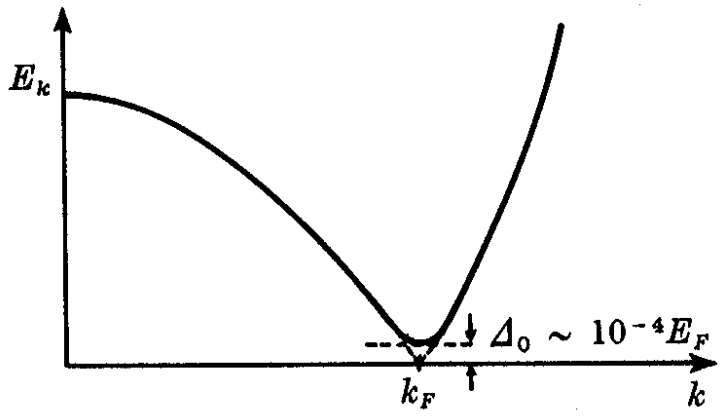

Fig. 4.4: The typical dispersion for bogolons out of the BCS reduced Hamiltonian. The quasiparticle excitation energy is plotted as a function of the wavevector modulus and differs from the corresponding free case only close to the Fermi level.

We can observe that the spectrum is fully gapped, with a minimum excitation energy equal to Δ_{k_F}. This is the reason why the order parameter was originally called "the gap" and it is now clear why the notation $E_{\mathbf{p}}$ was originally chosen. It is also clear that the Fermi energy still keeps a physical meaning also in the superconducting condensate. The phenomenon involves the main modifications in the occupation distribution exactly at the Fermi level and there the quasiparticle excitations with the smallest energies show up.

It is possible to obtain the GS expectation energy and the spectrum of the excitations in quite a different way, considering a Hamiltonian approach first introduced by Bogoliubov and Valatin ([90, 91]). We will briefly consider this treatment, which will lead us to the possibility of inclusion of external potentials and inhomogeneities quite easily. Many of these results will come out useful in our last chapter. The approach by Bogoliubov is essentially a generalization of the Hartree-Fock mean field treatment to the case of superconductivity.
We will therefore start with the full Hamiltonian of the system, including the presence of an external vector potential $\mathbf{A}(\mathbf{r})$ (this can be useful to describe magnetic field-related properties) and of an electrostatic modulation $U_0(\mathbf{r})$ (useful to treat system inhomogeneities). The homogeneous situation described by BCS will be recovered in the end as a particular case of this treatment.
The purpose of the Bogoliubov-de Gennes (BdG) approach is to diagonalize a mean-field Hamiltonian where anomalous averages have been explicitly taken into ac-

count. In this way the quasiparticle operators of the theory will come out automatically after the canonical transformation leading to the single particle diagonal form and the excitation spectrum will clearly show up as the quasiparticle kinetic operator.
Analogously to what seen in the BCS case we will assume a spin-independent attractive pointlike non-retarded four body interaction V. The effects related to retardation and momentum dependence of the interactions will be considered later within the field theoretical treatment of superconductors.
The Hamiltonian looks like

$$H = H_0 + H_1 \tag{4.39}$$

$$H_0 = \sum_s \int \mathrm{d}\mathbf{r}\, \psi_s^\dagger(\mathbf{r}) \left[\frac{1}{2m} \left(-i\hbar\nabla + \frac{e}{c}\mathbf{A}(\mathbf{r}) \right)^2 + U_0(\mathbf{r}) - \mu \right] \psi_s(\mathbf{r}) \tag{4.40}$$

$$H_1 = \frac{1}{2} V \sum_{s,s'} \int \mathrm{d}\mathbf{r}\, \psi_s^\dagger(\mathbf{r}) \psi_{s'}^\dagger(\mathbf{r}) \psi_{s'}(\mathbf{r}) \psi_s(\mathbf{r}) \tag{4.41}$$

where $\psi_s(\mathbf{r})$ is a field operator annihilating a particle with spin s at the position $\mathbf{r}$.
We will now consider a mean field treatment of the operator (4.39) where both normal averages $\langle \psi_s^\dagger(\mathbf{r}) \psi_s(\mathbf{r}) \rangle$ and anomalous ones like $\langle \psi_s(\mathbf{r}) \psi_{-s}(\mathbf{r}) \rangle$ and $\langle \psi_s^\dagger(\mathbf{r}) \psi_{-s}^\dagger(\mathbf{r}) \rangle$ are considered. As seen in the BCS equation, we will use the *notation* $\Delta(\mathbf{r}) = V \langle \psi_\downarrow(\mathbf{r}) \psi_\uparrow(\mathbf{r}) \rangle$.
The *normal* averages of the Hartree and Fock type generate a term of the form $\sum_s U(\mathbf{r}) \psi_s^\dagger(\mathbf{r}) \psi_s(\mathbf{r})$ with $U(\mathbf{r}) = V \langle \psi_\uparrow^\dagger(\mathbf{r}) \psi_\uparrow(\mathbf{r}) \rangle$. The mean-field Hamiltonian therefore is

$$\begin{aligned} H_{\mathrm{MF}} &= \sum_s \int \mathrm{d}\mathbf{r}\, \psi_s^\dagger(\mathbf{r}) \left[H_e + U(\mathbf{r}) \right] \psi_s(\mathbf{r}) + \\ &+ \int \mathrm{d}\mathbf{r}\, \left[\Delta(\mathbf{r})\, \psi_\uparrow^\dagger(\mathbf{r}) \psi_\downarrow^\dagger(\mathbf{r}) + \Delta^*(\mathbf{r})\, \psi_\downarrow(\mathbf{r}) \psi_\uparrow(\mathbf{r}) \right] \end{aligned} \tag{4.42}$$

where

$$H_e = \frac{1}{2m} \left(-i\hbar\nabla + \frac{e}{c}\mathbf{A}(\mathbf{r}) \right)^2 + U_0(\mathbf{r}) - \mu\ . \tag{4.43}$$

Here we face a delicate point. Indeed, we started with the Hamiltonian (4.39) which is invariant under the group $U(1)$. That is, by transforming every field operator with a $U(1)$ transformation, $\psi \to e^{i\theta}\psi$, the Hamiltonian is fully invariant for every choice of θ. This is nothing more to say that the particle number is conserved.
By making the mean-field approximation suggested by the binding effect discovered by Cooper, we end up with the Hamiltonian (4.42). This is *not any more invariant* under an arbitrary $U(1)$ transformation, unless $\theta = 0, \pi$ (called "the Z_2 group") and clearly does not preserve the particle number.
The symmetry of our problem is highly reduced due to the condensation instability. Such a phenomenon is called "Spontaneous Symmetry Breaking" and has crucial implications in the theory of phase transitions.
The consistency of the theory is recovered if we remember that also the new GS

does not have a conserved particle number, so that the physical expectation values of the anomalous mean field theory (4.42) on it assume a perfectly reasonable meaning.

The Hamiltonian (4.42) is quadratic in the field operators and can be diagonalized by a canonical transformation. However, the presence of the anomalous terms with two creation/annihilation operators forces us to choose, as new quasiparticle *operators*, a combination of particle and hole-like fields.
We can write the unitary transformation as

$$\psi_\uparrow(\mathbf{r}) = \sum_n \left[\gamma_{n\uparrow} u_n(\mathbf{r}) - \gamma^\dagger_{n\downarrow} v^*_n(\mathbf{r})\right] \tag{4.44}$$

$$\psi_\downarrow(\mathbf{r}) = \sum_n \left[\gamma_{n\downarrow} u_n(\mathbf{r}) + \gamma^\dagger_{n\uparrow} v^*_n(\mathbf{r})\right] \tag{4.45}$$

where $\gamma_{n\uparrow}$ and $\gamma_{n\downarrow}$ are annihilation operators for the new quasiparticles (Bogolons) in the eigenstates $|n\uparrow\rangle$ and $|n\downarrow\rangle$ (in the homogeneous case they are still momentum eigenstates, but this is not any longer the case when inhomogeneities are present, like vortices or disorder).
For the transformation (4.44) to be canonical, the fermionic commutation relations have to be fulfilled also by the new operators. In order to check it we can write the inverse transformation as

$$\gamma_{n\uparrow} = \int \mathrm{d}\mathbf{r}\ \left[u^*_n(\mathbf{r})\psi_\uparrow(\mathbf{r}) + v^*_n(\mathbf{r})\psi^\dagger_\downarrow(\mathbf{r})\right] \tag{4.46}$$

$$\gamma_{n\downarrow} = \int \mathrm{d}\mathbf{r}\ \left[u^*_n(\mathbf{r})\psi_\downarrow(\mathbf{r}) - v^*_n(\mathbf{r})\psi^\dagger_\uparrow(\mathbf{r})\right] \tag{4.47}$$

and impose the commutation relations

$$\{\gamma_{ns}, \gamma_{ms'}\} = 0 \tag{4.48}$$

$$\{\gamma_{ns}, \gamma^\dagger_{ms'}\} = \delta_{nm}\delta_{ss'}\ . \tag{4.49}$$

It is then easy to check that the (4.48) are fulfilled by imposing

$$\langle u_n|u_m\rangle + \langle v_n|v_m\rangle = \int \mathrm{d}\mathbf{r}\ [u^*_n(\mathbf{r})u_m(\mathbf{r}) + v^*_n(\mathbf{r})v_m(\mathbf{r})] = \delta_{nm} \tag{4.50}$$

$$\langle v_n|u^*_m\rangle - \langle u_n|v^*_m\rangle = \int \mathrm{d}\mathbf{r}\ [v^*_n(\mathbf{r})u^*_m(\mathbf{r}) - u^*_n(\mathbf{r})v^*_m(\mathbf{r})] = 0\ . \tag{4.51}$$

Our final task is to impose that the Hamiltonian in the new operators γ takes the diagonal form

$$H_{\mathrm{MF}} = E_{\mathrm{GS}} + \sum_{n,s} E_{ns}\, \gamma^\dagger_{ns}\gamma_{ns} \tag{4.52}$$

with E_{GS} the GS energy and E_{ns} the excitation energy of the eigenstate $|n, s\rangle$. The GS will be obtained as the vacuum of quasiparticle excitations.
In order to get to the equations that have to be satisfied by $u_n(\mathbf{r})$ and $v_n(\mathbf{r})$ we

consider the Heisenberg equations for the fields $\psi_s(\mathbf{r})$, $i\dot{\psi}_s = [\psi_s, H_{\rm MF}]$ and we obtain

$$i\dot{\psi}_s(\mathbf{r},t) = [H_e + U(\mathbf{r})]\,\psi_s(\mathbf{r},t) + s\,\Delta(\mathbf{r})\,\psi^\dagger_{-s}(\mathbf{r},t)\ . \tag{4.53}$$

The time dependence of the fields is then obtained from the evolution of the *diagonal* quasiparticle operators

$$\gamma_{ns}(t) = e^{-iE_{ns}t}\,\gamma_{ns}(t=0)\ . \tag{4.54}$$

Inserting (4.44) with the evolution (4.54) into the equations (4.53) for $\psi_\uparrow(\mathbf{r},t)$ and $\psi^\dagger_\downarrow(\mathbf{r},t)$ and collecting the terms containing, say, $\gamma_{n\uparrow}$, we obtain the desired equations (called Bogoliubov-de Gennes equations, in the following "BdG")

$$E_n u_n(\mathbf{r}) = [H_e + U(\mathbf{r})]\,u_n(\mathbf{r}) + \Delta(\mathbf{r})v_n(\mathbf{r}) \tag{4.55}$$

$$E_n v_n(\mathbf{r}) = -\,[H_e^* + U(\mathbf{r})]\,v_n(\mathbf{r}) + \Delta^*(\mathbf{r})u_n(\mathbf{r})\ . \tag{4.56}$$

They can be cast in the compact matrix form

$$E_n \begin{pmatrix} u_n(\mathbf{r}) \\ v_n(\mathbf{r}) \end{pmatrix} = \begin{pmatrix} [H_e + U(\mathbf{r})] & \Delta(\mathbf{r}) \\ \Delta^*(\mathbf{r}) & -[H_e^* + U(\mathbf{r})] \end{pmatrix} \begin{pmatrix} u_n(\mathbf{r}) \\ v_n(\mathbf{r}) \end{pmatrix}\ . \tag{4.57}$$

We will have to consider these equations in the last chapter, while discussing the presence of vortices in p-wave superconductors.
According to our definition $\Delta(\mathbf{r}) = V\langle\psi_\downarrow(\mathbf{r})\psi_\uparrow(\mathbf{r})\rangle$ we are now able to calculate the gap and its temperature dependence. In fact, by replacing the ψ operators with the eigenmodes γ, and using the expectation value

$$\langle\gamma^\dagger_{ms}\gamma_{ns'}\rangle = \delta_{ss'}\delta_{mn}\,\mathcal{F}(n,T) \tag{4.58}$$

with the Fermi-Dirac distribution $\mathcal{F}(n,T) = 1/(\exp[(E_n-\mu)/K_{\rm B}T]+1)$, we get

$$\Delta(\mathbf{r},T) = -V\sum_n u_n(\mathbf{r})v_n^*(\mathbf{r})\ (1-2\mathcal{F}(n,T))\ . \tag{4.59}$$

Notice that, having diagonalized the spectrum in terms of fermionic operators, the expectation values of a generic function of the γ fields has to be performed on a *normal* Fermi liquid-like Ground State, with the standard Fermi occupation at temperature T. The broken symmetry of the electronic GS is recovered in the language of the "old" fields ψ.
At this level we can consider, as a particular case, the homogeneous system described by the BCS treatment. Now the diagonalizing modes will still be momentum eigenstates and every spatial dependence of the Hamiltonian is absent. As in the BCS case we will incorporate the effects of the normal averages, contained in the term $U(\mathbf{r})$ of (4.42), into the single particle energy $\varepsilon_{\mathbf{k}}$, measured from the Fermi level. Thus, in the momentum representation, the BdG equations look like

$$E_{\mathbf{k}} \begin{pmatrix} u_{\mathbf{k}} \\ v_{\mathbf{k}} \end{pmatrix} = \begin{pmatrix} \varepsilon_{\mathbf{k}} & \Delta_{\mathbf{k}} \\ \Delta^*_{\mathbf{k}} & -\varepsilon_{\mathbf{k}} \end{pmatrix} \begin{pmatrix} u_{\mathbf{k}} \\ v_{\mathbf{k}} \end{pmatrix}\ . \tag{4.60}$$

The solvability of the system implies

$$E_{\mathbf{k}} = \sqrt{\varepsilon_{\mathbf{k}}^2 + |\Delta_{\mathbf{k}}^2|} \tag{4.61}$$

as already obtained in (4.37), and $u_{\mathbf{k}}$ and $v_{\mathbf{k}}$ satisfy the equations (4.20).
The gap equation (4.59) becomes

$$\Delta_{\mathbf{k}} = -V \sum_{\mathbf{k}'} \frac{\Delta_{\mathbf{k}'}}{2E_{\mathbf{k}'}} \tanh\left(\frac{E_{\mathbf{k}'}}{2K_{\mathrm{B}}T}\right). \tag{4.62}$$

For $T = 0$ equation (4.62) reduces to (4.32), where the momentum dependence of the interaction is included in the energy cutoff around the Fermi level. For finite temperatures the gap has a typical form depicted in Fig (4.5). There is a critical temperature T_{c} above which the gap vanishes and the energy gain in the condensation is lost, in favour of a stable Fermi-liquid like state.

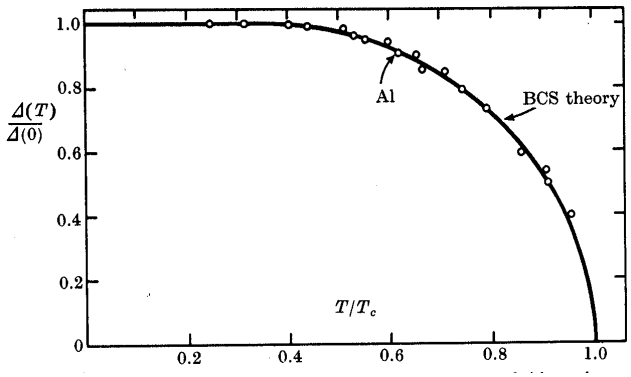

Fig. 4.5: The BCS gap (normalized to its zero temperature value $\Delta(0)$) as a function of temperature (normalized to the critical temperature T_{c}). Measured data from Al samples have been included, showing an impressive agreement between theory and experiment.

4.1.4 The BCS state in real space and p-wave superconductivity

Up to now we presented an introduction to the BCS theory with s-wave pairing as a condensation in momentum space. We have seen that the Cooper pairs in this problem are plane wave states with opposite momenta.
We could ask if, already in the absence of currents, this is the only possible pairing choice. Even further, we can ask what is the nature of the Cooper pairs when inhomogeneities are present in the system. All this sort of issues are essentially summarized in the question "Who pairs to whom?".

We will briefly analyze some of these questions here and a deep investigation about the nature of the Cooper pairs for an inhomogeneous p-wave superconductor will be presented in Chapter 6.

Within the BCS treatment it is customary to define a new function $g_{\mathbf{k}} = v_{\mathbf{k}}/u_{\mathbf{k}}$. In terms of it the normalized BCS state is

$$|\Psi_{\text{BCS}}\rangle = \prod_{\mathbf{k}} \frac{1 + g_{\mathbf{k}} c^{\dagger}_{\mathbf{k},\uparrow} c^{\dagger}_{-\mathbf{k},\downarrow}}{\sqrt{1 + |g^2_{\mathbf{k}}|}} |\text{vac}\rangle = \prod_{\mathbf{k}} \exp\left[\frac{g_{\mathbf{k}} c^{\dagger}_{\mathbf{k},\uparrow} c^{\dagger}_{-\mathbf{k},\downarrow}}{\sqrt{1 + |g^2_{\mathbf{k}}|}}\right] |\text{vac}\rangle. \tag{4.63}$$

The function $g_{\mathbf{k}}$ describes the ratio between the amplitudes of occupation and emptiness of the Cooper pair and clearly represents the k-space form of the pair wavefunction.
In analogy we can write the position representation of the GS as

$$|\Psi_{\text{BCS}}\rangle = \exp\left[\int \mathrm{d}\mathbf{r}\, \mathrm{d}\mathbf{r}'\; g(\mathbf{r}, \mathbf{r}')\, \psi^{\dagger}_{s}(\mathbf{r}) \psi^{\dagger}_{s'}(\mathbf{r}')\right] |\text{vac}\rangle \tag{4.64}$$

where the function $g(\mathbf{r}, \mathbf{r}')$ is already such that the GS is normalized, and describes the real space Cooper pair wavefunction.
If the spin pairing is chosen as in the BCS case ($s = \uparrow$, $s' = \downarrow$) then the antisymmetry of the pair state requires $g(\mathbf{r}, \mathbf{r}')$ to be an even function of its arguments.
However, in principle, we could write a trial paired state for equal spins $s = s'$, the so-called "Equal Spin Pairing" (ESP) configuration. In this case g will be a spatially odd function and it will be expanded in *odd* angular momenta components. The ESP is the simplest configuration to be considered while treating spin triplet Cooper pair condensation.
This and other non-standard pairing choices have been considered while discussing two-particles interactions with a repulsive small distance behaviour. Clearly, the antisymmetry of the pair wavefunction prevents two electrons to come close to each other thus lowering the energy cost due to the repulsive core.
In the case originally considered by Cooper the interaction was chosen to be constant and attractive and the s-wave pairing was then the natural choice to enhance the binding energy of the pairs. In real superconductors there is always some admixture of different pairing symmetries although one angular momentum channel is usually dominant over the others. In view of the future purposes we briefly describe the bulk properties of homogeneous spin triplet superconductors.
In general, when two particles enter a state with total spin $S = 1$, three possible components of S_z appear

$$S_z = 1 \Rightarrow |\uparrow\uparrow\rangle\,, \quad S_z = 0 \Rightarrow \frac{1}{\sqrt{2}} |\uparrow\downarrow + \downarrow\uparrow\rangle\,, \quad S_z = -1 \Rightarrow |\downarrow\downarrow\rangle\,. \tag{4.65}$$

Thus, in general, the Cooper pair wavefunction is of the form

$$\begin{aligned}\varphi(\mathbf{r}_1 - \mathbf{r}_2; s_1, s_2) = \varphi_{\uparrow\uparrow}(\mathbf{r}_1 - \mathbf{r}_2)|\uparrow\uparrow\rangle + \varphi_{\uparrow\downarrow}(\mathbf{r}_1 - \mathbf{r}_2)|\uparrow\downarrow + \downarrow\uparrow\rangle + \\ + \varphi_{\downarrow\downarrow}(\mathbf{r}_1 - \mathbf{r}_2)|\downarrow\downarrow\rangle\,.\end{aligned} \tag{4.66}$$

Again, the Pauli principle forces the spatial components to be *odd* functions of their arguments.
It may happen that a suitable choice of axes leads to the cancellation of $\varphi_{\uparrow\downarrow}(\mathbf{r}_1 - \mathbf{r}_2)$, thus leading us to the above mentioned ESP case. Analogously, ESP is the canonical way to describe the condensation of a fully spin polarized state, and this will be the case while discussing the GS at FQHE with $\nu = 5/2$ in chapter 6. In such a case we can neglect the spin index all the way and we are therefore forced to consider an antisymmetric function $g_{\mathbf{k}}$.
The treatment of this state is quite similar to the BCS picture presented in the last sections, with the GS taking the form

$$|\Psi_{\text{ESP}}\rangle = \prod_{\mathbf{k}}{}' \left(u_{\mathbf{k}} + v_{\mathbf{k}}\, c^{\dagger}_{\mathbf{k}} c^{\dagger}_{-\mathbf{k}}\right) |\text{vac}\rangle \tag{4.67}$$

with

$$|u_{\mathbf{k}}|^2 + |v_{\mathbf{k}}|^2 = 1 \tag{4.68}$$

and

$$\begin{cases} u_{-\mathbf{k}} = u_{\mathbf{k}} \\ v_{-\mathbf{k}} = -v_{\mathbf{k}} \end{cases} . \tag{4.69}$$

In (4.67) the prime indicates that the product should be taken considering a pair with momentum $\mathbf{k}$ only once.
Following a treatment completely analogous to the BCS one presented above, we obtain the relations (4.19) and the same gap equation (4.59). A deeper analysis of the BdG equations for ESP p-wave superconductors will be presented in chapter 6. The full treatment of spin singlet pairing, including all the components present in (4.66) is quite complicated and many different phases with different physical properties arise. The many phases of p-wave superconductors have played a crucial role in the theory of ^3He superfluidity, their crossovers being driven by external parameters, such as pressure or magnetic fields. Many details on this fascinating topic can be found in [93] and [94].

Up to now we essentially saw that the Cooper paired states in homogeneous systems are plane waves with opposite momenta, their spins being set by the singlet-triplet pairing choice. A relevant question would be to ask what is the nature of the Cooper pairs in case of an inhomogeneous system. A first answer to that, in the s-wave case, was given by Anderson soon after the BCS theory came out, and took the name of "Anderson's Theorem" [95].
He considered the case of a "very dirty superconductor" where the energy scale associated to scattering by the impurities is much larger than the gap. The essential outcome of his analysis was that the Cooper pairs in this case are made out of eigenstates of the disorder potential, paired with their time-reversed state. Surprisingly enough the gap is hardly affected by disorder at all for very large concentration of impurities, a fact which was simultaneously verified in experiments [96]. This argument relies on the time-reversal symmetry of the system. A small amount of magnetic impurities, which break the symmetry, is enough to reduce the gap drastically, finally destroying superconductivity [97].

A few comments are still to be spent on the BCS GS. As already stressed, one of its most extravagant peculiarities is to be a superposition of many body states with different number of particles. However when we think of a finite piece of metal being cooled down to small temperatures we reasonably imagine its number of electrons to be fixed. What kind of relevance should we therefore give to the bizzarre structure of the BCS state?
The answer to these questions can be many-faced. First of all it is questionable whether we can consider the metal as a truly isolated system. Often, while testing the sample, there are current-carrying contacts as well as voltage probes, and in general the system is immersed into a reservoir with which to share small particle number fluctuations.
Then it has also been shown that it is possible to write the wavefunction corresponding to a fixed number N of particles by means of a trick invented by Anderson [98]. Let us consider the family of BCS-like states

$$|\Psi_{\rm BCS}(\theta)\rangle = \prod_{\mathbf{k}} \left(u_{\mathbf{k}} + v_{\mathbf{k}} e^{i\theta} c^{\dagger}_{\mathbf{k},\uparrow} c^{\dagger}_{-\mathbf{k},\downarrow} \right) |\text{vac}\rangle \tag{4.70}$$

parametrized by the phase ϕ. The components with different particle numbers are associated to different phases. In particular, the N-particle component has a phase $\exp(i\theta N/2)$. If we now consider the linear superposition

$$|\Psi_{\rm N}\rangle = \frac{1}{2\pi} \int_0^{2\pi} d\theta \, e^{-iN\theta/2} |\Psi_{\rm BCS}(\theta)\rangle \tag{4.71}$$

it clearly comes out that this is exactly the N-particle state.

Up to now we showed some of the unique features arising when a superconductive condensation occurs and pointed out how a crucial ingredient is the existence of an effective attractive interaction between the original Landau quasiparticles close to the Fermi energy.
Some years before the BCS theory was developed, Frölich understood that the attractive coupling in metals is mediated by dynamically screened acoustic phonons together with a screened Coulomb repulsion [99]. In other words it is possible to obtain the leading small energy dynamical effective interaction by performing an RPA calculation of the screened Coulomb interaction where the RPA polarization is calculated considering both the e-e Coulomb coupling as well as the free phonon propagation. This corresponds to taking the series of bubble diagrams where the free bubbles (free since we are at RPA) are connected with each other by *single* Coulomb or phonon field lines.
For normal metals, we are used to write the screened Coulomb interaction $\mathcal{V}_{\rm C}(\mathbf{q},\omega)$ starting from the Dyson's equation

$$\mathcal{V}_{\rm C}(\mathbf{q},\omega) = V(\mathbf{q}) + V(\mathbf{q})\Pi(\mathbf{q},\omega)\mathcal{V}_{\rm C}(\mathbf{q},\omega) \tag{4.72}$$

with $V(\mathbf{q})$ the unscreened Coulomb potential and $\Pi(\mathbf{q},\omega)$ the exact irreducible polarization. Equation (4.72) can be rewritten as

$$\mathcal{V}_{\rm C}(\mathbf{q},\omega) = \frac{V(\mathbf{q})}{1 - V(\mathbf{q})\Pi(\mathbf{q},\omega)} \equiv \frac{V(\mathbf{q})}{\kappa(\mathbf{q},\omega)} \tag{4.73}$$

where $\kappa(\mathbf{q},\omega)$ is the dynamical dielectric function.
The pole of $\Pi(\mathbf{q},\omega)$ gives the dispersion of the collective excitations (the plasmon) and the vanishing of $\kappa(\mathbf{q},0)$ at small momenta leads to the static screening at large distances.
In the same way, when also the propagation of phonons is accounted for, the effective screened interaction becomes [55]

$$\mathcal{V}_{\text{Eff}}(\mathbf{q},\omega) \equiv \frac{V(\mathbf{q})}{\tilde{\kappa}(\mathbf{q},\omega)} = \frac{V(\mathbf{q})}{1 - V(\mathbf{q})\Pi(\mathbf{q},\omega) - \frac{\Omega^2(\mathbf{q})}{\omega^2}} \tag{4.74}$$

where $\tilde{\kappa}(\mathbf{q},\omega)$ is the new dielectric function, with $\Omega(\mathbf{q})$ the (linear) dispersion of a longitudinal phonon with momentum $\mathbf{q}$.
If we were to get the qualitative behaviour of (4.74), being interested mainly in the small energy limit, we could resort to the RPA to approximate the polarization function with the free one (Π^0) and use a jellium model to treat the phonons.
In particular we could get a feeling for the effective dressed interaction in 2D using the estimate of the small energy-momentum scaling given in Appendix A, $\Pi^0 \simeq -m/2\pi$, and approximate $\Omega(q) \simeq v_{\text{P}} q$ with v_{P} the typical small momentum group velocity for 2D acoustic phonons. Thus we would have

$$\mathcal{V}^{2D}_{\text{Eff}}(\mathbf{q},\omega) \approx \frac{\frac{2\pi e^2}{\epsilon q}}{1 + \frac{e^2 m}{\epsilon q} - \frac{v_{\text{P}}^2 q^2}{\omega^2}} \tag{4.75}$$

and clearly the effective interaction is attractive for $\omega/q \to 0$. In the small momentum regime it stays attractive for $\omega < [\epsilon v_{\text{P}}^2 q^3/me^2]^{1/2}$.
A qualitative picture of the frequency dependence of $\mathcal{V}_{\text{Eff}}(\mathbf{q},\omega)$ for a given momentum is presented in Fig (4.6).

Having identified the dressed acoustic phonons as mediators of the attraction in the small energy sector we can characterize the cutoff ω_{D} in the BCS analysis as their Debye energy.
For many years people tried to get superconductivity out of a perturbative treatment of the effective phonon-mediated interaction (4.74) within a normal Fermi Liquid framework, without success. The crucial ingredient missing was the inclusion of anomalous averages and a GS with a broken symmetry.

After presenting a brief introduction to the BCS theory of superconductivity we will now describe a field theoretical treatment, originally proposed by Nambu and Gor'kov [100, 101], in which the standard many-body techniques are tailored to the case where anomalous averages are automatically included.
These techniques will allow us to include retardation effects and the Green's functions apparatus into the field of superconductivity. We will consider a particular application of the Nambu formalism to the instabilities presented in Chapter 5.

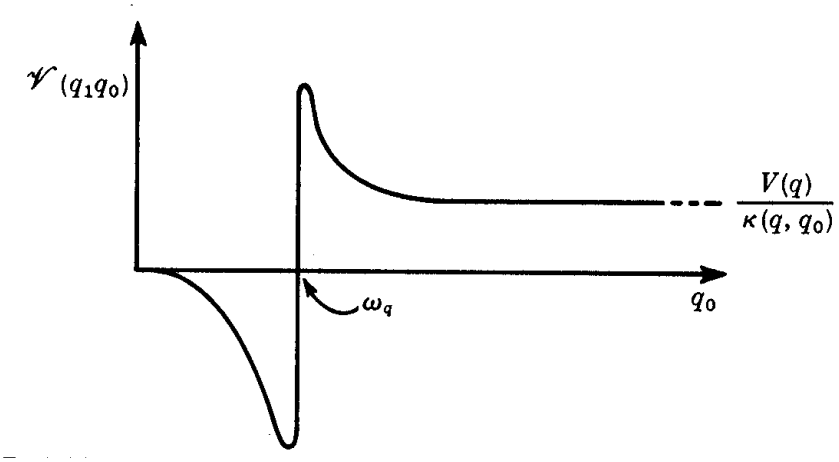

Fig. 4.6: The typical energy (q_0) dependence of the dressed effective interaction for a fixed momentum q. In the low energy sector, up to the acoustic phonon frequency ω_q, the interaction is attractive, leading to the condensation instability.

4.2 Green's functions for superconductors: the Nambu-Gor'kov formalism

Along the mean-field line of thinking used by Bogoliubov and Valatin it is possible to develop a field theoretical treatment of superconductors analogous to the well known many-body techniques applied to normal metals. This will allow an easier treatment of retardation effects in the interaction mediating the attraction and a systematic perturbation approach, together with the corresponding Feynman diagrammatic techniques.
The crucial ingredient to be introduced in the theory is the systematic inclusion of anomalous averages connected to the broken symmetry of the GS. Along with the normal averages $\langle \psi_s^\dagger \psi_s \rangle$ the anomalous ones associated with the superconductive condensation, $\langle \psi_s^\dagger \psi_{-s}^\dagger \rangle$ and $\langle \psi_s \psi_{-s} \rangle$, will have to be included in the definition of the single-particle Green's function.
Of course the mentioned ones are *not* the only possible anomalous averages conceivable. We could, for instance, consider $\langle \psi_s^\dagger \psi_{-s} \rangle$ (having to do with magnetic order in the symmetry-broken GS) and many others. The physical (experimental) information tells us that the vast majority of conventional superconductors show singlet pair structure; together with the condensation energy gain shown by Cooper we are naturally lead to the anomalous terms considered so far. The inclusion of different broken symmetries would however procede along the same line that will be shown, with suitable small changes.

Nambu realized that, by introducing the two components field operators

$$\Psi(\mathbf{r}) = \begin{pmatrix} \psi_\uparrow(\mathbf{r}) \\ \psi_\downarrow^\dagger(\mathbf{r}) \end{pmatrix}, \qquad \Psi^\dagger(\mathbf{r}) = \begin{pmatrix} \psi_\uparrow^\dagger(\mathbf{r}) & , \psi_\downarrow(\mathbf{r}) \end{pmatrix} \tag{4.76}$$

the mean-field BdG Hamiltonian (4.42) can be written in the compact matrix form

$$H_{\mathrm{MF}} = \int \mathrm{d}\mathbf{r}\ \Psi^\dagger(\mathbf{r})\, \mathbf{H}(\mathbf{r})\, \Psi(\mathbf{r}) \tag{4.77}$$

with

$$\mathbf{H}(\mathbf{r}) = \begin{pmatrix} H_e + U(\mathbf{r}) & \Delta(\mathbf{r}) \\ \Delta^*(\mathbf{r}) & -[H_e^* + U(\mathbf{r})] \end{pmatrix} \tag{4.78}$$

the Hamiltonian matrix.
On the basis of the Pauli matrices

$$\mathbf{1} = \begin{pmatrix} 1 & 0 \\ 0 & 1 \end{pmatrix} \quad \tau_1 = \begin{pmatrix} 0 & 1 \\ 1 & 0 \end{pmatrix} \quad \tau_2 = \begin{pmatrix} 0 & -i \\ i & 0 \end{pmatrix} \quad \tau_3 = \begin{pmatrix} 1 & 0 \\ 0 & -1 \end{pmatrix} \tag{4.79}$$

the Hamiltonian matrix has the form

$$\mathbf{H}(\mathbf{r}) = \mathbf{1}[i\,\mathrm{Im}H_e] + \tau_1[\mathrm{Re}\Delta(\mathbf{r})] + \tau_2[i\,\mathrm{Im}\Delta(\mathbf{r})] + \tau_3[\mathrm{Re}H_e + U(\mathbf{r})]\ . \tag{4.80}$$

In the absence of magnetic fields we can choose the phases of the fields such that the function Δ is real, thereby killing the contribution of the τ_2 matrix.
Having introduced a matrix form for the Hamiltonian of our system, it is then natural to introduce the matrix (Gor'kov) Green's function **G** out of the new field operators [101].
In analogy with the usual definition, the elements of **G** at $T = 0$ are

$$\mathbf{G}_{ab}(\mathbf{r}, t) = -\frac{i}{\hbar}\langle \mathcal{T}\left[\Psi_a(\mathbf{r}, t)\Psi_b^\dagger(\mathbf{0}, 0)\right]\rangle \tag{4.81}$$

where $\mathcal{T}$ is the time-ordering operator and $a, b \in \{1, 2\}$. The Gor'kov Green's function is thus

$$\mathbf{G}(\mathbf{r}, t) = \begin{pmatrix} -\frac{i}{\hbar}\langle \mathcal{T}\left[\Psi_\uparrow(\mathbf{r}, t)\Psi_\uparrow^\dagger(\mathbf{0}, 0)\right]\rangle & -\frac{i}{\hbar}\langle \mathcal{T}\left[\Psi_\uparrow(\mathbf{r}, t)\Psi_\downarrow^\dagger(\mathbf{0}, 0)\right]\rangle \\ -\frac{i}{\hbar}\langle \mathcal{T}\left[\Psi_\downarrow^\dagger(\mathbf{r}, t)\Psi_\uparrow^\dagger(\mathbf{0}, 0)\right]\rangle & -\frac{i}{\hbar}\langle \mathcal{T}\left[\Psi_\downarrow^\dagger(\mathbf{r}, t)\Psi_\downarrow(\mathbf{0}, 0)\right]\rangle \end{pmatrix}. \tag{4.82}$$

It is possible to introduce a diagrammatic representation of the matrix **G** (depicted as a thick double line) and of each of its normal and anomalous components shown in (4.82). Along the convention of letting the arrows come out of the creation fields $\psi^\dagger$ the diagrams associated to **G** and to $\mathbf{G}_{ab}(\mathbf{r}, t)$ are depicted in Fig (4.2).

Notice that the *free* Green's function matrix is diagonal, since the anomalous terms come out of selective contractions of the interaction part.
In the momentum representation the Nambu field operators are

$$\Psi(\mathbf{k}) = \begin{pmatrix} c_\uparrow(\mathbf{k}) \\ c_\downarrow^\dagger(-\mathbf{k}) \end{pmatrix} \tag{4.83}$$

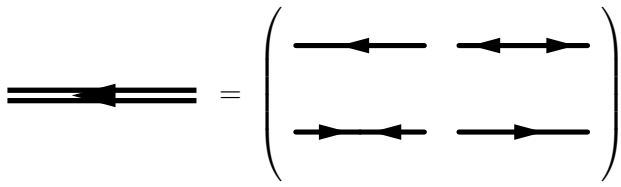

Fig. 4.7: The diagrammatic representation for the exact Gor'kov Green's function matrix, see (4.82). The thick double line represents the matrix $\mathbf{G}$ and the matrix elements $\mathbf{G}_{ab}$ are represented by thick single lines with arrows coming out of fermionic creation operators.

and they satisfy the fermionic commutation relations

$$\{\Psi(\mathbf{k}), \Psi^\dagger(\mathbf{k}')\} = \mathbf{1}\,\delta_{\mathbf{k}\mathbf{k}'} \quad , \quad \{\Psi(\mathbf{k}), \Psi(\mathbf{k}')\} = 0\,. \tag{4.84}$$

In the absence of magnetic fields the free fermionic Gor'kov Green's function in the momentum-energy representation is

$$\mathbf{G}^{(0)}(\mathbf{k}, E) = \begin{pmatrix} \frac{1}{E-\varepsilon_{\mathbf{k}}} & 0 \\ 0 & \frac{1}{E+\varepsilon_{\mathbf{k}}} \end{pmatrix}. \tag{4.85}$$

The exact Green's function can be obtained via the Dyson equation as

$$[\mathbf{G}(\mathbf{k}, E)]^{-1} = \left[\mathbf{G}^{(0)}(\mathbf{k}, E)\right]^{-1} - \mathbf{\Sigma}(\mathbf{k}, E) \tag{4.86}$$

where $\mathbf{\Sigma}$ is the matrix self-energy. Equation (4.86) is diagrammatically shown in components in Fig (4.2).

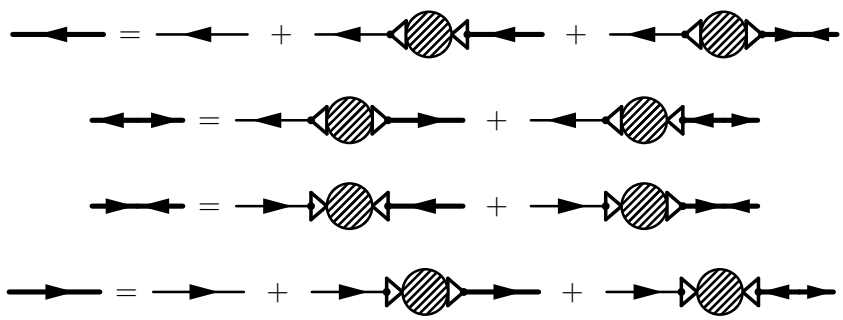

Fig. 4.8: The diagrammatic representation of the Dyson equation for the exact Gor'kov Green's function components $\mathbf{G}_{ab}$, see (4.86). Normal as well as anomalous selfenergy insertions are evident. Notice that, since the vertices always involve a fermionic part of the type $\psi^\dagger\psi$, the arrows "continue" in each of them and no *pair* creation or annihilation takes place.

The most general form for $\mathbf{\Sigma}$ can be written, on the basis of the Pauli matrices (4.79), as

$$\mathbf{\Sigma}(\mathbf{k}, E) = \mathbf{1}[E - EZ(\mathbf{k}, E)] + \tau_1[Z(\mathbf{k}, E)\Delta(\mathbf{k}, E)] + \tau_3[\delta\varepsilon_{\mathbf{k}}] \,, \tag{4.87}$$

again having chosen to kill the contribution of the τ_2 matrix. In (4.87) the so-called "mass-renormalization" function $Z(\mathbf{k}, E)$ has been introduced, together with the pairing function $\Delta(\mathbf{k}, E)$ and the single particle normal correction $\delta\varepsilon_{\mathbf{k}}$. We will see shortly that indeed the parameter $\Delta(\mathbf{k}, E)$ coincides with the gap we are used to from the BCS theory, and the reason of the name for the Z function will become clear. In the same spirit of the BCS treatment we will consider the *normal* selfenergy corrections as already incorporated in the single particle dispersion $\varepsilon_{\mathbf{k}}$, so that $\delta\varepsilon_{\mathbf{k}} = 0$ and the selfenergy matrix does not contain any τ_3 component (this is however not a crucial point, but it helps in simplifying the aspect of our expressions).
From (4.85,4.86,4.87) we extract the form for the matrix $\mathbf{G}$

$$\mathbf{G}(\mathbf{k}, E) = \frac{\mathbf{1}[E\, Z(\mathbf{k}, E)] + \tau_3[\varepsilon_{\mathbf{k}}] + \tau_1[Z(\mathbf{k}, E)\Delta(\mathbf{k}, E)]}{E^2\, Z^2(\mathbf{k}, E) - \varepsilon_{\mathbf{k}}^2 - Z^2(\mathbf{k}, E)\Delta^2(\mathbf{k}, E)} \,. \tag{4.88}$$

By studying the poles of this single particle Green's function we obtain informations about the spectrum of the excitations of the system. From the vanishing condition of the denominator in (4.88) we get the excitation energy

$$E^2 = \frac{\varepsilon_{\mathbf{k}}^2}{Z^2(\mathbf{k}, E)} + \Delta^2(\mathbf{k}, E) \tag{4.89}$$

closely resembling the Bogolons dispersion (4.61). Indeed it can be shown that in the BCS case $Z(\mathbf{k}, E) = 1$ and the reality of Δ comes from our phase choice (i.e. in the absence of magnetic fields Δ can always be chosen to be real).
Where the normal dispersion $\varepsilon_{\mathbf{k}}$ vanishes (i.e. at the Fermi level) we obtain the excitation gap Δ, justifying the choice of its name. Analogously, if the normal dispersion $\varepsilon_{\mathbf{k}}$ has the form $\varepsilon_{\mathbf{k}} \sim \hbar^2 k^2/2m$ the factor Z clearly renormalizes the electronic effective mass (again justifying the name chosen for it).
Up to now we did not make any assumption or choice about the form of the selfenergy with respect to the interaction and the fermionic Green's functions. To do so we can start discussing the perturbative treatment of the *matrix* Green's functions in line with the standard perturbation schemes for normal metals.
We have seen that the anomalous averages for the original fermionic operators come out naturally from *normal* averages of the Nambu field operators (see 4.82). Therefore we will have to consider a perturbation treatment *for the matrix Green's function* which is completely analogous to the one we are used to in *normal* metals. Every Green's function will be replaced by the corresponding matrix $\mathbf{G}$.
In order to incorporate the interactions in our treatment we notice the identity

$$\Psi^\dagger(\mathbf{k}+\mathbf{q})\tau_3\Psi(\mathbf{k}) = c_\uparrow^\dagger(\mathbf{k}+\mathbf{q})c_\uparrow(\mathbf{k}) + c_\downarrow^\dagger(-\mathbf{k})c_\downarrow(-\mathbf{k}-\mathbf{q}) - \delta_{\mathbf{q},0} \,. \tag{4.90}$$

A four fermion interaction term as in (4.26) is therefore written as

$$H_{\text{int}} = \frac{1}{2}\sum_{\mathbf{k},\mathbf{k}',\mathbf{q}} V(\mathbf{k}, \mathbf{k}', \mathbf{q}) \left[\Psi^\dagger(\mathbf{k}+\mathbf{q})\tau_3\Psi(\mathbf{k})\right] \left[\Psi^\dagger(\mathbf{k}'-\mathbf{q})\tau_3\Psi(\mathbf{k}')\right] \,. \tag{4.91}$$

In real cases this effective interaction is mediated by additional bosonic fields which must be coupled to the fermionic ones (we will see an explicit example in the next chapter).
In conventional superconductivity the bosonic fields are the dressed phonons mediating the residual attractive interaction close to the Fermi level. The dynamical bosonic field propagator entering the effective interaction will in general have a momentum-energy dependence, meaning a delay in the real time e-e coupling. The many body treatment we set up here is naturally suitable to treat these dynamical effects as well.
At this point the apparatus for the perturbative treatment is ready. We have to write selfenergy contributions in terms of the matrix Green's function and of the mediators of the interactions.
Every *selfconsistent* selfenergy diagram will in general be function of itself, through the form of the exact Green's functions. This implies we will find a system of nonlinear integral equations linking the two functions Z and Δ.
Let us take, for example, the selfconsistent Fock term due to the interaction (4.91), depicted in Fig(4.2).

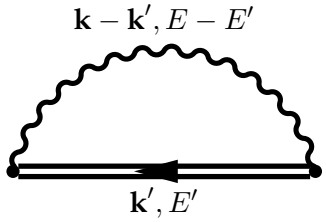

Fig. 4.9: The Fock type selfenergy correction to the single particle fermionic Gor'kov Green's function $\mathbf{G}^{(0)}(\mathbf{k}, E)$. Integration over internal momenta and frequency is implied.

Indeed, this was the first non trivial contribution considered by Eliashberg in his original treatment of the effects of the dynamical dressed phonons in the quasiparticle excitation spectrum of superconductors [102]. Thus

$$\mathbf{\Sigma}(\mathbf{k}, E) = i \int \frac{\mathrm{d}\mathbf{k}'\,\mathrm{d}E'}{(2\pi)^4}\, V(\mathbf{k}, \mathbf{k}', \mathbf{k}'-\mathbf{k}; E-E')\, \tau_3 \mathbf{G}(\mathbf{k}', E')\tau_3. \tag{4.92}$$

Substituting the form (4.87) for the selfenergy and the exact Green's function (4.88) we obtain

$$\mathbf{1}[E - EZ(\mathbf{k}, E)] + \tau_1[Z(\mathbf{k}, E)\Delta(\mathbf{k}, E)] = i \int \frac{\mathrm{d}\mathbf{k}'\,\mathrm{d}E'}{(2\pi)^4}\, V(\mathbf{k}, \mathbf{k}', \mathbf{k}'-\mathbf{k}; E-E') \times$$
$$\times \tau_3 \, \frac{\mathbf{1}[E'\, Z(\mathbf{k}', E')] + \tau_3[\varepsilon_{\mathbf{k}'}] + \tau_1[Z(\mathbf{k}', E')\Delta(\mathbf{k}', E')]}{E'^2\, Z^2(\mathbf{k}', E') - \varepsilon^2_{\mathbf{k}'} - Z^2(\mathbf{k}', E')\Delta^2(\mathbf{k}', E')}\, \tau_3 \,. \tag{4.93}$$

The formal inclusion of a frequency dependence in the effective interaction is automatic.

By writing the matrix equation in components we come out with a system of coupled integral equations for Z and Δ, called the "Eliashberg's equations".
It is in principle impossible to decouple exactly the mass renormalization equation from the gap one and even if this was done they would still be extremely difficult to solve separately. However, in some particular regimes, we can get a lot of important informations about the spectrum.
We will not dwell here on the original system considered by Eliashberg for his effective interaction. The interested reader can find more on that in [102, 103, 104].
We point out that the selfenergy diagram we just mentioned is only the simplest but non-trivial one (the Hartree contribution, being a constant energy shift, does not give rise to any new interesting effect). Further terms can be obtained by dressing the vertices, to reach the exact fermionic selfenergy.
In ordinary phonon-mediated superconductivity, however, it was shown by Migdal [105] that any additional bosonic insertion in the vertex part lead to corrections of order $\sqrt{m/M}$ where m is the electron mass and M the typical ionic mass. It was then natural to neglect these corrections and stick to the Fock term considered by Eliashberg.

In the next Chapter we will face the Eliashberg equations again and discuss their solutions in the case where dynamical bosonic gauge fields are the mediators of the residual attractive quasiparticle interaction.

5. SUPERCONDUCTIVE INSTABILITY OF COMPOSITE FERMIONS

In the previous chapters we have seen that several interesting phenomena take place close to the degeneracy of two LL of opposite spin at the Fermi energy.
This happens essentially because, at the crossing, the single particle fermionic energies of the two species coincide and the residual interactions between them is the leading energy scale to modify the GS properties.
In particular, the GS can be restructured and its spin-related properties can show anomalous behaviours. For example, as we saw in chapter 3, without quasiparticle interactions we cannot get the shoulder in the polarization observed around *every* CFLL crossing at the Fermi energy.
In this chapter we will consider the role of the residual interactions close to the degeneracy between two LL of fermions at the chemical potential.
Our approach will be essentially the following: we know from experiments that there is a point where the densities of the fermions belonging to the crossing modes coincide. This means that the two levels have an average filling $1/2$ each. We also know that a half filled LL of fermions can be mapped into a Fermi liquid of CF. Therefore we take, as a starting point, two Fermi liquids of CF (of two different species, which could be spin, or, more generally, pseudospins) and turn the interactions on.
The system we will consider is very close to what has been investigated in the field of bilayer Quantum Hall samples. A bilayer system can be realized in experiments by directly constructing two 2DES separated by a finite distance d or by producing a wide 2DES where two eigenstates of the confining potential in the z direction are occupied at the typical experimental densities. Clearly, in a bilayer system the pseudospin index coincides with the layer index.
In the following we will be mainly concerned in a *single* 2DEG where different fermion species coexist, being true spin eigenstates.
The main task will be to write the effective interaction coupling particles with the same as well as with opposite spins. The equal-spin interaction will essentially modify the single particle properties of CF, while the opposite-spin term can lead to more interesting effects. We will see, for instance, that the leading small energy interaction between particles with opposite spins and momenta can be attractive, leading to a condensation mechanism similar to what we just discussed in the framework of superconductivity [106]. The pairing instability of the CF liquid will be the main topic of the present chapter, and its outcomes will be discussed at the end of this section.
Along the chapter we will consider again the Chern-Simons Lagrangian, this time

for two species of fermions, and the related gauge field propagators mediating the residual CF interaction. To evaluate the superconductive properties of the system we will consider the Nambu-Gor'kov formalism and compute the energy gap in the spectrum by means of the Eliashberg equations described in the previous chapter.

5.1 The Chern-Simons Transformation with Spin

The first task of our analysis will be to write down the effective interaction between fermions with spins s and s'.
In analogy with what seen in chapter 2 the interaction is mediated by gauge field fluctuations. The effects of Coulomb as well as Chern-Simons terms will be incorporated in the gauge field propagator, while the coupling with the fermions is described by the vertices.
In order to obtain both the vertices and the propagators we start considering two coupled 2D Chern-Simons Fermi Liquids of opposite spins and equal quasiparticle mass m^* and densities, $\rho_\uparrow = \rho_\downarrow$. As suggested in chapter 3, the flux attachment generating the principal sequence of observed FQH states is performed independently for the two liquids, meaning that the Chern-Simons action is diagonal in the spins. The total real-time Lagrangian density is therefore (from now on we consider $\hbar = c = 1$, $e > 0$) [106, 107, 108],

$$\mathcal{L}(\mathbf{r},t) = \mathcal{L}_0(\mathbf{r},t) + \mathcal{L}_{\text{CS}}(\mathbf{r},t) + \mathcal{L}_{\text{Coul}}(\mathbf{r},t)\ . \tag{5.1}$$

The first term

$$\begin{aligned}\mathcal{L}_0(\mathbf{r},t) \quad = \quad & \sum_{s=\uparrow,\downarrow} \psi_s^\dagger(\mathbf{r},t)\Big\{ i\partial_t + \mu - e\mathcal{A}_0^s(\mathbf{r},t) \\ & -\frac{1}{2m^*}\Big[i\nabla - e\Big(\mathbf{A}(\mathbf{r}) - \boldsymbol{\mathcal{A}}^s(\mathbf{r},t)\Big)\Big]^2\Big\}\,\psi_s(\mathbf{r},t)\ ,\end{aligned} \tag{5.2}$$

describes Fermions with chemical potential μ, and spins $s = \pm 1 = \uparrow, \downarrow$ in the presence of the vector potential of the homogeneous external magnetic field, $\mathbf{B} = \nabla \times \mathbf{A}$, and the gauge fields $(\mathcal{A}_0^s, \boldsymbol{\mathcal{A}}^s)$ with $\boldsymbol{\mathcal{A}}^s = (\mathcal{A}_x^s, \mathcal{A}_y^s)$ corresponding to spin s. It clearly contains a free fermionic part and vertices connecting fermions with gauge fields.
The Chern-Simons Lagrangian of the gauge fields

$$\mathcal{L}_{\text{CS}}(\mathbf{r},t) = \frac{e}{\tilde{\varphi}\,\Phi_0}\sum_{s=\uparrow\downarrow} \mathcal{A}_0^s(\mathbf{r},t)\,\hat{\mathbf{z}}\cdot\nabla\times\boldsymbol{\mathcal{A}}^s(\mathbf{r},t)\ , \tag{5.3}$$

is responsible for attaching $\tilde{\varphi}$ flux quanta $\Phi_0 \equiv hc/e = 2\pi/e$ to each Fermion ($\hat{\mathbf{z}}$ is the unit vector in the direction perpendicular to the plane),

$$\hat{\mathbf{z}}\cdot\nabla\times\boldsymbol{\mathcal{A}}^s(\mathbf{r},t) \equiv b^s(\mathbf{r},t) = \tilde{\varphi}\Phi_0\rho_s(\mathbf{r},t)\ , \tag{5.4}$$

as can be seen by minimizing the action with respect to $\mathcal{A}_0^s$ (see (2.38)).
We have assumed here that the gauge term does not couple to the spins. This is equivalent to assuming that the orbital and the spin degrees of freedom are completely decoupled. In other words, this term corresponds to the Chern-Simons transformation (2.11) on the many electron wavefunction, depending only on the position of the particles. The Chern-Simons Lagrangian density clearly just contributes to the gauge fields propagators.

Finally, the Lagrangian of the Coulomb interaction between the fermions is

$$\mathcal{L}_{\text{Coul}}(\mathbf{r},t) = -\frac{1}{2}\sum_{s,s'=\uparrow,\downarrow}\int \mathrm{d}\mathbf{r}'\rho_s(\mathbf{r},t)\,V_{ss'}(\mathbf{r}-\mathbf{r}')\,\rho_{s'}(\mathbf{r}',t)\ , \tag{5.5}$$

and contains the densities of the Fermions with spin s, $\rho_s(\mathbf{r},t) \equiv \psi_s^\dagger(\mathbf{r},t)\psi_s(\mathbf{r},t)$. Using the constraint (5.4) we write $\mathcal{L}_{\text{Coul}}$ as a further term in the Lagrangian density for the gauge field fluctuations.
The existence of nonvanishing interspin interactions $V_{s,-s}$ means that the corresponding gauge field propagator is non diagonal in the spins.

For the interaction, we mention that $V_{\uparrow\uparrow} = V_{\downarrow\downarrow} = V_{\uparrow\downarrow} = V_{\downarrow\uparrow}$ and we assume a homogeneous isotropic potential $V(\mathbf{r}) = V(r) = V_\lambda/(r^2+d^2)^{\lambda/2}$ $(1 < \lambda < 2)$. For $\lambda = 1$, and $d \to 0$, this gives the pure Coulomb repulsion with $V_1 = e^2/\epsilon$. The Fourier transform of this is $V(q) = 2\pi e^2/\epsilon q$. For intermediate λ and $d \neq 0$, the potential decays as $r^{-\lambda}$ for large r, then for small q we have $V(q) \propto q^{\lambda-2}$. For $\lambda = 2$, $V(q \to 0) = \text{const}$.

In analogy to (2.42), the above total Lagrangian (5.1) can be shown to describe the same system of interacting electrons moving in a plane as without the Chern-Simons field.

With the Chern-Simons term, the effective magnetic field acting on a fermion with spin s is given by

$$B^s_{\text{eff}}(\mathbf{r},t) = B - b^s(\mathbf{r},t)\ . \tag{5.6}$$

If the filling factors for the two spin directions, $\nu_s = \rho_s\Phi_0/B$, are equal as in our case, $\nu_\uparrow = \nu_\downarrow = 1/2$, it is possible to compensate the external magnetic field B *for each spin channel* on the average by the *unique* choice $\tilde{\varphi} = 2$, preserving the fermionic statistics. Indeed, on the average, we get

$$\hat{\mathbf{z}}\cdot\nabla\times\langle\boldsymbol{\mathcal{A}}^s\rangle = \tilde{\varphi}\Phi_0\langle\rho_s\rangle \equiv B\ . \tag{5.7}$$

In the following we will consider the fluctuations of the gauge field with respect to its average by introducing

$$a^s_\mu = \mathcal{A}^s_\mu - \langle\mathcal{A}^s_\mu\rangle \tag{5.8}$$

with $\langle a^s_\mu\rangle = 0$.
The flux attachment constraint reads now

$$\rho_s(\mathbf{r},t) - \langle\rho_s\rangle = \frac{1}{\tilde{\varphi}\Phi_0}\,\hat{\mathbf{z}}\cdot\nabla\times\mathbf{a}^s(\mathbf{r},t)\ . \tag{5.9}$$

In this way the effect of the external vector potential $\mathbf{A}$ in $\mathcal{L}_0$ is compensated by $\langle\boldsymbol{\mathcal{A}}^s\rangle$. Moreover, since the average density contributes to the interaction Lagrangian just as an uninteresting constant, we can rewrite $\mathcal{L}_{\text{Coul}}$ in terms of density fluctuations, and then use the constraint (5.9) to cast it into a pure gauge fluctuation term.

The total lagrangian (5.1) is then rewritten as

$$\begin{aligned}
\mathcal{L}(\mathbf{r},t) &= \mathcal{L}_0(\mathbf{r},t)+\mathcal{L}_{\rm CS}(\mathbf{r},t)+\mathcal{L}_{\rm Coul}(\mathbf{r},t) \qquad (5.10)\\
\mathcal{L}_0(\mathbf{r},t) &= \sum_{s=\uparrow,\downarrow}\psi_s^\dagger(\mathbf{r},t)\Big\{i\partial_t+\mu-ea_0^s(\mathbf{r},t)+\\
&\qquad -\frac{1}{2m^*}\Big[i\nabla+e\mathbf{a}^s(\mathbf{r},t)\Big]^2\Big\}\psi_s(\mathbf{r},t)\ ,\\
\mathcal{L}_{\rm CS}(\mathbf{r},t) &= \frac{e}{\tilde\varphi\,\Phi_0}\sum_{s=\uparrow,\downarrow}a_0^s(\mathbf{r},t)\,\hat{\mathbf{z}}\cdot\nabla\times\mathbf{a}^s(\mathbf{r},t)\ ,\\
\mathcal{L}_{\rm Coul}(\mathbf{r},t) &= -\frac{1}{2(\tilde\varphi\,\Phi_0)^2}\sum_{s,s'=\uparrow,\downarrow}\int d\mathbf{r}'\,\hat{\mathbf{z}}\cdot\nabla\times\mathbf{a}^s(\mathbf{r},t)V_{ss'}(\mathbf{r}-\mathbf{r}')\hat{\mathbf{z}}\cdot\nabla\times\mathbf{a}^{s'}(\mathbf{r}',t)\ .
\end{aligned}$$

In the future we will write the propagators in the Matsubara imaginary-time representation. In order to obtain them we have therefore to write the Lagrangian density in the Euclidean space, $\mathcal{L}_{\rm E}$, by means of the substitutions

$$t\to -i\tau \quad ; \quad \partial_t\to i\partial_\tau \qquad (5.11)$$

$$\exp\left[i\mathcal{S}\right]\to\exp\left[\int_0^\beta d\tau\,\mathcal{L}(t=-i\tau)\right]\equiv\exp\left[-\int_0^\beta d\tau\,\mathcal{L}_{\rm E}(\tau)\right] \qquad (5.12)$$

where $\beta=1/{\rm K_B}T$ and $\rm K_B$ is the Boltzmann constant. Thus we obtain

$$\mathcal{L}_{\rm E}(\tau)=-\mathcal{L}(t=-i\tau)\ . \qquad (5.13)$$

In the Lagrangian density (5.10) we can identify three parts, describing free fermions, free gauge fields and the vertices between them. The resulting three Euclidean Lagrangians are then

$$\begin{aligned}
\mathcal{L}_{\rm E}(\mathbf{r},\tau) &= \mathcal{L}_{\rm F}(\mathbf{r},\tau)+\mathcal{L}_{\rm G}(\mathbf{r},\tau)+\mathcal{L}_{\rm Int}(\mathbf{r},\tau) \qquad (5.14)\\
\mathcal{L}_{\rm F}(\mathbf{r},\tau) &= \sum_{s=\uparrow,\downarrow}\psi_s^\dagger(\mathbf{r},\tau)\Big\{\partial_\tau-\mu-\frac{\nabla^2}{2m^*}\Big\}\psi_s(\mathbf{r},\tau) \qquad (5.15)\\
\mathcal{L}_{\rm G}(\mathbf{r},\tau) &= \sum_{s=\uparrow,\downarrow}\Big\{-\frac{e}{\tilde\varphi\,\Phi_0}\,a_0^s(\mathbf{r},\tau)\,\hat{\mathbf{z}}\cdot\nabla\times\mathbf{a}^s(\mathbf{r},\tau)+ \qquad (5.16)\\
&\qquad +\frac{1}{2(\tilde\varphi\,\Phi_0)^2}\sum_{s'=\uparrow,\downarrow}\int d\mathbf{r}'\,\hat{\mathbf{z}}\cdot\nabla\times\mathbf{a}^s(\mathbf{r},\tau)\,V_{ss'}(\mathbf{r}-\mathbf{r}')\,\hat{\mathbf{z}}\cdot\nabla\times\mathbf{a}^{s'}(\mathbf{r}',\tau)\Big\}\\
\mathcal{L}_{\rm Int}(\mathbf{r},\tau) &= \sum_{s=\uparrow,\downarrow}\psi_s^\dagger(\mathbf{r},\tau)\Big\{ea_0^s(\mathbf{r},\tau)+\frac{ie}{2m^*}\Big[\nabla\cdot\mathbf{a}^s(\mathbf{r},\tau)+\mathbf{a}^s(\mathbf{r},\tau)\cdot\nabla\Big]+\\
&\qquad +\frac{e^2}{2m^*}\,\mathbf{a}^s(\mathbf{r},\tau)\cdot\mathbf{a}^s(\mathbf{r},\tau)\Big\}\psi_s(\mathbf{r},\tau) \qquad (5.17)
\end{aligned}$$

5.2 The Free Propagators and the vertices

We will now consider the free propagators for fermions, gauge fields and the vertices described by the Lagrangian density (5.14). As usual, it will be more conve-

nient to work in the energy-momentum space with the definitions (for a generic field ϕ_μ)

$$\phi_\mu(\mathbf{r},\tau) = \beta^{-1} \sum_{n=-\infty}^{+\infty} \int \frac{\mathrm{d}\mathbf{k}}{(2\pi)^2}\, e^{i(\mathbf{k}\cdot\mathbf{r}-\omega_n\tau)} \phi_\mu(\mathbf{k},\omega_n) \tag{5.18}$$

$$\phi_\mu(\mathbf{k},\omega_n) = \int \mathrm{d}\mathbf{r} \int_0^\beta \mathrm{d}\tau\, e^{-i(\mathbf{k}\cdot\mathbf{r}-\omega_n\tau)} \phi_\mu(\mathbf{r},\tau) \tag{5.19}$$

with $n \in \mathbb{Z}$ and

$$\omega_n = \begin{cases} (2n+1)\pi\beta^{-1}, & \text{for fermions} \\ 2n\pi\beta^{-1}, & \text{for bosons} \end{cases} \tag{5.20}$$

5.2.1 The free fermion propagator

Let us first consider the free fermionic action

$$\mathcal{S}_\mathrm{F} = \int \mathrm{d}\mathbf{r} \int_0^\beta \mathrm{d}\tau\, \mathcal{L}_\mathrm{F}(\mathbf{r},\tau)\ . \tag{5.21}$$

In the Fourier space it reads

$$\mathcal{S}_\mathrm{F} = -\beta^{-1} \sum_s \sum_{n=-\infty}^{+\infty} \int \frac{\mathrm{d}\mathbf{k}}{(2\pi)^2}\, \psi_s^\dagger(\mathbf{k},\omega_n) \left[i\omega_n - \varepsilon_\mathbf{k}\right] \psi_s(\mathbf{k},\omega_n) \tag{5.22}$$

with the definition $\varepsilon_\mathbf{k} = k^2/2m^* - \mu$.
On the other side we know that the fermionic action is linked to the Matsubara Green's function via the relation

$$\mathcal{S}_\mathrm{F} = -\beta^{-1} \sum_{n=-\infty}^{+\infty} \int \frac{\mathrm{d}\mathbf{k}}{(2\pi)^2}\, \psi^\dagger(\mathbf{k},\omega_n) \left[\mathcal{G}^0(\mathbf{k},\omega_n)\right]^{-1} \psi(\mathbf{k},\omega_n) \tag{5.23}$$

whence we deduce that, in our case

$$\left[\mathcal{G}_s^0(\mathbf{k},\omega_n)\right]^{-1} = i\omega_n - \varepsilon_\mathbf{k} \tag{5.24}$$

and is independent on spin.

5.2.2 The free gauge field propagator

In analogy to what done before, we now derive the propagator of the gauge fields out of the Free action

$$\mathcal{S}_\mathrm{G} = \int \mathrm{d}\mathbf{r} \int_0^\beta \mathrm{d}\tau\, \mathcal{L}_\mathrm{G}(\mathbf{r},\tau)\ . \tag{5.25}$$

We choose the transverse gauge, $\nabla \cdot \mathbf{a}^s = 0$ which, in the Fourier space, becomes $\mathbf{q} \cdot \mathbf{a}^s(\mathbf{q}) = 0$.

If we then project the vector $\mathbf{a}^s(\mathbf{q})$ on the 2D versors orthogonal ($\hat{e}_{\rm T}(\mathbf{q}) = \hat{\mathbf{z}} \times \mathbf{q}/q$) and parallel ($\hat{e}_{\rm L}(\mathbf{q}) = \mathbf{q}/q$) to $\mathbf{q}$,

$$\mathbf{a}^s(\mathbf{q}) = a_1^s(\mathbf{q})\, \hat{e}_{\rm T}(\mathbf{q}) + a_2^s(\mathbf{q})\, \hat{e}_{\rm L}(\mathbf{q}) \,, \tag{5.26}$$

the gauge choice implies $a_2^s(\mathbf{q}) = 0$.
From now on we will use the notation a_μ^s, ($\mu = 0, 1$), and we have

$$a_0^{s\dagger}(\mathbf{q}, \Omega_n) = a_0^s(-\mathbf{q}, \Omega_n) \qquad a_1^{s\dagger}(\mathbf{q}, \Omega_n) = -a_1^s(-\mathbf{q}, \Omega_n) \,. \tag{5.27}$$

with bosonic frequencies Ω_n. The relations (5.27) have been obtained imposing the reality of $a_\mu^s(\mathbf{r})$ and considering that $\hat{e}_{\rm T}(-\mathbf{q}) = -\hat{e}_{\rm T}(\mathbf{q})$.
Using the identity (2.63) the gauge fields action $\mathcal{S}_{\rm G}$ becomes

$$\mathcal{S}_{\rm G} = -\beta^{-1} \sum_{s,s'=\uparrow,\downarrow} \sum_{n=-\infty}^{+\infty} \int \frac{\mathrm{d}\mathbf{q}}{(2\pi)^2} \Big\{ a_0^s(\mathbf{q}, \Omega_n)\, \frac{ieq}{\tilde{\varphi}\, \Phi_0}\, a_1^s(-\mathbf{q}, \Omega_n) + \\ + a_1^s(\mathbf{q}, \Omega_n)\, \frac{q^2 V_{ss'}(q)}{2(\tilde{\varphi}\, \Phi_0)^2}\, a_1^{s'}(-\mathbf{q}, \Omega_n) \Big\} \,. \tag{5.28}$$

Due to the existence of the term $V_{s,-s}$ the gauge field propagator is non diagonal in the spins. We can however define diagonal gauge modes as symmetric and anti-symmetric spin combinations

$$a_\mu^\alpha = \frac{1}{2}(a_\mu^\uparrow + \alpha\, a_\mu^\downarrow) \,, \tag{5.29}$$

with $\alpha = \pm$. The inverse relation yields

$$a_\mu^\uparrow = a_\mu^+ + a_\mu^- \qquad , \qquad a_\mu^\downarrow = a_\mu^+ - a_\mu^- \,, \tag{5.30}$$

thanks to which the free diagonal gauge field action becomes

$$\mathcal{S}_{\rm G} = -\frac{1}{2} \sum_{\mu\nu,\alpha=\pm} \sum_{n=-\infty}^{+\infty} \int \frac{\mathrm{d}\mathbf{q}}{(2\pi)^2}\, a_\mu^{\alpha\dagger}(\mathbf{q}, \Omega_n) \left[\mathcal{D}_{\mu\nu}^{0\alpha}(\mathbf{q}, \Omega_n)\right]^{-1} a_\nu^\alpha(\mathbf{q}, \Omega_n) \tag{5.31}$$

with the free Matsubara inverse gauge field propagator

$$\left[\mathcal{D}_{\mu\nu}^{0\alpha}(\mathbf{q}, \Omega_n)\right]^{-1} = \begin{pmatrix} 0 & \frac{2ieq}{\tilde{\varphi}\Phi_0} \\ -\frac{2ieq}{\tilde{\varphi}\Phi_0} & -\frac{4q^2 V(q)}{\tilde{\varphi}^2 \Phi_0^2}\, \delta_{\alpha,+} \end{pmatrix} . \tag{5.32}$$

The diagonal free gauge field Green's functions, obtained inverting the matrix (5.32), are

$$\mathcal{D}_{\mu\nu}^{0\alpha}(\mathbf{q}, \Omega_n) = \left(\frac{\tilde{\varphi}\Phi_0}{2eq}\right)^2 \begin{pmatrix} \frac{4q^2 V(q)}{\tilde{\varphi}^2 \Phi_0^2}\, \delta_{\alpha,+} & \frac{2ieq}{\tilde{\varphi}\Phi_0} \\ -\frac{2ieq}{\tilde{\varphi}\Phi_0} & 0 \end{pmatrix} . \tag{5.33}$$

The antisymmetric component $\mathcal{D}^{0(-)}_{\mu\nu}(\mathbf{q},\Omega_n)$ is not affected by the Coulomb term. This comes out by considering that the antisymmetric gauge field $a^{(-)}_\mu$ feels the $V_{s,s} - V_{s,-s}$ combination, which vanishes due to the spin independent nature of $V_{s,s'}$.
On the contrary, the $\mathcal{D}^{0(+)}_{\mu\nu}(\mathbf{q},\Omega_n)$ mode is renormalized by the combination $V_{s,s} + V_{s,-s} = 2V_{s,s'}$.
As in chapter 2, the dynamics of the gauge field propagators will come out of the coupling with the fermions. For the Coulomb case, each matrix element of (5.33) scales as $1/q$ and the RPA will therefore be a good approximation in describing their small momentum dominant behaviour.

5.2.3 Interactions and vertices between fermions and gauge fields

The last part of the Lagrangian density (5.14) to be considered is $\mathcal{L}_{\text{Int}}$ describing the vertices between the fermions and the gauge field fluctuations. In the Fourier space it has the form

$$\mathcal{L}_{\text{Int}}(\tau) = \sum_{s=\uparrow,\downarrow} \int \frac{\mathrm{d}\mathbf{k}}{(2\pi)^2}\frac{\mathrm{d}\mathbf{q}}{(2\pi)^2}\Big[\psi^\dagger_s(\mathbf{k}+\mathbf{q},\tau)\Big(ea^s_0(\mathbf{q},\tau) - \frac{e}{2m^*}(2\mathbf{k}+\mathbf{q})\cdot\mathbf{a}^s(\mathbf{q},\tau)\Big)\psi_s(\mathbf{k},\tau) + \\ + \int \frac{\mathrm{d}\mathbf{k}'}{(2\pi)^2}\,\psi^\dagger_s(\mathbf{k}+\mathbf{q},\tau)\Big(\frac{e^2}{2m^*}\,\mathbf{a}^s(\mathbf{q},\tau)\cdot\mathbf{a}^s(\mathbf{q}',\tau)\Big)\psi_s(\mathbf{k}+\mathbf{q}',\tau)\Big]\,. \tag{5.34}$$

It can be rewritten as

$$\mathcal{L}_{\text{Int}}(\tau) = \sum_{s=\uparrow,\downarrow} \int \frac{\mathrm{d}\mathbf{k}}{(2\pi)^2}\frac{\mathrm{d}\mathbf{q}}{(2\pi)^2}\Big[\sum_\mu v^s_\mu(\mathbf{k},\mathbf{q})\psi^\dagger_s(\mathbf{k}+\mathbf{q},\tau)a^s_\mu(\mathbf{q},\tau)\psi_s(\mathbf{k},\tau) + \\ + \frac{1}{2}\sum_{\mu,\nu}\int \frac{\mathrm{d}\mathbf{k}'}{(2\pi)^2}\,w^s_{\mu\nu}\;\psi^\dagger_s(\mathbf{k}+\mathbf{q},\tau)a^s_\mu(\mathbf{q},\tau)a^s_\nu(\mathbf{q}',\tau)\psi_s(\mathbf{k}+\mathbf{q}',\tau)\Big]\,. \tag{5.35}$$

with the vertices

$$v^s_\mu(\mathbf{k},\mathbf{q}) = \begin{cases} e, & \text{for } \mu = 0 \\ \frac{e}{m^*}\,\hat{\mathbf{z}}\cdot\frac{\mathbf{k}\times\mathbf{q}}{q}, & \text{for } \mu = 1 \end{cases}$$
$$w^s_{\mu\nu}(\mathbf{q},\mathbf{q}') = \frac{e^2}{m^*}\,\frac{\mathbf{q}\cdot\mathbf{q}'}{qq'}\,\delta_{\mu 1}\delta_{\nu 1}\,. \tag{5.36}$$

In diagrammatic terms they are represented in Fig (2.3.3).
Rewriting the gauge fields a^s in terms of their diagonal components $a^\pm$ we can see that a fermionic line with spin s has vertices with *both* the symmetric and antisymmetric gauge field fluctuations. Since the effective interaction $V_{ss'}$ between the fermions will be obtained by considering two vertices and the internal gauge field propagator we can directly see how *both* D^+ and D^- contribute to the *same* (s,s') channel.
Thus, in the symmetric-antisymmetric representation a vertex involving fermions with spin $s = \pm 1$ and a gauge field of the type α comes together with a factor $(\delta_{\alpha,+} + s\,\delta_{\alpha,-})$.

Having introduced the free Green's functions for fermions and gauge fields and their actions we can start considering the perturbation expansion of the propagators in terms of the vertices described by the Lagrangian (5.35).
The exact gauge field propagator is defined as

$$\mathcal{D}_{\mu\nu}(\mathbf{q},\tau) = -\langle \mathrm{T}_\tau \left[a_\mu(\mathbf{q},\tau) a^\dagger_\nu(\mathbf{q},0) \right] \rangle \tag{5.37}$$

analogously to the fermionic Green's function

$$\mathcal{G}_s(\mathbf{k},\tau) = -\langle \mathrm{T}_\tau \left[\psi_s(\mathbf{k},\tau) \psi^\dagger_s(\mathbf{k},0) \right] \rangle \ , \tag{5.38}$$

where T_τ is the imaginary time ordering operator. They can also be obtained as

$$\mathcal{D}_{\mu\nu}(\mathbf{q},\tau) = -\frac{1}{\mathcal{Z}} \int \mathcal{D}\psi^\dagger_{\mathbf{k}} \mathcal{D}\psi_{\mathbf{k}} \mathcal{D}a_\mu(\mathbf{q})\, e^{-\mathcal{S}_\mathrm{E}} a_\mu(\mathbf{q},\tau) a^\dagger_\nu(\mathbf{q},0) \tag{5.39}$$

and the analogous for $\mathcal{G}_s$, with $\mathcal{S}_\mathrm{E} = \int \mathrm{d}\mathbf{r}\, \mathrm{d}\tau\, \mathcal{L}_\mathrm{E}(\mathbf{r},\tau)$ and the partition function

$$\mathcal{Z} = \int \mathcal{D}\psi^\dagger_{\mathbf{k}} \mathcal{D}\psi_{\mathbf{k}} \mathcal{D}a_\mu(\mathbf{q})\, e^{-\mathcal{S}_\mathrm{E}} \ . \tag{5.40}$$

Expanding the exponential of the interaction action contained in $\mathcal{S}_\mathrm{E}$ as

$$e^{-\mathcal{S}_\mathrm{int}} = \sum_{n=0}^{\infty} \frac{(-1)^n}{n!} \left(\mathcal{S}_\mathrm{int}\right)^n \tag{5.41}$$

and taking all the possible contractions of couple of fermions and gauge field operators we produce the corresponding Green's functions according to (5.37) and (5.38). That is, using Wick's theorem we will break the average of the product of many operators into contractions of couples of them, with the relations

$$\langle a^\alpha_\mu(\mathbf{q},\tau) a^\alpha_\nu(\mathbf{q}',\tau') \rangle = -\,(-1)^\nu\, \mathcal{D}^{(0)\alpha}_{\mu\nu}(\mathbf{q},\tau-\tau')\, \delta(\mathbf{q}+\mathbf{q}') \tag{5.42}$$

$$\langle \psi_s(\mathbf{k},\tau) \psi^\dagger_{s'}(\mathbf{k}',\tau') \rangle = -\,\mathcal{G}^{(0)}_s(\mathbf{k},\tau-\tau')\, \delta_{ss'}\, \delta(\mathbf{k}-\mathbf{k}') \ . \tag{5.43}$$

As usual, we will concentrate on connected diagrams with free internal Green's functions.

With the formal apparatus of perturbation theory we can now address the Random Phase Approximation for the gauge field propagators.

5.3 The RPA for the Gauge field propagator

The RPA for the gauge field propagator will be obtained considering the free polarization function in the Dyson equation (2.78). In the Matsubara representation we have

$$\Pi^0_{\mu\nu}(\mathbf{q},\Omega_n) = \beta^{-1} \sum_s \sum_m w^s_{\mu\nu}(\mathbf{q},\mathbf{q}) \int \frac{\mathrm{d}\mathbf{k}}{(2\pi)^2}\, \mathcal{G}^0_s(\mathbf{k},\omega_m)\, e^{i\omega_m 0^+} + \\ + \beta^{-1} \sum_s \sum_m \int \frac{\mathrm{d}\mathbf{k}}{(2\pi)^2}\, v^s_\mu(\mathbf{k},\mathbf{q}) \mathcal{G}^0_s(\mathbf{k}-\mathbf{q},\omega_m-\Omega_n) \mathcal{G}^0_s(\mathbf{k},\omega_m) v^s_\nu(\mathbf{k},\mathbf{q}) \ . \tag{5.44}$$

These polarization terms correspond to the diagrams of Fig (2.4).
In the following we will be mainly interested in processes close to the Fermi energy of the two degenerate CF Fermi liquids. In particular we will be interested in the possibility of the superconductive restructuration of the GS by the effective fermionic interaction, taking place close to the Fermi level. This means that we will need the small energy behaviour of the gauge field propagator mediating the coupling.
To get this, we then consider the polarization Π^0 in the regime $|\Omega_n| \ll v_{\rm F} q \ll v_{\rm F} k_{\rm F}$. The result (see Appendix A) is

$$\Pi^0(\mathbf{q},\Omega_n) = \begin{pmatrix} -\frac{e^2 m^*}{\pi}\left(1-\frac{|\Omega_n|}{q v_{\rm F}}\right) & 0 \\ 0 & \frac{e^2 q^2}{12\pi m^*} + \frac{4e^2|\Omega_n|\rho}{m^* q v_{\rm F}} \end{pmatrix} . \tag{5.45}$$

Replacing this result in the exact polarization present in the Dyson equation we get the propagator in Random Phase Approximation ($\alpha = \pm 1$)

$$\begin{aligned} \mathcal{D}^{\alpha}(\mathbf{q},\Omega_m) &= \frac{1}{\zeta(q)[\gamma^+(q)\delta_{\alpha,+} + \gamma^-(q) - \eta|\Omega_m|/q] - \beta^2 q^2} \\ &\times \begin{pmatrix} \gamma^+(q)\delta_{\alpha,+} + \gamma^-(q) - \eta\frac{|\Omega_m|}{q} & -i\beta q \\ i\beta q & \zeta(q) \end{pmatrix} \end{aligned} \tag{5.46}$$

where $\zeta(q) = e^2 m^*(1-|\Omega_n|/q v_{\rm F})/\pi$, $\beta = 2e/\tilde{\varphi}\Phi_0$, $\gamma^+(q) = -4q^2 V(q)/\tilde{\varphi}^2\Phi_0^2$, $\gamma^-(q) = -q^2 e^2/12\pi m^*$, $\eta = 2e^2\rho/m^* v_{\rm F}$. Notice that for zero Coulomb interaction $\gamma^+ = 0$ the symmetric and antisymmetric propagators are equal $\mathcal{D}^+ = \mathcal{D}^-$. For small q and Ω_n, the dominant matrix elements are

$$\mathcal{D}_{11}^+(\mathbf{q},\Omega_n) \approx \frac{-q}{\alpha_+(q)q^2 + \alpha_- q^3 + \eta|\Omega_n|} \tag{5.47}$$

$$\mathcal{D}_{11}^-(\mathbf{q},\Omega_n) \approx \frac{-q}{\alpha_- q^3 + \eta|\Omega_n|} \tag{5.48}$$

with $\alpha_+ = 4qV(q)/\tilde{\varphi}^2\Phi_0^2$ and $\alpha_- = (e^2/12\pi + 4\pi/\tilde{\varphi}^2\Phi_0^2)/m^*$.
For Coulomb interaction ($\lambda = 1$), $V(q) \propto 1/q$ and $\alpha^+ \approx$ const. In this case, the matrix element $\mathcal{D}_{11}^-$ is much larger than $\mathcal{D}_{11}^+$ for $q \to 0$.
On the other hand, when the interaction is screened ($\lambda = 2$), $V(q \to 0)$= const, $\alpha^+ \propto q$, and $\mathcal{D}_{11}^-$ and $\mathcal{D}_{11}^+$ are of the same order.
From now on we will focus on the unscreened Coulomb interaction ($\lambda = 1$), neglecting in eq. (5.47) the sub-leading term α^-.
From (5.47,5.48) by analytical continuation we can deduce the real frequency form

of the retarded gauge field propagators

$$D_{11}^{R(+)}(\mathbf{q},\Omega) \approx \frac{-q}{\alpha_+(q)q^2+\alpha_- q^3 - i\eta\Omega} \tag{5.49}$$

$$D_{11}^{R(-)}(\mathbf{q},\Omega) \approx \frac{-q}{\alpha_- q^3 - i\eta\Omega}\ . \tag{5.50}$$

These Green's function have poles at the complex frequencies

$$\Omega^{(+)} = -i\,\frac{\alpha_+(q)q^2+\alpha_- q^3}{\eta} \tag{5.51}$$

$$\Omega^{(-)} = -i\,\frac{\alpha_- q^3}{\eta}\ . \tag{5.52}$$

They correspond to slowly decaying modes and in the case of Coulomb interaction, for small momentum, the pole $\Omega^{(-)}$ is the smallest one. In this case the antisymmetric mode is the slowest to decay and becomes the leading coupling channel between the fermions in the low energy regime.

Having identified the dominant sector ($\mu=\nu=1$) we can write explicitly the effective interaction describing the low energy process where a fermion of spin s and momentum $\mathbf{k}$ scatters another fermion of spin s' and momentum $\mathbf{k}'$ with a three-momentum transfer $(\mathbf{q},\Omega_n)$. Such a scattering event is depicted in Fig (4.1.2) and we have

$$V_{\text{eff}}^{ss'}(\mathbf{k},\mathbf{k}',\mathbf{q};\Omega_n) = -\,v_{\mu=1}^{s}(\mathbf{k},\mathbf{q})v_{\nu=1}^{s'}(\mathbf{k}',-\mathbf{q})\left(\mathcal{D}_{11}^{+}(\mathbf{q},\Omega_n)+ss'\mathcal{D}_{11}^{-}(\mathbf{q},\Omega_n)\right)\ . \tag{5.53}$$

A similar analysis has been carried out in [110].
The frequency dependence of the effective interactions means a real-time retardation effect due to the dynamical screening of the gauge field fluctuation by the fermions. This aspect is incorporated naturally in the field theoretical language of the Green's functions rather than in a Hamiltonian approach as we used in the weak coupling theory of superconductivity.
From (5.53) we can see that, in the Cooper channel ($s'=-s,\mathbf{k}'=-\mathbf{k}$) we have

$$V_{\text{eff}}^{s,-s}(\mathbf{k},-\mathbf{k},\mathbf{q};\Omega_n) = \left(\frac{e}{m^*}\right)^2\left(\frac{\mathbf{k}\times\mathbf{q}}{q}\right)^2\left(\mathcal{D}_{11}^{-}(\mathbf{q},\Omega_n)-\mathcal{D}_{11}^{+}(\mathbf{q},\Omega_n)\right)\ . \tag{5.54}$$

Since the antisymmetric channel dominates over the symmetric one, and having determined their leading form (5.47,5.48), we see that for small energies the leading coupling is attractive and can lead to an instability of the Fermi liquid GS as in the case of phonon-mediated superconductivity. This is exactly what we will investigate in the next section by explicitly calculating the energy gap in the spectrum close to the Fermi level via the Eliashberg techniques.
It is not immediate to grasp the physical reason for an effective attractive interaction in the antisymmetric channel. It comes more natural if we think in terms of a bilayer system (the spin being a layer index) with a very small interlayer separation d. By this we mean that d is much smaller than the typical distance between

the fermions in each layer.
In this system the $\mathcal{D}^{(-)}$ propagator is coupled to the antisymmetric combination of the fermionic density between the layers. This means that to any positive density fluctuation in one layer it corresponds a negative fluctuation in the other. Thus, to any quasiparticle the antisymmetric mode offers a quasihole at a characteristic distance d, a process which tends to lower effectively the energy.

Before considering the superconductive instability of the GS, we could ask what would be the influence of the new interaction channel $\mathcal{D}^{(-)}$ on the quasiparticle properties of the Normal Fermi liquid phase. For instance, we could investigate the Landau quasiparticle effective mass close to the Fermi level, in analogy to what seen in chapter 2.
We should then calculate the fermionic selfenergy (see (2.93)) with the dominant antisymmetric channel $\alpha = -$,

$$\delta\Sigma(\mathbf{k},\omega) \simeq i \int \frac{\mathrm{d}\mathbf{k}'}{(2\pi)^2} \frac{\mathrm{d}\Omega}{2\pi} v_1(\mathbf{k},\mathbf{k}')^2 D_{11}^-(\mathbf{k}-\mathbf{k}',\Omega) \left[G^0(\mathbf{k}',\omega-\Omega) - G^0(\mathbf{k}',-\Omega)\right] . \tag{5.55}$$

The calculation is essentially analogous to what done to obtain (2.104), except from the integral over q. In fact, the q^{-2} quasistatic divergence of the antisymmetric gauge field propagator produces, in the small energy regime,

$$\int_0^{2k_\mathrm{F}} \mathrm{d}q\, D_{11}^-(q,\Omega) = \int_0^{2k_\mathrm{F}} \mathrm{d}q\, \frac{-q}{\alpha_- q^3 - i\eta\Omega} \simeq -\frac{2\pi\sqrt{3}}{9} \left[\frac{i}{\alpha_-^2\, \eta\, \Omega}\right]^{1/3} \tag{5.56}$$

with the final result for (5.55) [112]

$$\delta\Sigma(\mathbf{k},\omega) \simeq -\frac{\pi}{\sqrt{3}} \left[\frac{i}{\alpha_-^2 \eta}\right]^{1/3} \omega^{2/3} . \tag{5.57}$$

This form of the selfenergy would produce an effective mass diverging as $\omega^{-1/3}$ close to the Fermi level.
The Ward identities occurring for the exactness of the first order selfenergy term in the spinless case work in this case as well. The result (5.57) should thus be exact [113].
Again, the experimental test of such a divergence would be a difficult task, even because we would need a fully unpolarized even denominator state. The spin polarization experiment by Kukushkin [61] showed that $\nu = 1/2$ is *fully polarized* for $B > 9.3$ T, the spin polarization decreasing smoothly while lowering the field. This means that for high enough fields the regime of the logarithmic mass correction can be accessed. On the contrary, the *fully unpolarized* $\nu = 1/2$ state was never reached and is probably expected only for $B \to 0$.
However, we believe that the predicted power law corrections in the unpolarized case can become relevant close to the SCFLL degeneracy in modifying the low energy excitation spectrum for the Normal liquid phase. This issue is presently under consideration [112].

Together with the mentioned singular normal phase corrections, the residual interaction due to the antisymmetric gauge field channel mediates an attraction between Fermions in the s-wave Cooper channel.
In the next section we will concentrate on the interaction-induced instability to the Cooper pair formation. To verify whether the phenomenon occurs we study the selfconsistent equations connecting normal and anomalous fermionic Green's functions and finally deal with the possibility of an outcoming non-vanishing gap.

5.4 The Dyson Equation for the fermionic Nambu-Gor'kov Green's function

To get informations about the spectrum of the quasiparticle excitations of the two coupled Fermi Liquids we investigate the single particle fermionic Green's function. The possibility of a superconductive instability will be considered, taking into account non-vanishing anomalous contributions. As seen in the previous chapter this issue is automatically included in the Nambu-Gor'kov treatment of the propagators.
We start from the Nambu field

$$\mathbf{\Phi}(\mathbf{k},\tau) = \begin{pmatrix} \psi_\uparrow(\mathbf{k},\tau) \\ \psi^\dagger_\downarrow(-\mathbf{k},\tau) \end{pmatrix} \equiv \begin{pmatrix} \Phi_1(\mathbf{k},\tau) \\ \Phi^\dagger_2(\mathbf{k},\tau) \end{pmatrix} . \tag{5.58}$$

Using the imaginary-time definition of the Nambu Green's function

$$\boldsymbol{\mathcal{G}}(\mathbf{k},\tau) = -\langle T_\tau \mathbf{\Phi}(\mathbf{k},\tau)\mathbf{\Phi}^\dagger(\mathbf{k},0)\rangle \tag{5.59}$$

we get the 2×2-matrix

$$\mathcal{G}_{ij}(\mathbf{k},\tau) = \begin{pmatrix} -\langle T_\tau \psi_\uparrow(\mathbf{k},\tau)\psi^\dagger_\uparrow(\mathbf{k},0)\rangle & -\langle T_\tau \psi_\uparrow(\mathbf{k},\tau)\psi_\downarrow(-\mathbf{k},0)\rangle \\ -\langle T_\tau \psi^\dagger_\downarrow(-\mathbf{k},\tau)\psi^\dagger_\uparrow(\mathbf{k},0)\rangle & -\langle T_\tau \psi^\dagger_\downarrow(-\mathbf{k},\tau)\psi_\downarrow(-\mathbf{k},0)\rangle \end{pmatrix} .$$

The off-diagonal elements will be assumed to be different from zero. This has to be verified selconsistently at the end of the calculation.
The frequency-dependent Matsubara Green's function is given by the Dyson equation

$$\boldsymbol{\mathcal{G}}^{-1}(\mathbf{k},\omega_n) = \boldsymbol{\mathcal{G}}_0^{-1}(\mathbf{k},\omega_n) - \boldsymbol{\Sigma}(\mathbf{k},\omega_n) \tag{5.60}$$

with the free CF Green's function

$$\boldsymbol{\mathcal{G}}^{\mathbf{0}}(\mathbf{k},\omega_n) = \begin{pmatrix} \frac{1}{i\omega_n - (k^2/2m^* - \mu)} & 0 \\ 0 & \frac{1}{i\omega_n + (k^2/2m^* - \mu)} \end{pmatrix} \equiv \begin{pmatrix} \frac{1}{i\omega_n - \varepsilon_k} & 0 \\ 0 & \frac{1}{i\omega_n + \varepsilon_k} \end{pmatrix} \tag{5.61}$$

and the fermionic matrix selfenergy $\mathbf{\Sigma}(\mathbf{k},\omega_n)$.

As in the case of the Eliashberg's equations for real superconductors we will consider a Fock type selfenergy, whose matrix elements are determined by the in-

teraction terms proportional to v_μ $(i = 1, 2; j = 1, 2)$

$$\Sigma_{ii}(\mathbf{k}, \omega_n) = -\frac{1}{\beta}\sum_{\mu\nu}(-1)^\nu \int \frac{\mathrm{d}\mathbf{q}}{(2\pi)^2}\sum_{\Omega_m}\left[\mathcal{D}^+_{\mu\nu}(\mathbf{q}, \Omega_m) + \mathcal{D}^-_{\mu\nu}(\mathbf{q}, \Omega_m)\right] \times \\ \times v_\mu(\mathbf{k}, \mathbf{q}) v_\nu(\mathbf{k}, -\mathbf{q}) \mathcal{G}_{11}(\mathbf{k} - \mathbf{q}, \omega_n - \Omega_m) \tag{5.62}$$

$$\Sigma_{i\neq j}(\mathbf{k}, \omega_n) = \frac{1}{\beta}\sum_{\mu\nu}(-1)^\nu \int \frac{\mathrm{d}\mathbf{q}}{(2\pi)^2}\sum_{\Omega_m}\left[\mathcal{D}^+_{\mu\nu}(\mathbf{q}, \Omega_m) - \mathcal{D}^-_{\mu\nu}(\mathbf{q}, \Omega_m)\right] \times \\ \times v_\mu(\mathbf{k}, \mathbf{q}) v_\nu(-\mathbf{k}, -\mathbf{q}) \mathcal{G}_{12}(\mathbf{k} - \mathbf{q}, \omega_n - \Omega_m)\ . \tag{5.63}$$

Notice the factors $(-1)^\nu$ stemming from (5.27), used to transform the gauge-field operators a into $a^\dagger$.
The self-energies can be chosen to satisfy the relations [11]

$$\Sigma_{21}(\mathbf{k}, \omega_n) = \Sigma_{12}(\mathbf{k}, \omega_n), \qquad \Sigma_{22}(\mathbf{k}, \omega_n) = -\Sigma_{11}(-\mathbf{k}, -\omega_n) \tag{5.64}$$

which can be obtained from the definitions (5.62), and (5.63) and from the definition of the Nambu Green function (5.58).
The Dyson equation (5.60) together with the above (5.62) and (5.63) establish a self consistent set of equations for the Green functions.

5.4.1 Solution of the Dyson Equation

In order to solve the set of equations for the self energies it is useful to transform from the Matsubara propagators to the retarded propagators via analytic continuation to real frequencies [11]. One obtains for the self-energies

$$\Sigma^{\mathrm{R}}_{11}(\mathbf{k}, \epsilon) = -\frac{1}{2\pi^2}\sum_{\mu\nu}(-1)^\nu \int \frac{\mathrm{d}\mathbf{q}}{(2\pi)^2}\int_{-\infty}^{\infty}\mathrm{d}\omega\,\mathrm{d}\epsilon_1 \tag{5.65}$$
$$\frac{\mathrm{Im}\left[D^{+,\mathrm{R}}_{\mu\nu}(\mathbf{k} - \mathbf{q}, \omega) + D^{-,\mathrm{R}}_{\mu\nu}(\mathbf{k} - \mathbf{q}, \omega)\right]}{\omega + \epsilon_1 - \epsilon - i\delta}$$
$$\times v_\mu(\mathbf{k}, \mathbf{k} - \mathbf{q})\, v_\nu(\mathbf{k}, \mathbf{q} - \mathbf{k})\, \mathrm{Im}G^{\mathrm{R}}_{11}(\mathbf{q}, \epsilon_1)\left(\tanh\frac{\epsilon_1}{2T} + \coth\frac{\omega}{2T}\right)$$

$$\Sigma^{\mathrm{R}}_{12}(\mathbf{k}, \epsilon) = \frac{1}{2\pi^2}\sum_{\mu\nu}(-1)^\nu \int \frac{\mathrm{d}\mathbf{q}}{(2\pi)^2}\int_{-\infty}^{\infty}\mathrm{d}\omega\,\mathrm{d}\epsilon_1 \tag{5.66}$$
$$\frac{\mathrm{Im}\left[D^{+,\mathrm{R}}_{\mu\nu}(\mathbf{k} - \mathbf{q}, \omega) - D^{-,\mathrm{R}}_{\mu\nu}(\mathbf{k} - \mathbf{q}, \omega)\right]}{\omega + \epsilon_1 - \epsilon - i\delta}$$
$$\times v_\mu(\mathbf{k}, \mathbf{k} - \mathbf{q})\, v_\nu(-\mathbf{k}, \mathbf{q} - \mathbf{k})\, \mathrm{Im}G^{\mathrm{R}}_{12}(\mathbf{q}, \epsilon_1)\left(\tanh\frac{\epsilon_1}{2T} + \coth\frac{\omega}{2T}\right)\ .$$

The imaginary parts of G^{R}_{11} and G^{R}_{12} are obtained from the analytic continuation of $\mathcal{G}^{\mathrm{R}}_{11}$ and $\mathcal{G}^{\mathrm{R}}_{12}$ by observing that the Σ-functions depend only on the modulus of

the momentum in an isotropic system

$$G^{\mathrm{R}}_{11}(\mathbf{q},\epsilon_1) = \frac{\epsilon_1 + \varepsilon_q + {\Sigma^{\mathrm{R}}_{11}}^*(q,-\epsilon_1)}{[\epsilon_1 - \varepsilon_q - \Sigma^{\mathrm{R}}_{11}(q,\epsilon_1)][\epsilon_1 + \varepsilon_q + {\Sigma^{\mathrm{R}}_{11}}^*(q,-\epsilon_1)] - [\Sigma^{\mathrm{R}}_{12}(q,\epsilon_1)]^2} \tag{5.67}$$

$$G^{\mathrm{R}}_{12}(\mathbf{q},\epsilon_1) = \frac{\Sigma^{\mathrm{R}}_{12}(q,\epsilon_1)}{[\epsilon_1 - \varepsilon_q - \Sigma^{\mathrm{R}}_{11}(q,\epsilon_1)][\epsilon_1 + \varepsilon_q + {\Sigma^{\mathrm{R}}_{11}}^*(q,-\epsilon_1)] - [\Sigma^{\mathrm{R}}_{12}(q,\epsilon_1)]^2} \tag{5.68}$$

$$\varepsilon_q \equiv q^2/2m^* - \mu\,. \tag{5.69}$$

This can be rewritten in the form

$$G^{\mathrm{R}}_{11}(q,\epsilon_1) = \frac{\epsilon_1 + \varepsilon_q - \Sigma^{\mathrm{R}}_{11}(q,\epsilon_1)}{[\epsilon_1 - \Sigma^{\mathrm{R}}_{11}(q,\epsilon_1)]^2 - \varepsilon_q^2 - [\Sigma^{\mathrm{R}}_{12}(q,\epsilon_1)]^2} \tag{5.70}$$

$$G^{\mathrm{R}}_{12}(q,\epsilon_1) = \frac{\Sigma^{\mathrm{R}}_{12}(q,\epsilon_1)}{[\epsilon_1 - \Sigma^{\mathrm{R}}_{11}(q,\epsilon_1)]^2 - \varepsilon_q^2 - [\Sigma^{\mathrm{R}}_{12}(q,\epsilon_1)]^2} \tag{5.71}$$

due to the fact that $\mathrm{Im}\Sigma^{\mathrm{R}}_{11}$ is an even function of ϵ_1.
We are interested only in the odd part of $\mathrm{Re}\Sigma^{\mathrm{R}}_{11}$ since the even part gives just a correction to the chemical potential that does not depend on the temperature [102]. We evaluate the imaginary parts of G^{R}_{11} and G^{R}_{12} for small imaginary parts of the self-energy, i.e. in the limit $\mathrm{Im}\Sigma^{\mathrm{R}}_{11}, \mathrm{Im}\Sigma^{\mathrm{R}}_{12} \to 0$. Since we are interested in the region of momenta close to the Fermi surface, we assume

$$\Sigma^{\mathrm{R}}_{11}(k_{\mathrm{F}},\epsilon_1) = \Sigma(\epsilon_1) - i\Gamma(\epsilon_1) \tag{5.72}$$

$$\Sigma^{\mathrm{R}}_{12}(k_{\mathrm{F}},\epsilon_1) = \phi(\epsilon_1) - i\Theta(\epsilon_1) \tag{5.73}$$

with $\Theta, \Gamma > 0$ because of the analytical properties of the retarded Green functions. Thus

$$\mathrm{Im}G^{\mathrm{R}}_{11}(q,\epsilon_1) = (A + \varepsilon_q)\,\frac{-2\Gamma A}{B^2 + 4\Gamma^2 A^2} \tag{5.74}$$

$$\mathrm{Im}G^{\mathrm{R}}_{12}(q,\epsilon_1) = \phi\,\frac{-2\Gamma A}{B^2 + 4\Gamma^2 A^2} \tag{5.75}$$

with the definitions $A \equiv \epsilon_1 - \Sigma(\epsilon_1)$ and $B = A^2 - \phi^2(\epsilon_1) - \varepsilon_q^2$.
For $\Gamma \to 0$ and $\Theta \to 0$ we get

$$\begin{aligned}\mathrm{Im}G^{\mathrm{R}}_{11}(q,\epsilon_1) &= -\pi\,(A + \varepsilon_q)\,\delta(B)\,\mathrm{sgn}\,A \\ &= -\pi\,\mathrm{sgn}\,[\epsilon_1 - \Sigma(\epsilon_1)]\,\frac{\epsilon_1 - \Sigma(\epsilon_1) + \varepsilon_q}{2\Omega_1(\epsilon_1)} \\ &\quad \times \{\delta[\varepsilon_q - \Omega_1(\epsilon_1)] + \delta[\varepsilon_q + \Omega_1(\epsilon_1)]\}\end{aligned} \tag{5.76}$$

$$\begin{aligned}\mathrm{Im}G^{\mathrm{R}}_{12}(q,\epsilon_1) &= -\pi\,\phi\,\delta(B)\,\mathrm{sgn}\,A \\ &= -\pi\,\mathrm{sgn}\,[\epsilon_1 - \Sigma(\epsilon_1)]\,\frac{\phi(\epsilon_1)}{2\Omega_1(\epsilon_1)} \\ &\quad \times \{\delta[\varepsilon_q - \Omega_1(\epsilon_1)] + \delta[\varepsilon_q + \Omega_1(\epsilon_1)]\}\end{aligned} \tag{5.77}$$

with

$$\Omega_1(\epsilon_1) = \sqrt{[\epsilon_1 - \Sigma(\epsilon_1)]^2 - \phi^2(\epsilon_1)}\,. \tag{5.78}$$

In order to perform the **q**-integrations in (5.65) and (5.66), we consider the dominant contribution D_{11} and rewrite the expressions for the vertices with $p \equiv |\mathbf{k}-\mathbf{q}|$

$$v_1(\mathbf{k},\mathbf{k}-\mathbf{q})\, v_1(\mathbf{k},\mathbf{q}-\mathbf{k}) = -\frac{e^2}{m^{*2}}\frac{k^2q^2}{p^2}\sin^2\theta \tag{5.79}$$

where θ is the angle between **k** and **q**. Aligning the q_x axis parallel the $\hat{k}$-direction, the measure is changed to

$$\int_0^\infty q\,\mathrm{d}q \int_0^{2\pi} \mathrm{d}\theta = 2\int_0^\infty \mathrm{d}q \int_{|k-q|}^{k+q} \mathrm{d}p\, \frac{p}{k\sin\theta} \tag{5.80}$$

with

$$\sin\theta = \sqrt{1 - \Big[\frac{k^2+q^2-p^2}{2kq}\Big]^2}\,. \tag{5.81}$$

If we assume for the external momentum $k \approx k_\mathrm{F}$ and consider only the dominant contributions due to $q \sim k_\mathrm{F}$ we get for $\Sigma^\mathrm{R}_{11}(k_\mathrm{F},\epsilon) \approx \Sigma(\epsilon)$ and $\Sigma^\mathrm{R}_{12}(k_\mathrm{F},\epsilon) \approx \phi(\epsilon)$

$$\Sigma(\epsilon) = \frac{-1}{4\pi^4}\frac{k_\mathrm{F}^2e^2}{m^{*2}}\int_0^\infty \mathrm{d}q \int_0^{2k_\mathrm{F}} \mathrm{d}p \sqrt{1-\frac{p^2}{4k_\mathrm{F}^2}} \int \mathrm{d}\omega\, \mathrm{d}\epsilon_1 \tag{5.82}$$
$$\frac{\mathrm{Im}\left[D_{11}^{+,\mathrm{R}}(p,\omega) + D_{11}^{-,\mathrm{R}}(p,\omega)\right]}{\omega+\epsilon_1-\epsilon-i\delta}\,\mathrm{Im}G^\mathrm{R}_{11}(q,\epsilon_1)\left(\tanh\frac{\epsilon_1}{2T} + \coth\frac{\omega}{2T}\right)$$

$$\phi(\epsilon) = \frac{-1}{4\pi^4}\frac{k_\mathrm{F}^2e^2}{m^{*2}}\int_0^\infty \mathrm{d}q \int_0^{2k_\mathrm{F}} \mathrm{d}p \sqrt{1-\frac{p^2}{4k_\mathrm{F}^2}} \int \mathrm{d}\omega\, \mathrm{d}\epsilon_1 \tag{5.83}$$
$$\frac{\mathrm{Im}\left[D_{11}^{+,\mathrm{R}}(p,\omega) - D_{11}^{-,\mathrm{R}}(p,\omega)\right]}{\omega+\epsilon_1-\epsilon-i\delta}\,\mathrm{Im}G^\mathrm{R}_{12}(q,\epsilon_1)\left(\tanh\frac{\epsilon_1}{2T} + \coth\frac{\omega}{2T}\right)$$

since the $D_{11}^\pm$ depend only on the modulus of their argument.

The q-integral involves only ImG and yields, when linearizing $\varepsilon_q \sim v_\mathrm{F}(q-k_\mathrm{F})$,

$$\int \mathrm{d}q\,\mathrm{Im}G^\mathrm{R}_{11}(q,\epsilon_1) = -\frac{\pi}{v_\mathrm{F}}\,\mathrm{sgn}\left[\epsilon_1-\Sigma(\epsilon_1)\right]\frac{\epsilon_1-\Sigma(\epsilon_1)}{\Omega_1(\epsilon_1)} \tag{5.84}$$

$$\int \mathrm{d}q\,\mathrm{Im}G^\mathrm{R}_{12}(q,\epsilon_1) = -\frac{\pi}{v_\mathrm{F}}\,\mathrm{sgn}\left[\epsilon_1-\Sigma(\epsilon_1)\right]\frac{\phi(\epsilon_1)}{\Omega_1(\epsilon_1)}\,. \tag{5.85}$$

In evaluating this integral, some assumptions have been made. First of all, Σ_{11} and Σ_{12} (cf.(5.72), (5.73)), are assumed to have imaginary parts that are much smaller than the real parts. We have also neglected contributions to the self-energy that do not depend on the frequency. Although at this stage these assumption cannot

really be justified they are *a posteriori* found to be consistent with the results. In any case, they are necessary in order to be consistent with the Fermi liquid picture for the Composite Fermions. The equations above are valid if Ω_1 is real, i.e. for $(\epsilon_1 - \Sigma)^2 - \phi^2 \geq 0$, otherwise, the integrals are zero due to the δ-functions.

By introducing the quantity

$$\epsilon z(\epsilon) \equiv \epsilon - \Sigma(\epsilon) \tag{5.86}$$

and defining the gap Δ,

$$\Delta(\epsilon) z(\epsilon) \equiv \phi(\epsilon) \ , \tag{5.87}$$

such that

$$\Omega_1(\epsilon_1) = |z(\epsilon_1)| \sqrt{\epsilon_1^2 - \Delta^2(\epsilon_1)} \ , \tag{5.88}$$

we also can write (5.84) and (5.85) in the form

$$\int \mathrm{d}q \, \mathrm{Im} G_{11}^{\mathrm{R}}(q, \epsilon_1) = -\frac{\pi}{v_{\mathrm{F}}} \frac{|\epsilon_1|}{\sqrt{\epsilon_1^2 - \Delta^2(\epsilon_1)}} \tag{5.89}$$

$$\int \mathrm{d}q \, \mathrm{Im} G_{12}^{\mathrm{R}}(q, \epsilon_1) = -\frac{\pi}{v_{\mathrm{F}}} \frac{\mathrm{sgn}\, \epsilon_1 \Delta(\epsilon_1)}{\sqrt{\epsilon_1^2 - \Delta^2(\epsilon_1)}} \ . \tag{5.90}$$

We can now perform the p-integrations assuming $p \ll k_{\mathrm{F}}$, thus retaining only the first order in the square root. Using (5.47) and (5.48) and defining the integrals

$$P^+(\omega) = \int_0^\infty \mathrm{d}p \, \mathrm{Im} D_{11}^{+,\mathrm{R}}(p, \omega) = -\frac{\pi}{4\alpha_+} \mathrm{sgn}\, \omega \tag{5.91}$$

$$P^-(\omega) = \int_0^\infty \mathrm{d}p \, \mathrm{Im} D_{11}^{-,\mathrm{R}}(p, \omega) = -\frac{\pi}{3\sqrt{3}} \frac{1}{\alpha_-^{2/3} \eta^{1/3}} \omega^{-1/3} \tag{5.92}$$

we, find in the limit $T \to 0$ where

$$\tanh \frac{\epsilon_1}{2T} \to \mathrm{sgn}\, \epsilon_1 \qquad , \qquad \coth \frac{\omega}{2T} \to \mathrm{sgn}\, \omega \ , \tag{5.93}$$

the expressions for the self-energies

$$\Sigma(\epsilon) = \frac{1}{4\pi^3} \frac{k_{\mathrm{F}} e^2}{m^*} \int \mathrm{d}\omega \, \mathrm{d}\epsilon_1 \, \frac{\mathrm{sgn}\, \epsilon_1 + \mathrm{sgn}\, \omega}{\omega + \epsilon_1 - \epsilon - i\delta} \left[P^+(\omega) + P^-(\omega) \right] \times \mathrm{sgn}\, \epsilon_1 \frac{\epsilon_1}{\sqrt{\epsilon_1^2 - \Delta^2(\epsilon_1)}} \tag{5.94}$$

$$\phi(\epsilon) = \frac{1}{4\pi^3} \frac{k_{\mathrm{F}} e^2}{m^*} \int \mathrm{d}\omega \, \mathrm{d}\epsilon_1 \, \frac{\mathrm{sgn}\, \epsilon_1 + \mathrm{sgn}\, \omega}{\omega + \epsilon_1 - \epsilon - i\delta} \left[P^+(\omega) - P^-(\omega) \right] \times \mathrm{sgn}\, \epsilon_1 \frac{\Delta(\epsilon_1)}{\sqrt{\epsilon_1^2 - \Delta^2(\epsilon_1)}} \ . \tag{5.95}$$

Now the energy integrations have to be performed. We begin by defining the integrals

$$F_+(\epsilon,\epsilon_1) = \int \mathrm{d}\omega\, \mathrm{sgn}\,\omega\, \frac{\mathrm{sgn}\,\epsilon_1 + \mathrm{sgn}\,\omega}{\omega + \epsilon_1 - \epsilon - i\delta} \tag{5.96}$$

$$F_-(\epsilon,\epsilon_1) = \int \mathrm{d}\omega\, \omega^{-1/3}\, \frac{\mathrm{sgn}\,\epsilon_1 + \mathrm{sgn}\,\omega}{\omega + \epsilon_1 - \epsilon - i\delta} \tag{5.97}$$

that must be evaluated as principal values. For F_-,

$$\mathrm{Re}F_-(\epsilon,\epsilon_1) = -\frac{\pi}{\sqrt{3}} \frac{[1 + 3\,\mathrm{sgn}\,\epsilon_1\,\mathrm{sgn}\,(\epsilon_1 - \epsilon)]}{(\epsilon - \epsilon_1)^{1/3}}\ , \tag{5.98}$$

$$\mathrm{Im}F_-(\epsilon,\epsilon_1) = \pi\, \frac{\mathrm{sgn}\,\epsilon_1 + \mathrm{sgn}\,(\epsilon - \epsilon_1)}{(\epsilon - \epsilon_1)^{1/3}}\ . \tag{5.99}$$

The integral F_+ must be calculated by introducing a cutoff Λ_c,

$$\mathrm{Re}F_+(\epsilon,\epsilon_1) = \int_{-\Lambda_\mathrm{c}}^{\Lambda_\mathrm{c}} \frac{\mathrm{d}\omega}{\omega + \epsilon_1 - \epsilon} + \mathrm{sgn}\,\epsilon_1 \int_{-\Lambda_\mathrm{c}}^{\Lambda_\mathrm{c}} \mathrm{d}\omega\, \frac{\mathrm{sgn}\,\omega}{\omega + \epsilon_1 - \epsilon}\ , \tag{5.100}$$

$$\mathrm{Im}F_+(\epsilon,\epsilon_1) = \pi(1 - \mathrm{sgn}\ \epsilon_1 \mathrm{sgn}\,(\epsilon_1 - \epsilon))\ . \tag{5.101}$$

We finally find for the real part

$$\mathrm{Re}F_+(\epsilon,\epsilon_1) = \log \frac{|\Lambda_\mathrm{c} + \epsilon_1 - \epsilon|}{|\Lambda_\mathrm{c} - \epsilon_1 + \epsilon|} + \mathrm{sgn}\,\epsilon_1 \log \frac{|\Lambda_\mathrm{c}^2 - (\epsilon_1 - \epsilon)^2|}{(\epsilon_1 - \epsilon)^2}\ . \tag{5.102}$$

The physically meaningful value of the cut-off can be estimated by considering with more detail the behavior of the integral over $\mathrm{Im}D_{11}^{\pm,\mathrm{R}}(p,\omega)$,

$$\int_0^{2k_\mathrm{F}} \mathrm{d}p\, \mathrm{Im}D_{11}^{\pm,\mathrm{R}}(p,\omega) = -\frac{1}{2\alpha_+}\left(\frac{\pi}{2} - \arctan\frac{\eta\omega}{4k_\mathrm{F}^2\alpha_+}\right)\ . \tag{5.103}$$

This vanishes for $\omega \to \infty$. The scale for the vanishing of the integral can be obtained by considering the argument of the $\arctan$-function

$$\frac{\eta\omega}{4k_\mathrm{F}^2\alpha_+} = \frac{\omega}{e^2/\epsilon\ell}\frac{1}{2k_\mathrm{F}\ell} \tag{5.104}$$

where $E_\mathrm{C} = e^2/\epsilon\ell$ is the energy scale of the Coulomb interaction and ℓ is the magnetic length. Therefore, it is reasonable to choose as the cut-off $\Lambda_\mathrm{c} = \Lambda k_\mathrm{F}\ell E_\mathrm{C}$, where Λ represents the numerical value of the cut-off itself.

5.5 The Energy Gap

In order to find the solutions of the above non-linear Eliashberg equations (5.94) and (5.95) it is convenient to define the constant

$$C = \frac{1}{4\pi^3}\frac{k_\mathrm{F}e^2}{m^*}\ , \tag{5.105}$$

and

$$M^+(\epsilon,\epsilon_1) = \int \mathrm{d}\omega\, P^+(\omega)\, \frac{\mathrm{sgn}\,\epsilon_1 + \mathrm{sgn}\,\omega}{\omega+\epsilon_1-\epsilon-i\delta} = -\frac{\pi}{4\alpha_+} F^+(\epsilon,\epsilon_1)\,, \tag{5.106}$$

$$M^-(\epsilon,\epsilon_1) = \int \mathrm{d}\omega\, P^-(\omega)\, \frac{\mathrm{sgn}\,\epsilon_1 + \mathrm{sgn}\,\omega}{\omega+\epsilon_1-\epsilon-i\delta} = -\frac{\pi}{3\sqrt{3}} \frac{1}{\alpha_-^{2/3}\eta^{1/3}} F^-(\epsilon,\epsilon_1)\,, \tag{5.107}$$

such that

$$\Sigma(\epsilon) = C \int \mathrm{d}\epsilon_1 [M^+(\epsilon,\epsilon_1) + M^-(\epsilon,\epsilon_1)] \mathrm{sgn}\,\epsilon_1\, \frac{\epsilon_1}{\sqrt{\epsilon_1^2 - \Delta^2(\epsilon_1)}} \tag{5.108}$$

$$\phi(\epsilon) = C \int \mathrm{d}\epsilon_1 [M^+(\epsilon,\epsilon_1) - M^-(\epsilon,\epsilon_1)] \mathrm{sgn}\,\epsilon_1\, \frac{\Delta(\epsilon_1)}{\sqrt{\epsilon_1^2 - \Delta^2(\epsilon_1)}} \tag{5.109}$$

which give, after using the definitions (5.86), (5.87),

$$\begin{aligned} \Delta(\epsilon) \;\; = \;\; & C \int \frac{\mathrm{sgn}\,\epsilon_1 \mathrm{d}\epsilon_1}{\sqrt{\epsilon_1^2 - \Delta^2(\epsilon_1)}} \\ & \times \left\{ [M_+(\epsilon,\epsilon_1) + M_-(\epsilon,\epsilon_1)] \frac{\epsilon_1}{\epsilon} \Delta(\epsilon) + [M_+(\epsilon,\epsilon_1) - M_-(\epsilon,\epsilon_1)] \Delta(\epsilon_1) \right\}. \end{aligned} \tag{5.110}$$

If we assume that the gap is energy-independent, $\Delta(\epsilon) \approx \Delta$, this gives finally for the gap the condition

$$I_+ + I_- = 1\,, \tag{5.111}$$

with quantities $I_\pm$ that can be calculated by expanding with respect to ϵ_1 around $\epsilon = 0$.
We first note that the imaginary parts of F_+, F_- do not give contributions to the ϵ_1-integral. Then, with $|\epsilon_1| > |\Delta|$, and assuming $\Delta > 0$, we get

$$\begin{aligned} I_- &= \frac{16\pi^2}{27} \eta^{-1/3} \alpha_-^{-2/3} \int_\Delta^\infty \frac{\mathrm{d}\epsilon_1 \epsilon_1^{-1/3}}{\sqrt{\epsilon_1^2 - \Delta^2}} \\ &= \frac{16\pi^{5/2}}{9} \eta^{-1/3} \alpha_-^{-2/3} \frac{\Gamma(7/6)}{\Gamma(2/3)} \Delta^{-1/3}\,, \end{aligned} \tag{5.112}$$

$$\begin{aligned} I_+ &= -\frac{\pi}{\alpha_+} \int_\Delta^{\Lambda_\mathrm{c}} \mathrm{d}\epsilon_1 \frac{1}{\sqrt{\epsilon_1^2 - \Delta^2}} \left(\log \frac{\Lambda_\mathrm{c} + \epsilon_1}{\epsilon_1} + \frac{\Lambda_\mathrm{c}}{\Lambda_\mathrm{c} + \epsilon_1} \right) \\ &\approx -\frac{\pi}{\alpha_+} \left[\frac{1}{2} \log^2 \left(\frac{\Lambda_\mathrm{c}}{\Delta} \right) + \frac{\Lambda_\mathrm{c}}{\sqrt{\Lambda_\mathrm{c}^2 - \Delta^2}} \log \left(\frac{\Lambda_\mathrm{c}}{\Delta} \right) \right] \end{aligned} \tag{5.113}$$

in the limit $\Lambda_\mathrm{c}/\Delta \gg 1$.

By replacing the expressions for η and $\alpha_\pm$ and Λ_c we find the final result

$$1 = C_- \left(\frac{E_\mathrm{F}}{\Delta} \right)^{1/3} - C_+ \left[\log^2 \left(\Lambda' \frac{E_\mathrm{F}}{\Delta} \right) + \frac{\Lambda' E_\mathrm{F}}{\sqrt{(\Lambda' E_\mathrm{F})^2 - \Delta^2}} \log \left(\Lambda' \frac{E_\mathrm{F}}{\Delta} \right) \right] \tag{5.114}$$

with $\Lambda' \equiv 2\pi\Lambda/C_+$ and the constants

$$C_- \approx 1.4 \qquad C_+ = \frac{E_{\rm F}}{2\pi e^2 k_{\rm F}/\varepsilon} = \frac{E_{\rm F}}{E_{\rm C}} \frac{1}{2\pi k_{\rm F}\ell}\,. \tag{5.115}$$

The first term in (5.114) is completely independent of the interaction and describes the contribution due to D^-. The second term is due to D^+ and stems from the interaction between particles.

Independently on the value of the magnetic field there is *always* a solution $\Delta \neq 0$ to this equation. For $E_{\rm F}$ larger than $E_{\rm C}$ ($C_+ \gg 1$) Δ becomes vanishingly small. If $E_{\rm C}$ is much larger than $E_{\rm F}$ ($C_+ \ll 1$), the gap is nearly independent on the Coulomb interaction.

5.6 Discussion of the results

We just obtained equation (5.114) which was our principal aim. This equation always has a non-vanishing solution for the gap Δ and shows that indeed the system is instable towards the Cooper condensation.
A similar line of thinking has been followed in the bilayer systems in [111, 109].
Up to now the solution depends on many parameters, like the ratio between the Fermi energy of the original Fermi Liquid $E_{\rm F}$ and the Coulomb repulsion $E_{\rm C}$, the cutoff, etc. According to the different situations where this argument applies we can have quite different results depending on the real values of the parameters.
Let us define a function

$$F(x) = C_- x^{1/3} - C_+ \left[\log^2(\Lambda' x) + \frac{\Lambda' x}{\sqrt{(\Lambda' x)^2 - 1}} \log(\Lambda' x) \right] - 1 \tag{5.116}$$

where $x = E_{\rm F}/\Delta$. The zero of $F(x)$ determines the value of the gap.

In order to see a direct quantitative application of this calculation we can consider again the LL crossings giving rise to the shoulders in the polarization experiments described in chapter 3.
In this case we have to remember that only a part of the total fermionic density takes part into the two Fermi liquids. Let us consider $\nu = 2/5$ for example. Here we have two occupied LL for fermions, but only half of a LL contributes to the density of *each* spin channel. So we have $\rho_\uparrow = \rho_\downarrow = 1/4\,\rho$ with ρ the total density. Thus

$$k_{\rm F} = \sqrt{4\pi\rho_s} = \sqrt{\pi\rho} = \frac{1}{\ell\sqrt{5}} \tag{5.117}$$

Moreover the effective mass m^* is given by the CF mass $m^* = m_0\alpha\sqrt{B\,[\mathrm{T}]}$, with $\alpha \sim 0.2$. This implies that the Fermi energy of the two coupled Fermi liquids is just proportional to the Coulomb interaction. Bearing in mind the value of the cyclotron energy in vacuum $eB/m_0 = 1.5\,B\,[\mathrm{T}]$ K we deduce

$$E_{\rm F} = \frac{k_{\rm F}^2}{2m^*} = \frac{eB}{m^*}\frac{k_{\rm F}^2}{2eB} = \frac{eB}{m_0}\frac{1}{\alpha\sqrt{B}}\frac{\nu}{4} = 0.75\sqrt{B[\mathrm{T}]}\,\mathrm{K}\,. \tag{5.118}$$

Comparing it with the Coulomb energy

$$E_{\mathrm{C}} = 51\,\sqrt{B[\mathrm{T}]}\,\mathrm{K} \tag{5.119}$$

we deduce

$$\frac{E_{\mathrm{F}}}{E_{\mathrm{C}}} = 0.015\,. \tag{5.120}$$

Thus we have

$$C_{+} = \frac{E_{\mathrm{F}}}{E_{\mathrm{C}}}\,\frac{\sqrt{5}}{2\pi} \simeq 0.005\,. \tag{5.121}$$

Finally, by considering the result (5.103), we can estimate the value of the cutoff. The function (5.103) is essentially negligible when (5.104) is larger than 100. This implies $\Lambda \simeq 200$ and $\Lambda' \simeq 2.5 \cdot 10^5$.
With these choices the gap equation $F(E_{\mathrm{F}}/\Delta) = 0$ leads to

$$\Delta \simeq 0.36\,E_{\mathrm{F}} \simeq 0.27\,\sqrt{B[\mathrm{T}]}\,\mathrm{K}\,. \tag{5.122}$$

The spin polarization transition for $\nu = 2/5$ occurs close to $B = 3$ T, implying a gap $\Delta^{\mathrm{c}}_{2/5} \simeq 0.45$ K. As already noticed in chapter 3, the characteristic energy involved in modifying the crossover is of this order of magnitude [63].

Having a superconductive restructuration of the GS close to the LL crossings at the Fermi energy would imply the shoulder at zero temperature.
In fact, if singlet Cooper pairs form near the LL degeneracy, we would have to pay a minimum energy Δ to add or subtract a single fermion of a given spin. This would imply a rigidity of the spin polarization of the system.
Unless the energy difference between the two SCFLL becomes larger than Δ it is energetically favourable to keep the superconductive structure with equal spin populations. This means that, for a certain interval of magnetic fields close to the transition, the spin polarization is unaltered. The width of the shoulder is then linked to the energy gap, and the quantitative estimate we obtain seems to be in good agreement with experiments [106, 114, 108].
The argument we presented here would be *generic* for every LL crossing at the Fermi energy and the outcoming superconductive GS has *isotropic* properties. This is what should be expected in a homogeneous configuration like the one in the experiments, where the magnetic field is purely perpendicular and the disorder potential does not have, a priori, any preferential anisotropy direction.
Our result is just the first step in the way to understanding the effects of the dominant fermionic interaction terms. In the future we plan to investigate the role of the vertex corrections and higher order diagrams which have been neglected up to now.

Recently, the issue of the partly polarized states has been investigated in a couple of papers [115]. A first attempt to explain the effect with a charge-density wave GS was numerically shown to be inappropriate. Subsequently, after further simulations on small-size systems with modified Haldane pseudopotentials, an excitonic condensate GS has been proposed. However, the true nature of the partly polarized state still remains mysterious and further experiments are needed to pin it down

clearly.

The calculation above produces a uniform non-vanishing order parameter Δ for a 2D system with a superconductive instability.
However, in 2D and 1D the quantum fluctuations would tend to destroy the stable phase and produce an average vanishing gap, as was shown by Hohenberg [116]. What happens in reality is that, for low enough temperatures $T < T_c$ ($T_c \simeq \Delta/K_B$), although the average over the space of the gap function vanishes, its autocorrelation function $\langle \Delta(\mathbf{r})\Delta(\mathbf{r}') \rangle$ decays as a power law of $|\mathbf{r} - \mathbf{r}'|$ with a characteristic decay length R_0. For $T > T_c$ the decay would be exponential. This is one example of Kosterlitz-Thouless phase transition [117]. Essentially the behaviour of the system is superconductive in "paddles" of typical linear size R_0.
This means that, in principle and for a sample with typical size $L \gg R_0$, the transport properties of the whole sample can be dissipative (as it seems the case in experiments very close to the spin transition) but still its spin-related properties can show rigidity due to the superconductive areas.
Very recently, experiments showed very high supercurrents in *single* 2DES [118]. According to Hohenberg's theorem such an effect should be impossible. However, the superconductive behaviour still survives due to the fact that the physical properties of the system are essentially determined by its correlation functions, rather than by having a fully developed uniform gap [119].

In order to experimentally address the properties of the suggested GS close to the crossing we believe that further low-temperatures measurements of the spin polarization would be in need. Local photon absorption experiments are currently being set up at the *Weizmann Institute of Science* [120] that would furnish a spatial map of the degree of spin-polarization of the 2DES. Such an investigation would allow the observation of rigid-spin paddles as well as eventual domain formation in the GS.
In principle, having proposed superconductive correlations forming close to the CFLL degeneracy, we could expect peculiar effects like Josephson currents to show up for small enough samples (smaller than the typical Kosterlitz-Thouless correlation length). Indeed, a possible experimental setup to test this issue would be to consider two QHE systems in the same plane, separated by a tunnel junction. Suppose the bar is immersed in a perpendicular magnetic field and the filling factor in one of the two halves is kept fixed at one incompressible fraction exactly at the density where the spin polarization transition occurs. Then, by tuning the density in the other half plane to the value of the point of degeneracy a "Josephson current" should flow. Such a current should vanish as soon as one of the two densities is detuned.

6. THE 5/2 FQHE AND QUANTUM NON-ABELIAN STATISTICS

Up to now we presented several features connected to different FQH states. Incompressibility for fractions belonging to the principal sequence has been considered within the Composite Fermions picture in presence of a finite residual magnetic field. Moreover the Chern-Simons field theories have been used to treat the compressible "even denominator" states in both the spinless and spinful cases. Finally, the effective CF interaction has been shown to induce superconductive instabilities at the degeneracy of two CF Fermi Liquids with equal densities.

In this chapter we will consider a somewhat "exotic" FQH state, showing up at $\nu = 5/2$. Together with $\nu = 7/2$, this is the only (up to now) observed even denominator state showing the FQHE, i.e. the quantization in the Hall resistance and the corresponding vanishing magnetoresistance.
In 1991, Moore and Read proposed a many body wavefunction, called "the Pfaffian state", as a candidate Ground State for the $5/2$ effect [131]. Using subtle conformal field theory arguments they obtained a formal description of the GS and of its quasiparticle excitations, induced as usual, by an excess (or defect) of uncompensated magnetic flux quanta.
In analogy with Laughlin quasiparticles, the vortices in the Pfaffian state have a fractional charge. However, surprisingly their statistics was argued to be non-Abelian, meaning that an interchange of two vortices amounts to a non-commutative matrix representation of the braiding group, rather than to a unitary modulus complex number. The statistical matrices act on a set of wavefunctions describing a subspace of degenerate GS showing up in the many-vortices configuration [135].
Recently, in a beautiful paper, Read and Green proposed a more physical picture of the $5/2$ state as a p-wave condensation of fully polarized CF in the last half filled LL [133]. The quasiparticle excitations are then viewed as vortices in this p-wave BCS state, each carrying a zero-energy excitation mode which is finally responsible for the GS degeneracy [136, 137].

In analogy with the s-wave CF condensation described in the last chapter, here we investigate the p-wave CF BCS state and the properties of the vortex excitations. We will identify the different degenerate GS occurring in the many-vortices configuration and determine their structure. As a byproduct of our analysis we will address the non-abelian statistics of the vortices on physical grounds. The crucial issues coming out will be the nature of the zero mode in each vortex core and the necessary entanglement between quasiparticles states living on different vortices.
Furthermore we will devote the last part of the chapter to the identification of the Cooper pairs in the many vortices state, addressing the unsolved issue of pairing for p-wave superconductors in presence of vortex-like inhomogeneities.

6.1 The $\nu = 5/2$ FQH state: basic experimental facts

For several years since the first Quantum Hall measurements, the even denominator states in the first as well as higher LL did not show any sign of FQHE. In these cases, typically, the Hall resistance does not show plateaux or shoulders and the longitudinal resistance has a smooth behaviour as a function of the external magnetic field, with a *finite* central value.
With time, the mobility of samples was increased significantly and lower temperatures were accessed. It was thanks to these technical achievements that in 1987 Willett and co-workers reported the observation of a developing fragile magnetoresistance minimum at $\nu = 5/2$, which was easily washed away by temperature [121]. As usual for new developing FQH states, the minima in R_{xx} did not go to zero but was strengthening for decreasing temperatures. In 1999, with an exceptionally clean sample, Pan et al. finally observed the full $5/2$ FQHE state [122], with a well quantized R_{xy} plateaux and a vanishing magnetoresistance (see Fig.(6.1)).

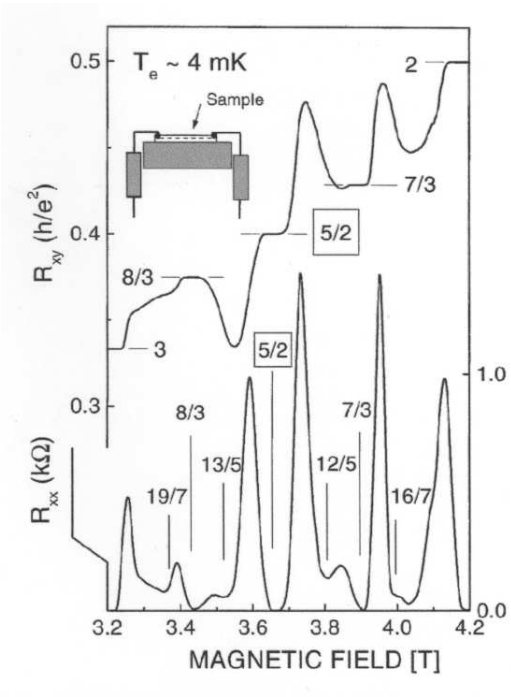

Fig. 6.1: The Hall and longitudinal resistances (R_{xy}, R_{xx}) close to $\nu = 5/2$ [122]. The temperature is exceptionally low ($T = 4.0$ mK) as well as the mobility extremely large ($\mu = 1.7 \times 10^7$ cm^2/Vs). The fully developed FQH state at $5/2$ is clearly visible.

If we analyze the sequence of half filled LLs we find "pairs" of particle-hole conju-

gate states with similar behaviours.

- For $\nu = 1/2$ and $3/2$ (LL index $n = 0$, two-fold spin split) we have *compressible isotropic* states (no FQHE) well described as CF Fermi liquids, their spin polarization being smooth in the external field. For the sake of clarity, while speaking of the spin-polarization of the even-denominator states, we will refer to the polarization of the last half filled LL only.
- At $\nu = 5/2$ and $7/2$ (LL index $n = 1$) *incompressible* states are observed, showing the FQHE at very small temperatures in extremely clean samples [122].
- For $\nu = 9/2$ and $11/2$ (LL index $n = 2$) we have again *compressible* states with *no FQHE* which are naturally anisotropic even in the purely perpendicular field configuration [123], with the anisotropy direction easily oriented by an eventual in-plane field.

For not too small magnetic fields the essential physics in these states takes place in the last half-filled LL, the lower full LLs being frozen out by the electronic Fermi statistics. This notwithstanding, the half filled LL states are quite different among themselves. The role of the LL index seems crucial in determining the effective e-e interactions setting the final structure of the GS.
In what follows we will not be particularly concerned in determining the effective interaction leading to the different half-filled states, but rather in analyzing the properties of a particularly significant function which has been proposed to describe the GS for the $5/2$ FQHE. The reader interested in the effective quasiparticle interactions in higher LL can find more on that in [124].

In order to probe further properties of the new $5/2$ FQH state, the effect of an in-plane $B_{\|}$ on it was studied in tilted magnetic field configurations [125]. The main result was that the $5/2$ state was weakening for increasing $B_{\|}$ and was finally destroyed at a critical field.
This feature induced people to think of a spin unpolarized (or at least partially polarized) GS, which should soon be destroyed by the increasing Zeeman split induced by the in-plane field.
However, further analysis showed that, for quite large $B_{\|}$ anisotropic transport was observed, the anisotropy direction being orthogonal to $B_{\|}$ itself [126, 127], much like in the $9/2$ state. This was the first element shedding doubts on the issue of the partial spin polarization at $5/2$.
It was then suggested that the main role of $B_{\|}$ could be to couple with the finite thickness of the 2DES thus modifying the effective e-e interaction towards the $9/2$ and $11/2$ compressible cases.
Recently, with transport measurements at different densities, it has been shown that the activation gap at *constant* $\nu = 5/2$ is highly insensitive to the (purely orthogonal) magnetic field [128]. In particular, no sign of reentrant gap shows up that could indicate a spin polarization transition in the GS. Several experiments seem now to agree on the fully polarized nature of the $5/2$ GS.
Finally, for temperature larger than the $5/2$ gap, where no FQHE resists, a Fermi liquid behaviour has been probed with periodic density modulation on the 2DES

[129]. The results are consistent with the formation of a stable CF Fermi liquid in the last half-filled LL. The present understanding of the $5/2$ incompressibility is a BCS-like condensation of this FL below a critical temperature, as we will see.
There are no principle reasons why only $5/2$ and $7/2$ condense, and the effect has to do with the details of the e-e interactions. It can easily be that the typical experimental parameters are such that these two even-denominator states have the largest critical temperatures and therefore appear as the first FQH half-filled states. Other CF Fermi liquids could as well condense, probably with smaller energy gaps, their discovery having to await for even cleaner samples and lower temperatures.

6.2 Introduction to the theory of the $5/2$ FQHE: the Pfaffian state

The "standard" FQH states are observed for odd denominator fractions and, as we saw, their principal sequence can be obtained straightforwardly within the CF picture.
The Halperin wavefunctions we presented at the end of chapter 1 [38] could however generate even denominator states, like $1/2$. In this picture the incompressible even denominators would be interpreted as Laughlin-like states for charge 2 bosons (in units of the electronic charge) formed by the eventual pair-binding of two electrons. The Laughlin quasiparticle excitations (or vortices) out of these states would have a charge $\pm\nu/2$ (in particular, at $\nu = 1/2$, the vortex charge would be $\pm 1/4$). The quasiparticle charge comes from inserting a flux quantum per state, which in this case is the two-electrons pair, with the final outcome of halving the original Laughlin result.

In order to theoretically investigate the $5/2$ state the standard approach has been to consider different condensations of the last half filled LL, without considering the lower full LL. In this sense the $5/2$ and $1/2$ problems formally coincide. Their physical difference has to do with the different e-e interactions in the last LL and with the typical experimental range of parameters where they show up. Numerical investigations [124] seem to suggest that the $1/2$ state has a much lower tendency to condense and this could be the reason why it is still detected as a CF Fermi Liquid even at the lowest experimentally available temperatures.

Immediately after the experimental discovery, Haldane and Rezayi (HR) proposed a spin-singlet (unpolarized) wavefunction at $\nu = 1/2$ as a possible GS, arguing it to be incompressible [130]. The HR state was shown to be the exact GS for a hollow-core Hamiltonian where the angular momentum 1 is the only non-vanishing e-e interaction channel.
In 1991 Moore and Read proposed a different interpretation of the GS along the picture of a paired many body wavefunction [131]. In their point of view the HR state is a spin-singlet d-wave condensate. With conformal field theory arguments they constructed a *p-wave polarized* state, called the "Pfaffian" state. The quasiparticle excitations out of the Pfaffian have fractional charge, as for other paired states, but they are expected to obey a non-Abelian, rather than fractional, statistics.
With time, a lot of numerical work has been undertaken to investigate the nature of the $5/2$ state. The Pfaffian state is actually believed to describe the correct GS [124],

and the presence of an in-plane field has been indeed shown to modify the interaction parameters such that the incompressibility is lost in favour of a compressible striped phase [132].
Motivated by the arguments above, we will thus concentrate on the properties of this fascinating state, inquiring on its structure as well as on its quasiparticle excitations.

The Moore-Read, or "Pfaffian" state at $\nu = 1/2m$ ($m \in \mathbb{N}$) has been proposed in the form

$$\boxed{\Psi_{\text{MR}}(z_1, ..., z_N) = \text{Pf}\left(\frac{1}{z_i - z_j}\right) \prod_{i<j=1}^{N} \left(\frac{z_i - z_j}{\ell}\right)^{2m} \prod_{j=1}^{N} e^{-\frac{1}{4\ell^2}|z_j|^2}} \tag{6.1}$$

where z_i is the 2D complex coordinate of the i-th particle. Apart from the usual gaussian factors, we point out the presence of the Vandermonde polynomial with *even* exponent needed to produce the correct flux attachment for CF at $1/2m$ filling. Finally, the Pfaffian term is defined as

$$\text{Pf}\left(M_{ij}\right) = \mathcal{A}\left[M_{12}M_{34}...M_{N-1,N}\right] \tag{6.2}$$

for an antisymmetric matrix M_{ij}, where $\mathcal{A}$ is the normalized antisymmetrization operator. In particular

$$\text{Pf}\left(\frac{1}{z_i - z_j}\right) = \mathcal{N}\left[\frac{1}{z_1 - z_2} \cdot \frac{1}{z_3 - z_4}... - \frac{1}{z_1 - z_3} \cdot \frac{1}{z_2 - z_4}... + \frac{1}{z_1 - z_4} \cdot \frac{1}{z_2 - z_3}...\right] . \tag{6.3}$$

with $\mathcal{N}$ a normalization factor.
The Pfaffian term (6.3) therefore describes a paired many-body state of spinless (or fully spin-polarized) CF with fixed particle number, where the pair wavefunction is $1/(z_i - z_j)$ for the (i, j) pair. This can be seen by direct comparison with the position representation of the N-particle paired state (4.14), which we can now write as

$$\Psi(z_1, ..., z_N) = \text{Pf}\left(g(z_i - z_j)\right) \tag{6.4}$$

where, as usual, $g(z_i - z_j)$ is the pair wavefunction. Indeed, the Pfaffian is the general structure of the position form of the BCS state sector with a fixed particle number generated by the second quantized state (4.64).
In the Moore-Read state (6.1) the CF pair wavefunction is clearly *odd* with respect to particle interchange, leading us to an odd-angular momentum pairing of spinless fermions. If we denote as $z = z_i - z_j$ the relative coordinate in the pair, we have $g(z) = 1/z$, leading to the angular momentum pairing channel $l = -1$ and to the momentum-space form $g_{\mathbf{k}} = 1/(k_x + ik_y)$.
To pursue the BCS analogy further [133], let us consider again the ESP state (4.67) presented in section 4.1.4, i.e. the spinless p-wave BCS state

$$|\Psi_{\text{ESP}}\rangle = \prod_{\mathbf{k}}{}' \left(u_{\mathbf{k}} + v_{\mathbf{k}}\, c^{\dagger}_{\mathbf{k}} c^{\dagger}_{-\mathbf{k}}\right) |\text{vac}\rangle \ . \tag{6.5}$$

This is the GS for the mean-field Hamiltonian

$$H_{\text{MF}} = \int \frac{\mathrm{d}\mathbf{k}}{(2\pi)^2} \left[\varepsilon_{\mathbf{k}} c^\dagger_{\mathbf{k}} c_{\mathbf{k}} + \frac{1}{2} \left(\Delta^*_{\mathbf{k}}\, c_{-\mathbf{k}} c_{\mathbf{k}} + \Delta_{\mathbf{k}}\, c^\dagger_{\mathbf{k}} c^\dagger_{-\mathbf{k}} \right) \right] \tag{6.6}$$

where the small momentum Fermi-liquid like dispersion $\varepsilon_{\mathbf{k}} = k^2/2m^* - \mu$ is assumed. In usual superconductors μ is the chemical potential, while in our case it will also assume a different meaning, as a parameter responsible for tuning the different phases arising in the GS.
In analogy with what argued above, we will take the order parameter in the $l = -1$ channel, its *small momentum* behaviour being

$$\Delta_{\mathbf{k}} = \Delta \cdot (k_x - i k_y) \equiv -i\Delta \cdot \left(\partial_x - i \partial_y \right) \tag{6.7}$$

with Δ a constant, in the uniform case. Notice that $\Delta_{-\mathbf{k}} = -\Delta_{\mathbf{k}}$ and $\Delta^*_{\mathbf{k}} = \Delta \cdot (k_x + i k_y) \equiv -i\Delta \cdot \left(\partial_x + i \partial_y \right)$.
In analogy with what seen in chapter 4 we can diagonalize the Hamiltonian with the Bogoliubov transformation

$$\gamma_{\mathbf{k}} = u_{\mathbf{k}} c_{\mathbf{k}} + v_{\mathbf{k}} c^\dagger_{-\mathbf{k}} \tag{6.8}$$

the fermionic statistics being preserved by the condition $|u^2_{\mathbf{k}}| + |v^2_{\mathbf{k}}| = 1$, $\forall\, \mathbf{k}$. The p-wave requirement produces $u_{\mathbf{k}} = u_{-\mathbf{k}}$ and $v_{\mathbf{k}} = -v_{-\mathbf{k}}$.
Imposing the final diagonal form

$$H_{\text{MF}} = E_{\text{GS}} + \sum_{\mathbf{k}} E_{\mathbf{k}}\, \gamma^\dagger_{\mathbf{k}} \gamma_{\mathbf{k}} \tag{6.9}$$

we obtain the Bogoliubov-de Gennes (BdG) equations

$$E_{\mathbf{k}} \begin{pmatrix} u_{\mathbf{k}} \\ v_{\mathbf{k}} \end{pmatrix} = \begin{pmatrix} \varepsilon_{\mathbf{k}} & \Delta^*_{\mathbf{k}} \\ \Delta_{\mathbf{k}} & -\varepsilon_{\mathbf{k}} \end{pmatrix} \begin{pmatrix} u_{\mathbf{k}} \\ v_{\mathbf{k}} \end{pmatrix} . \tag{6.10}$$

It can be directly checked that, differently from the s-wave case, if the spinor (u, v) is solution with energy E, then there is a solution with energy $-E$ associated to the spinor (v^*, u^*). This issue will have crucial implications in the following.
The BdG equations (6.10) imply the Bogolon dispersion

$$E_{\mathbf{k}} = \sqrt{\varepsilon^2_{\mathbf{k}} + |\Delta_{\mathbf{k}}|^2} \tag{6.11}$$

and further

$$g_{\mathbf{k}} = \frac{v_{\mathbf{k}}}{u_{\mathbf{k}}} = \frac{\varepsilon_{\mathbf{k}} - E_{\mathbf{k}}}{\Delta^*_{\mathbf{k}}} \tag{6.12}$$

with

$$|u_{\mathbf{k}}|^2 = \frac{1}{2} \left(1 + \frac{\varepsilon_{\mathbf{k}}}{E_{\mathbf{k}}} \right) \tag{6.13}$$

$$|v_{\mathbf{k}}|^2 = \frac{1}{2} \left(1 - \frac{\varepsilon_{\mathbf{k}}}{E_{\mathbf{k}}} \right) . \tag{6.14}$$

The plan in the following will be to characterize the properties of the Pfaffian state by studying its BCS form. We will not attempt to solve the full BCS problem for the whole momentum range, but rather concentrate in the large distance (small momenta) scaling of the different phases. In fact, apart from quantitative changes, the qualitative properties of the phases are generic once the phase is reached, and we will see that the critical point of the theory will be in the small momentum range, around $\mu = 0$.

Let us consider the general first quantized free Hamiltonian in the position representation, in presence of a generic vector potential $\mathbf{A}(\mathbf{r})$ as well as of an external electrostatic potential $U_0(\mathbf{r})$ (see (4.39))

$$H_0 = \frac{1}{2m}\left(-i\hbar\nabla + \frac{e}{c}\,\mathbf{A}(\mathbf{r})\right)^2 + U_0(\mathbf{r}) - \mu\ . \tag{6.15}$$

The scalar potential can be incorporated into a position dependent effective "chemical potential" $\mu(\mathbf{r}) = \mu - U_0(\mathbf{r})$, while μ is the true constant Fermi energy, at $T = 0$. The function $\mu(\mathbf{r})$ varies in space and can be thought as a local parameter entering the BCS problem.
For example, a strong external confining potential can be described by a rapidly growing function $U_0(\mathbf{r})$ eventually diverging to $+\infty$. In terms of the function $\mu(\mathbf{r})$, the confinement would result in a diverging scaling $\mu(\mathbf{r}) \to -\infty$ outside the confinement area. In the following we will drop the $\mathbf{r}$-dependence of $\mu(\mathbf{r})$ and simply indicate it as μ, and it is intended we explore local properties of a certain phase.
Considering the spectrum (6.11) we observe that a transition occurs at $\mu = 0$ for $\mathbf{k} = \mathbf{0}$, where the bogolon dispersion vanishes. Indeed, in the small momentum limit, we have $\varepsilon_{\mathbf{k}} \simeq -\mu$ and $\Delta_{\mathbf{k}} \simeq \Delta \cdot \mathbf{k}^*$ so that

$$E_{\mathbf{k}\to 0} \simeq \sqrt{\mu^2 + |\Delta|^2 k^2}\ . \tag{6.16}$$

The pair wavefunction is determined by the behaviour of $g_{\mathbf{k}}$ (6.12), which in its turn depends crucially on $E_{\mathbf{k}}$. In order to investigate the properties of the pairing in the different phases, we focus on the small momentum regimes in the two sides of, and at, the transition $\mu = 0$. The three relevant cases are

1. $\mu > 0$: $E_{\mathbf{k}} \simeq \mu\left(1 + \frac{1}{2}\frac{|\Delta|^2 k^2}{\mu^2}\right)$, leading to $g_{\mathbf{k}} \simeq -2\,\frac{\mu}{\Delta}\cdot\frac{1}{\mathbf{k}}$
2. $\mu = 0$: $E_{\mathbf{k}} \simeq \Delta \cdot \mathbf{k}^*$, leading to $g_{\mathbf{k}} \simeq -\frac{\mathbf{k}^*}{k}$
3. $\mu < 0$: $E_{\mathbf{k}} \simeq -\mu\left(1 + \frac{1}{2}\frac{|\Delta|^2 k^2}{\mu^2}\right)$, leading to $g_{\mathbf{k}} \simeq \frac{1}{\Delta}\left(\frac{1}{2m} + \frac{|\Delta|^2}{2\mu}\right)\cdot\mathbf{k}^*$.

The first case, $\mu > 0$ is conceptually analogous to our view of conventional p-wave superconductors. It will be denoted "the weak pairing" case, since it is directly connected to the BCS-like weak coupling phase. However, strictly speaking, close to the transition we are quite far from the conventional "weak coupling" condition, since the minimum excitation energy *does not* occur at k_{F} but at $\mathbf{k} = \mathbf{0}$.
The function $g_{\mathbf{k}}$ in this phase has a $1/\mathbf{k}$ small-momentum scaling, as expected for the Pfaffian state (see above). This means that the position-representation form of the pair wavefunction has the expected $1/z$ behaviour at large distances. In the

Pfaffian state this scaling is valid all the way down to small distances. The weak pairing p-wave BCS phase will be then identified as describing the essential properties of the Pfaffian state.
The divergence of $g_{\mathbf{k}}$ at small-momenta is due to the independent scalings $|v_{\mathbf{k}}| \to 1$ and $|u_{\mathbf{k}}| \to 0$, indicating a dominant occupation of long wavelength states in the BCS wavefunction, as expected in the weak-coupling regime, as well as in the utterly non-interacting Fermi-gas case.
Finally, notice, in $g_{\mathbf{k}}$, the appearance of the factor μ/Δ, the only characteristic inverse-length scale in the problem.

In the second case, $\mu = 0$, we have $|v_{\mathbf{k}}|^2 \to 1/2$ and $|u_{\mathbf{k}}|^2 \to 1/2$, with the outcoming pair wavefunction $g(z) \propto 1/(z|z|)$. Clearly, the particles in the pair are now more tightly bound than in the weak-pairing phase.

Finally, in the third case, $\mu < 0$, we have that $g_{\mathbf{k}}$ is analytical at small momenta, leading to an exponentially decaying pair wavefunction for large distances. In this phase the paired particles are exponentially bound, justifying the name "strong pairing" used to identify it. At small momenta we have $|v_{\mathbf{k}}| \to 0$ and $|u_{\mathbf{k}}| \to 1$, indicating a dominant occupation weight shifted to the small wavelength states. For $\mu < 0$ we expect to describe situations where the superconducting particle density is strongly reduced, like outside confinement edges or in the core of vortices.

Apart from the different scaling of the pair wavefunction in the position or momentum representation, the three phases are topologically distinguished [134]. To see this, let us consider the BdG spinor $\mathbf{s}_{\mathbf{k}} \equiv (u_{\mathbf{k}}, v_{\mathbf{k}})$ *parametrized* by the 2D momentum $\mathbf{k} \in \mathbb{R}^2$. The condition $|u_{\mathbf{k}}|^2 + |v_{\mathbf{k}}|^2 = 1$ implies the unitary modulus of $\mathbf{s}_{\mathbf{k}}$. Moreover, multiplying both its components by the same phase does not have any physical effect.
Altogether, this spinor representation maps the 2D momentum-space $\mathbb{R}^2$ into the unitary sphere S^2 embedded in $\mathbb{R}^3$, the polar angle being simply the global multiplicative phase for the BdG solution. In particular, the $(u_{\mathbf{k}} = 1, v_{\mathbf{k}} = 0)$ spinor describes the North pole of the sphere, while $(u_{\mathbf{k}} = 0, v_{\mathbf{k}} = 1)$ is the South pole. The convergence of the particle number implies $v_{k\to\infty} \to 0$, meaning that the "infinite-momentum states", are mapped to the North pole. Since $\mathbb{R}^2$ plus the point at infinite is itself an S^2 space, the spinorial representation builds up a mapping between the S^2-momentum space and the S^2-BdG spinor space with the North pole mapping into itself.

$$\mathbf{s}_{\mathbf{k}} : \; S^2_{\mathbf{k}} \longmapsto S^2_{\text{BdG}} \tag{6.17}$$

The maps are topologically classified into equivalence classes (called "homotopy" classes) and maps belonging to the same homotopy class can be deformed into each other continuously. The equivalence classes are identified by the number of times a certain point (different from the fixed point common to all, the North pole) in the target space, let it be the South pole, is reached by the full mapping. In other terms, the n-th homotopy class describes mappings that cover the target BdG spinor space n times while spanning the whole $\mathbf{k}$-space only once.
We can directly see that in the *strong* pairing phase the South pole is never reached since $g_{\mathbf{k}}$ vanishes when the gap goes to zero ($k = 0$). This means that the strongly paired case belongs to the 0-th homotopy class and it can be continuously deformed

in the trivial mapping where all the $\mathbf{k}$ points are identified with the North Pole.
On the contrary, the $\mathbf{k} = \mathbf{0}$ state in the *weak* pairing phase is directly mapped into the South Pole. This phase thus belongs *at least* to the 1-st homotopy class. It is likely that indeed the South Pole is reached only once, for the vanishing momentum state. However it is clear that the two phases cannot be continuously deformed into one another and are thus topologically distinguished.
Finally, the critical phase $\mu = 0$ is a separatrix between the other two, with the $\mathbf{k} = \mathbf{0}$ state being mapped onto the equator.

The arguments above suggest to identify the Moore-Read state *at* $\nu = 5/2$ with the weak-pairing uniform BCS-like phase at $\mu > 0$. The Cooper pairs for this wavefunction are CF states of well defined and opposite momenta. In the clean limit we do not have density modulations and if the filling is *exactly* $5/2$ the GS is *unique* with *no* vortex-like quasiparticle excitations.
The topologically distinguished strongly paired case $\mu < 0$ is associated to regions where the superconductive particle density vanishes, like strong confinements or the deep-core regions of externally induced vortices. In particular, the vacuum is expected to be topologically connected to the strongly-paired phase.

In the following we concentrate on what happens when Laughlin-like quasiparticle excitations are induced in the sample by varying the magnetic field with respect to where $5/2$ forms. As we saw in chapter 1, the uncompensated magnetic flux quanta enter the sample in form of vortices, locally suppressing the superconducting correlations. As long as they are trapped by the small amount of disorder present in the sample, the conductivity properties are not affected and the FQH plateau is acquainted for. However, as we will see, their internal structure has deep consequences on their statistics.
We will consider the problem of the structure of the GS in presence of several well-separated vortices. The non-Abelian nature of the quasiparticle statistics will be addressed on physical grounds. Finally we will consider the issue of the paired wavefunctions in the inhomogeneous many vortices configuration.

6.3 Vortex-like excitations in the Pfaffian state

Let us consider the effect of introducing an uncompensated magnetic flux quantum in the Pfaffian state. We could perform this operation as in (1.59), acting on the position representation of the Pfaffian state (6.1) with the Laughlin quasi-hole creation operator at position Z

$$\Psi_Z^{(+)}(z_1, ..., z_N) = \prod_{j=1}^{N} \left(\frac{z_j - Z}{\ell} \right) \Psi_{\rm MR}(z_1, ..., z_N) \ . \tag{6.18}$$

This wavefunction approach has been followed in [135]. Here we will consider a different perspective, examining the effect of the flux attachment as a vortex insertion in the corresponding *weakly paired* p-wave BCS state.
Recently, the role of vortices in 2D p-wave superconductors, like He^3, has attracted

a lot of theoretical interest [136, 137]. They have been shown to require a much smaller creation energy than that needed to break a Cooper pair into two far apart Bogolons. Finally, since a vortex implies a non-vanishing phase winding, they must be created in pairs in order to preserve the original boundary conditions at infinity. The typical features associated to a vortex are the linear vanishing of the gap with the radial distance from its core, and the additional $e^{i\theta}$ phase accumulated by the order parameter (θ being the polar angle in the cylindrical coordinates centered in the vortex core). Here we will not be interested in solving the gap equation self-consistently in presence of a vortex, but rather to characterize the nature of its BdG eigenstates of smallest energy. Thus we will consider the effect of the vortex phase in the BdG equations, but neglect the detailed radial dependence of the gap function, which can be appreciated only in the extreme proximity of the vortex core.
In the s-wave case it has been shown [138] that the excitation spectrum in a vortex has the harmonic oscillator form $(n+1/2)\Delta_0$, with $n \in \mathbb{N}$ and $\Delta_0 \sim \Delta^2/E_{\mathrm{F}}$ (Δ the bulk gap). Therefore the minimal BdG excitation energy in this case is $\Delta_0/2$, which is small but finite.
On the contrary, in the p-wave case, the analogous calculation [136] produces an internal spectrum of the type $n \cdot \Delta_0$, ($n \in \mathbb{N}$), and has a peculiar zero-energy excitation mode for $n = 0$ (we will call it "zero mode" (ZM)). Essentially, the reason for that is the cancellation between the vortex phase with the original p-wave order parameter phase. Clearly, in the s-wave case, this does not happen, leaving a residual uncompensated vortex phase responsible for the zero point finite energy.
The ZM is one allowed BdG solution, producing a spinor (u, v) which, in its turn generates a bogolon operator with zero excitation energy localized around the vortex core. The nature of this BdG state is peculiar, as we will see, and has deep consequences on the quasiparticle statistics.
Let us imagine to have several, say $2n$, far-apart vortices in the sample, each carrying its localized ZM, and ask what will be the GS *in presence of the vortices*. To make this point clear, we stress that vortices can be viewed as *excitations* for the Pfaffian state, but once the external magnetic field is tuned to a value that induces $2n$ vortices in the original $5/2$ state, the system will relax to the configuration of smallest energy. *This* configuration is what we are interested in.
If the ZM do not significantly overlap (meaning the vortex distances being ideally infinite), then there are $2n$ localized zero energy states. If we occupy them or leave them empty, the *total* energy of the configurations *does not* change, leading to many possible degenerate GS.
It may be tempting to think that there is a two-fold degeneracy per vortex (the ZM being empty or occupied). This would lead to a picture of the degenerate GS as made of independent pseudospin states on each vortex, corresponding to a GS subspace degeneracy of 2^{2n}.
However this is *not correct*. We will see that the BdG ZM are not true fermionic operators, but Majorana (real) fields. To produce a true (complex) zero energy fermionic creation/annihilation operator we need to build it up from two separate ZM living on different vortices, making the situation somewhat non-local. This effect will halve the number of possibilities and the correct final GS subspace degeneracy will be 2^n for $2n$ vortices.

This nontrivial degeneracy is the fundamental issue connected to the non-Abelian quasiparticle statistics. In fact, if we imagine to adiabatically interchange two quasiparticles, the final result will be a unitary operation *in the subspace of the degenerate GS*, corresponding to a matrix with size $2^n \times 2^n$. Successive quasiparticle interchanges will then correspond to the product of the associated matrices, *in the correct order* (the first interchange-matrix acting first, and so on). Choosing a different order of the quasiparticle permutations will correspond to a different matrix product. The result of the two permutation cycles, therefore, is not the same, since the statistical matrices do not commute.
The non-commutativity of the statistical matrices is the equivalent of the non-Abelian quasiparticle statistics. It is clear that such an effect depends crucially on the GS degeneracy, in its turn originated by the characteristics of the ZM BdG operators. The fractional Abelian statistics of ordinary Laughlin-quasiparticles came from a unique, non degenerate, GS.
Motivated by these considerations we will now inquire in the nature of the ZM BdG states, and then procede to characterize the GS in presence of vortices. The non-Abelian statistics will come out as a byproduct of the GS analysis.

6.3.1 The BdG equations for a vortex in the p-wave BCS state

A vortex in a 2D p-wave BCS state can be described in cylindrical coordinates (r, θ) by [88]

$$\Delta(\mathbf{r}) = \Delta(r)\, e^{-i\theta} \tag{6.19}$$

with $\Delta(r)$ a *real* function depending only on the radius, measured from the vortex core, chosen as the coordinate origin.
The full selfconsistent treatment of the BdG equations produces a $\Delta(r)$ vanishing linearly for $r \to 0$. This is however an effect which affects the close proximity of the vortex core, while the winding phase θ of the order parameter will persist even in the large distances. In the following we will not be concerned with the full selfconsistent solution of the problem at any length, and we will drop the r dependence of $\Delta(r)$, keeping the winding phase responsible for the properties of the vortex spectrum. Thus we will consider a vortex described by $\Delta(\mathbf{r}) = \Delta\, e^{-i\theta}$ with Δ a constant.
Our focus will be on the BdG equations for small momenta, as discussed above, where we will essentially neglect the laplacian term in the kinetic Hamiltonian, which will simply be expanded as $\varepsilon_{\mathbf{k}} = -\mu$, chosen to be locally constant in a given pairing phase. Moreover, the order parameter is not any longer uniform, and in particular it does not trivially commute with the momentum in (6.7). Thus the properly symmetrized BdG equations (6.10) become

$$\begin{cases} E\, u(\mathbf{r}) = -\mu\, u(\mathbf{r}) + \frac{1}{2}\left\{\Delta^*(\mathbf{r}), -i\partial_x + \partial_y\right\} v(\mathbf{r}) \\ E\, v(\mathbf{r}) = \mu\, v(\mathbf{r}) + \frac{1}{2}\left\{\Delta(\mathbf{r}), -i\partial_x - \partial_y\right\} u(\mathbf{r}) \end{cases} . \tag{6.20}$$

We remind that the BdG spinor solution at energy E, $(u_E(\mathbf{r})\,,\,v_E(\mathbf{r}))$ is associated to the quasiparticle field

$$\gamma_E = \int \mathrm{d}\mathbf{r}\,\left[u_E(\mathbf{r})\psi(\mathbf{r}) + v_E(\mathbf{r})\psi^\dagger(\mathbf{r})\right]\,. \tag{6.21}$$

The *positive energy* sector is associated to the quasiparticle excitation annihilators which, by definition, destroy the GS.
Inserting the form of the gap in presence of the vortex and using the cylindrical representation of the gradient

$$\nabla = e^{i\theta}\left(\partial_r + \frac{i}{r}\,\partial_\theta\right) \tag{6.22}$$

the (6.20) are rewritten as

$$\begin{cases} (E+\mu)\,u(\mathbf{r}) = -i\,\Delta\cdot\left(\partial_r + \frac{i}{r}\,\partial_\theta + \frac{1}{2r}\right)v(\mathbf{r}) \\ (E-\mu)\,v(\mathbf{r}) = -i\,\Delta\cdot\left(\partial_r - \frac{i}{r}\,\partial_\theta + \frac{1}{2r}\right)u(\mathbf{r}) \end{cases} \tag{6.23}$$

where the terms in $1/2r$ come from the direct evaluation of the anticommutator.
Already at this level we notice an extremely relevant fact. From (6.23), by complex conjugation, we see that, if we have a BdG spinor solution $(u_E(\mathbf{r})\,,\,v_E(\mathbf{r}))$ at energy E, the solution at energy $-E$ is the spinor $(v_E^*(\mathbf{r})\,,\,u_E^*(\mathbf{r}))$. In particular, for $E=0$ (Zero Mode) we get the spinor $(u_{E=0}(\mathbf{r})\,,\,u_{E=0}^*(\mathbf{r}))$. The corresponding BdG field operator is then

$$\gamma_{E=0} = \int \mathrm{d}\mathbf{r}\,\left[u_{E=0}(\mathbf{r})\psi(\mathbf{r}) + u_{E=0}^*(\mathbf{r})\psi^\dagger(\mathbf{r})\right] = \gamma_{E=0}^\dagger\,. \tag{6.24}$$

That is, the Bogolon operator associated to the zero energy state is a Majorana (or real) fermion operator. Therefore, in itself, it *does not* create or annihilate a true (complex) fermion. This fact is responsible for the above mentioned "non-locality" of the GS in the many vortices configuration, and to the halving of the exponent in the dimension of the degenerate GS subspace.

In order to characterize the BdG spinors, we consider (6.23) in more depth. The global angular dependence of $u(\mathbf{r})$ and $v(\mathbf{r})$ will not matter and can be neglected in both, such that the term in ∂_θ can be dropped.
By defining

$$\begin{cases} u(\mathbf{r}) = \frac{U(r)}{\sqrt{r}} \\ v(\mathbf{r}) = \frac{V(r)}{\sqrt{r}} \end{cases} \tag{6.25}$$

the (6.23) become

$$\begin{cases} (E+\mu)\,U(r) = -i\,\Delta\,\partial_r V(r) \\ (E-\mu)\,V(r) = -i\,\Delta\,\partial_r U(r) \end{cases}\,. \tag{6.26}$$

In the following we will have to evaluate projections of different BdG functions, like $\langle u_E|u_{E'}\rangle$, $\langle u_E|v_{E'}\rangle$ and so on. For example

$$\langle u_E|v_{E'}\rangle = \int \mathrm{d}\mathbf{r}\, u_E^*(\mathbf{r})\, v_{E'}(\mathbf{r}) = 2\pi \int \mathrm{d}r\, U_E^*(r)\, V_{E'}(r) \tag{6.27}$$

so that it can be calculated as a 1D integral using the functions U and V and dropping the factor r in the 2D measure.
Finally, we can define the *real* functions $q(r)$ and $p(r)$ via

$$\begin{cases} U(r) = \sqrt{i}\, q(r) \\ V(r) = -\frac{1}{\sqrt{i}}\, p(r) \end{cases} \tag{6.28}$$

producing the BdG system

$$\begin{cases} (E+\mu)\, q(r) = \Delta\, \partial_r p(r) \\ (E-\mu)\, p(r) = -\Delta\, \partial_r q(r) \end{cases} . \tag{6.29}$$

Resuming our previous definitions we can write the BdG functions as

$$\begin{cases} u(\mathbf{r}) = \sqrt{\frac{i}{r}}\, q(r) \\ v(\mathbf{r}) = -\sqrt{\frac{1}{i\, r}}\, p(r) \end{cases} . \tag{6.30}$$

If we consider the case $E = 0$ in (6.29), we get two possibilities, $q(r) = p(r)$ or $q(r) = -p(r)$, both leading to exponential solutions. As we mentioned, we are considering the insertion of vortices in the weakly paired BCS phase, i.e. $\mu > 0$. Thus, the choice $q(r) = p(r)$ produces an exponentially diverging solution for large r, which cannot be normalized and is therefore discarded. The only remaining possibility is $q(r) = -p(r)$, leading to

$$q_{E=0}(r) = -p_{E=0}(r) = \mathcal{N} e^{-\frac{\mu}{\Delta} r} . \tag{6.31}$$

with $\mathcal{N}$ a normalization factor to be fixed. Again, we notice, in the exponent, the factor μ/Δ, the only characteristic inverse-length in the problem. It can readily be checked that, indeed, for the Zero Mode, we have $v^*(\mathbf{r}) = u(\mathbf{r})$.

We have then shown the existence of a zero-energy BdG eigenstate, exponentially localized around the vortex center. As stressed in (6.24), the associated Bogolon field is a Majorana operator, acting *locally* on the single vortex on which the ZM lives.
Having presented some of the properties of a single vortex in the p-wave state, we now turn to describe the Ground State in presence of many vortex-like quasiparticles [139]. The essential features are captured by considering the two-vortices configuration, from which we start.

6.4 The GS in presence of vortices

Let us consider the situation of two vortices in the otherwise uniform p-wave BCS state. Let $\mathbf{R}_k = (R_k, \Omega_k)$ be their 2D positions in cylindrical coordinates, with $k = 1, 2$ the label index for the two vortices.
In the proximity of $\mathbf{R}_k$ the gap has the form $\Delta(\mathbf{r}) = \Delta(r - R_k)\, e^{i(\Omega_k + \theta)}$, with θ the phase of the relative coordinate $\mathbf{r} - \mathbf{R}_k$.
As stated above, we will assume the vortices to be far-apart, so that no overlap between them has to be considered. If they were brought closer, the tunneling overlap between them would split the two degenerate Zero Modes producing two eigenmodes with exponentially small positive-negative energy. At the typical temperature T where experiments are performed they would still result as essentially degenerate, their energy split being much smaller than T.
If no tunneling takes place, we can describe the two ZM Majorana operators as

$$\begin{aligned} \alpha_k^{(0)} &= \int \mathrm{d}\mathbf{r} \left[w_k^{(0)}(\mathbf{r} - \mathbf{R}_k)\, e^{i\Omega_k/2}\, \psi(\mathbf{r}) + w_k^{(0)*}(\mathbf{r} - \mathbf{R}_k)\, e^{-i\Omega_k/2}\, \psi^\dagger(\mathbf{r}) \right] \\ &\equiv \frac{1}{\sqrt{2}} \left(\Psi_k^{(0)} + \Psi_k^{(0)\dagger} \right) = \alpha_k^{(0)\dagger} \end{aligned} \tag{6.32}$$

with $w_k^{(0)}(\mathbf{r}) = u_{k,E=0}(\mathbf{r})$, of the exponentially localized form obtained in (6.30,6.31) (the notation has been changed for successive convenience). The superscript (0) will be called "generation index", and will acquire a meaning soon. For simplicity, in the following we will drop the shift coordinate $\mathbf{R}_k$, assuming the operators with index k act *locally* around the positions $\mathbf{R}_k$.
Thus, the Majorana fermions (6.32) are generated by the ZM BdG spinors

$$A_k^{(0)} \equiv \begin{pmatrix} w_k^{(0)}(\mathbf{r}) \\ w_k^{(0)*}(\mathbf{r}) \end{pmatrix} . \tag{6.33}$$

In (6.32) we introduced $\Psi_k^{(0)}$ the *true fermionic* annihilation operator on the ZM state, with

$$\Psi_k^{(0)} = \sqrt{2} \int \mathrm{d}\mathbf{r}\, w_k^{(0)}(\mathbf{r})\, e^{i\Omega_k/2}\, \psi(\mathbf{r}) . \tag{6.34}$$

We stress that $\Psi_k^{(0)}$ acts *locally*, just on the ZM of the k-th vortex.
We can define the occupation representation for the true-fermionic ZM by introducing the states $|0\rangle_k$ and $|1\rangle_k$ according to

$$\Psi_k^{(0)} |0\rangle_k = 0 \qquad\qquad \Psi_k^{(0)\dagger} |0\rangle_k = e^{-i\Omega_k/2}\, |1\rangle_k . \tag{6.35}$$

In the two-vortices case we would have four basis states

$$|00\rangle \tag{6.36}$$

$$e^{-i\Omega_2/2}\, |01\rangle = \Psi_2^{(0)\dagger} |00\rangle \tag{6.37}$$

$$e^{-i\Omega_1/2}\, |10\rangle = \Psi_1^{(0)\dagger} |00\rangle \tag{6.38}$$

$$e^{-i(\Omega_1 + \Omega_2)/2}\, |11\rangle \equiv \Psi_1^{(0)\dagger} \Psi_2^{(0)\dagger} |00\rangle . \tag{6.39}$$

Notice that $\Psi_1^{(0)\dagger} e^{-i\Omega_2/2}\,|01\rangle = -\Psi_2^{(0)\dagger} e^{-i\Omega_1/2}\,|10\rangle = e^{-i(\Omega_1+\Omega_2)/2}\,|11\rangle$, $\Psi_1^{(0)}|11\rangle = e^{-i\Omega_2/2}\,|01\rangle$ and $\Psi_2^{(0)}|11\rangle = -e^{-i\Omega_1/2}\,|10\rangle$.
If the BdG ZM were true fermionic operators, we could generate different orthogonal degenerate GS by creating fermions in the localized states with zero energy, as in (6.36). With $2n$ vortices we would then have a GS degeneracy of 2^{2n}, since each ZM could be empty or singly occupied. However this is not the case, and the ZM fields are sums of localized true fermionic creation and annihilation operators. In particular, the states (6.36) *are not* the GS, as we will see, but they form a basis on which the GS can be written.
We can construct a different BdG spinor for the k-th vortex, orthogonal by construction to the ZM one, as

$$B_k^{(0)} = \begin{pmatrix} i\,w_k^{(0)}(\mathbf{r}) \\ -i\,w_k^{(0)*}(\mathbf{r}) \end{pmatrix}\,, \tag{6.40}$$

generating a second Majorana operator

$$\begin{aligned} x_k^{(0)} &= \int \mathrm{d}\mathbf{r}\,\left[i\,w_k^{(0)}(\mathbf{r})\,e^{i\Omega_k/2}\;\psi(\mathbf{r}) - i\,w_k^{(0)*}(\mathbf{r})\,e^{-i\Omega_k/2}\;\psi^\dagger(\mathbf{r})\right] \\ &\equiv \frac{i}{\sqrt{2}}\left(\Psi_k^{(0)} - \Psi_k^{(0)\dagger}\right) = x_k^{(0)\dagger}\,. \end{aligned} \tag{6.41}$$

Being orthogonal to $A_k^{(0)}$, the spinor $B_k^{(0)}$ can be expanded on all the BdG solutions with *finite* energy (both positive and negative, but *not* zero), described by the spinors

$$S_{E,k} = \begin{pmatrix} u_{E,k}(\mathbf{r}) \\ v_{E,k}(\mathbf{r}) \end{pmatrix}\,. \tag{6.42}$$

The expansion results in

$$B_k^{(0)} = \begin{pmatrix} i\,w_k^{(0)}(\mathbf{r}) \\ -i\,w_k^{(0)*}(\mathbf{r}) \end{pmatrix} = \sum_{E\neq 0} C_{E,k}^{(1)} \begin{pmatrix} u_{E,k}(\mathbf{r}) \\ v_{E,k}(\mathbf{r}) \end{pmatrix} = \sum_{E\neq 0} C_{E,k}^{(1)} S_{E,k} \tag{6.43}$$

with the coefficients

$$C_{E,k}^{(1)} = S_{E,k}^\dagger B_k^{(0)} = \int \mathrm{d}\mathbf{r}\,\left[i\,u_{E,k}^*(\mathbf{r}) w_k^{(0)}(\mathbf{r}) - i\,v_{E,k}^*(\mathbf{r}) w_k^{(0)*}(\mathbf{r})\right]\,. \tag{6.44}$$

The *positive energy* part of $B_k^{(0)}$ is associated to the *annihilation* operator on the 0-generation states. Explicitly, this *fermionic* annihilator is generated by

$$Y_k^{(1)} = \sum_{E>0} C_{E,k}^{(1)} S_{E,k} = \frac{1}{2}\left(B_k^{(0)} - i\,A_k^{(1)}\right) \tag{6.45}$$

with

$$A_k^{(1)} = i \sum_{E\neq 0} \mathrm{sgn}(E) C_{E,k}^{(1)} S_{E,k} \equiv \begin{pmatrix} w_k^{(1)}(\mathbf{r}) \\ w_k^{(1)*}(\mathbf{r}) \end{pmatrix}\,. \tag{6.46}$$

Notice that, having used the relation $v_{-E,k} = u^*_{E,k}$, we obtained that $A^{(1)}_k$ is again a Majorana spinor, this time called of "1-generation". The 0-generation quasiparticle-excitation annihilator (6.45) can then be written as

$$y^{(1)}_k = \frac{i}{2\sqrt{2}} \left(\Psi^{(0)}_k - \Psi^{(0)\dagger}_k - \Psi^{(1)}_k - \Psi^{(1)\dagger}_k \right) \tag{6.47}$$

with obvious notations.
We can already see that the fermionic ZM occupation states on the k-th vortex, $|0\rangle_k$ and $e^{-i\Omega_k/2}|1\rangle_k$, do not represent two independent GS. In fact, the true GS must be destroyed by (6.47), but if we act with it on the two states above we obtain

$$y^{(1)}_k |0\rangle_k = -\frac{i}{2\sqrt{2}}\, e^{-i\Omega_k/2}\, |1\rangle_k \qquad\qquad y^{(1)}_k e^{-i\Omega_k/2}\, |1\rangle_k = \frac{i}{2\sqrt{2}}\, |0\rangle_k \ . \tag{6.48}$$

Thus, we can already predict that the true GS will imply entanglement of the fermionic ZM occupation states.
At this point we can iterate the arguments. Out of $A^{(1)}_k$ we can construct the orthogonal Majorana spinor

$$B^{(1)}_k = \begin{pmatrix} i\, w^{(1)}_k(\mathbf{r}) \\ -i\, w^{(1)*}_k(\mathbf{r}) \end{pmatrix} = \sum_{E\neq 0} C^{(2)}_{E,k} S_{E,k} \tag{6.49}$$

with

$$C^{(2)}_{E,k} = S^\dagger_{E,k} B^{(1)}_k \ . \tag{6.50}$$

The *positive energy* part of $B^{(1)}_k$ generates the *annihilation* operator on the 1-generation states

$$Y^{(2)}_k = \sum_{E>0} C^{(2)}_{E,k} S_{E,k} = \frac{1}{2} \left(B^{(1)}_k - i\, A^{(2)}_k \right) \tag{6.51}$$

with

$$A^{(2)}_k = i \sum_{E\neq 0} \mathrm{sgn}(E) C^{(2)}_{E,k} S_{E,k} \equiv \begin{pmatrix} w^{(2)}_k(\mathbf{r}) \\ w^{(2)*}_k(\mathbf{r}) \end{pmatrix} \tag{6.52}$$

and so on for successive generations.
The j-generation localized functions $w^{(j)}(\mathbf{r})$ are generic, until the BdG functions in $S_{E,k}$ are obtained explicitly. Still, it is possible to show generally (see Appendix B) that *each* $w^{(j)}(\mathbf{r})$ is orthogonal to *every other* $w^{(j')}(\mathbf{r})$ if $j \neq j'$. This implies that all the $A^{(j)}_k$ and $B^{(j)}_k$ spinors are orthogonal to one another if they belong to different generations, apart from being trivially orthogonal, due to their localization, if they sit on different vortices.
This iteration automatically produces orthogonal localized wavefunctions that can be used as a functional basis around each vortex (completeness is still to be proved, but we believe it holds in the case of infinitely far vortices). The successive generation essentially stops whenever the w functions start overlapping with those of other vortices.

Let me express my deep appreciation to Ady Stern for inventing this beautiful procedure.
Apart from its clean logical beauty, the generation procedure presented above turns out to be extremely suitable to address the nature of the GS in the many vortices case.

In order to produce a *zero energy* true fermionic field with *two* vortices we consider the operator

$$\alpha^{(0)} = \alpha_1^{(0)} - i\,\alpha_2^{(0)} = \frac{1}{\sqrt{2}}\left(\Psi_1^{(0)} + \Psi_1^{(0)\dagger} - i\Psi_2^{(0)} - i\Psi_2^{(0)\dagger}\right) . \tag{6.53}$$

In complete analogy we can build

$$x^{(0)} = x_1^{(0)} - i\,x_2^{(0)} = \frac{1}{\sqrt{2}}\left(i\Psi_1^{(0)} - i\Psi_1^{(0)\dagger} + \Psi_2^{(0)} - \Psi_2^{(0)\dagger}\right) \tag{6.54}$$

and introduce four orthogonal states

$$|\downarrow\downarrow\rangle \tag{6.55}$$
$$|\uparrow\downarrow\rangle = \alpha^{(0)\dagger}|\downarrow\downarrow\rangle \tag{6.56}$$
$$|\downarrow\uparrow\rangle = x^{(0)\dagger}|\downarrow\downarrow\rangle \tag{6.57}$$
$$|\uparrow\uparrow\rangle \equiv \alpha^{(0)\dagger}x^{(0)\dagger}|\downarrow\downarrow\rangle \tag{6.58}$$

with the conditions

$$\alpha^{(0)}|\downarrow\downarrow\rangle = x^{(0)}|\downarrow\downarrow\rangle = 0 . \tag{6.59}$$

To get the relation between this "spin" description and the occupation representation we write the state $|\downarrow\downarrow\rangle$ on the basis (6.36) as

$$|\downarrow\downarrow\rangle = a\,|00\rangle + b\,e^{-i\Omega_2/2}\,|01\rangle + c\,e^{-i\Omega_1/2}\,|10\rangle + d\,e^{-i(\Omega_1+\Omega_2)/2}\,|11\rangle . \tag{6.60}$$

Imposing (6.59) with the definitions (6.53,6.54) we get the conditions $a = d = 0$ and $c = i \cdot b$, producing

$$|\downarrow\downarrow\rangle = \frac{1}{\sqrt{2}}\left(e^{-i\Omega_1/2}\,|10\rangle - i\,e^{-i\Omega_2/2}\,|01\rangle\right) \tag{6.61}$$

where normalization has been implemented.
The successive terms in (6.55) give

$$\begin{aligned}
|\downarrow\uparrow\rangle &= \frac{1}{\sqrt{2}}\left(|00\rangle + i\,e^{-i(\Omega_1+\Omega_2)/2}\,|11\rangle\right) \\
|\uparrow\downarrow\rangle &= \frac{1}{\sqrt{2}}\left(|00\rangle - i\,e^{-i(\Omega_1+\Omega_2)/2}\,|11\rangle\right) \\
|\uparrow\uparrow\rangle &= \frac{1}{\sqrt{2}}\left(e^{-i\Omega_1/2}\,|10\rangle + i\,e^{-i\Omega_2/2}\,|01\rangle\right) .
\end{aligned} \tag{6.62}$$

Altogether, we see that each spin-description state implies entanglement in the occupation representation. Notice that no tunneling is ever considered. The entanglement holds for states on different vortices and is therefore non-local, somehow

resembling what happens in the EPR (Einstein-Podolski-Rosen) paradox.
As discussed qualitatively above, for two vortices we expect *two* GS. In the spin-representation they are easily identified as the two possible states for the zero-energy operator $\alpha^{(0)}$. By tracing over the "right" spin states and stopping at the 0-generation level, we obtain the two possibilities

$$|\downarrow\rangle = |\downarrow\downarrow\rangle + |\downarrow\uparrow\rangle \tag{6.63}$$
$$|\uparrow\rangle = |\uparrow\downarrow\rangle + |\uparrow\uparrow\rangle \, . \tag{6.64}$$

Using the (6.61,6.62) we can finally express the two GS in the occupation representation. The entanglement between states of the same generation is evident, and we observe that each GS is a superposition of many-body configurations with different particle numbers, as we already saw for the BCS state (chapter 4).
Before characterizing completely the structure of the GS for the next generations, we can already address the issue of non-Abelian quasiparticle statistics. The question is, as seen in chapter 1, what happens when one of the two vortices encircles the other.
We can for instance drag vortex 2 adiabatically in a closed loop around vortex 1 (which can be chosen to sit in the origin). The occupation of the ZM is not affected by this operation, but the phase Ω_2 goes into $\Omega_2 + 2\pi$. The final effect is thus a change of sign for the states with vortex 2 occupied in the family (6.61,6.62). Therefore, in (6.63) the GS $|\downarrow\rangle$ is transformed into $|\uparrow\rangle$ and viceversa. These statistical factors coincide with those obtained in [135, 140].
Our derivation offers a quite physical picture of the non-Abelian statistics. The ingredients which have been shown to be crucial in our discussion are the presence of ZM in the vortex cores leading to the GS degeneracy, the entanglement between states living on different vortices and the phase accumulated by a vortex dragged around a closed loop in the 2DES.

Having obtained the mapping between the occupation and "spin" representations, we can now procede to determine the full structure of the GS. In particular, once we solved the issue of entanglement at the 0-generation level, we want to address what happens to the further generations.
We saw that, while building the quasiparticle-excitation annihilators on the j-th generation $y_k^{(j+1)}$, we automatically produced the Majorana spinor of $j+1$ generation $A_k^{(j+1)}$. The annihilators will therefore constitute the bridges between different generations.
To see this, we need a two-spins ket *per each generation* j, of the form $|s_j, S_j\rangle$ with $s_j, S_j = \uparrow / \downarrow$, such that $\alpha^{(j)}$ ($x^{(j)}$) lowers the spin value s_j (S_j), exactly as in (6.55). The two GS in the two-vortices case are therefore identified with $s^{(0)} = \uparrow, \downarrow$, as in (6.63). To keep trace of the next generations we can (tensor)-multiply each two-spin ket $|s_j, S_j\rangle$ with a "bath" of states describing the further generations, indicated as

$\mathcal{B}^{(j+1)}_{S_j}$. In this notation we write the two GS as

$$|\downarrow\rangle = |\downarrow\downarrow\rangle|\mathcal{B}^{(1)}_{\downarrow}\rangle + |\downarrow\uparrow\rangle|\mathcal{B}^{(1)}_{\uparrow}\rangle \tag{6.65}$$

$$|\uparrow\rangle = |\uparrow\downarrow\rangle|\mathcal{B}^{(1)}_{\downarrow}\rangle + |\uparrow\uparrow\rangle|\mathcal{B}^{(1)}_{\uparrow}\rangle \tag{6.66}$$

or, more compactly

$$|s_0\rangle = \sum_{S_0} |s_0, S_0\rangle|\mathcal{B}^{(1)}_{S_0}\rangle \ . \tag{6.67}$$

At this point we *impose* that the GS are destroyed by the annihilators $y^{(1)}_k$ (6.47). More conveniently we can define the operators

$$y^{(j)}_{\pm} = y^{(j)}_1 \pm i y^{(j)}_2 \tag{6.68}$$

with

$$y^{(j)}_{+} = \frac{1}{2}\left(x^{(j-1)\dagger} - i\alpha^{(j)\dagger}\right) \tag{6.69}$$

$$y^{(j)}_{-} = \frac{1}{2}\left(x^{(j-1)} - i\alpha^{(j)}\right) \ . \tag{6.70}$$

By requesting

$$y^{(1)}_{+}|s_0\rangle = 0 \tag{6.71}$$

$$y^{(1)}_{-}|s_0\rangle = 0 \tag{6.72}$$

for $s_0 = \uparrow, \downarrow$, and bracketing (6.71) with $\langle s_0, S_0|$ for every $S_0 = \uparrow, \downarrow$, we obtain four equations for the baths

$$\alpha^{(1)\dagger}|\mathcal{B}^{(1)}_{S_0=\uparrow}\rangle = i\,|\mathcal{B}^{(1)}_{S_0=\downarrow}\rangle \tag{6.73}$$

$$\alpha^{(1)\dagger}|\mathcal{B}^{(1)}_{S_0=\downarrow}\rangle = 0 \tag{6.74}$$

$$\alpha^{(1)}|\mathcal{B}^{(1)}_{S_0=\uparrow}\rangle = 0 \tag{6.75}$$

$$\alpha^{(1)}|\mathcal{B}^{(1)}_{S_0=\downarrow}\rangle = -i\,|\mathcal{B}^{(1)}_{S_0=\uparrow}\rangle \ . \tag{6.76}$$

Therefore the bath $|\mathcal{B}^{(1)}_{S_0}\rangle$ has the typical behaviour of the spin state with $s_1 = -S_0$ and can then be written as

$$|\mathcal{B}^{(1)}_{S_0}\rangle = i^{S_0/2}\sum_{S_1} |s_1 = -S_0, S_1\rangle|\mathcal{B}^{(2)}_{S_1}\rangle \tag{6.77}$$

where we associate $S_j = \downarrow \equiv -1$ and $S_j = \uparrow \equiv 1$ (same for s_j). Analogous arguments can be repeated for baths of successive generations.
The GS have therefore a beautiful self-similar structure. Along with the *vortex-entanglement at the same generation level* implied in the two-spins kets $|s_j, S_j\rangle$ (see

(6.55)) the (6.71) also produce *entanglement between neighbour generations*. The final form of the GS will therefore be

$$|s_0\rangle = \sum_{S_0} |s_0, S_0\rangle i^{S_0/2} \sum_{S_1} |s_1 = -S_0, S_1\rangle i^{S_1/2} \sum_{S_2} |s_2 = -S_1, S_2\rangle i^{S_2/2} \times \\ \times \sum_{S_3} \dots i^{S_n/2} \sum_{S_{n+1}} |s_{n+1} = -S_n, S_{n+1}\rangle |\mathcal{B}^{(n+2)}_{S_{n+1}}\rangle \ . \tag{6.78}$$

The index n indicates the upper limit of the generation procedure, occurring when the $w_k^{(n)}$ functions on different vortices start overlapping.
In the case of four (and more) vortices the arguments are quite analogous. The vortices will be divided in many pairs. Within each pair the two ZM will be combined to form a single complex true-fermionic operator, and the successive generation procedure works as already presented.
The analysis presented up to now is completely general and highlights the complex structure of the GS.
We could however dig deeper into the knowledge of the properties of our system if we succeeded in solving the spectrum of spinor BdG eigenstates. This would allow to address the localized states $w_k^{(j)}$ explicitly and would produce a different basis on which to expand the paired wavefunctions.
Indeed, one aspect which is still to be solved is the issue of pairing in the inhomogeneous p-wave state. That is, we would now like to determine what is the nature of the Cooper pairs wavefunctions, i.e. address the open question "who pairs to whom?".
In order to do that we will now consider a case in which the BdG equations can be solved exactly and finally write the GS on the basis of the BdG states.

6.5 The issue of Cooper-pairing in the GS with vortices

In what follows we will concentrate on a particular case where the BdG equations can be solved explicitly and the pairing structure of the GS becomes evident. The nature of the Cooper pairs wavefunctions in presence of vortices will be addressed [141].

6.5.1 Explicit solution of the BdG equations for a step-like model

In this section we will consider the explicit case of a disk-like sample with a large circular edge of radius x_{E} enclosing a weakly paired phase and a vortex in the disk center.
As shown by Read and Green [133], and as we mentioned previously, we can describe this situation with a function $\mu(\mathbf{r})$ ($\mathbf{r} = (x, \theta)$ in cylindrical coordinates) which is negative in the extreme vortex core and outside the external edge, and positive in the bulk of the sample. Thus the vortex, apart from its phase winding appearing directly in the BdG equations, can be described as a small circular domain boundary with radius $x_{\mathrm{V}} \ll x_{\mathrm{E}}$, separating the strongly paired internal phase from the

weakly paired bulk.
As seen previously in (6.29), the interesting BdG problem is purely radial if $\mu(\mathbf{r})$ does not have any angular dependence (we will assume this and simply write $\mu(x)$). Finally, for simplicity we will set $x_{\mathrm{V}} = 0$ and $x_{\mathrm{E}} = L$, so that the configuration resembles that of a Corbino disk.
Using (6.30), the Bogoliubov-de Gennes equations at energy E in the circular geometry can be written as

$$\begin{cases} \partial_x q(x) = \frac{\mu(x)-E}{\Delta}\, p(x) \\ \\ \partial_x p(x) = \frac{\mu(x)+E}{\Delta}\, q(x) \end{cases} . \tag{6.79}$$

The effective chemical potential $\mu(x)$ is negative for $x < 0$ and $x > L$ and positive for $0 < x < L$. Without further specification about the functional form $\mu(x)$ these coupled equations are not solvable in general terms.
We can however observe that the system (6.79) describes a 1D harmonic oscillator where q and p are canonical coordinates (position-momentum), x taking the place of time, with a "time"-dependent oscillation frequency $\omega^2(x) = (\mu^2(x) - E^2)/\Delta^2$.
The problem could be tackled approximately by choosing the time-dependence of the oscillator frequency to be much slower than the characteristic time evolution of the system. This would be accomplished by choosing a slowly varying potential $\mu(x)$ and the approximate solutions for q and p would result from the action conservation principle for classical adiabatic transformations [142, 143].
For calculational purposes, however, in order to obtain *exact* BdG solutions we resort to a step-like function $\mu(x)$ of the form

$$\mu(x) = \begin{cases} -\mu_\infty & \text{for } x < 0 \text{ (Region 1)} \\ \\ \mu & \text{for } 0 < x < L \text{ (Region 2)} \\ \\ -\mu_\infty & \text{for } x > L \text{ (Region 3)} \end{cases} \tag{6.80}$$

with $\mu, \mu_\infty > 0$ and $\mu_\infty \to +\infty$. With this choice every phase is *uniform* and equations (6.79) reduce to those of a 1D harmonic oscillator with a constant frequency *in every region*.
The general normalizable solutions for q and p with $E > \mu$ in the three regions are

$$\boxed{E > \mu} \begin{cases} q_1(x) = A_1\, e^{\frac{\mu_\infty}{\Delta} x} \\ \\ q_2(x) = A_2\, \cos(kx) + B_2\, \sin(kx) \\ \\ q_3(x) = A_3\, e^{-\frac{\mu_\infty}{\Delta}(x-L)} \end{cases} \tag{6.81}$$

and

$$\boxed{E > \mu} \begin{cases} p_1(x) = -A_1\, e^{\frac{\mu_\infty}{\Delta} x} \\ \\ p_2(x) = \gamma_k\, (-A_2\, \sin(kx) + B_2\, \cos(kx)) \\ \\ p_3(x) = A_3\, e^{-\frac{\mu_\infty}{\Delta}(x-L)} \end{cases} \tag{6.82}$$

where

$$\begin{cases} k = \frac{\sqrt{|E^2-\mu^2|}}{\Delta} \\ \\ \gamma_k = \frac{k}{a-\sqrt{a^2+k^2}} \end{cases} \tag{6.83}$$

having introduced the inverse decay length $a = \mu/\Delta$.
Imposing the continuity of $q(x)$ and $p(x)$ in $x = 0$ and $x = L$ we obtain the conditions

$$\begin{cases} A_2 = A_1 \\ B_2 = -\frac{1}{\gamma_k} A_1 \\ A_3 = A_1 \left(\cos(kL) - \frac{1}{\gamma_k}\sin(kL)\right) \\ A_3 = -A_1 \left(\gamma_k \sin(kL) + \cos(kL)\right) \end{cases} \tag{6.84}$$

whence the quantization condition for the allowed k's

$$\tan(kL) = \frac{k}{a} \, . \tag{6.85}$$

The positive solutions for k to (6.85) are labelled as k_i, i a positive integer, with $k_1 = 0$.
For $aL > 1$ we have $k_i \in \left((i-1)\frac{\pi}{L}, (i-1)\frac{\pi}{L} + \frac{\pi}{2L}\right)$, so that $\mathrm{sgn}\left(\sin(k_i L)\right) = \mathrm{sgn}\left(\cos(k_i L)\right) = (-1)^{i+1}$. Denoting $q_{k_i}(x)$ and $p_{k_i}(x)$ the allowed solutions for the whole range of x we have $q_{k_i}(x) = q_{-k_i}(x)$ and $p_{k_i}(x) = p_{-k_i}(x)$ and we can only care about the positive k's.
From (6.85) we can then extract

$$\begin{cases} \sin(k_i L) = (-1)^{i+1} \frac{k_i}{\sqrt{a^2+k_i^2}} \\ \\ \cos(k_i L) = (-1)^{i+1} \frac{a}{\sqrt{a^2+k_i^2}} \end{cases} \tag{6.86}$$

In the end the A_1's are k-dependent, and such that the normalization condition $\langle q_k | q_{k'} \rangle + \langle p_k | p_{k'} \rangle = \delta_{kk'}$ is fulfilled: we will label them as A_i for the solution k_i.
It can be checked that $q_k(L-x) = \pm q_k(x)$, $p_k(L-x) = \mp p_k(x)$ and obviously $p_k(0) = -q_k(0)$. This is not surprising, since in our model $\mu(x)$ is symmetric with respect to $x_{\mathrm{M}} = \frac{L}{2}$ and the solutions to the BdG system must be eigenfunctions of the parity centered in x_{M}. In particular, the parity of two successive allowed solutions for q (as well as for p), i.e. with index i differing by a factor 1, is opposite. Thus, ordering the BdG eigenspinors according to their integer indices i we will have an even-odd-even-odd-... effect.
In addition to these oscillatory solutions there is a *zero energy* state formed by the tunneling combination of the zero modes centered on the vortex and the edge. Its form is

$$\begin{cases} q_{\mathrm{Z}}(x) = A_{\mathrm{Z}} \left(e^{-ax} + \sigma e^{a(x-L)}\right) \\ \\ p_{\mathrm{Z}}(x) = A_{\mathrm{Z}} \left(-e^{-ax} + \sigma e^{a(x-L)}\right) \end{cases} \tag{6.87}$$

for $x \in [0, L]$ and the negligible $e^{\frac{\mu_\infty}{\Delta}x}$ outside this interval. We will later specify whether it is even or odd with respect to parity around $x_{\rm M}$, i.e. $\sigma = \pm 1$.
Finally it should be noticed that the (in principle allowed) $k_1 = 0$ solution has to be rejected, being trivially $q_{k=0}(x) = p_{k=0}(x) = 0$, and therefore not normalizable.
In the end we can produce a vector of the solutions $q_i(x)$ where we identify the $q_{i=1}$ state with the zero mode $q_{\rm Z}$ and $q_i = q_{k_i}$, $i \neq 1$.
As far as the prefactors A_i are concerned, they can be calculated imposing $\langle q_i|q_j\rangle + \langle p_i|p_j\rangle = \delta_{ij}$ with the result

$$\begin{cases} A_1 = \left[\frac{2}{a}(1 - e^{-2aL})\right]^{-1/2} \\ \\ A_{i\neq 1} = \left[2L\left(\frac{k_i}{a-\sqrt{a^2+k_i^2}} + \frac{a}{k_i}\right)^2 - \frac{2a}{k_i^2}\right]^{-1/2} \end{cases} \tag{6.88}$$

Clearly, for large system size L, A_i is scaling as $L^{-1/2}$ for $i \neq 1$ and is L-independent for the zero-mode case $i = 1$.

6.5.2 The GS and the formal paired wavefunctions

We now turn to address the nature of the paired wavefunctions in our case of a p-wave superconductor with one vortex and one edge. We can view this case as a two-vortices configuration, the second vortex being at infinity, surrounded by the external edge. This is easier to imagine in a spherical geometry, the two vortices sitting on the two poles. If we imagine to send the sphere radius to infinity and stretch continuously the circular edge surrounding one of the two vortices across the equator we exactly obtain our 2D planar configuration.
In chapter 4 we already discussed the issue of pairing in the uniform and dirty s-wave superconductors, as well as in the uniform ESP p-wave case. Thanks to the arguments by Cooper we know that states of opposite momenta are coupled in the two uniform cases, with opposite spins for s-wave and the same spin for p-wave. Moreover, the Anderson's Theorem clarifies that the Cooper pairs for a very disordered s-wave superconductor are localized eigenstates of the inhomogeneous potential paired with themselves, with opposite spin indices.
There is no analog of such a theorem for the disordered p-wave ESP case, essentially because, due to Fermi statistics, we cannot occupy the same localized eigenstate twice since we do not have two orthogonal spin indices.
Our analysis will allow us to characterize the Cooper pairs for this unsolved ESP problem. Although our step-like model is a particular one we still get the feeling for many generic properties of the paired wavefunctions.

In the fully polarized case we are considering, the general form of a BCS-like GS is

$$|\Psi_{\rm ESP}\rangle = \exp\left[\frac{1}{2}\int \mathbf{dr}\,\mathbf{ds}\; g(\mathbf{r},\mathbf{s})\,\psi^\dagger(\mathbf{r})\psi^\dagger(\mathbf{s})\right]\,|\text{vac}\rangle \tag{6.89}$$

with $g(\mathbf{r},\mathbf{s})$ an antisymmetric function.
In order to characterize the function g entering the true GS we *impose* that (6.89) is

destroyed by *every* BdG quasiparticle annihilator

$$\Gamma_{k_i} = \int \mathrm{d}\mathbf{r} \left[u_{k_i}(\mathbf{r})\psi(\mathbf{r}) + v_{k_i}(\mathbf{r})\psi^\dagger(\mathbf{r}) \right] \tag{6.90}$$

with k_i satisfying the quantization condition (6.85).
Imposing this constraint on the first expansion terms of (6.89) we deduce that $g(\mathbf{r},\mathbf{s})$ has to satisfy the relation

$$\int \mathrm{d}\mathbf{r}\, g(\mathbf{r},\mathbf{s})\, u_{k_i}(\mathbf{r}) = -\, v_{k_i}(\mathbf{s}) \tag{6.91}$$

for every $i \in \mathbb{N}$.
In a seminal paper in 1962 Bloch & Messiah considered the mathematical structure of a generic antisymmetric tensor (like $g(\mathbf{r},\mathbf{s})$) in connection with superconductivity [144]. They showed that it can always be reduced, via a unitary transformation, to a block-diagonal (called "canonical") form, the blocks being 2×2 antisymmetric matrices.
In our case, this implies that $g(\mathbf{r},\mathbf{s})$ can be reduced to the paired form

$$g(\mathbf{r},\mathbf{s}) = \sum_m \alpha_m \left[\phi^*_m(\mathbf{r})\phi^*_{m'}(\mathbf{s}) - \phi^*_m(\mathbf{s})\phi^*_{m'}(\mathbf{r}) \right] \tag{6.92}$$

with ϕ_m orthogonal to $\phi_{m'}$.
Clearly, inserting (6.92) into (6.89) we see that ϕ_m and $\phi_{m'}$ are the Cooper pairs of our problem.
In order to determine them explicitly we apply the conditions (6.91) on the canonical form (6.92). We then obtain two equations for two generic paired wave-functions ϕ_{m_0} and $\phi_{m'_0}$

$$\alpha_{m_0} N_{m_0} \int \mathrm{d}\mathbf{r}\, \phi^*_{m'_0}(\mathbf{r}) u_k(\mathbf{r}) = \int \mathrm{d}\mathbf{r}\, \phi_{m_0}(\mathbf{r}) v_k(\mathbf{r}) \tag{6.93}$$

$$\alpha_{m_0} N_{m'_0} \int \mathrm{d}\mathbf{r}\, \phi^*_{m_0}(\mathbf{r}) u_k(\mathbf{r}) = -\int \mathrm{d}\mathbf{r}\, \phi_{m'_0}(\mathbf{r}) v_k(\mathbf{r}) \tag{6.94}$$

to be satisfied for all the allowed k's, where

$$N_{m_0} = \int \mathrm{d}\mathbf{r}\, \left|\phi_{m_0}(\mathbf{r})\right|^2 \tag{6.95}$$

$$N_{m'_0} = \int \mathrm{d}\mathbf{r}\, \left|\phi_{m'_0}(\mathbf{r})\right|^2 \tag{6.96}$$

are the squared norms of the Cooper-paired states.
Introducing the spinor notation

$$|M_0\rangle = \begin{pmatrix} \phi_{m_0}(\mathbf{r}) \\ \phi^*_{m'_0}(\mathbf{r}) \end{pmatrix} \tag{6.97}$$

$$|k_{\mathrm{P}\alpha}\rangle = \begin{pmatrix} \alpha_{m_0} N_{m'_0} u_k(\mathbf{r}) \\ v_k(\mathbf{r}) \end{pmatrix} \quad , \quad |-k_{\mathrm{P}\alpha}\rangle = \begin{pmatrix} v^*_k(\mathbf{r}) \\ \alpha^*_{m_0} N_{m'_0} u^*_k(\mathbf{r}) \end{pmatrix} \tag{6.98}$$

$$|k_{\mathrm{M}\alpha}\rangle = \begin{pmatrix} \alpha_{m_0} N_{m_0} u_k(\mathbf{r}) \\ -v_k(\mathbf{r}) \end{pmatrix} \quad , \quad |-k_{\mathrm{M}\alpha}\rangle = \begin{pmatrix} -v^*_k(\mathbf{r}) \\ \alpha^*_{m_0} N_{m_0} u^*_k(\mathbf{r}) \end{pmatrix} \tag{6.99}$$

the two (6.93) are compactly rewritten as

$$\langle M_0|k_{\mathrm{P}\alpha}\rangle = 0 \tag{6.100}$$
$$\langle -k_{\mathrm{M}\alpha}|M_0\rangle = 0\ . \tag{6.101}$$

From the properties (4.48) of the BdG solutions u_k and v_k it is easy to verify that $\langle -k'_{\mathrm{P}\alpha}|k_{\mathrm{P}\alpha}\rangle = \langle -k'_{\mathrm{M}\alpha}|k_{\mathrm{M}\alpha}\rangle = 0, \forall k, k'$.
It is then possible to automatically fulfil (6.100) by constructing the vector $|M_0\rangle$ on the basis $|-n_{\mathrm{P}\alpha}\rangle$ as

$$|M_0\rangle = \sum_n \gamma_n\, |-n_{\mathrm{P}\alpha}\rangle\ . \tag{6.102}$$

It remains to impose

$$0 = \langle -k_{\mathrm{M}\alpha}|M_0\rangle = \sum_n \gamma_n \langle -k_{\mathrm{M}\alpha}|-n_{\mathrm{P}\alpha}\rangle\ , \tag{6.103}$$

i.e. the vector $\boldsymbol{\gamma}$ with elements γ_n has to be a nontrivial eigenvector of the matrix $K_{\mathrm{MP}} = \langle -k_{\mathrm{M}\alpha}|-n_{\mathrm{P}\alpha}\rangle$ with eigenvalue 0.
Notice that, by themselves, the BdG functions u and v, do not directly represent the Cooper pairs wavefunctions nor they give much information about the paired states. But they constitute a basis *on which* we can systematically build the Cooper pairs.
It is easy to see that

$$K_{\mathrm{MP}} = \left(\left|\alpha_{m_0}\right|^2 N_{m_0} N^*_{m'_0} + 1\right) \langle u^*_k|u^*_n\rangle - \delta_{kn}\ . \tag{6.104}$$

Therefore we have to carefully consider the symmetric matrix Q with elements (see (6.27))

$$Q_{ij} = \langle u^*_{k_i}|u^*_{k_j}\rangle = \int_0^L \mathrm{d}x\, q_{k_i}(x) q_{k_j}(x)\ , \tag{6.105}$$

where we neglect the small contribution due to regions 1 and 3. Since we ruled out the $k = 0$ state, we will order the matrix elements so that $i = 1$ is associated to the zero mode, $i = 2$ to the first allowed oscillatory mode q_{k_2}, and so on.
Once the eigenvector $\boldsymbol{\gamma}$ is known, via (6.102) we deduce the functional form of the Cooper pair wavefunctions.

6.5.3 The matrix elements for the explicit construction of the paired states

There are essentially two different cathegories of Q_{ij} according to whether $i, j = 1$, or i *and* $j \neq 1$.

1. First Case: $i = 1$

In this case we have

$$Q_{1j}(\sigma) = \frac{1}{2}\,\delta_{j1} + (1-\delta_{j1})\; A_1 A_j \;\left[(1+\sigma(-1)^{j+1})\frac{1}{\sqrt{a^2+k_j^2}} + \right.$$
$$\left. +(\sigma+(-1)^{j+1})\; e^{-aL}\left(\frac{1}{\sqrt{a^2+k_j^2}} - \frac{2a}{a^2+k_j^2}\right)\right]. \qquad (6.106)$$

It can be checked directly that $Q_{1j}(\sigma)$ is zero for ($\sigma = 1, j$ even) or ($\sigma = -1, j$ odd) as it should for symmetry reasons.

2. Second Case: *i and $j \neq 1$*
In this case we have

$$Q_{ij}(i\neq 1, j\neq 1) = \; A_i\, A_j \left[CC_{ij}(x) + \frac{1}{\gamma_{k_i}\gamma_{k_j}}\; SS_{ij}(x) - \frac{1}{\gamma_{k_j}}\; SC_{ji}(x) - \frac{1}{\gamma_{k_i}}\; SC_{ij}(x)\right]_0^L \qquad (6.107)$$

where

$$CC_{ij}(x) = \int \mathrm{d}x\;\cos(k_i x)\cos(k_j x) = \frac{1}{2}\left(\frac{\sin[(k_i+k_j)x]}{k_i+k_j} + \frac{\sin[(k_i-k_j)x]}{k_i-k_j}\right) \qquad (6.108)$$

$$SS_{ij}(x) = \int \mathrm{d}x\;\sin(k_i x)\sin(k_j x) = \frac{1}{2}\left(\frac{\sin[(k_i-k_j)x]}{k_i-k_j} - \frac{\sin[(k_i+k_j)x]}{k_i+k_j}\right) \qquad (6.109)$$

$$SC_{ij}(x) = \int \mathrm{d}x\;\sin(k_i x)\cos(k_j x) = -\frac{1}{2}\left(\frac{\cos[(k_i+k_j)x]}{k_i+k_j} + \frac{\left(1-\delta_{ij}\right)\cdot\cos[(k_i-k_j)x]}{k_i-k_j}\right) \qquad (6.110)$$

and the case $i=j$ has to be intended as $\lim_{k_i\to k_j}$.
Using (6.86) into (6.107) we obtain the explicit form of Q_{ij}

$$Q_{ij}(1\neq i\neq j\neq 1) = \; A_i\, A_j\,[f_{ij} - g_{ij} - g_{ji}] \qquad (6.111)$$

with

$$f_{ij} = \frac{(-1)^{i+j}\,a}{\sqrt{(a^2+k_i^2)(a^2+k_j^2)}} \qquad (6.112)$$

$$g_{ij} = \frac{a-\sqrt{a^2+k_i^2}}{k_i^2-k_j^2}\;\left(1-(-1)^{i+j}\sqrt{\frac{a^2+k_j^2}{a^2+k_i^2}}\right)\;. \qquad (6.113)$$

Since the parity of the solutions $q_{k_i}(x)$ is $(-1)^{i+1}$ we can directly test that $Q_{ij}=0$ when $i+j=$ odd.
In the same way we extract ($i\neq 1$)

$$Q_{ii} = A_i^2\left[L\left(1+\frac{a}{\gamma_{k_i}\cdot k_i}\right) - \frac{1}{\gamma_{k_i}\cdot k_i}\right]\;. \qquad (6.114)$$

Thus we realize that the Q_{ii} are L-independent, $Q_{1i} \sim 1/\sqrt{L}$ and $Q_{ij}(1 \neq i \neq j \neq 1) \sim 1/L$, apart from the selection rules due to parity.

At first, due to their L-dependence and the destructive interference between oscillations with different wave-numbers, it could be tempting to neglect the off-diagonal terms and keep only the Q_{1i} and Q_{ii} elements.
Let us try this approximation out (called "Almost Diagonal Approximation", ADA), which has the nice feature of being analytically exploitable.
Later we will argue about the validity of ADA and work out an exact treatment.

6.5.4 Almost-Diagonal-Approximation (ADA)

As mentioned, within ADA we retain the first line and column of the *symmetric* matrix Q as well as the diagonal, but discard the other matrix elements scaling as $1/L$.
Following (6.104), within ADA we look for zero-eigenvalue eigenvectors $\boldsymbol{\gamma}$ of the matrix

$$\beta\,(K_{\mathrm{MP}})_{ij} = Q_{ij} - \beta\delta_{ij}\ , \tag{6.115}$$

where we define $\beta = \left[|\alpha_{m_0}|^2 N_{m_0} N^*_{m'_0} + 1\right]^{-1}$.
It is easy to determine the elements γ_i of $\boldsymbol{\gamma}$

$$\begin{cases} \gamma_{i\neq 1} = -\frac{Q_{1i}}{Q_{ii}-\beta}\ \gamma_1 \\ \\ (Q_{11}-\beta)\,\gamma_1 = -\sum_{i\neq 1} Q_{1i}\,\gamma_i \end{cases} \tag{6.116}$$

whence the condition for β

$$Q_{11} - \beta = \sum_{i\neq 1} \frac{Q_{1i}^2}{Q_{ii}-\beta}\ . \tag{6.117}$$

It is possible to grasp the essential features of the solutions for β by rewriting

$$\sum_{i\neq 1} \frac{Q_{1i}^2}{Q_{ii}-\beta} \equiv F(\beta) \tag{6.118}$$

and considering that $Q_{11} = 1/2$. Then (6.117) is rewritten as

$$\frac{1}{2} - \beta = F(\beta)\ . \tag{6.119}$$

The function $F(\beta)$ has poles for $\beta = Q_{ii} \in [0, \frac{1}{2}]$ and $\lim_{\beta\to+\infty} F(\beta) = 0^-$. There are essentially two kind of solutions to (6.119) for β.

1. If $\beta \in [0, \frac{1}{2}]$, the β solutions to (6.119) will be very close to some Q_{ii}, meaning that the component γ_i dominates in the vector $\boldsymbol{\gamma}$ (see (6.116)). The outcoming spinor $|M_0\rangle = \sum_n \gamma_n |-n_{\mathrm{P}\alpha}\rangle \sim \gamma_i |-i_{\mathrm{P}\alpha}\rangle$ where the *extended functions* $q_i(x)$ and $p_i(x)$ give the leading contribution.
2. If, on the contrary, we pick the solution $\beta > \frac{1}{2}$ there is no "preferred γ_i" and practically all the $q_i(x)$ and $p_i(x)$ contribute to produce the paired functions ϕ and ϕ', which, due to interference "in the bulk" (Region 2), result *localized* around the vortex *and* the edge.

Once we have obtained the β's, the vector $\boldsymbol{\gamma}$ is completely determined (using the free γ_1 for the normalization), as well as the state ϕ, its norm N_{m_0} and the state $\frac{1}{\alpha^*_{m_0} N^*_{m'_0}} \phi^*_{m_0}$. From the definition (6.95) we can fix also the product $|\alpha_{m_0}|^2 N^*_{m'_0}$. In order for these arguments to be correct we have then to check the selfconsistency between the obtained β and the consequent product $\left|\alpha_{m_0}\right|^2 N^*_{m'_0} N_{m_0}$.

The ADA thus produces two kinds of Cooper pairs

- *one* pair made out of localized states around the vortex *and* the edge, characterized by a value of $\beta > 1/2$
- *many* pairs of extended states, each dominated by one BdG component, occurring for values $\beta < 1/2$

Notice that the localized Cooper pair is *not* due to a dominant occupation of the localized ZM BdG states (the *only* localized BdG states within our step-like model), but rather due to destructive interference of all the extended BdG wavefunctions in Region 2.
The explicit Cooper pairs for ADA will be presented in the next section, where they will be compared to the "exact" solutions deduced from the original matrix Q without any approximation. The price we pay for the exact solution is that we cannot any longer solve the problem analytically. We therefore resort to a numerical diagonalization of the problem, looking for the exact eigenstates of Q. In analogy with ADA, the values of β's ($>$ or $< 1/2$) will be associated to localized or extended paired wavefunctions.

6.5.5 Numerical Analysis: beyond ADA

We now turn to discuss the results obtained for the *exact* matrix Q (let us call it "EQ" case) and compare them with those coming out of the ADA. The problem is now extremely complex, due to the presence of the off-diagonal terms in Q_{ij}. Relations (6.116) are no more valid and we have to turn to a numerical analysis of the true Q. In analogy with the previous ADA analysis we look for zero eigenvalues of (6.115) or, analogously, to the eigenvalues (β) and eigenvectors ($\boldsymbol{\gamma}$) of Q. Again we expect that the largest β will generate localized functions ϕ and ϕ'.
We performed the analysis on three matrices with $i, j \in \{1, 2, ..., N_{\mathrm{Matr}}\}$, and $N_{\mathrm{Matr}} = 300, 600, 1000$.
As already mentioned $k_i \sim i\pi/L$: in order to span both the regimes $k_i \ll a$ and

$k_i \gg a$ we need $\pi/L \ll a$, as well as $N_{\text{Matr}}\pi/L \gg a$. Our choice of parameters was then $L = 1000$ and $a = 0.05$ (corresponding to a characteristic exponential decay length of 20, still much smaller than L) and we tested that the results were non depending on small variations of a.
In what follows we will essentially present the results for $N_{\text{Matr}} = 1000$ but they are equivalent to those obtained for the smaller sizes, apart from small numerical differences that will be pointed out.

The first quantities of interest are the eigenvalues β of Q: it comes out that the general features for the β's are qualitatively and semiquantitatively similar for EQ and ADA, as seen in Fig. (6.5.5) for the case $N_{\text{Matr}} = 1000$. The large majority of β's

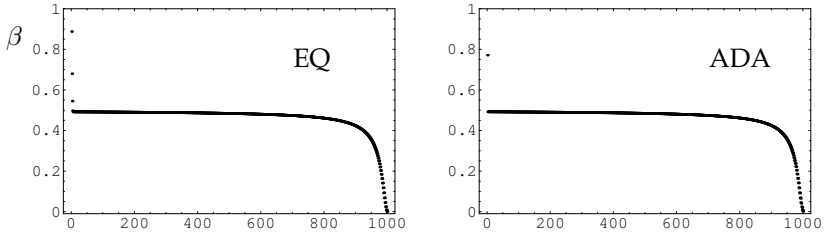

Fig. 6.2: The eigenvalues β of Q (ordered from the largest to the smallest) within EQ and ADA for $\sigma = 1$, $N_{\text{Matr}} = 1000$. Notice the first three anomalous β's in the EQ case, while only one is observed in ADA.

lie within $[0, \frac{1}{2}]$ apart very few with $\beta > 1/2$ (called "anomalous" eigenvalues).
Indeed, we realized that increasing the matrix size produces more anomalous eigenvalues, their number rising very slowly with N_{Matr}. For the 300×300 matrix the anomalous β are two, while they become three in the 1000×1000 case (their first values are 0.887528, 0.679783, 0.544785, 0.497542, 0.492036, 0.49203...). We remind that within ADA, independently on the matrix size, we always got *one* anomalous β only.
We cannot extract a size dependence of the number of anomalous eigenstates, but we tend to believe that they will slowly diverge for the ideal $N_{\text{Matr}} \to \infty$ case.
Furthermore, a closer investigation reveals that, for EQ ($\sigma = -1$), one eigenvalue goes to zero (within the numerical error) for all matrix sizes, a feature not observable with ADA. This effect is not present for $\sigma = 1$. Such an eigenvalue would then force one among ϕ and ϕ' to identically vanish, which is physically meaningless. This tells us that the only physical case for our investigation will be $\sigma = 1$, i.e. an even $q_Z(x)$.
Moreover, the non-critical eigenvalues ($\beta < 1/2$) within EQ always "go in pairs" (each is two-fold degenerate) reminding the $\mathbf{k}$ and $-\mathbf{k}$ states of the uniform system (again, this effect is not observed for ADA).

We can now address the nature of the Cooper pairs directly by producing the wavefunctions $\phi_j(x)$ and $\phi_{j'}(x)$ associated to the various eigenvalues β_j via (6.102). First of all we can concentrate on testing the connection between anomalous β's and

wavefunction localization.
The eigenvector γ associated to a certain β is written on the basis of the BdG-eigenstates. A strongly peaked eigenvector will thus generate a Cooper pair where one particular BdG spinor dominates, leading to essentially oscillatory extended wavefunctions (unless all the weight is given to the ZM). On the contrary, an "extended" γ will weight many BdG spinors almost equally, their interference producing localization in Region 2.
To check our arguments, in Fig. (6.5.5) we present the eigenvectors associated to the first five β's for the 1000×1000 matrix Q in both the EQ and ADA cases. Indeed, we observe that the anomalous β are associated to extended eigenvectors in both the EQ and ADA treatments. Within EQ we also observe an extended eigenvector also for the first non-anomalous β.
A closer analysis reveals that, in both EQ and ADA, every eigenvector has non-vanishing elements only for positions with a given parity (e.g. the first eigenvector, corresponding to the largest β, has non-vanishing elements only in the odd positions). Since the parity of the BdG solution q_i is $(-1)^{i+1}$ (and that of p_i is $(-1)^i$) this means that the Cooper wavefunctions (ϕ_j, $\phi_{j'}$) associated to the j-th eigenvalue have well defined (and opposite) parity and are therefore automatically orthogonal.
The position representation of the Cooper pairs for some anomalous and regular β's is shown in Fig. (6.5.5). The envelope of the Cooper pair wavefunctions reveals their localized/extended nature. In Fig. (6.5.5) short-wavelength oscillations are reproducibly observed for every localized (ϕ_j, $\phi_{j'}$), due to the finite size of the matrix producing a minimum period $\sim L/N_{\text{Matr}}$.
For every Cooper pair wavefunctions we explicitly calculated their norms N_j and $N_{j'}$, obtaining that $N_j + N_{j'} = 1$ ($\forall j$), and we tested the fulfilment of the selfconsistency check for β. Moreover we notice that $N_{j'} = \beta_j$ ($\forall j$) leading to $\alpha_j = 1/\beta_j$.
Introducing the normalized functions $\phi_j^{(\mathrm{N})}(\mathbf{r}) = N_j^{-1/2} \cdot \phi_j(\mathbf{r})$ and $\phi_{j'}^{(\mathrm{N})}(\mathbf{r}) = N_{j'}^{-1/2} \cdot \phi_{j'}(\mathbf{r})$ the (6.92) can be written as

$$g(\mathbf{r},\mathbf{s}) = \sum_m \sqrt{\frac{1-\beta_m}{\beta_m}} \left[\phi_m^{(\mathrm{N})*}(\mathbf{r})\phi_{m'}^{(\mathrm{N})*}(\mathbf{s}) - \phi_m^{(\mathrm{N})*}(\mathbf{s})\phi_{m'}^{(\mathrm{N})*}(\mathbf{r})\right] \tag{6.120}$$

where we have now access to any information concerning the paired states as well as their occupation.
In fact, from (6.120), in analogy with the uniform BCS state, we know that $[(1-\beta_m)/\beta_m]^{1/2}$ represent the ratio between the amplitudes of occupation and emptyness of the pair with index m. In the standard BCS case the pairs of states with small momenta are the most occupied. In our case (6.120) their analog are the pairs with small β.
As in the uniform case, we also checked that $\langle\phi_j^{(\mathrm{N})}|\phi_l^{(\mathrm{N})}\rangle = \delta_{jl}$ and $\langle\phi_j^{(\mathrm{N})}|\phi_{l'}^{(\mathrm{N})}\rangle = 0$, $\forall j, l$.

The step-like model for μ we used up to now allows direct exact investigations of the BdG solutions, thereby producing a basis on which to construct the paired

wavefunctions. Despite its simplicity, the model highlights many interesting features of the Cooper pairs for the inhomogeneous p-wave state.
We have found that the presence of vortices tends to localize an ensemble of Cooper pairs around the vortex cores, their number probably diverging in the exact thermodinamic limit. The localized pairs are described by wavefunctions which are shared between different vortices, reminding the entangled states of successive generations we discussed in the previous sections.
The large majority of Cooper pairs are extended and typically dominated by one BdG pair each.
The choice of the BdG solutions as a basis on which to expand the paired states is of course arbitrary. At present we are investigating a similar construction using the basis of the $w_k^{(j)}$ functions which should be naturally suitable to describe the localized Cooper pairs. Using the exact BdG spinors for the step-like model we can in fact produce the w's of successive generations. The final aim of the investigation will be a full comparison between the GS in the two representations, with the purpose of extracting the universal properties involved in the issue of pairing for inhomogeneous systems.

6.6 Summary of the results

In this chapter we investigated the properties of paired states of fully spin-polarized CF close to half LL filling.
Exactly *at* $\nu = 1/2$ there is no residual flux quantum and the condensation takes place as in uniform ESP p-wave superconductors.
Interestingly, different topologically distinct phases of the GS show up when significant density modulations are imposed on the 2DES, like for strong confinement potentials or vortices depressing the superconducting correlations. In particular, the Pfaffian state, proposed as the GS for the $5/2$ FQHE has been identified with the weakly-paired phase, qualitatively resembling the usual BCS state.
Whenever a finite (but small) residual magnetic flux is present, it enters the sample in form of vortex-like quasiparticle excitations for the Pfaffian GS. Due to the underlying p-wave structure of the many-body wavefunction, these vortices carry a zero-energy BdG excitation level each, associated to a Majorana (real) bogolonic field.
We then studied the structure of the GS occurring in the many-vortices configurations from different perspectives. The role of the localized zero-modes on the vortices is two-fold. On one side, due to their zero energy, they induce a degeneracy of the GS. On the other side, their "Majorana" nature forces us to consider non-local combination of localized states to build up true fermionic creation/annihilation operators. The result of the two combined effects is a non-trivial GS-subspace degeneracy of 2^n for the $2n$ vortices case.
The different degenerate GS have been identified and their structure highlighted. We were able to produce a basis of localized states on each vortex built up systematically, generation by generation, by the formal knowledge of the zero-mode real operators. The non-locality of the true fermionic operators implies entanglement

between states living on different vortices. Moreover, entanglement takes place between localized states on the same vortex belonging to different generations.
As a byproduct of our analysis we could investigate the non-Abelian statistics of vortex-like quasiparticles. The crucial ingredients highlighted by our treatment are the GS subspace degeneracy and the entangled nature of the zero-mode sector of each degenerate GS.
Subsequently, we addressed the issue of Cooper pairing in the many-vortices case. By solving explicitly the BdG problem in one particularly simple case we succeeded in identifying the Cooper pairs of our problem. The insertion of vortices in the p-wave state has the effect of localizing a family of paired wavefunctions around the vortices themselves. Localization takes place non-trivially due to a destructive interference of many (ideally infinite) extended BdG solutions.

Many issues are still to be addressed in this fascinating problem. On a fundamental level, in the future we would like to obtain a full mapping between the GS in the different representations. Moreover, having the explicit form of the paired GS, we can address many properties of the system by direct calculation.
In parallel, many experimental issues concerning the $5/2$ state are still open. The spin polarization of the last half-filled LL is still to be directly measured, as well as the fractional charge of the quasiparticle-excitations. These experiments are particularly difficult to realize due the small excitation gap of the $5/2$ FQH state. Extremely low temperatures and high mobilities are requested in order to observe the state at all.
Finally, there is still no experiment proposed to investigate the non-Abelian statistics of the vortices. Indeed, still the fractional Abelian statistics of Laughlin quasiparticles has to be addressed in experiments. It is likely that the quasiparticle statistics at $5/2$ will be an even tougher challenge for the years to come.

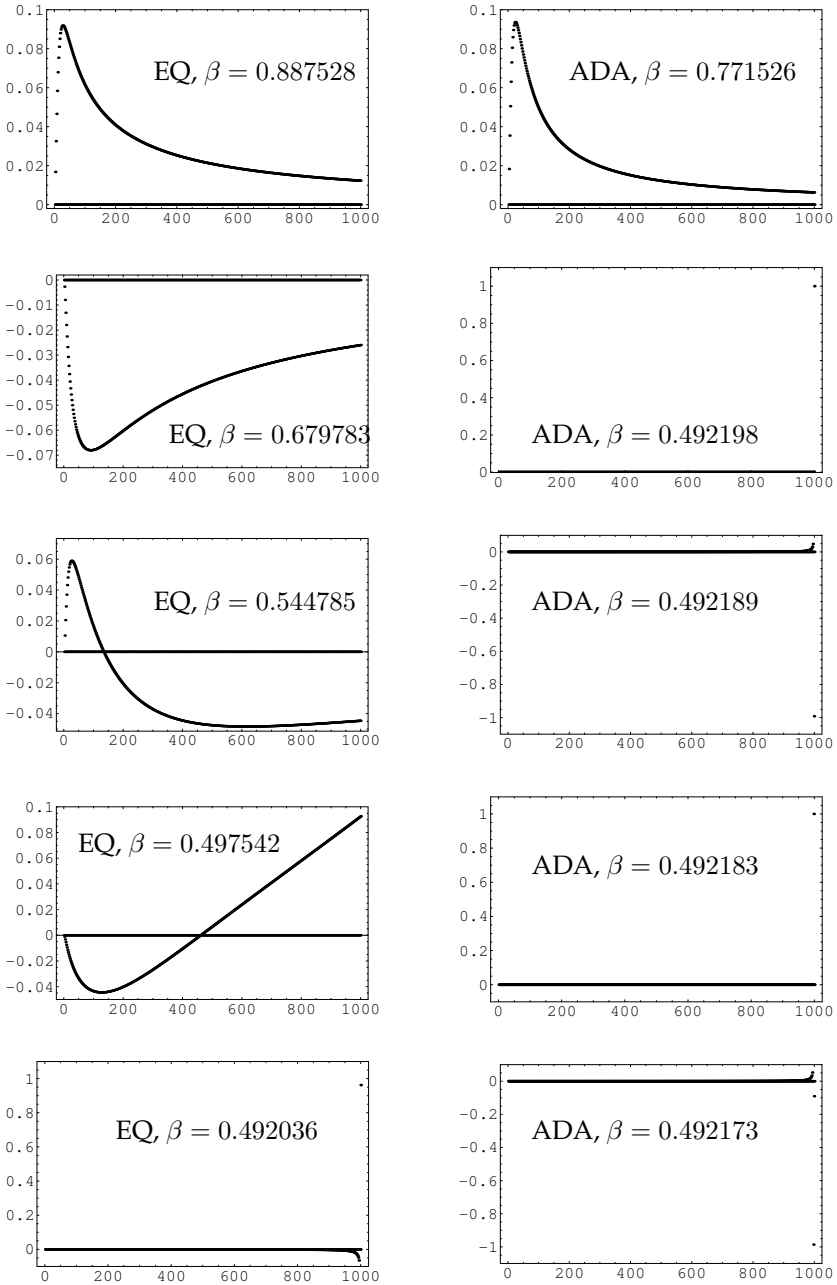

Fig. 6.3: The first five eigenvectors of Q in both EQ and ADA cases. Their corresponding eigenvalues β are indicated in the figures. Notice how EQ and ADA agree qualitatively only for the very first localized eigenstate. The remaining "anomalous" β (as well as the "regular" $\beta = 0.497542$) for EQ have extended eigenvectors giving rise to localized Cooper pairs wavefunctions. The transition between extended and localized eigenvectors is dramatic already for the close EQ values $\beta = 0.497542,\ 0.492036$.

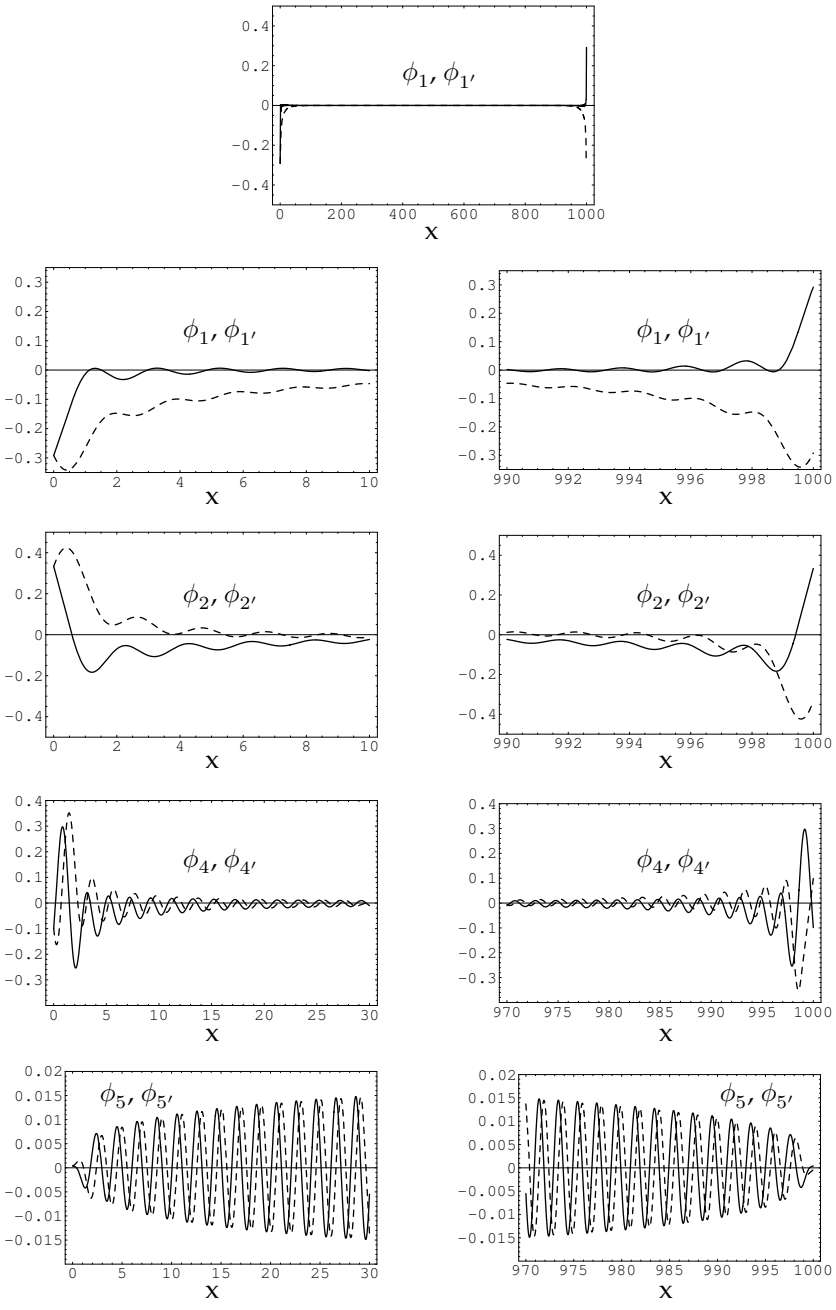

Fig. 6.4: Some localized and extended Cooper pairs in the position space. The real part of both ϕ_j (full lines) and $\phi_{j'}$ (dashed lines) are plotted as a function of the radius x for different eigenvalues β_j in the EQ case. The eigenvalues are $\beta_1 = 0.887528$, $\beta_2 = 0.679783$, $\beta_4 = 0.497542$, $\beta_5 = 0.492036$. Notice the clear localization in the whole range $[0, L]$ as well as the parity effects visible in the symmetrical regions close to the edges of the radius interval. Moreover, notice the drastic localization-delocalization crossover between $j = 4$ and $j = 5$.

7. CONCLUSIONS

In this thesis we analyzed some important characteristics of Composite Fermions in the Fractional Quantum Hall Effect, especially related to their spin and pairing instabilities.
The main outcome is their extreme versatility in addressing a vast amount of experimental results. Already at the independent (non-interacting) quasiparticle level they grasp many essential features due to the *collective* electronic states responsible for the FQHE.
The inclusion of the spin degree of freedom, i.e. of the Zeeman energy scale, produces a whole variety of spin-related quantum phase transitions already at the mean field level. This independent quasiparticle model can be used to interpret, and even predict, quantitative measurable effects in extremely good agreement with the experimental data available up to now.
Having shown the model to be a valuable starting point, we considered correlation effects due to the residual CF interactions. In the normal state, they produce marginal-Fermi-liquid-like corrections to the quasiparticle effective parameters. More interestingly, we considered the possibility of spontaneously broken symmetries in the FQH systems, interpreted as quasiparticle pairing instabilities of the superconductive type.
The CF s-wave pairing case has been considered close to the degeneracy of two Landau Levels with opposite spins. The consequent rigidity of the Ground State can be used to interpret some recent, and still unsolved, experimentally observed partly-polarized states. Our self-consistent mean field treatment, although just a first-step analysis of the problem, highlights the possible dramatic effects that CF coupling can induce in a single 2D electronic system. Higher order corrections and a close analysis of the role of disorder and quantum fluctuations on our state will be the subject of further investigations I plan to address in the near future.
Furthermore, we considered another symmetry-broken Ground State showing up at filling factor $5/2$. In the CF language it can be addressed as a p-wave quasiparticle paired state, whose superconductive gap acquaints for the experimentally observed incompressibility. We investigated its vortex-like quasiparticle excitations from different perspectives. Their quantum non-Abelian statistics has been addressed by the explicit identification of the degenerate Ground States in the many vortices configuration. The entangled structure of these many-body states has been derived, clarifying the origin of the non-Abelian statistics from a physical point of view. Furthermore, the open issue of Cooper-pairing for inhomogeneous p-wave superconductors has been addressed for an exactly solvable case, highlighting the tendency of vortices to localize some of the Cooper-pair wavefunctions.

I believe that the arguments treated in this thesis confirm once more how fascinating the field of Quantum Hall research can be. In order to address many of the issues in the document we had to combine physical and technical knowledge belonging to otherwise different, and usually far apart, contexts. In my thesis, the special connection was between FQHE and superconductivity, in both the wavefunction as well as the field theoretical language. Of course, a thorough analysis should consider other symmetry-breaking mechanisms, along the line of excitonic condensation or magnetic phase transitions. These will be among the plans of further research I would like to address in my post-doctoral academic period.

8. APPENDIX A: EXPLICIT EVALUATION OF $\Pi^0_{\mu\nu}(\mathbf{Q}, \Omega_M)$

For simplicity of notation, in this appendix the effective mass m^* will be denoted as the free one, m.
We remind the definition

$$\Pi^0_{\mu\nu}(\mathbf{q}, \Omega_n) = \beta^{-1} \sum_s \sum_m w^s_{\mu\nu}(\mathbf{q}, \mathbf{q}) \int \frac{\mathrm{d}\mathbf{k}}{(2\pi)^2} \, \mathcal{G}^0_s(\mathbf{k}, \omega_m) \, e^{i\omega_m 0^+} +$$
$$+\beta^{-1} \sum_s \sum_m \int \frac{\mathrm{d}\mathbf{k}}{(2\pi)^2} \, v^s_\mu(\mathbf{k}, \mathbf{q}) \mathcal{G}^0_s(\mathbf{k} - \mathbf{q}, \omega_m - \Omega_n) \mathcal{G}^0_s(\mathbf{k}, \omega_m) v^s_\nu(\mathbf{k}, \mathbf{q}) \; . \tag{8.1}$$

with

$$v^s_\mu(\mathbf{k}, \mathbf{q}) = \begin{cases} e, & \text{for } \mu = 0 \\ \frac{e}{m^*} \, \hat{\mathbf{z}} \cdot \frac{\mathbf{k} \times \mathbf{q}}{q}, & \text{for } \mu = 1 \end{cases}$$
$$w^s_{\mu\nu}(\mathbf{q}, \mathbf{q}') = \frac{e^2}{m} \, \frac{\mathbf{q} \cdot \mathbf{q}'}{q q'} \, \delta_{\mu 1} \delta_{\nu 1} \; . \tag{8.2}$$

whence $w^s_{\mu\nu}(\mathbf{q}, \mathbf{q}) = e^2/m \, \delta_{\mu 1} \delta_{\nu 1}$.
Due to symmetry reasons we have

$$\Pi^0_{\mu\nu}(\mathbf{q}, \Omega_m) = \Pi^0_{\mu\mu}(\mathbf{q}, \Omega_n) \; \delta_{\mu\nu} \tag{8.3}$$

and from the definition of the free electronic Green's function we get

$$\mathcal{G}^0_s(\mathbf{k} - \mathbf{q}, \omega_m - \Omega_n) \mathcal{G}^0_s(\mathbf{k}, \omega_m) = \frac{1}{i\omega_n - i\Omega_n - \varepsilon_{\boldsymbol{k}-\mathbf{q}}} \cdot \frac{1}{i\omega_m - \varepsilon_{\boldsymbol{k}}}$$
$$= \frac{1}{i\Omega_n + \varepsilon_{\boldsymbol{k}-\mathbf{q}} - \varepsilon_{\boldsymbol{k}}} \left(\frac{1}{i\omega_m - i\Omega_n - \varepsilon_{\boldsymbol{k}-\mathbf{q}}} - \frac{1}{i\omega_m - \varepsilon_{\boldsymbol{k}}} \right) .$$

Using the Poisson sum method we can then evaluate

$$\beta^{-1} \sum_m \left(\frac{1}{i\omega_m - i\Omega_n - \varepsilon_{\boldsymbol{k}-\mathbf{q}}} - \frac{1}{i\omega_m - \varepsilon_{\boldsymbol{k}}} \right) \tag{8.4a}$$
$$= - \frac{1}{2\pi i} \int_C \mathrm{d}\xi \; f(\xi) \left(\frac{1}{\xi - i\Omega_n - \varepsilon_{\boldsymbol{k}-\mathbf{q}}} - \frac{1}{\xi - \varepsilon_{\boldsymbol{k}}} \right) \tag{8.4b}$$

where $f(\xi)$ is the Fermi function, diverging for $\xi = i\omega_m$ with residue $-\beta^{-1}$, and the integral is performed on the contour C enclosing the points $\xi = i\omega_m$ in the

counterclockwise sense.
Notice that the integrand in (8.4b) is singular only in $\xi=\varepsilon_{\boldsymbol{k}}$ and $\xi=\varepsilon_{\boldsymbol{k}-\mathbf{q}}+i\Omega_n$ and the integral along the circle at infinity vanishes. The only surviving contributions come from the residues in the two singularities. Using $f(x\pm i\Omega_n)=f(x)$ we get

$$-\frac{1}{2\pi i}\int_C \mathrm{d}\xi\; f(\xi)\left(\frac{1}{\xi-i\Omega_n-\varepsilon_{\boldsymbol{k}-\mathbf{q}}}-\frac{1}{\xi-\varepsilon_{\boldsymbol{k}}}\right)=f(\varepsilon_{\boldsymbol{k}-\mathbf{q}})-f(\varepsilon_{\boldsymbol{k}})$$

whence

$$\beta^{-1}\sum_s\sum_m \mathcal{G}^0_s(\mathbf{k}-\mathbf{q},\omega_m-\Omega_n)\mathcal{G}^0_s(\mathbf{k},\omega_m)=-\frac{f(\varepsilon_{\boldsymbol{k}})-f(\varepsilon_{\boldsymbol{k}-\mathbf{q}})}{i\Omega_n-(\varepsilon_{\boldsymbol{k}}-\varepsilon_{\boldsymbol{k}-\mathbf{q}})} \tag{8.5}$$

The first term in (8.1) is then easily evaluated to be

$$\begin{aligned}
&\beta^{-1}\sum_s\sum_m w^s_{\mu\nu}(\mathbf{q},\mathbf{q})\int\frac{\mathrm{d}\mathbf{k}}{(2\pi)^2}\,\mathcal{G}^0_s(\mathbf{k},\omega_m)\,e^{i\omega_m 0^+}=\\
&=\frac{e^2}{m}\,\delta_{\mu 1}\delta_{\nu 1}\sum_s\int\frac{\mathrm{d}\mathbf{k}}{(2\pi)^2}\int_C\frac{\mathrm{d}\xi}{2\pi i}\;f(\xi)\,\frac{1}{\xi-i\Omega_n-\varepsilon_{\mathbf{k}}}=\\
&=\frac{2e^2}{m}\,\delta_{\mu 1}\delta_{\nu 1}\int_0^{k_{\mathrm{F}}}\frac{k\,\mathrm{d}k}{2\pi}\;f(\varepsilon_{\mathbf{k}})=\frac{2e^2}{2\pi}\,\delta_{\mu 1}\delta_{\nu 1}\int_0^{E_{\mathrm{F}}}\mathrm{d}\varepsilon\;f(\varepsilon)=\\
&=\frac{2e^2\rho}{m}\,\delta_{\mu 1}\delta_{\nu 1}
\end{aligned} \tag{8.6}$$

where we used the relation $k_{\mathrm{F}}^2=4\pi\rho$. Finally, introducing $\omega_{\mathbf{k}\,\mathbf{q}}=\varepsilon_{\boldsymbol{k}}-\varepsilon_{\boldsymbol{k}-\mathbf{q}'}$ we obtain

$$\Pi^0_{00}(\mathbf{q},\Omega_n)=-\,2\,e^2\sum_{\mathbf{k}}\frac{f(\varepsilon_{\boldsymbol{k}})-f(\varepsilon_{\boldsymbol{k}-\mathbf{q}})}{i\Omega_n-\omega_{\mathbf{k}\,\mathbf{q}}} \tag{8.7}$$

$$\Pi^0_{11}(\mathbf{q},\Omega_n)=\frac{2e^2\rho}{m}-\frac{2\,e^2}{m^2}\sum_{\mathbf{k}}\frac{|\mathbf{k}\times\mathbf{q}|^2}{q^2}\cdot\frac{f(\varepsilon_{\boldsymbol{k}})-f(\varepsilon_{\boldsymbol{k}-\mathbf{q}})}{i\Omega_n-\omega_{\mathbf{k}\,\mathbf{q}}} \tag{8.8}$$

Let us then evaluate the retarded part $\Pi^{0\mathrm{r}}_{\mu\nu}(\mathbf{q},\omega)=\Pi^0_{\mu\nu}(\mathbf{q},-i\omega+\delta)$ ($\delta=0^+$), transforming the second term in (8.7) and (8.8) via the substitution $\mathbf{k}\to-\mathbf{k}'+\mathbf{q}$

$$\varepsilon_{\boldsymbol{k}}\longrightarrow\varepsilon_{-\mathbf{k}'+\mathbf{q}}\equiv\varepsilon_{\boldsymbol{k}'-\mathbf{q}}\quad;\quad\varepsilon_{\boldsymbol{k}-\mathbf{q}}\longrightarrow\varepsilon_{-\mathbf{k}'}\equiv\varepsilon_{\mathbf{k}'}\quad;\quad\omega_{\mathbf{k}\,\mathbf{q}}\longrightarrow-\omega_{\mathbf{k}'\,\mathbf{q}}$$

We get

$$\Pi^{0\mathrm{r}}_{00}(\mathbf{q},\omega)=-\,2e^2\sum_{\mathbf{k}}f(\varepsilon_{\boldsymbol{k}})\Big(\frac{1}{\omega-\omega_{\mathbf{k}\,\mathbf{q}}+i\,\delta}-\frac{1}{\omega+\omega_{\mathbf{k}\,\mathbf{q}}+i\,\delta}\Big) \tag{8.9}$$

$$\Pi^{0\mathrm{r}}_{11}(\mathbf{q},\Omega_n)=\frac{2e^2\rho}{m}-2\frac{e^2}{m^{*2}}\sum_{\mathbf{k}}\frac{|\mathbf{k}\times\mathbf{q}|^2}{q^2}\;f(\varepsilon_{\boldsymbol{k}})\Big(\frac{1}{\omega-\omega_{\mathbf{k}\,\mathbf{q}}+i\,\delta}-\frac{1}{\omega+\omega_{\mathbf{k}\,\mathbf{q}}+i\,\delta}\Big) \tag{8.10}$$

8.1 $\Pi^{0\mathrm{r}}_{00}(\boldsymbol{q},\omega)$ at $T=0$

At zero temperature the Fermi distribution becomes a step-function, whence the integral over the momenta is limited from above by k_{F}. Let us also introduce adimensional variables

$$\boxed{|\mathbf{k}| = \xi\, k_{\mathrm{F}} \quad ; \quad |\mathbf{q}| = \bar{q}\, 2k_{\mathrm{F}} \quad ; \quad \omega = \bar{\omega}\, \frac{2k_{\mathrm{F}}^2}{m}}$$

In 2D we have

$$\frac{1}{(2\pi)^2}\int \mathrm{d}\mathbf{k}\; \Theta(\varepsilon_{\boldsymbol{k}})\; \ldots = \frac{k_{\mathrm{F}}^2}{(2\pi)^2}\int_0^1 \mathrm{d}\xi\, \xi \int_0^{2\pi} \mathrm{d}\theta\; \ldots$$

which, together with $\omega_{\mathbf{k}\,\mathbf{q}} = \dfrac{1}{2m}\,(2\mathbf{k}\cdot\mathbf{q} - \mathbf{q}^2) = \dfrac{2k_{\mathrm{F}}^2}{m}\,\bar{q}\,(\xi\cos\theta - \bar{q})$, produces

$$\Pi^{0\mathrm{r}}_{00}(\mathbf{q},\omega) = -\frac{e^2}{4\pi^2}\,\frac{m}{\bar{q}}\int_0^1 \mathrm{d}\xi\, \xi \int_0^{2\pi} \mathrm{d}\theta\, \left(\frac{1}{\nu_+ - \xi\cos\theta + i\,\delta} - \frac{1}{\nu_- + \xi\cos\theta + i\,\delta}\right) \tag{8.11}$$

where we defined $\nu_\pm = \dfrac{\bar{\omega}}{\bar{q}} \pm \bar{q}$.

In agreement with the fluctuation-dissipation theorem and respecting causality we notice that

$$\Re\mathrm{e}\,\Pi^{0\mathrm{r}}_{00}(\mathbf{q},\omega) = \Re\mathrm{e}\,\Pi^{0\mathrm{r}}_{00}(\mathbf{q},-\omega) \quad ; \quad \Im\mathrm{m}\,\Pi^{0\mathrm{r}}_{00}(\mathbf{q},\omega) = -\,\Im\mathrm{m}\,\Pi^{0\mathrm{r}}_{00}(\mathbf{q},-\omega)$$

Separating real and imaginary parts we have

$$\Im\mathrm{m}\,\Pi^{0\mathrm{r}}_{00}(\mathbf{q},\omega) = \frac{e^2}{4\pi}\,\frac{m}{\bar{q}}\int_0^1 \mathrm{d}\xi\, \xi \int_0^{2\pi} \mathrm{d}\theta\, \Big[\delta\big(\nu_+ - \xi\cos\theta\big) - \delta\big(\nu_- + \xi\,\cos\theta\big)\Big] \tag{8.12a}$$

$$\Re\mathrm{e}\,\Pi^{0\mathrm{r}}_{00}(\mathbf{q},\omega) = -\,\frac{e^2}{4\pi^2}\,\frac{m}{\bar{q}}\,\mathsf{P}\int_0^1 \mathrm{d}\xi\, \xi \int_0^{2\pi} \mathrm{d}\theta\, \left(\frac{1}{\nu_+ - \xi\cos\theta} - \frac{1}{\nu_- + \xi\cos\theta}\right) \tag{8.12b}$$

where P indicates the principal-value integration.

1.A $\Im\mathrm{m}\,\Pi^{0\mathrm{r}}_{00}(\mathbf{q},\omega)$

For the imaginary part (8.12a), using

$$\int \mathrm{d}x\; \delta\big(f(x)\big) = \sum_i \frac{1}{\big|f'(x_i)\big|} \tag{8.13}$$

where $f(x_i) = 0$, we get

$$\begin{aligned}\int_0^1 \mathrm{d}\xi\, \xi \int_0^{2\pi} \mathrm{d}\theta\; \delta\big(\pm\nu_\pm - \xi\cos\theta\big) &= \int_0^1 \mathrm{d}\xi\; \frac{2\xi}{\sqrt{\xi^2 - \nu_\pm^2}}\; \Theta\big(\xi^2 - \nu_\pm^2\big) \\ &= 2\,\Theta\big(1-\nu_\pm^2\big)\,\sqrt{\big(1-\nu_\pm^2\big)}\end{aligned}$$

Using this result in (8.12a) we finally obtain

$$\Im\mathrm{m}\,\Pi^{0\mathrm{r}}_{00}(\mathbf{q},\omega)=e^2\frac{m}{2\pi}\frac{1}{\bar{q}}\Big[\Theta\big(1-\nu_+^2\big)\sqrt{\big(1-\nu_+^2\big)}-\Theta\big(1-\nu_-^2\big)\sqrt{\big(1-\nu_-^2\big)}\Big] \tag{8.14}$$

1. In the limit $\bar{\omega},\ \bar{q}\gg 1$ we have $\nu_\pm\gg 1$ implying $\Im\mathrm{m}\,\Pi^{0\mathrm{r}}_{00}(\mathbf{q},\omega)=0$.
2. In the limit $\bar{q}\ll 1$ *and* $\bar{\omega}\ll\bar{q}$, $|\nu_\pm|\ll 1$ producing

$$\Im\mathrm{m}\,\Pi^{0\mathrm{r}}_{00}(\mathbf{q},\omega)\approx e^2\frac{m}{2\pi}\frac{1}{2\bar{q}}\left[\nu_-^2-\nu_+^2\right]\approx -e^2\frac{m}{\pi}\frac{\bar{\omega}}{\bar{q}}$$

$$\boxed{\Im\mathrm{m}\,\Pi^{0\mathrm{r}}_{00}(\mathbf{q},\omega)\approx -e^2\frac{m}{\pi}\frac{\omega}{v_{\mathrm{F}}\,q}} \tag{8.15}$$

Notice that m/π is the density of states for free spinful fermions in 2D. In 3D the result is analogous, replacing m/π by the 3D DOS at the Fermi level.

1.B $\Re\mathrm{e}\,\Pi^{0\mathrm{r}}_{00}(\mathbf{q},\omega)$

Let us rewrite (8.12b) as

$$\Re\mathrm{e}\,\Pi^{0\mathrm{r}}_{00}(\mathbf{q},\omega)=-e^2\frac{m}{2\pi}\frac{1}{\bar{q}}\left[\mathcal{I}_0\big(\nu_+\big)+\mathcal{I}_0\big(-\nu_-\big)\right] \tag{8.16}$$

where $\mathcal{I}_0(\nu)$ is defined as

$$\mathcal{I}_0(\nu)=\frac{\mathsf{P}}{2\pi}\int_0^1\mathrm{d}\xi\,\xi\int_0^{2\pi}\mathrm{d}\theta\,\frac{1}{\nu-\xi\cos\theta}$$

It can be easily shown that

$$\mathcal{I}_0(\nu)=\int_0^1\mathrm{d}\xi\,\frac{\xi}{\sqrt{\nu^2-\xi^2}}\,\Theta\big(\nu^2-\xi^2\big)\,\mathrm{sign}\,[\nu-\xi]$$

producing

$$\begin{aligned}\mathcal{I}_0(\nu)&=\Theta\big(\nu^2-1\big)\,\mathrm{sign}\,[\nu]\int_0^1\mathrm{d}\xi\,\frac{\xi}{\sqrt{\nu^2-\xi^2}}+\Theta\big(1-\nu^2\big)\,\mathrm{sign}\,[\nu]\int_0^{|\nu|}\mathrm{d}\xi\,\frac{\xi}{\sqrt{\nu^2-\xi^2}}\\&=\nu-\Theta\big(\nu^2-1\big)\,\mathrm{sign}\,[\nu]\,\sqrt{\nu^2-1}\end{aligned} \tag{8.17}$$

Finally, replacing (8.17) into (8.16) we get

$$\Re\mathrm{e}\,\Pi^{0\mathrm{r}}_{00}(\mathbf{q},\omega)=-e^2\frac{m}{\pi}\Big[1-\frac{1}{2\bar{q}}\sum_{\pm}\pm\big(\nu_\pm^2-1\big)^{1/2}\,\Theta\big(\nu_\pm^2-1\big)\,\mathrm{sign}\,\big[\nu_\pm\big]\Big] \tag{8.18}$$

1. Static limit ($\omega = 0$). Being $\Im\mathrm{m}\,\Pi^{0\mathrm{r}}_{00}(\mathbf{q},0) = 0$

$$\Pi^{0\mathrm{r}}_{00}(\mathbf{q},0) = -e^2\frac{m}{\pi}\Big[1 - \frac{\sqrt{\bar{q}^2-1}}{\bar{q}}\,\Theta\big(\bar{q}^2-1\big)\Big] \tag{8.19}$$

   (a) For $q \leqslant 2k_{\mathrm{F}}$,

$$\Pi^{0\mathrm{r}}_{00}(\mathbf{q},0) = -e^2\,\frac{m}{\pi}$$

   independent on q.

   (b) For $q \gtrsim 2k_{\mathrm{F}}$,

$$\Pi^{0\mathrm{r}}_{00}(\mathbf{q},0) \approx -e^2\,\frac{m}{\pi}\left[1 - \sqrt{\frac{q-2k_{\mathrm{F}}}{k_{\mathrm{F}}}}\right]$$

   (c) For $q \gg 2k_{\mathrm{F}}$,

$$\Pi^{0\mathrm{r}}_{00}(\mathbf{q},0) \approx -2\,e^2\,\frac{m}{\pi}\,\frac{k_{\mathrm{F}}^2}{q^2}$$

2. $\bar{\omega} \ll \bar{q}$ and $\bar{q} \ll 1$ ($\omega \ll v_{\mathrm{F}}\,q$ and $q \ll 2k_{\mathrm{F}}\,q$)

$$\boxed{\Re\mathrm{e}\,\Pi^{0\mathrm{r}}_{00}(\mathbf{q},\omega) \approx -e^2\frac{m}{\pi}} \tag{8.20}$$

   that, together with (8.15) implies the small frequency-small momenta limit

$$\boxed{\Pi^{0\mathrm{r}}_{00}(\mathbf{q},\omega) \approx -e^2\frac{m}{\pi}\Big(1 + i\,\frac{\omega}{v_{\mathrm{F}}\,q}\Big)} \tag{8.21}$$

3. $\bar{q} \ll 1$ and $\bar{\omega} \gg \bar{q}$. In this limit $\Im\mathrm{m}\,\Pi^{0\mathrm{r}}_{00}(\mathbf{q},0) = 0$, and

$$\Pi^{0\mathrm{r}}_{00}(\mathbf{q},\omega) \approx e^2\frac{m}{\pi}\,\frac{\bar{q}^2}{2\bar{\omega}^2} = e^2\frac{m\,v_{\mathrm{F}}^2}{2\pi}\,\frac{q^2}{\omega^2}$$

$$\boxed{\Pi^{0\mathrm{r}}_{00}(\mathbf{q},\omega) \approx e^2\,\frac{2\rho}{m}\,\frac{q^2}{\omega^2}} \tag{8.22}$$

   directly related with the Kohn's Theorem.

8.2 $\Pi^{0\mathrm{r}}_{11}(\boldsymbol{q},\omega)$ at $T = 0$

Analogously to the previous section, for the real and imaginary parts of $\Pi^{0\mathrm{r}}_{11}$ we get

$$\Im\mathrm{m}\,\Pi^{0\mathrm{r}}_{11}(\mathbf{q},\omega) = \frac{e^2\rho}{m}\,\frac{1}{\bar{q}}\int_0^1 \mathrm{d}\xi \int_0^{2\pi}\mathrm{d}\theta\;\xi^3\,\sin^2\theta \Big[\delta\big(\nu_+ - \xi\cos\theta\big) - \delta\big(\nu_- + \xi\,\cos\theta\big)\Big] \tag{8.23a}$$

$$\Re\mathrm{e}\,\Pi^{0\mathrm{r}}_{11}(\mathbf{q},\omega) = \frac{2e^2\rho}{m} - \frac{e^2\rho}{m}\,\frac{1}{\pi\bar{q}}\,\mathsf{P}\int_0^1 \mathrm{d}\xi \int_0^{2\pi}\mathrm{d}\theta\,\Big(\frac{\xi^3\,\sin^2\theta}{\nu_+ - \xi\cos\theta} - \frac{\xi^3\,\sin^2\theta}{\nu_- + \xi\cos\theta}\Big) \tag{8.23b}$$

having used $\big|(\mathbf{k}\times\hat{\mathbf{q}})\big|^2 = k_{\rm F}^2\,\xi^2\sin^2\theta$.

2.A $\Im\mathrm{m}\,\Pi^{0\mathrm{r}}_{11}(\mathbf{q},\omega)$

Using (8.13) we obtain

$$\int_0^1\mathrm{d}\xi\int_0^{2\pi}\mathrm{d}\theta\;\xi^3\;\sin^2\theta\,\delta\big(\pm\nu_\pm-\xi\cos\theta\big)=\int_0^1\mathrm{d}\xi\;2\xi\,\sqrt{\xi^2-\nu_\pm^2}\;\Theta\big(\xi^2-\nu_\pm^2\big)$$
$$=\frac{2}{3}\,\Theta\big(1-\nu_\pm^2\big)\,\big(1-\nu_\pm^2\big)^{\frac{3}{2}}\;.$$

Using this result into (8.23a) we get

$$\Im\mathrm{m}\,\Pi^{0\mathrm{r}}_{11}(\mathbf{q},\omega)=\frac{2e^2\rho}{m}\frac{1}{3\bar{q}}\big[\Theta\big(1-\nu_+^2\big)\,\big(1-\nu_+^2\big)^{\frac{3}{2}}-\Theta\big(1-\nu_-^2\big)\,\big(1-\nu_-^2\big)^{\frac{3}{2}}\big]\tag{8.24}$$

In the limit $\bar{q}\ll 1$ *and* $\bar{\omega}\ll\bar{q}$ ($q\ll 2k_{\rm F}$ and $\omega\ll v_{\rm F}\,q$), $|\nu_\pm|\ll 1$ and the result is

$$\Im\mathrm{m}\,\Pi^{0\mathrm{r}}_{11}(\mathbf{q},\omega)\approx\frac{e^2\rho}{m}\,\frac{1}{\bar{q}}\,\big[\nu_-^2-\nu_+^2\big]\approx-\frac{2e^2\rho}{m}\,\frac{\bar{\omega}}{\bar{q}}$$

$$\boxed{\Im\mathrm{m}\,\Pi^{0\mathrm{r}}_{11}(\mathbf{q},\omega)\approx-\frac{4e^2\rho}{m}\,\frac{\omega}{v_{\rm F}\,q}}\tag{8.25}$$

2.B $\Re\mathrm{e}\,\Pi^{0\mathrm{r}}_{11}(\mathbf{q},\omega)$

We can rewrite (8.23b) in the form

$$\Re\mathrm{e}\,\Pi^{0\mathrm{r}}_{11}(\mathbf{q},\omega)=\frac{2e^2\rho}{m}-\frac{2e^2\rho}{m\bar{q}}\;\big[\mathcal{I}_1\big(\nu_+\big)+\mathcal{I}_1\big(-\nu_-\big)\big]\tag{8.26}$$

where $\mathcal{I}_1(\nu)$ is

$$\mathcal{I}_1(\nu)=\frac{\mathsf{P}}{2\pi}\int_0^1\mathrm{d}\xi\int_0^{2\pi}\mathrm{d}\theta\;\frac{\xi^3\;\sin^2\theta}{\nu-\xi\cos\theta}$$

Again, we can deduce

$$\mathcal{I}_1(\nu)=\frac{1}{2}\,\nu-\int_0^1\mathrm{d}\xi\;\xi\,\sqrt{\nu^2-\xi^2}\,\mathrm{sign}\,[\xi+\nu]\;\Theta\big(\nu^2-\xi^2\big)\tag{8.27}$$

as well as

$$\mathcal{I}_1(\nu)=\frac{1}{2}\,\nu-\frac{1}{3}\,\nu^3+\frac{1}{3}\,\Theta\big(\nu^2-1\big)\;\mathrm{sign}\,[\nu]\,(\nu^2-1)^{\frac{3}{2}}\tag{8.28}$$

Using (8.28) into (8.26) we obtain

$$\Re\mathrm{e}\,\Pi^{0\mathrm{r}}_{11}(\mathbf{q},\omega)=\frac{2e^2\rho}{m}-\frac{2e^2\rho}{m}\;\left\{1-\frac{1}{3\bar{q}}\sum_{\pm}\pm\Big[\nu_\pm^3-\Theta\big(\nu_\pm^2-1\big)\;\mathrm{sign}\,[\nu_\pm]\;\big(\nu_\pm^2-1\big)^{\frac{3}{2}}\Big]\right\}\tag{8.29}$$

1. Static limit ($\omega = 0$). Being $\Im\mathrm{m}\,\Pi^{0\mathrm{r}}_{11}(\mathbf{q},\omega) = 0$:

$$\Pi^{0\mathrm{r}}_{11}(\mathbf{q},0) = \frac{4e^2\rho}{3m}\,\bar{q}^2\left[1-\left(1-\frac{1}{\bar{q}^2}\right)^{\frac{3}{2}}\,\Theta(\bar{q}^2-1)\right] \tag{8.30}$$

   (a) For $q \leqslant 2k_{\mathrm{F}}$:

$$\Pi^{0\mathrm{r}}_{11}(\mathbf{q},0) = \frac{e^2q^2}{12\pi m}$$

   (b) For $q \gtrsim 2k_{\mathrm{F}}$,

$$\Pi^{0\mathrm{r}}_{11}(\mathbf{q},0) \approx \frac{2e^2\rho}{m} - \frac{2}{3}\frac{e^2\rho}{m}\,\left[1+2\left(\frac{q-2k_{\mathrm{F}}}{k_{\mathrm{F}}}\right)^{\frac{3}{2}}\right]$$

   (c) For $q \gg 2k_{\mathrm{F}}$,

$$\Pi^{0\mathrm{r}}_{11}(\mathbf{q},0) \approx \frac{2e^2\rho}{m}\left(1-\frac{2k_{\mathrm{F}}^2}{q^2}\right)$$

2. In the small-frequency and small-momenta limit $\omega \ll v_{\mathrm{F}}q$, $q \ll 2k_{\mathrm{F}}$:

$$\boxed{\Re\mathrm{e}\,\Pi^{0\mathrm{r}}_{11}(\mathbf{q},\omega) = \frac{2e^2\rho}{m}\left[\frac{2}{3}\,\bar{q}^2 + \mathcal{O}\Big(\Big(\frac{\bar{\omega}}{\bar{q}}\Big)^2\Big)\right]} \tag{8.31}$$

   Collecting (8.31) and (8.25) we get

$$\boxed{\Pi^{0\mathrm{r}}_{11}(\mathbf{q},\omega) \approx \frac{e^2q^2}{12\pi m} - i\,\frac{4e^2\rho}{m}\frac{\omega}{v_{\mathrm{F}}\,q}\Big)} \tag{8.32}$$

3. Small momenta ($\bar{q} \ll 1$) and finite frequencies ($\bar{\omega} \gg \bar{q}$) $\nu_\pm \gg 1$:

$$\Re\mathrm{e}\,\Pi^{0\mathrm{r}}_{11}(\mathbf{q},\omega) = -\frac{2e^2\rho}{m}\cdot\frac{1}{3\bar{q}}\Big(-\nu_+^3+\nu_-^3+(\nu_+^2-1)^{\frac{3}{2}}-(\nu_-^2-1)^{\frac{3}{2}}\Big)$$

$$\boxed{\Re\mathrm{e}\,\Pi^{0\mathrm{r}}_{11}(\mathbf{q},\omega) = \frac{2e^2\rho}{m} + \frac{e^2\rho}{m}\,\frac{\bar{q}^2}{\bar{\omega}^2} = \frac{2e^2\rho}{m} + \frac{e^2\rho}{m}\,\frac{v_{\mathrm{F}}^2q^2}{\omega^2}} \tag{8.33}$$

9. APPENDIX B: ORTHOGONALITY RELATIONS BETWEEN FUNCTIONS OF DIFFERENT GENERATIONS

In this Appendix we will show the orthogonality between the localized functions $w_k^{(j)}(\mathbf{r})$ of different generations j, living around the k-th vortex. Due to their localization, they are trivially orthogonal if they belong to different vortices, so in the following we neglect the index k and just consider different generations on a single vortex. For compactness of the notations, the explicit position dependence will be omitted as well.
We remind the spinor notations

$$|A^{(j)}\rangle = \begin{pmatrix} w^{(j)} \\ w^{(j)*} \end{pmatrix} \qquad |B^{(j)}\rangle = \begin{pmatrix} i\, w^{(j)} \\ -i\, w^{(j)*} \end{pmatrix} \tag{9.1}$$

and their expansions on *finite energy* BdG spinors $|S_E\rangle$

$$|A^{(j)}\rangle = i \sum_{E\neq 0} \mathrm{sgn}(E)\, C_E^{(j)} |S_E\rangle \tag{9.2}$$

$$|B^{(j)}\rangle = \sum_{E\neq 0} C_E^{(j+1)} |S_E\rangle \ . \tag{9.3}$$

This same fact guarantees the *spinor* orthogonalities

$$\langle A^{(0)}|A^{(l)}\rangle = \langle A^{(0)}|B^{(m)}\rangle = 0 \quad \forall l \in \mathbb{N}\setminus\{0\}, \forall m \in \mathbb{N} \tag{9.4}$$

since $|A^{(0)}\rangle$ is the *zero energy* BdG mode.
One first useful identity we can show is

$$C_{-E}^{(j)*} = \langle S_{-E}|B^{(j-1)}\rangle^* = \langle S_E|B^{(j-1)}\rangle = C_E^{(j)} \tag{9.5}$$

having used $u_{-E}^* = v_E$.
Equation (9.2)

$$|A^{(j)}\rangle = i \sum_{E\neq 0} \mathrm{sgn}(E)\, C_E^{(j)} |S_E\rangle = i \sum_{E\neq 0} \mathrm{sgn}(E) |S_E\rangle\langle S_E|B^{(j-1)}\rangle \ . \tag{9.6}$$

can be rewritten, using the Pauli matrix σ_z, as

$$|A^{(j)}\rangle \equiv \begin{pmatrix} w^{(j)} \\ w^{(j)*} \end{pmatrix} = -\sum_{E\neq 0} \mathrm{sgn}(E) |S_E\rangle\langle S_E|\sigma_z \begin{pmatrix} w^{(j-1)} \\ w^{(j-1)*} \end{pmatrix} \equiv$$

$$\equiv K \begin{pmatrix} w^{(j-1)} \\ w^{(j-1)*} \end{pmatrix} = K\, |A^{(j-1)}\rangle \tag{9.7}$$

having defined the operator

$$K = -\sum_{E\neq 0} \mathrm{sgn}(E)|S_E\rangle\langle S_E|\sigma_z = -A\,\sigma_z \tag{9.8}$$

with

$$A = \sum_{E\neq 0} \mathrm{sgn}(E)|S_E\rangle\langle S_E| = A^\dagger\ . \tag{9.9}$$

From (9.5) we have

$$\langle A^{(1)}|B^{(0)}\rangle = -i\sum_{E\neq 0} \mathrm{sgn}(E)\,|C_E^{(1)}|^2 = 0 \tag{9.10}$$

which, together with (9.4), leads to the first orthogonality relation

$$\langle w^{(1)}|w^{(0)}\rangle = 0\ . \tag{9.11}$$

In general, to show that $\langle w^{(l)}|w^{(m)}\rangle = 0$ we need to prove separately the relations $\langle A^{(l)}|A^{(m)}\rangle = 0$ *and* $\langle A^{(l)}|B^{(m)}\rangle = 0$.
Willing to prove the orthogonality $\langle w^{(2)}|w^{(0)}\rangle = 0$ we just need to show that $\langle A^{(2)}|B^{(0)}\rangle = 0$, since $\langle A^{(2)}|A^{(0)}\rangle = 0$ by construction (9.4). However

$$\langle A^{(2)}|B^{(0)}\rangle = \langle A^{(1)}|K^\dagger|B^{(0)}\rangle = -i\langle A^{(1)}|\sigma_z A\sigma_z|A^{(0)}\rangle = i\langle A^{(1)}|\sigma_z|A^{(1)}\rangle = 0 \tag{9.12}$$

due to the vanishing trace of Pauli matrices. Thus we also proved

$$\langle w^{(2)}|w^{(0)}\rangle = 0\ . \tag{9.13}$$

In order to compute $\langle w^{(2)}|w^{(1)}\rangle$ we notice that

$$K^\dagger K = \sigma_z A^2\sigma_z = \sigma_z\left(\mathbf{1} - |A^{(0)}\rangle\langle A^{(0)}|\right)\sigma_z = \mathbf{1} - \sigma_z|A^{(0)}\rangle\langle A^{(0)}|\sigma_z\ . \tag{9.14}$$

Thus

$$\langle A^{(2)}|A^{(1)}\rangle = \langle A^{(1)}|K^\dagger K|A^{(0)}\rangle = \langle A^{(1)}|A^{(0)}\rangle - \langle A^{(1)}|\sigma_z|A^{(0)}\rangle\langle A^{(0)}|\sigma_z|A^{(0)}\rangle = 0\ . \tag{9.15}$$

Together with

$$\langle A^{(2)}|B^{(1)}\rangle = -i\sum_{E\neq 0} \mathrm{sgn}(E)\,|C_E^{(2)}|^2 = 0 \tag{9.16}$$

we prove that

$$\langle w^{(2)}|w^{(1)}\rangle = 0\ . \tag{9.17}$$

At the n-th iteration step we have already shown that $\langle w^{(n-1)}|w^{(j)}\rangle = 0\ \forall j \leq (n-2)$, and in particular $\langle w^{(n-1)}|w^{(0)}\rangle = \langle w^{(n-1)}|w^{(1)}\rangle = 0$. Then we have

$$\langle A^{(n)}|B^{(0)}\rangle = -i\langle A^{(n-1)}|\sigma_z A\sigma_z|A^{(0)}\rangle = i\langle A^{(n-1)}|\sigma_z|A^{(1)}\rangle = 0\ . \tag{9.18}$$

Having $\langle A^{(n)}|A^{(0)}\rangle = 0$ by construction, we have then shown

$$\langle w^{(n)}|w^{(0)}\rangle = 0\ . \tag{9.19}$$

Furthermore, to consider $\langle w^{(n)}|w^{(j)}\rangle\ \forall j \leq (n-2)$ we evaluate

$$\begin{aligned}\langle A^{(n)}|A^{(j)}\rangle &= \langle A^{(n-1)}|K^\dagger K|A^{(j-1)}\rangle = \\ &= \langle A^{(n-1)}|A^{(j-1)}\rangle - \langle A^{(n-1)}|\sigma_z|A^{(0)}\rangle\langle A^{(0)}|\sigma_z|A^{(j-1)}\rangle = 0\end{aligned} \tag{9.20}$$

and

$$\langle A^{(n)}|B^{(j)}\rangle = -i\langle A^{(n-1)}|\sigma_z A\sigma_z|A^{(j)}\rangle = i\langle A^{(n-1)}|\sigma_z|A^{(j+1)}\rangle = 0 \tag{9.21}$$

with the result

$$\langle w^{(n)}|w^{(j)}\rangle = 0 \qquad \forall j \leq (n-2)\ . \tag{9.22}$$

Finally

$$\begin{aligned}\langle A^{(n)}|A^{(n-1)}\rangle &= \langle A^{(n-1)}|K^\dagger K|A^{(n-2)}\rangle = \\ &= \langle A^{(n-1)}|A^{(n-2)}\rangle - \langle A^{(n-1)}|\sigma_z|A^{(0)}\rangle\langle A^{(0)}|\sigma_z|A^{(n-2)}\rangle = 0\end{aligned} \tag{9.23}$$

and

$$\langle A^{(n)}|B^{(n-1)}\rangle = -i\sum_{E\neq 0}\mathrm{sgn}(E)\,|C_E^{(n)}|^2 = 0 \tag{9.24}$$

so that we deduce

$$\langle w^{(n)}|w^{(j)}\rangle = 0 \qquad \forall j \leq (n-1)\ . \tag{9.25}$$

With this the full orthogonality between all the different generations have been proven, q.e.d.

10. ACKNOWLEDGEMENTS

At the end of this work I would like to express my gratitude to a certain amount of people.

A first great "thanks" goes to my supervisor, Prof. Bernhard Kramer, for many different reasons.
First I have to thank him for having given me the possibility and freedom of investigating such *different* and *fundamental* research areas and melting them in a unified way, thus broadening my physical horizon. From a cultural point of view it was a priceless opportunity. In this way I have been stimulated to grow my own ideas and develop independence in the work, an issue of fundamental importance for my future academic experiences.
Although leaving me a great autonomy, he always kept supporting enthusiastically the development of my research projects and directing my efforts to a focused target.
Thanks to him I had the opportunity to take part in a vast amount of scientific meetings where he always strongly supported me to present my work to a large international audience.
Thank you, Bernhard.

Among the experiences I could not have undergone without him was my six-months visit to the *Weizmann Institute of Science* (WIS, Israel). This has been the most extraordinary scientific experience in my life, so far.
There are definitely several people at the WIS I would like to thank.
Clearly, above all, Prof. Ady Stern. It is not easy to speak properly about this wonderful physicist and extraordinary human being. I just say that it is a pleasure to know and work together with such an exemplar person, from all the point of views. I thank him for all he taught to me in physics and for the exceptional example of humanity and warmth he shows in every moment.
Thank you Ady, Ruty, Noga and Uri.

There are other people at the WIS without whom my visit could not have taken place. In this sense I would like to express my deep gratitude to Dr. Hadas Shtrikman and Prof. Moty Heiblum.
A special mention goes to Roby Tsabary, a wonderful secretary who also became a second-mother to me during my stay in Israel.
I would also like to thank Alessandro Silva and his family, for the friendly atmosphere we shared.
Among the people at the WIS I acknowledge excellent discussions with Joe Imry, Sasha Finkel'stein, Israel Bar-Joseph, Uri Sivan, Misha Reznikov, Yunchul Chung,

Yang Ji, Yuval Oreg, Alex Punnoose, Moshe Shekter, Ophir Auslaender.

Cosí vid'i' adunar la bella scola
di quel segnor de l'altissimo canto
che sovra li altri com'aquila vola
(Dante, Inf. IV, 94)

Coming back to Hamburg, I want to thank Franco Napoli for being a true friend and for sharing with me the taste for several topics and techniques. Besides having been a careful dissertation-referee, he taught me a lot in the field of many-body systems and we spent many excellent moments together.

I would also like to express my gratitude to the people of the *I. Institut für Theoretische Physik* for many discussions and their friendly attitude towards me: among them Daniela Pfannkuche, Alexander Chudnovskij, Alex Struck, Siawoosh Mohammadi, Sebastian Papazoglou and the many people of the rooms nearby.
A particular "thank you" goes to Stefan Kettemann, besides hundreds of discussions, for his example of dedication to physics, scientific ethics and profound enthusiasm.
A special mention goes to Riki Mazzarello, my three-year-long room-mate (in the office and at the conferences), for plenty of discussions about physics and a huge variety of different topics. Thank you also for standing me day after day and for giving some excellent examples of passion for physics and knowledge in general.

I thank many other people in Genova and elsewhere in the world for a lot of discussions and support. Among them let me mention Maura Sassetti and her family, Nico Magnoli, Matteo Merlo, Ale Braggio, Tobias Brandes and, further on, Felix von Oppen, Rudy Morf, Hideo Aoki, Yuval Gefen, Klaus von Klitzing, Jurgen Smet, Igor Kukushkin, Rolf Haug, Uli Zeitler, Friedl Kuchar, Dieter Weiss, Jens Siewert, Giovanni Cuniberti, Saro Fazio, Pino Falci, Arturo Tagliacozzo and his family.

On a more private level let me thank several friends in (and out of) physics: Michele, Andrea, Rob, Valentina and the whole "Accademia della Crozza", Tobias Kleimann for his generous hospitality, Chiara, Franz, Valeria, Ila, Andrea and Chiara (with the new entry Daniela), Leo and Maja, Dany, Marco and the other silly guys together with Dodo.
I would also like to express my deep gratitude to Katia, although our story couldn't resist distance...
A special mention to my deepest friend Paolo, thank you for everything.

Finally, I want to thank, above all, my family.
First of all my parents, for supporting me fully in all my experiences, comforting me in hard times and leaving me free in any decision, even the most "unusual" ones. You were always there, although "by long distance".
Then, my grandparents and aunt, for being always close to me.
Thank you all!

And, once more, thank's to Glenn, Keith, Pat and Stanley!

"O frati", dissi "che per cento milia
perigli siete giunti a l'occidente,
a questa tanto picciola vigilia

d'i nostri sensi ch'é del rimanente,
non vogliate negar l'esperienza,
di retro al sol, del mondo sanza gente.

Considerate la vostra semenza:
fatti non foste a viver come bruti,
ma per seguir virtute e canoscenza".

(Dante, Inf. XXVI, 112)

BIBLIOGRAPHY

[1] N. M. Ashcroft, N. D. Mermin, *Solid State Physics*, SAUNDERS COLLEGE, Philadelphia (1976).

[2] E. H. Hall, *Amer. J. Math.* **2**, 287 (1879).

[3] L. Onsager, *Phys. Rev.* **37**, 405 (1931); **38**, 2265 (1931).

[4] K. von Klitzing, G. Dorda, M. Pepper, *Phys. Rev. Lett.* **45**, 494 (1980).

[5] K. von Klitzing, *Rev. Mod. Phys.* **58**, 519 (1986).

[6] D.C. Tsui, H.L. Stormer, A.C. Gossard, *Phys. Rev. Lett.* **50**, 1559 (1982).

[7] H. L. Stormer, *Physica B* **177**, 401 (1992).

[8] L. D. Landau, *Soviet Phys. JETP* **3**, 920 (1956).

[9] T. Ando, Y. Uemura, *J. Phys. Soc. Japan* **36**, 959 (1974).

[10] S. Doniach and E. H. Sondheimer, *Green's functions for Solid State physicists*, W. A. BENJAMIN, INC., London (1974)

[11] A. A. Abrikosov, L. P. Gorkov, I. E. Dzyaloshinski, *Methods of quantum field theory in statistical physics*, PRENTICE-HALL, INC., Englewood Cliffs, New Jersey (1964).

[12] A.L. Fetter, J.D. Walecka, *Quantum Theory of Many-Particle Systems*, MCGRAW-HILL, New York (1971).

[13] P. Nozieres, *Theory of interacting Fermi systems*, W. A. BENJAMIN, INC., New York (1964)

[14] E. M. Lifshitz and L. P. Pitaevskii, *Statistical Physics* (Part 2), PERGAMON PRESS, New York, (1980)

[15] J. W. Negele and H. Orland, *Quantum many-particle Systems*, ADDISON-WESLEY, Redwood City (1988).

[16] F. Wegner, *Z. Phys. B* **51**, 279 (1983).

[17] E. Abrahams, P. W. Anderson, D. C. Licciardello and T. V. Ramakrishnan, *Phys. Rev. Lett.* **42**, 673 (1979).

[18] M. Morgenstern, J. Klijn, Chr. Meyer and R. Wiesendanger, *Phys. Rev. Lett.* **90**, 056804-1 (2003).

[19] Courtesy of Markus Morgenstern

[20] Courtesy of Alexander Struck

[21] M. E. Levinshtein, B. I. Shklovskii, M. S. Shur and A. L. Efros, *Zh. ksp. Teor. Fiz.*, **69**, 386 (1975) [*Sov. Phys. JETP*, **42**, 197 (1975)].

[22] B Huckestein and B. Kramer, *Phys. Rev. Lett.* **64**, 1437 (1990).

[23] B. Kramer and A. Mac Kinnon, *Rep. Prog. Phys.* **56**, 1469 (1994).

[24] R. B. Laughlin, *Phys. Rev. B* **23**, 5632 (1981).

[25] B. I. Halperin, *Phys. Rev. B* **25**, 2185 (1982).

[26] S. R. E. Yang, A. H. MacDonald and B. Huckestein, *Phys. Rev. Lett.* **74**, 3229 (1995).

[27] R. B. Laughlin, *Phys. Rev. Lett.* **50**, 1935 (1983).

[28] R. de Picciotto, M. Reznikov, M. Heiblum, V. Umansky, G. Bunin and D. Mahalu, *Nature* **389**, 162 (1997).

[29] L. Saminadayar, D. C. Glattli, Y. Jin and B. Etienne, *Phys. Rev. Lett.* **79**, 2526 (1997).

[30] S. M. Girvin and T. Jach, *Phys. Rev. B* **29**, 5617 (1984).

[31] R. E. Prange, S. M. Girvin (eds.), *The Quantum Hall Effect*, SPRINGER-VERLAG, New York (1990).

[32] G. S. Boebinger, A. M. Chang, H. L. Stormer, and D. C. Tsui, *Phys. Rev. Lett.* **55**, 1606 (1985).

[33] T. Chakraborty, *Phys. Rev. B* **31**, 4026 (1985).

[34] R. Morf and B. I. Halperin, *Phys. Rev. B* **33**, 2221 (1986).

[35] D. Arovas, J. R. Schrieffer and F. Wilczek, *Phys. Rev. Lett.* **53**, 722 (1984).

[36] S. M. Girvin, in *Topological Aspects of Low Dimensional Systems*, ed. A. Comtet et al., SPRINGER-VERLAG, Berlin (2000); `cond-mat/9907002`.

[37] M. V. Berry, *Proc. Roy. Soc.* (London) A**392**, 45 (1984).

[38] B. I. Halperin, *Helv. Phys. Acta* **56**, 75 (1983)

[39] S. Das Sarma and A. Pinczuk (Eds.), *Perspectives in Quantum Hall Effects*, WILEY, New York, (1997).

[40] T. Chakraborty and P. Pietiläinen, *The Quantum Hall Effects*, SPRINGER-VERLAG, Berlin Heidelberg (1995).

[41] F. D. M. Haldane, *Phys. Rev. Lett.* **51**, 605 (1983).

[42] J. K. Jain, *Phys. Rev. Lett.* **63**, 199 (1989).

[43] N. Read, *Surf. Sci.* **361**, 7 (1996).

[44] O. Heinonen (Ed.), *Composite Fermions*, WORLD SCIENTIFIC, Singapore (1998).

[45] B. I. Halperin, P. A. Lee, N. Read, *Phys. Rev. B* **47**, 7312 (1993).

[46] W. Pan, H. L. Stormer, D. C. Tsui, L. N. Pfeiffer, K. W. Baldwin, and K. W. West Phys. Rev. Lett. 90, 016801 (2003).

[47] H. W. Jiang, H. L. Stormer, D. C. Tsui, L. N. Pfeiffer and K. W. West, *Phys. Rev. B* **40**, 12013 (1989).

[48] J. H. Smet, S. Jobst, K. von Klitzing, D. Weiss, W. Wegscheider and V. Umansky, *Phys. Rev. Lett.* **83**, 2620 (1999).

[49] R. R. Du, H. L. Stormer, D. C. Tsui, L. N. Pfeiffer and K. W. West, *Phys. Rev. Lett.* **70**, 2944 (1993).

[50] A. Lopez, E. Fradkin, *Phys. Rev. B* **44** 5246 (1991).

[51] S. C. Zhang, *Int. J. Mod. Phys.* **6**, 25 (1992).

[52] A. L. Fetter, C. B. Hanna and R. B. Laughlin, *Phys. Rev. B* **39**, 9679 (1989).

[53] P. Ramond, *Field Theory: A Modern Primer*, BENJAMIN-CUMMINGS PUBLISHING COMPANY (1981).

[54] A. Stern, B. I. Halperin, *Phys. Rev. B* **52**, 5890 (1995).

[55] J. R. Schrieffer, *Theory of superconductivity*, W. A. BENJAMIN, INC., New York (1964).

[56] R. R. Du, H. L. Stormer, D. C. Tsui, A. S. Yeh, L. N. Pfeiffer and K. W. West, *Phys. Rev. Lett.* **73**, 3274 (1994).

[57] T. Chakraborty and F. C. Zhang, *Phys. Rev. B* **29**, 7032 (1984); F. C. Zhang and T. Chakraborty, *Phys. Rev. B* **30**, 7320 (1984).

[58] X. C. Xie, Y. Guo, and F. C. Zhang, *Phys. Rev. B* **40** , 3487 (1989); P. Beran and R. Morf, *Phys. Rev. B* **43**, 12654 (1991).

[59] U. Zeitler, H. W. Schumacher, A. G. M. Jansen and R. J. Haug, *Phys. Rev. Lett.* **86**, 866 (2001)

[60] J. T. Chalker, D. G. Polyakov, F. Evers, A. D. Mirlin, and P. Wlfle, *Phys. Rev. B* **66**, 161317 (2002)

[61] I. V. Kukushkin, K. v.Klitzing, and K. Eberl, *Phys. Rev. Lett.* **82**, 3665 (1999).

[62] I. V. Kukushkin, K. v.Klitzing, K. G. Levchenko, and Yu. E. Lozovik, *JETP Letters* **70**, 730 (1999).

[63] I. V. Kukushkin, J. H. Smet, K. v.Klitzing, and K. Eberl, *Phys. Rev. Lett.* **85**, 3688 (2000).

[64] E. Mariani, R. Mazzarello, M. Sassetti and B. Kramer, *Ann. Phys. (Leipzig)* **11**, 926 (2002)

[65] A. Lopez and E. Fradkin, *Phys. Rev. B* **51**, 4347 (1995).

[66] S. S. Mandal and V. Ravishankar, *Phys. Rev. B* **54** , 8688 (1996).

[67] N. d'Ambrumenil and R. H. Morf, *Phys. Rev. B* **40**, 6108 (1989).

[68] K. Park and J. K. Jain, *Phys. Rev. Lett.* **80**, 4237 (1998).

[69] R. Shankar, *Phys. Rev. B* **63**, 085322 (2001); G. Murthy, `cond-mat/0004334`; G. Murthy, `cond-mat/0008259`.

[70] I. V. Kukushkin, J. H. Smet, K. von Klitzing, and W. Wegscheider, *Nature* **415**, 409 (2002).

[71] S. S. Mandal and J. K. Jain, `cond-mat/0103631`.

[72] R. R. Du, A. S. Yeh, H. L. Stormer, D. C. Tsui, L. N. Pfeiffer, and K. W. West, *Phys. Rev. Lett.* **75**, 3926 (1995).

[73] T. Chakraborty, P. Pietiläinen and F. C. Zhang, *Phys. Rev. Lett.* **57**, 130 (1986).

[74] S. Melinte, N. Freytag, M. Horvatic, C. Berthier, L. P. Levy, V. Bayot, and M. Shayegan, *Phys. Rev. Lett.* **84**, 354 (2000).

[75] B. L. Altshuler and L. B. Ioffe, *Phys. Rev. Lett.* **69** , 2979 (1992).

[76] D. V. Khveshchenko and S. V. Meshkov, *Phys. Rev. B*, **47**, 12051 (1993).

[77] E. Altshuler, A. G. Aronov, A. D. Mirlin and P. Woelfle, *Europhys. Lett.* **29**, 239 (1995).

[78] D. V. Khveshchenko, *Phys. Rev. Lett.* **77**, 1817 (1996).

[79] A. Shelankov, *Phys. Rev. B* **62**, 3196 (2000).

[80] A. D. Mirlin, D. G. Polyakov and P. Woelfle, *Phys. Rev. Lett.* **80**, 2429 (1998).

[81] T. Ando, J. Phys. Soc. Jpn., **37**, 1233 (1974).

[82] T. Ando, Y. Matsumoto, Y. Uemura, J. Phys. Soc. Jpn., **39**, 279 (1975).

[83] V. I. Falko, *Phys. Rev. B* **46**, 4320 (1992).

[84] G. F. Giuliani, and J. J. Quinn, *Phys. Rev. B* **31**, 6228 (1985).

[85] S. Yarlagadda, *Phys. Rev. B* **44**, 13101 (1991).

[86] H. Kamerlingh-Onnes, *Comm. Phys. Lab. Univ. Leiden*, Nos. 119, 120, 122 (1911).

[87] W. Meissner and R. Ochsenfeld, *Naturwiss.* **21**, 787 (1933).

[88] P. G. deGennes, *Superconductivity of metals and alloys*, W. A. BENJAMIN, INC., New York (1966).

[89] J. Bardeen, L. N. Cooper and J. R. Schrieffer, *Phys. Rev.* **106**, 162 (1957); *Phys. Rev.* **108**, 1175 (1957).

[90] N. N. Bogoliubov, *Nuovo Cimento* **7**, 794 (1958).

[91] J. Valatin, *Nuovo Cimento* **7**, 843 (1958).

[92] L. N. Cooper, *Phys. Rev.* **104**, 1189 (1956).

[93] A. J. Leggett, *Rev. Mod. Phys.* **47**, 331 (1975).

[94] D. Vollhardt, and P. Woelfle, *The superfluid phases of Helium 3*, TAYLOR & FRANCIS, London (1990).

[95] P. W. Anderson, *J. Phys. Chem. Solids* **11**, 26 (1959).

[96] B. T. Matthias, E. A. Wood, E. Corenzwit and V. B. Bala, *J. Phys. Chem. Solids* **1**, 188 (1956).

[97] A. A. Abrikosov and L. P. Gor'kov, *Sov. Phys. JETP* **10**, 593 (1960); M. A. Woolf and F. Reif, *Phys. Rev.* **137A**, 557 (1965).

[98] P. W. Anderson, *Phys. Rev.* **112**, 1900 (1958).

[99] H. Frolich, *Phys. Rev.* **79**, 845 (1950).

[100] Y. Nambu, *Phys. Rev.* **117**, 648 (1960).

[101] L. P. Gor'kov, *Sov. Phys. JETP* **7**, 505 (1958).

[102] G. M. Eliashberg, *Sov. Phys. JETP* **11**, 696 (1960).

[103] S. V. Vonsovsky, Yu. A. Izyumov and E. Z. Kurmaev, *Superconductivity of transition metals*, SPRINGER-VERLAG, Berlin Heidelberg (1982).

[104] A. M. Zagoskin, *Quantum theory of many-body systems*, SPRINGER-VERLAG, New York (1998).

[105] A. B. Migdal, *Sov. Phys. JETP* **1**, 996 (1958).

[106] E. Mariani, N. Magnoli, F. Napoli, M. Sassetti and B. Kramer, *Phys. Rev. B* **66**, 241303(R) (2002).
cond-mat/0212422

[107] B. Kramer, E. Mariani, N. Magnoli, M. Merlo, F. Napoli and M. Sassetti, *Phys. Stat. Sol. (b)* **234**, 221 (2002).

[108] B. Kramer, N. Magnoli, E. Mariani, M. Merlo, F. Napoli and M. Sassetti, "Composite Fermions with Spin at $\nu = 1/2$", *Proceedings of the Varenna Summer School "E. Fermi", Course CLI "Quantum Phenomena in Mesoscopic Systems"*, July 2002.
cond-mat/0212423

[109] D. V. Khveshchenko, *Phys. Rev. B* **47**, 3446 (1993).

[110] N. E. Bonesteel, *Phys. Rev. B* **48**, 11484 (1993).

[111] N. E. Bonesteel, I. A. McDonald, and C. Nayak, *Phys. Rev. Lett.* **77**, 3009 (1996).

[112] E. Mariani, unpublished.

[113] Ady Stern, private communications.

[114] B. Kramer, N. Magnoli, E. Mariani, M. Merlo, and M. Sassetti, *J. Phys. Soc. Jpn.* **72**, 42 (2003).

[115] G. Murthy, *Phys. Rev. Lett.* **84**, 350 (2000); V. M. Apalkov, T. Chakraborty, P. Pietilainen, and K. Niemela, cond-mat/0007043; V. M. Apalkov, T. Chakraborty, P. Pietilainen, and K. Niemela, *Phys. Rev. Lett.* **86**, 1311 (2001).

[116] P. C. Hohenberg, *Phys. Rev.* **158**, 383 (1967).

[117] J. M. Kosterlitz and D. J. Thouless, *J. Phys. C* **6**, 1181 (1973).

[118] G. Balestrino, P. G. Medaglia, P. Orgiani, A. Tebano, C. Aruta, S. Lavanga, and A. A. Varlamov, *Phys. Rev. Lett.* **89**, 156402 (2002).

[119] A. I. Larkin, and A. A.Varlamov, "Fluctuation Phenomena in Superconductors", in *Handbook on Superconductivity: Conventional and Unconventional Superconductors* ed. K. H. Bennemann and J. B. Ketterson, SPRINGER (2002).

[120] I. Bar-Joseph, private communications.

[121] R. L. Willett, J. P. Eisenstein, H. L. Stormer, D. C. Tsui, A. C. Gossard and J. H. English, *Phys. Rev. Lett.* **59**, 1776 (1987).

[122] W. Pan, J. S. Xia, V. Schvarts, D. E. Adams, H. L. Stormer, D. C. Tsui, L. N. Pfeiffer, K. W. Baldwin and K. W. West, *Phys. Rev. Lett.* **83**, 3530 (1999).

[123] M. P. Lilly, K. B. Cooper, J. P. Eisenstein, L. N. Pfeiffer and K. W. West, *Phys. Rev. Lett.* **82**, 394 (1999).

[124] R. H. Morf, *Phys. Rev. Lett.* **80**, 1505 (1998).

[125] J. P. Eisenstein, R. L. Willett, H. L. Stormer, D. C. Tsui, A. C. Gossard and J. H. English, *Phys. Rev. Lett.* **61**, 997 (1988).

[126] W. Pan, R. R. Du, H. L. Stormer, D. C. Tsui, L. N. Pfeiffer, K. W. Baldwin and K. W. West, *Phys. Rev. Lett.* **83**, 820 (1999).

[127] M. P. Lilly, K. B. Cooper, J. P. Eisenstein, L. N. Pfeiffer and K. W. West, *Phys. Rev. Lett.* **83**, 824 (1999).

[128] W. Pan, H. L. Stormer, D. C. Tsui, L. N. Pfeiffer, K. W. Baldwin, K. W. West, `cond-mat/0103144`.

[129] R. L. Willett, K. W. West and L. N. Pfeiffer, *Phys. Rev. Lett.* **88**, 066801 (2002).

[130] F. D. M. Haldane and E. H. Rezayi, *Phys. Rev. Lett.* **60**, 956, 1886 (E) (1988).

[131] G. Moore and N. Read, *Nucl. Phys. B* **360**, 362 (1991).

[132] E. H. Rezayi and F. D. M. Haldane, *Phys. Rev. Lett.* **84**, 4685 (2000).

[133] N. Read and D. Green, *Phys. Rev. B* **61**, 10267 (2000).

[134] G. E. Volovik, *Zh. ksp. Teor. Fiz.* **94**, 123 (1988) [*Sov. Phys. JETP* **67**, 1804 (1988)].

[135] C. Nayak and F. Wilczek, *Nucl. Phys. B* **479**, 529 (1996).

[136] N. B. Kopnin and M. M. Salomaa, *Phys. Rev. B* **44**, 9667 (1991).

[137] G. E. Volovik and V. M. Yakovenko, *J. Phys.: Condens. Matter* **1**, 5263 (1989); G. E. Volovik, *Physica B* **162**, 222 (1990); G. E. Volovik, *Zh. ksp. Teor. Fiz.* **51**, 111 (1990) [*JETP Lett.* **51**, 125 (1990)]; G. E. Volovik, *Zh. ksp. Teor. Fiz.* **55**, 363 (1992) [*JETP Lett.* **55**, 368 (1992)].

[138] C. Caroli, P. G. de Gennes and J. Matricon, *Phys. Lett.* **9**, 307 (1964).

[139] A. Stern, F. von Oppen and E. Mariani, in preparation.

[140] D. A. Ivanov, `cond-mat/0005069`.

[141] E. Mariani and A. Stern, in preparation.

[142] J. Schwinger, *Quantum Mechanics*, SPRINGER, New York (2001).

[143] R. Abraham and J. E. Marsden, *Foundations of Mechanics*, ADDISON-WESLEY INC. (1978).

[144] C. Bloch and A. Messiah, *Nucl. Phys.* **39**, 95 (1962)